Combating HIV with Novel Antibody Architectures

Thesis by

Rachel P Galimidi

In Partial Fulfillment of the Requirements for the degree of

Doctor of Philosophy

CALIFORNIA INSTITUTE OF TECHNOLOGY

Pasadena, California

2016

(Defended February 5, 2016)

© 2016

Rachel P Galimidi
All Rights Reserved

ACKNOWLEDGEMENTS

ABSTRACT

More than 30 years has passed since the discovery of Human Immunodeficiency Virus (HIV) yet it remains one of the most important current threats to global public health. HIV is a T-lymphotrophic retrovirus that is the causative agent of Acquired Immune Deficiency Syndrome, and despite decades of research, there remains no cure. Vaccines are most effective when they are able to induce broadly neutralizing antibodies at concentrations capable of blocking viral infection. Notwithstanding all of the effort, a successful vaccine that is capable of inducing complete protection from the immune system has yet to be found. In this thesis, the first chapter provides a history of the discovery of HIV, the origins of the virus, description of the HIV genome, focusing primarily on the envelope glycoprotein, a trimeric spike on the surface of the HIV virion necessary for viral fusion and the sole epitope for broadly neutralizing antibodies. Lastly, the first chapter reviews an overview of the antiviral immune response specifically the role of humoral immune branch and broadly neutralizing antibodies, as well as their limitations in protection against HIV. Antibodies developed during HIV-1 infection lose efficacy as the viral spike mutates. In addition to structural features of HIV's envelope spike that facilitate antibody evasion, we proposed that the low-density and limited lateral mobility of HIV spikes impedes bivalent binding by antibodies. The resulting predominantly monovalent binding minimizes avidity and thereby high affinity binding and potent neutralization, thus expanding the range of HIV mutations permitting antibody evasion. The work described in subsequent chapters attempts to overcome HIV's evasion strategy of low spike density through the design of novel antibody architectures.

We postulated that anti-HIV-1 spike antibodies primarily bind monovalently because HIV's low spike density impedes bivalent binding through inter-spike crosslinking, and the spike trimer structure prohibits bivalent binding through intra-spike crosslinking. Monovalent binding reduces avidity and neutralization potency, thus expanding the range of mutations permitting antibody evasion. To test this idea, we engineered antibody-based molecules capable of bivalent binding through intra-spike crosslinking. We used DNA as a "molecular ruler" to measure intra-epitope distances on virion-bound spikes and to construct intra-spike crosslinking molecules. Optimal bivalent reagents exhibited up to 2.5 orders of magnitude of increased potency (>100-fold average increases across a virus panel) and identified conformational states of virion-bound spikes. The demonstration that intra-spike crosslinking lowers the concentration of antibodies required for neutralization supports the hypothesis that low spike densities facilitate antibody evasion and the use of molecules capable of intra-spike crosslinking for therapy or passive protection. These results shed light on dynamic spike conformations and are relevant to therapeutic interventions.

PUBLISHED CONTENT AND CONTRIBUTIONS

Chapter Two:

Barbian, H.J., Decker, J.M., Bibollet-Ruche, F., **Galimidi, R.P.**, West, A.P., Jr., Learn, G.H., Parrish, N.F., Iyer, S.S., Li, Y., Pace, C.S., Song, R., Huang, Y., Denny, T.N., Mouquet, H., Martin, L., Acharya, P., Zhang, B., Kwong, P.D., Mascola, J.R., Verrips, C.T., Strokappe, N.M., Rutten, L., McCoy,L.E., Weiss,R.A., Brown,C.S., Jackson, R., Silvestri, G., Connors, M., Burton, D.R., Shaw, G.M., Nussenzweig, M.C., Bjorkman, P.J., Ho, D.D., Farzan,M., and Hahn, B.H., (2015). Neutralization properties of simian immunodeficiency viruses infecting chimpanzees and gorillas. mBio *6*.

Parrish NF, Gao F, Li H, Giorgi EE, Barbian HJ, Parrish EH, Zajic L, Iyer SS, Decker JM, Kumar A, Hora B, Berg A, Cai F, Hopper J, Denny TN, Ding H, Ochsenbauer C, Kappes JC, **Galimidi RP**, West AP Jr, Bjorkman PJ, Wilen CB, Doms RW, O'Brien M, Bhardwaj N, Borrow P, Haynes BF, Muldoon M, Theiler JP, Korber B, Shaw GM, Hahn BH. (2013) Phenotypic properties of transmitted founder HIV-1. Proc Natl Acad Sci U S A. 2013 Apr 23;110(17):6626-33.

West, A.P., Jr., **Galimidi, R.P.,** Foglesong, C.P., Gnanapragasam, P.N.P., Klein, J.S., Bjorkman, P.J. (2010) Evaluation of alternative CD4-CD4i antibody architectures yields potent, broadly cross-reactive anti-HIV reagents. J. Virol. 84:261-269

This chapter describes the characterization of an antibody-based reagent for the treatment of an endangered population of chimpanzees infected with SIV in Tanzania. My contribution to this work involved the repurposing and redesign of a reagent from previous research that I had done prior to beginning as a graduate student at Caltech. I designed and preformed initial characterization of the second generation reagents that

were later tested for use against SIV. This work was a collaboration with Anthony West and Alysia Ahmed in the Bjorkman lab, Hannah Barbian and other members of Beatrice Hahn's lab at UPENN, as well as Michael Farzan at HMS.

Chapter Three:

Galimidi, R.P., Klein, J.S., Politzer, M.S., Bai, S., Seaman, M.S., Nussenzweig, M.C., West, A.P., Jr., and Bjorkman, P.J. (2015). Intra-spike crosslinking overcomes antibody evasion by HIV-1. Cell *160*, 433-446.

This chapter describes the development of a series of broadly neutralizing antibody-based reagents capable of intraspike cross-linking on an HIV envelope spike. These bivalent engineered reagents bind with high-avidity leading to >100 fold average increased neutralization potencies. These data further validate a hypothesis first described in Pamela Bjorkman's lab suggesting that the low spike density on HIV-1 virions evolved to facilitate antibody evasion. Here we also describe a novel molecular tool to measure distances on a virtually sub-nanometer scale.

My contributions to this work was to be the lead researcher on the project, I helped to conceive the study, prepared the reagents needed to test the hypothesis, performed the assays to test the reagents, analyzed the data and wrote the paper.

Chapter Four:

Klein J.S*., Jiang S.*, **Galimidi R.P.*,** Keeffe J.R., Bjorkman P.J. (2014) Design and Characterization of Structured Protein linkers with differing flexibilities. Protein Eng Des Sel. 2014 Oct;21 (10):325-30.

*Authors contributed equally to work.

This chapter describes the characterization of engineered protein linkers. This work was a collaboration between Joshua Klein, Siduo Jiang, Jennifer Keeffe and myself. Joshua Klein, Siduo Jiang and I each contributed equally to this work. The conception and many of the initial designs of linkers, were by Joshua Klein. Joshua also performed early experiments and analyzed initial data. Siduo Jiang cloned, expressed, and purified protein linker reagents; performed experiments; analyzed data; and aided in the design of various protein linkers. My contribution to this work was the design of a subset of the structured linkers; cloning, expression, purification of linker reagents; performed experiments; as well as analysis and characterization of the protein linkers. In addition, throughout Siduo Jiang's time as an undergraduate researcher in the lab, I was his primary mentor, and oversaw all of the work that was done.

Appendix B:

West, A.P., Jr., **Galimidi, R.P.,** Gnanapragasam, P.N.P, Bjorkman, P.J.(2011) Single Chain Fv-based anti-HIV proteins: Potential and Limitations. J. Virol. 2011 Oct 19.

This appendix describes the strengths and weaknesses of a class of antibody based reagents for the use in immunotherapies against HIV. This work was done in collaboration with Anthony West, and Priyanthi Gnanapragasam. My contribution to this work was in aiding Anthony in initial construct design, cloning of DNA, protein purification, and preliminary characterization of the reagents.

TABLE OF CONTENTS

Chapter One: Introduction

Introduction

The Discovery of HIV

The year was 1981: doctors in Los Angeles, San Francisco, and New York are left baffled at cases of pneumonia and a rare yet aggressive cancer that seems to be spreading among seemingly healthy young men (Gottlieb et al., 1981). The cause of the outbreak is unknown but the only common thread is that the men are homosexual. By the end of the year there will be 41 reported cases and 8 victims dead within 24 months after their initial diagnosis (Altman, 1981). This sudden form of the rare cancer, called Kaposi's Sarcoma, originally described by Moritz Kaposi in 1872, presented with pigmented epidermal lesions, and led doctors and soon the media into a frenzy trying to find the cause. One of the earliest doctors to arrive on the scene was Dr. Michael Gottlieb, of UCLA, who first postulated that these patients must be suffering from a potentially sexually transmissible immune deficiency (Gottlieb et al., 1981). During this time, two independent labs were about to discover how right Dr. Gottlieb and colleagues were.

We will all soon know this condition as AIDS, or Acquired Immune Deficiency Syndrome, and despite it being over 35 years since the emergence of the AIDS epidemic there remains no cure. The cause of AIDS, HIV– or human immunodeficiency virus– would eventually be discovered two years later, in the labs of Robert Gallo, Luc Montagnier, and Franciose Barre-Sinoussi. Montagnier and Barre-Sinoussi would later receive the Nobel Prize in Physiology and Medicine for their heroic efforts. The cause: a retrovirus, similar to that of HTLV-1 first discovered in 1980 (Gallo and Montagnier, 2003; Gallo, 2005) which was shown to be linked to adult T-cell leukemia. Retroviruses

are a family of viruses which obtained their name when the discovery of reverse transcriptase by David Baltimore and Howard Temin showed that some viruses had RNA genomes which were copied to DNA (Gallo and Montagnier, 2003). Unlike HTLV, HIV proved to be of the lentivirus genus, which is best classified by the slow progression to disease, and the clinical latency phase can last over 20 years which made it exceedingly difficult in the early 80s to pinpoint (Levy, 1993; Moir et al., 2011) .

Within 15 years, huge progress was made first with repurposing of the nucleoside analog, zidovudine (AZT) (Fischl et al., 1987). Previously synthesized as a potential cancer therapeutic, AZT failed in mouse trials and was forgotten until after the discovery of its use as an inhibitor to the Friend Virus, a known retrovirus that causes murine Friend Leukemia Virus (FLV) (Ostertag et al., 1974). By 1985, pharmaceutical companies were itching to find a treatment for the ever growing population of people being infected and dying of AIDS. During those six years since the emergence, an estimated one million Americans were infected with the virus and 15,000 had already succumbed to the disease (Boffey, 1986). When the Borroughs Welcome Company dusted AZT off the shelf and sent it to the National Institute of Health and the National Cancer Institute to test against HIV-infected cells, it was there that they found that the zidovudine could successfully inhibit the virus without harming the cells. It was not long after that AZT went into animals and the FDA approved it for clinical trials ("A Failure led to drug against AIDS",1986).

Unfortunately, the AZT craze was short sided, and the effects were only temporary; with the harsh side effects and only modest improvement on life span there was still no effective treatment (Fischl et al., 1987). It wasn't until 1996, that the development of

highly active antiretroviral therapy (HAART) was credited with the effective decrease in AIDS related mortality and morbidity in the United States and other industrialized countries (Palella et al., 1998). However, the cost associated with HAART and lack of a strong health care foundation has limited its use in developing countries (UNAIDS, 2015). Since the onset of the virus, nearly 39 million people have died from the HIV/AIDS related illnesses, with currently 37 million people living with HIV. Despite this, only 15 million people living with HIV even have access to anti-retroviral therapy (UNAIDS and Sabin, 2015). Looking at a regional picture, the numbers become even more devastating, with more than two thirds of all people currently living with HIV residing in Sub-Saharan Africa alone. Strikingly, within Sub-Saharan Africa resides 88% of the worlds HIV+ children (UNAIDS and Sabin, 2015).

In 1984, during an unsubstantiated moment of hubris, the U.S. Secretary of Health and Human Services, Margaret Heckler, announced that through the discovery of the virus that causes AIDS "they" believed that a vaccine would soon follow: "We hope to have such a vaccine ready for testing in approximately two years" (Watkins, 2008). Unfortunately, despite nearly 35 years since the emergence of the HIV/AIDS epidemic and massive efforts there remains no cure or vaccine in sight. In order to understand the difficulty in obtaining a feasible vaccine, one must appreciate the virus' inherent diversity and ability to mutate and change over time.

The HIV genome

HIV is a roughly spherical enveloped lentivirus that contains two copies of a positive sense RNA genome (Levy, 1993). Encasing the RNA is a cone-shaped capsid with a layer known as matrix dividing it from envelope (Figure 1). Similar to other lentiviruses, such as Simian immunodeficiency syndrome (SIV) and Equine infectious anemia virus (EIAV), HIV is known for its immunosuppressive properties, as referenced in its name. HIV has an intricate genome that spans 9.8 kilobases (kb), and contains both regulatory and accessory genes necessary to encode all of the viral proteins, that are defined by three regions of the genome (Figure 1): *gag*, *pol* and *env* (Flint et al., 2008).

Gag, or group-specific antigen gene produces p55, or the Gag precursor protein, a 55 kilodalton (kDa) protein expressed from the unspliced viral RNA. Following translation, p55 is myristoylated at its N-terminus, which enables p55 to interact with the cytoplasmic region of the cell membrane. Once it is associated with the cell membrane, p55 then recruits other viral and cellular proteins and viral genomic RNA to induce budding of the virus particle from the infected cell (Flint et al., 2008; Hutchinson, 2001). Post budding, viral maturation occurs and p55 is then cleaved by a virally encoded protease into matrix, capsid, nucleocapsid, and p6 (Cook et al., 2014). Matrix is derived from the N'-terminus of p55 and is responsible for stabilizing the viral particle by attaching to the virion envelope via the insertion of the myristoyl group into a phosphoinosotide in the plasma membrane (Ganser-Pornillos et al., 2008). The capsid protein forms the canonical cone-like core of the viral particles **(FIGURE)** encapsulating the RNA genome (Ganser-Pornillos et al., 2008), while the nucleocapsid protein is responsible for condensing the RNA genome (Briggs and Krausslich, 2011). Lastly, p6 is

necessary for efficient budding of the virions from infected cells as well as facilitating the interaction between p55 and Vpr, a viral accessory gene, and aids in the incorporation of Vpr into the fully assembled virion (Paxton et al., 1993).

The Pol proteins (Integrase, Protease, Reverse transcriptase, and RNase H) are synthesized from the Pol-Gag precursor, p160. Synthesis of this fusion protein occurs due to a ribosomal frameshift event initiated by a cis-acting RNA motif in the distal region of the *Gag* RNA (Parkin et al., 1992). When ribosomes recognize this motif, a frameshift occurs approximately five percent of the time, allowing for the entire *pol* reading frame to be translated without interruption (Parkin et al., 1992). Similarly to p55, during viral maturation, the virally encoded Protease that is packaged in the virion cleaves p160 into the aforementioned *pol* proteins (Parkin et al., 1992). HIV protease is a dimeric aspartyl protease that is packaged in the virion during viral maturation, and as mentioned above, is essential for the cleavage of both p55 and p160 (Pettit et al., 2004). Reverse transcriptase, a hallmark of retroviruses, produces double-stranded DNA from the viral RNA genome (Baltimore, 1970). During this process, RNase H is required to eliminate the original RNA template to ensure the complementary strand of DNA is synthesized (Flint et al., 2008). The last *pol* protein, Integrase, facilitates the incorporation of the provirus DNA into the host cell's genomic DNA (Flint et al., 2008).

The third gene, envelope (*env*), encodes for a 160 kDa glycoprotein known as gp160. Env functions as the initiator of virion and host cell interactions and is heavily glycosylated. HIV utilizes glycosylation of the env protein as a mechanism to evade the host immune response. Indeed, following translation gp160 is targeted to the Golgi, where N-linked glycans are added to roughly thirty sites on the gp160 surface (Go et al.,

2013; Pritchard et al., 2015a). While still in the Golgi network, HIV utilizes Furin, a ubiquitous protease enriched in the trans-golgi, to cleave gp160 into its active subunits, gp120 and gp41 (Figure 1) (Freed and Mouland, 2006; Ganser-Pornillos et al., 2008; Pantophlet and Burton, 2006; Pritchard et al., 2015a). The *env* proteins are then transported to the cell membrane where they form a trimer of gp120-gp41 heterodimers (Figure 1). The gp120-gp41 trimer, along with the host cell's lipid bilayer, form the envelope coating the HIV virion, where gp41 contains the transmembrane domain, and gp120 is located on the surface of the infected cell or virion (Capon and Ward, 1991). The gp160 trimer or viral spike is required to mediate infection into the host cell and the primary site of the immune system's humoral response against HIV; the mechanism of each will be discussed later in this chapter.

In addition to Gag, Pol, and Env, the HIV genome encodes regulatory proteins Rev and Tat, as well as accessory proteins Nef, Vif, Vpr, and Vpu (Briggs and Krausslich, 2011; Cook et al., 2014). Both Rev and Tat are proteins produced from fully spliced mRNA. Rev, an RNA binding protein, is responsible for facilitating the shift from early to late phase gene expression. Tat acts as a transcriptional transactivator in HIV-1 replication and works in aiding to produce full-length HIV-1 transcripts (Feinberg et al., 1991; Felber et al., 1990). Unlike Rev and Tat, the accessory proteins are not required for viral replication but affect virulence.

Nef, or negative factor, is a protein encoded a single exon located partially within the 3' Long terminal repeat (LTR) and is an early sign of HIV infection, as it is the first virally encoded protein to accumulate in an infected cell. Nef has been shown to increase virulence of the HIV via downregulation of CD4, the primary receptor necessary for

infection in T-Cells allowing for overexpression of Env on the cell surface. In addition, Nef has been shown to downregulate major histocompatibility complex (MHC) on the infected cell in an attempt to evade the host immune response (Lama et al., 2001; Ross et al., 1999).

Unlike Nef, Vpr, Vpu, and Vif are products of incomplete splicing of mRNA and therefore are only produced during the Rev induced late phase of infection. Similar to Nef, Vpu is a protein that aids in the propagation of HIV-1 through its ability to downregulate CD4, as well as the novel function of enhancing the release of viral buds through the acting as an antagonist to a human type 2 integral membrane protein, known as tetherin. Interestingly, Vpu, while found in HIV-1, is not encoded in HIV-2, perhaps due to its redundancy with Nef (Magadán et al., 2010; McNatt et al., 2013). Vpr, through an interaction with the c-termini of the p55 protein, accumulates in the viral particles and aids in the ability of HIV to infect non-dividing cells and inhibits cell division (Jowett et al., 1995). Finally, Vif, the last accessory protein, also packaged in the mature virion, is known to assist in the replication of HIV in non-CD4 expressing lymphocytes (Lake et al., 2003), through depletion of APOBEC3G, an endogenous enzyme known to inhibit retroviral replication in HIV-infected T-cells (Stopak et al., 2003).

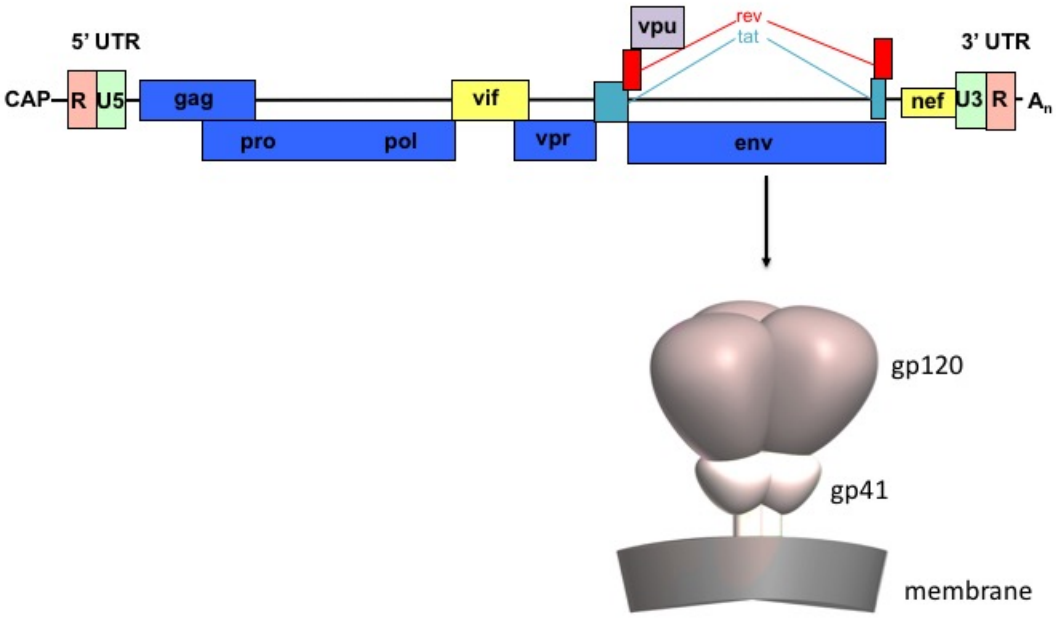

Figure 1. Genome organization of HIV and HIV envelope structure.

Origin and genetic diversity of HIV

Based on phylogenic analysis of the HIV genome and pathogenesis, there are two types of HIV viruses: HIV-1 and HIV-2. While HIV-1 and HIV-2 can both lead to AIDS, and share traits such as mode of transmission, basic genetic composition, and replication pathways, HIV-2 accounts for only 2% of HIV incidence rates worldwide and is characterized by slower progression to AIDS and increased immunogenicity (Wu, 2015). Moreover, the two viruses only share an overall genetic sequence identity of less than 50% (Wu, 2015). Unlike the worldwide epidemic of HIV-1, HIV-2 is largely contained to Western Africa, and is largely tolerated without the need of medication. Based on this, in general much less effort has been made to research HIV-2 biology.

Through phylogenetic analysis, it is hypothesized that HIV-1 and HIV-2 are derived from separate cross-species transmission incidents (Figure 2) (Hutchinson, 2001). HIV-1, is more closely related to chimpanzee simian immunodeficiency virus, SIVcpz, which suggests that the known HIV-1 progenitor was passed from chimpanzees, while HIV-2 is more closely related to an SIV strain known to infect sooty mangabeys (Figure 2) (Sharp and Hahn, 2011). Moreover, HIV-1 viral strains can be further divided into four groups: major (M), outlier (O), non-outlier and non-major (N), and P (pending the identification of further human cases) (Figure 2). These groups, likely emerged from three separate and independent transmission events. HIV-1 groups M and N are thought to have arisen from chimpanzees, with similar strains found in currently SIV infected chimps. Group O seems to be the true outlier, diverging from M and N, and only recently has thought to have stemmed from a progenitor in gorillas (Figure 2) (Sharp and Hahn, 2011). Interestingly, group P, having similar origins to Group O in gorillas, was

discovered in an HIV-1 infected Cameroonian woman in France, and despite extensive research in the area, only one other person (also from Cameroon) has been identified with the same virus (Sharp and Hahn, 2011).

The genetic diversity of HIV can be attributed to an inherent mechanism that the virus uses to produce rapid viral evolution. Most notably, reverse transcriptase, the enzyme required to generate DNA from a retroviral RNA genome, is highly error prone, with a mutation rate of approximately 3.4×10^{-5} mutations per base per replication cycle (Baltimore, 1970). With a genome of approximately 10^4 bases, and an estimated average of 1.03×10^{10} virions produced per day, this means that on average there is at least 1 mutation per genome per cycle, and millions of viral mutants produced daily within every infected individual (Perelson et al., 1996).

The predominant group of HIV-1 currently in circulation is aptly named Main or Group M. This group can be further sub-divided into subtypes or clades that can be linked to specific geographic areas (Figure 3) (UNAIDS and Sabin, 2015). The world-wide distribution of the ten clades, denoted A to K, is depicted in Figure 3. The distribution observed is likely due to a founder effect, which resulted in a local predominance of a certain transmitted subtype (Buonaguro et al., 2007). HIV-1 subtypes A, B, and C are the most prevalent globally, with subtype C accounting for approximately 50% of all HIV-1 infections. As depicted in Figure 3, subtype A viruses are widely spread through eastern and central Africa and eastern Europe. Subtype B, on the other hand, is predominant in western and central Europe, Australia, the western hemisphere, Northern Africa, and Southeast Asia. Unsurprisingly, subtype C viruses are predominant in Sub-Saharan Africa, India, and other high-risk populated countries

(Buonaguro et al., 2007). In addition to the 10 subtypes of Group M, in areas where multiple subtypes are found, there are "intersubtype" recombinant forms that are believed to be created from individuals infected with multiple viral strains. These "intersubtypes" are known as circulating recombinant forms or CRF. CRFs currently account for ~20% of infections and represent predominant forms of the virus found in Southeast Asia and Western Africa (Figure 3) (Buonaguro et al., 2007). Interaction between the virus and host may differ between viral subtypes and can potentially influence HIV transmission and progression to AIDS. Further understanding of the mechanism of HIV infection may shed light on the inherent differences seen between subtypes.

Currently, the earliest documented case of an individual infected with HIV-1 Group M was from a city in the Democratic Republic of Congo now known as Kinshasa, concerning a sailor who passed away from AIDS-like symptoms in 1959. Despite mainly being restricted to Western Africa, genetic material from a less common subtype, Group O, was first found in the early 1970's in the remains of a Norwegian family (Zhu et al., 1998).

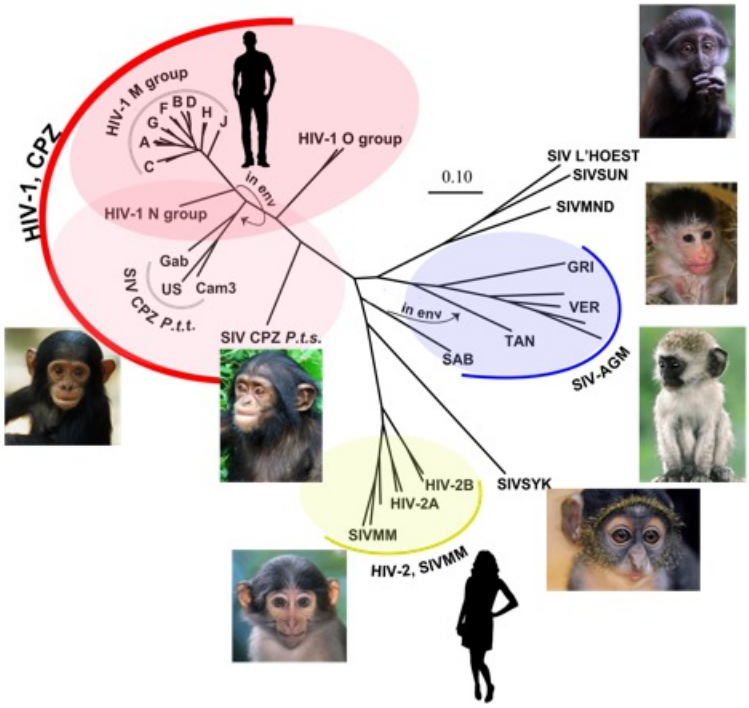

Figure 2. Phylogenetic Tree based on *pol* and *env* sequences. Most similarly related are grouped by color. Images depict main species infected. Tree adapted from Los Alamos HIV Phylogenetic Consortium.

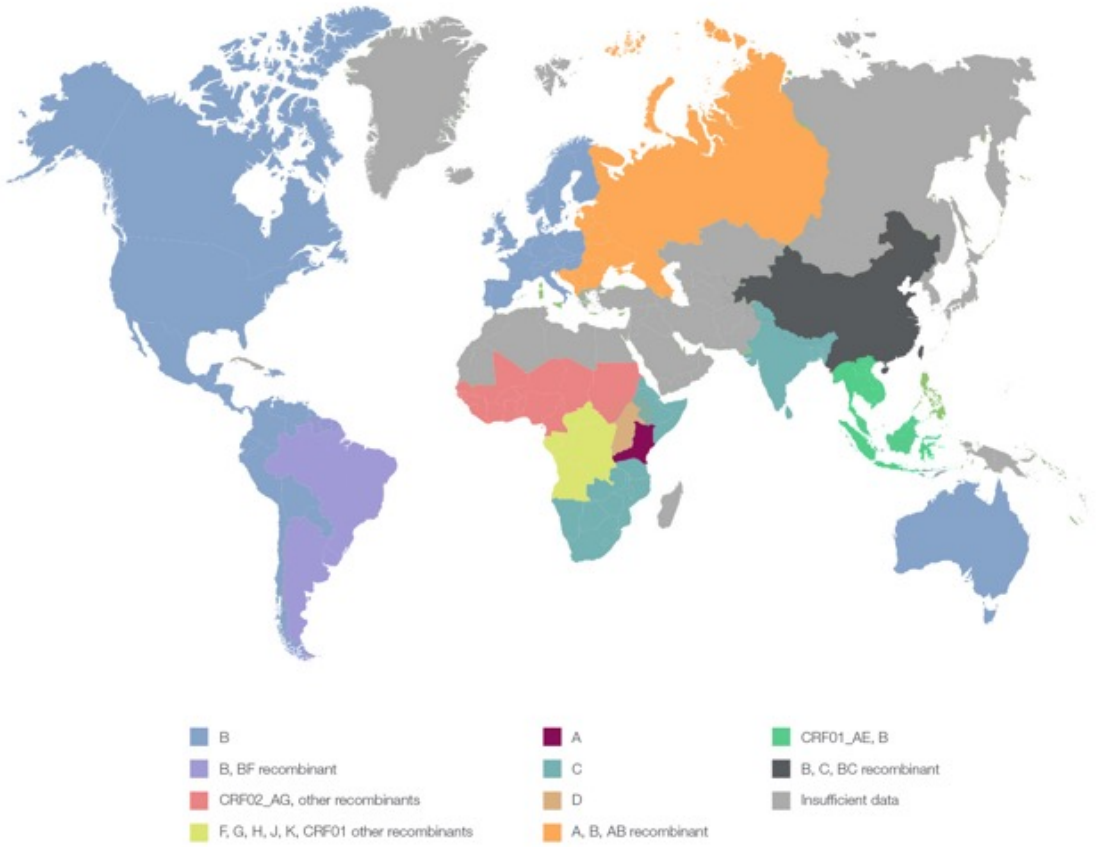

Figure 3. World-wide distribution and prevalence of HIV-1.

The distribution observed is likely due to a founder effect, which resulted in a local predominance of a certain transmitted subtype. HIV-1 subtypes A, B, and C are the most prevalent globally, with subtype C accounting for approximately 50% of all HIV-1 infections.

Epidemiology, Transmission and Pathogenesis of HIV

Today, the routes through which HIV infection has spread are most commonly through sexual transmission and through the sharing of needles (UNAIDS, 2015; UNAIDS and Sabin, 2015). Bodily fluids such as blood, semen, pre-seminal fluid, rectal and vaginal secretions, and breast milk can carry and transmit the virus if they come in contact with mucosal membranes, damaged tissues, or, in the case of intra-venous drug use or blood transfusions, if they are directly injected into the bloodstream (Pritchard et al., 2015b). The most common route of HIV transmission is through exposure of free virus or cell-associated virus present in mucosal surfaces or semen (Haase, 1999; Mehellou and De Clercq, 2010; Moir et al., 2011). While heterosexual intercourse is the most common globally, in first world countries such as the United States, the highest-risk population are those of the MSM (men who have sex with men) community, followed by heterosexual women (CDC, 2012).

While HIV transmission through intravenous drug use or blood transfusions seems clear, in order to establish and infection in either the female reproductive tract or through the rectal mucosa, HIV in semen must first cross the genital or rectal epithelium as well as bypass both innate and adaptive immune responses and then manage to establish an infection (Figure 4). Potential pathways for crossing the mucosal epithelium include mechanical mechanisms such as the virus traversing through micro-tears that can occur during sex due to friction. Lubricants and anti-microbial lotions can also increase HIV incidence rate by causing irritation to the epithelial layers. It is also hypothesized that the dendritic cells or Langerhans cells which can span the epithelial layers can potentially allow for HIV to cross the epithelium via mechanisms such as endocytosis,

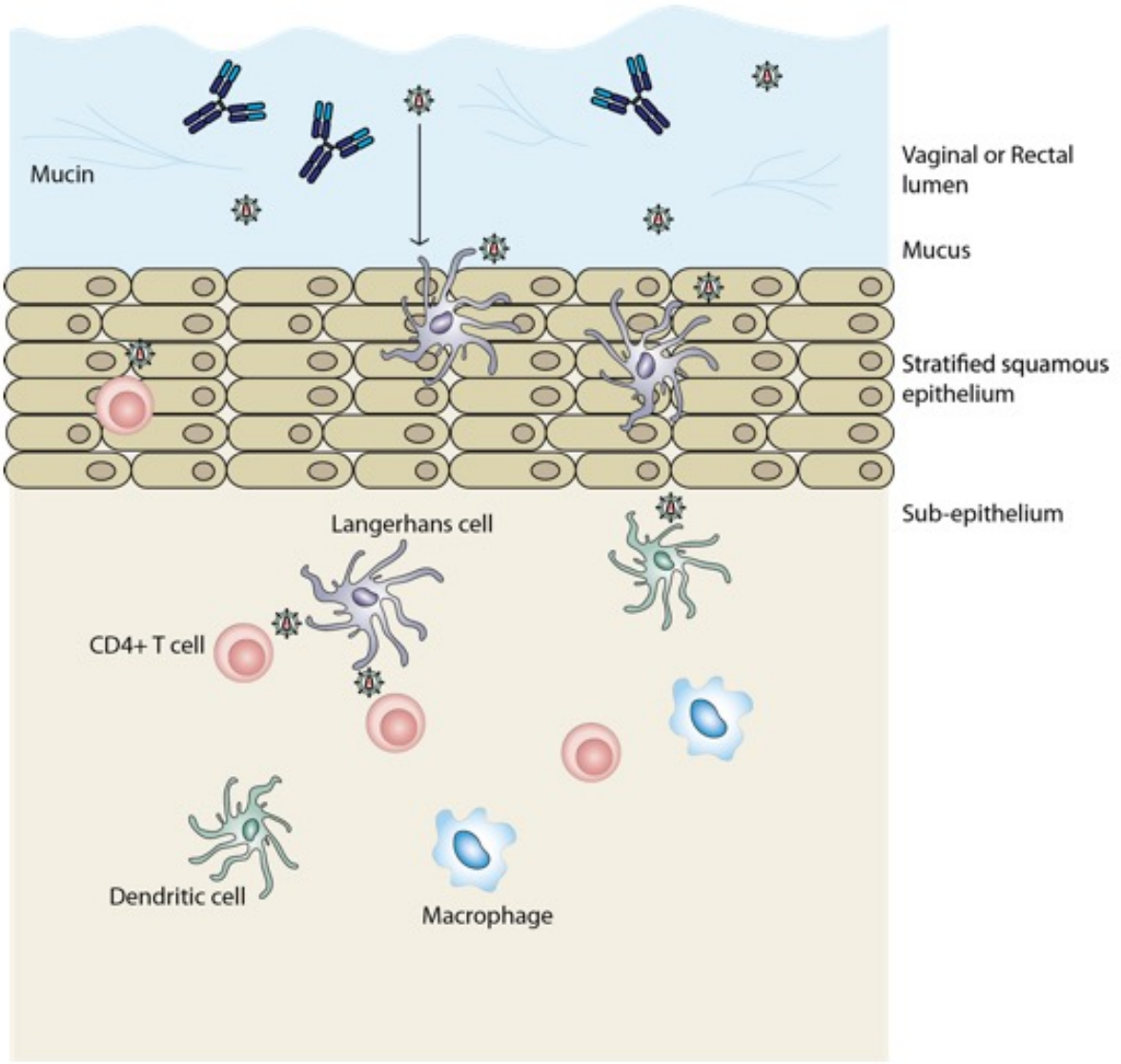

Figure 4. HIV transmission through the vaginal or rectal lumen.

transcytosis, or binding to cell receptors such as DC-SIGN on dendritic cells (Geijtenbeek et al., 2000).

Early on in the discovery of HIV, physicians noticed that the hallmark of HIV and AIDS progression was the depletion of CD4+ T-cells (also known has TH or Helper T-cells) in the patient. Once the CD4+ T-cell count fell below 200 per microliter of blood, an individual was classified as having AIDS and therefore susceptible to the AIDS-related opportunistic infections and cancers. It has been shown that other cells expressing CD4, such as macrophages and dendritic cells, are also capable of being infected, which may mediate HIV transmission, but to a lesser degree. This can be attributed to the need of the co-receptors either CCR5 or CXCR4 found on helper T-Cells in order for the virus to effectively fuse to the cell (Alkhatib, 2007). Following the initial infection, it has been shown through rhesus macaque models of the infection that the preliminary site of CD4 T-cell depletion is in the gut-associated lymphoid tissue (GALT); it is here that the virus first finds residence in the body, leading to rapid proliferation of the virus (Boggiano and Littman, 2007).

Within a few weeks post initial transmission, people infected with HIV typically suffer from flu-like symptoms, potentially due to the high viremia as well as proliferation and activation of cytotoxic T lymphocytes specific HIV flooding the immune system (Simon et al., 2006). Following the initial acute viremia, the immune system seems to be able to control the infection, leading to a precipitous drop in viral load and the recovery of CD4+ T-cells. This asymptomatic stage, common with many lentiviral infections, can last for years before the virus can rebound again leading to the fall of CD4+ T-cells

below 500 cells/microliter, which allows opportunistic infections to occur, resulting in the progression to AIDS and then ultimately to death (Coffin and Swanstrom, 2013).

The mechanism of HIV fusion is well established, with HIV's envelope proteins gp120 and gp41 facilitating the interaction. In order for infection to occur, it has been found that both CD4 and a G-protein-coupled receptor (GPCR) need be on the surface of the cell (Alkhatib, 2007). CCR5 and CXCR4 are the most commonly used GPCRs for HIV infection, with CCR5 being the principal co-receptor (Alkhatib, 2007). HIV isolates are commonly characterized by a preference for either CCR5 or CXCR4. Interestingly, it has been shown that CCR5-tropic viruses, also known as R5 isolates, are thought to be the first virus to infect cells during transmission by targeting macrophages and activated CD4+ memory T-cells (Freed and Mouland, 2006; Geijtenbeek et al., 2000). R5-tropic strains predominate the infection during early stages of HIV; however, as the virus mutates its preference for GPCRs changes as well, and the viral population selects for X4 isolates, preferentially binding to CXCR4 (Waters et al., 2008). As the tropism changes from R5 to X4, so does the cell preference, with CXCR4 on naïve CD4+T-Cells (Waters et al., 2008). This marketed switch from memory to naïve CD4+ T-cells is likely due to the T-cell population decreasing and the lack of available memory cells.

Mechanism of HIV Fusion and the structure of HIV's trimeric env spike

The HIV gp120 glycoprotein was first defined by as having two major features, the first being the gp120 core, and the variable regions. The gp120 core, composed of five constant regions, is responsible for the interactions that are necessary for the key binding events to occur for fusion. The second feature is the variable region defined as

the five variable loops, which have been shown to be mainly responsible for shielding and protecting the core from immune detection (Starcich et al., 1986). While this first designation of the regions remains largely correct, the V3 loop has been shown to mediate co-receptor binding (Tamamis and Floudas, 2014). In addition to the variable loops of the gp120, the presence of the glycan shield aids in the virus' ability to occlude key sites of its envelope in order to evade the immune system. First described as the 'silent face' of the gp120 protein, the glycans on the surface of the protein account for 50% of the total surface area (Wyatt et al., 1998). These glycans produced by the host during viral synthesis allow the virus to remain shielded from the potential immune response that host cells may deem it self (Wyatt et al., 1998). The variable regions and the glycan shield together with the virus' mutation rate and the ability to hide conserved regions such as the co-receptor binding site at interfaces produced by the oligomerization of the Env trimer, have been the prevailing ideas for how the virus can evade the humoral response (Kwong et al., 2002; Labrijn et al., 2003; Moore and Sodroski, 1996).

During HIV fusion, gp120 of the HIV trimer engages with the CD4 receptor, leading to a conformational change that reveals the co-receptor binding site. It is then that the virus can bind to the co-receptor (CCR5 or CXCR4) and form a very stable attachment to the CD4+T-cell. Post attachment, the gp41 induces an additional conformational change where the N-terminus forms as a fusion peptide (HR1) that is inserted into the host cell to form a pre-hairpin intermediate state (Harrison, 2015). During this process, the gp120 proteins shed from the envelope spike and the fusion continues, where the individual monomers of C-terminal heptad repeat region of gp41 (HR2) bind to the N-terminal HR1, forming a six helical bundle composed of both the

HR1 and HR2, bringing the host membrane within close proximity to the viral membrane and anchoring to form a stable pore where the virus' genomic and protein content can then be deposited (Chan et al., 1997; Chan and Kim, 1998).

There has been a great effort within the scientific community to understand the HIV envelope trimer in an attempt to understand how to develop an effective vaccine. To date, there has yet to be an effective vaccine developed despite clinical trials and massive efforts in design (Graham, 2002; McMichael, 2006; Picker et al., 2012; Watkins, 2008). Learning more about the structure and function of the envelope trimer has been an intensively studied area of HIV biology, as it is the primary focus for broadly neutralizing antibodies, an important arm of the humoral immune system (Mascola and Montefiori, 2010).

The first crystal structure of HIV envelope protein gp120 was solved in 1998 to 2.5 Å by Peter Kwong and Wayne Hendrickson at Columbia University (Kwong et al., 1998; Rizzuto et al., 1998). In order for gp120 to be crystallized, the N-and C-termini of gp120 and variable loops V1/V2 and V3 were truncated to produce a core version of gp120, and N-linked glycans were truncated using enzymatic deglycosylation (Kwong et al., 1998). This structure contained the core gp120 from HIV strain HxBc2, a soluble version of CD4 containing the first two domains, and the fragment antigen binding (Fab) portion of 17b, an antibody known to recognize the co-receptor binding site on gp120 (Kwong et al., 1998; Rizzuto et al., 1998). The gp120 structure consisted of an inner and outer domain connected by a bridging sheet. Residue Phe43 of CD4 was shown to reach into a recessed hydrophobic pocket on gp120, defining for the first time HIV Env evolved to interact with its host receptor.

The structure of the ectodomain of gp41, solved by two independent groups in 1997, revealed a six-helical bundle in which two helical regions from each subunit of the trimer, HR1 and HR2, both formed an anti-parallel alpha-helical coiled coil (Chan et al., 1997; Weissenhorn et al., 1997). The structure was interpreted as depicting the post-fusion state of the gp41 domain, in which fusion peptide that is N-terminal to HR1 is embedded in the host cell membrane while the C-terminal transmembrane domain is embedded in the viral membrane.

While the gp120 and gp41 structures facilitated understanding the HIV spike and the neutralizing antibodies that can bind them, determining the structure of the trimeric gp160 complex remained an important area of research in order to learn more about the trimer structures in context. In 2006, the first images of the SIV Env trimer were revealed by electron tomography of SIV virions by Zhu et al.: the trimer was described as consisting of a head (composed of the gp120 proteins) and gp41 forming a tripod-like structure holding up the gp120 trimer (Zhu et al., 2006). Aspects of the model were refuted in 2008 when a group at the NIH published new structures of the HIV envelope trimer (Liu et al., 2008). It was in this study that we first saw visual confirmation that the conformational changes induced by the binding of CD4, first hypothesized in 1991 (Sattentau and Moore, 1991), were valid. Interestingly, this study also found that CD4 binding site antibodies such as b12 can also induce conformational changes (Liu et al., 2008). Despite the low resolution of these structures (~20 Å), these early electron tomography efforts by Subramaniam were later validated by EM structures of a soluble, furin-cleaved form of a gp140 trimer comprising the gp160 ectodomain, which is produced by truncating gp160 prior to the predicted transmembrane domain of

gp41(Harris et al., 2011; Tran et al., 2012). Developed by the Moore lab at Cornell Weill (Sanders et al., 2002; Schulke et al., 2002), the SOSIP gp140 trimer is thought to be the most native-like soluble version of the trimer to date (Klasse et al., 2013; Schulke et al., 2002). SOSIP gp140 trimers are soluble, furin-cleaved trimers that are stabilized through engineering of an intermolecular disulfide bond between the gp41 and gp120 subunits (SOS), which prevents dissociation of gp120 monomers (Schulke et al., 2002), and the substitution of a single residue in the gp41 subunit (I559P; IP), which was found to increase the proportion of soluble trimers (Sanders et al., 2002).

While the early electron tomography efforts by Subramaniam were crucial to understanding the envelope trimer on HIV virions, due to the low resolution of the cryo-EM tomography/sub-tomogram averaging procedure required to produce the Env structures, the structures only depicted a rough outline of the shape of the trimer and gross conformational changes in the complex, and allowed modeling of the gp120 core region through docking of gp120 crystal structures into the EM maps. The gp41 subunit and the variable loops of gp120 in the context of the trimer remained largely a mystery until recent EM and crystal structures of SOSIP trimers were solved.

Within the past four years there has been technological advancements in the area of X-ray crystallography and molecular biology, which have allowed for the first high resolution structures of the HIV envelope trimer to be solved. The first structures involved a SOSIP trimer constructed form the clade-A HIV-1 isolate BG505, which naturally exhibited a more stable trimer that was efficiently cleaved into gp120 and gp41 subunits (Sanders et al., 2013). Between 2013 and today, a series of high resolution X-ray and EM structures BG505 SOSIP.664 env trimer have been solved (Do Kwon et al.,

2015; Julien et al., 2013b; Lyumkis et al., 2013; Pancera et al., 2014a; Scharf et al., 2015). The X-ray crystallographic and EM structures solved to a range of 3Å-6Å allowed for greater understanding of the role of gp41 in the context of the trimer prior to fusion and provided information concerning the various loops that had been truncated in gp120 structures (Julien et al., 2013b; Lyumkis et al., 2013; Pancera et al., 2014a; Scharf et al., 2015). With the variable loops now intact, these data suggest that the variable loops V1, V2, and V3 encompass the trimer apex, aiding in trimer stabilization via previously-undescribed inter-protomer contacts. In an attempt to mask the co-receptor binding site, V3 lies behind an N-linked glycan attached to gp120 position Asn197 of the adjacent protomer and beneath the V1-V2 loops (Julien et al., 2013b; Lyumkis et al., 2013). Through the most recent high-resolution structures, a more complete gp41 structure can be seen elucidating in further detail the interaction between gp41 and gp120 (Garces et al., 2015; Pancera et al., 2014a; Scharf et al., 2015). It is within these structures that we first see gp41 hydrophobic residues wrap around the N-termini of the gp120 proteins to obtain a similar topology as seen with other viral spike proteins found in Ebola and influenza viruses (Garces et al., 2015; Pancera et al., 2014a).

The structures of the Env trimer described above were crucial to the understanding of the work described in the following chapters.

The Anti-Viral Immune Response

In order to develop effective therapeutics against HIV, it is important to understand the natural immune response against viruses. This section is dedicated to discussing the role

of the immune system during an active infection, in an effort to understand current limitations and find strategies to work around it.

Innate Immune System

In order to protect an individual from an infection, the immune system must be able to perform the following four tasks: recognize the pathogen, respond to and clear the microorganism, self-regulate the response in order to keep homeostasis, allowing for minimal damage to the body, and finally, generation of an immunological memory so that when encountered by the pathogen again it can respond more effectively.

Leukocytes are the component of the blood responsible for both the innate and adaptive immune system. The innate cells are derived from a common myeloid progenitor in the bone marrow, and differentiate into dendritic cells, macrophages, granulocytes, and mast cells. Natural Killer cells (NK cells) are an innate immune cell derived from the common lymphoid progenitor; unlike other lymphocytes described later in the chapter, not antigen specific and have the ability to kill abnormal cells such as tumor cells and are thought to hold viral infections at bay until the adaptive immune system can respond. All of these cells get recruited to the location of the pathogen within the first few hours and days of the infection (Murphy et al., 2012).

The first method of defense to pathogens that the body employs is physical and chemical barriers at sites of transmission. The physical barriers include the skin, tight junctions between epithelial cells, cilia located in the nose, lung and gut "shield and sweep" the microbes away from vulnerable sites of infection, the production of mucus as a barrier, and peristalsis of the gut to name a few. If the organism has managed to escape the physical hurdles, it is then barred through a series of chemical barriers present in the

blood, extracellular fluid and epithelial secretion such as antimicrobial enzymes and peptides that are able to lyse bacterial cell membranes (Murphy et al., 2012). These antimicrobial peptides and enzymes are secreted by a group of epithelial cells known as paneth cells in the crypts of the small intestine, and by phagocytes such as macrophages and dendritic cells circulating in the blood and in infected tissues (Murphy et al., 2012).

Another innate response against pathogens is the complement system, consisting of a series of proteins in the plasma. The complement pathway can be activated directly by the pathogen, that leads to a cascade of events on the microbe's surface and leads to the degradation of the pathogen by phagocytes. If all the above fail to stop the entry of the pathogen, the immune system is poised and ready to defend (Murphy et al., 2012).

Phagocytosis and the ability to recognize the pathogen as foreign are two processes of the innate immune system that are particularly important in protecting the host from microbial pathogens. Phagocytosis performed by cells, including macrophages and dendritic cells, work in the removal of the pathogen in two ways: first by the degradation of the microbe and second by the presentation of pathogen-derived peptide antigen (Medzhitov, 2007; Medzhitov and Janeway, 2000). In the case of viruses, as well as bacterial infections, the viral genomic material and proteins are distinguished from self by a series of receptors known as pattern recognition receptors or PRRs. PRRs are expressed on innate immune cells and work by recognizing the pathogen-associated molecular patterns (PAMPs) that are present on the pathogen but not on self. Depending on what it detects, the PRRs are present on either the on the cell membrane surface or within the cytoplasm, where they can detect various viral components (Murphy et al., 2012). It is the detection of these PAMPs through the PRRs that activates the innate

immune cells as well as catalyzes the adaptive immune system through the gene expression of inflammatory cytokines and co-stimulatory molecules (Murphy et al., 2012). PRRs including toll-like receptors (TLRs) and Rig-I-like helicases (RLHs) are known to be especially important in sensing viral infections. In the case of HIV, TLR7/8 and 9 sensing single stranded RNA and CpG methylated DNA has been implicated in aiding the humoral immune response against the HIV-1 spike (Moody et al., 2014). RIG-I, a RNA helicase like domain widely expressed across various tissues and cell types has also been implicated in innate sensing of HIV by the detection of viral RNA in the cytoplasm of infected cells (Solis et al., 2011).

In addition to engulfment of the pathogen via phagocytosis, macrophages and dendritic cells secrete cytokines such as IL-8 and IL-12 to recruit and activate cells to the site of the infection, as well as the secretion of TNF-α, which leads to the increase in vascular permeability to allow for entry of immune cells, complement, and antibodies to the damaged tissue (Murphy et al., 2012). In the case of HIV infection, immune cells, including macrophages, neutrophils and monocytes, secrete chemokines CCL3 and CCL4, which are known to compete with HIV-1 binding to the co-receptor site CCR5, as described in this chapter (Altfeld and Gale, 2015).

Adaptive Immune Response

Leukocytes responsible for the adaptive immune response are known as lymphocytes and are derived from the common lymphocyte progenitor (Murphy et al., 2012). Unlike the common-myeloid progenitor cells, lymphocytes are mainly antigen specific and aid in both the clearance of a pathogen, as well as immunological memory of

the pathogen. Lymphocytes can be differentiated into two major groups: B- and T-lymphocytes. B- and T- lymphocytes have complementary but different roles in the adaptive immune system. Moreover, they aid in separating the adaptive immune response into two branches: cell mediated immunity where the protective function is associated with cells utilizing mainly Cytotoxic T-lymphocytes (CTLs or CD8+ T-cells), and the humoral immune response, which utilizes antibodies produced by B lymphocytes (B-Cells) as the primary mode of protection (Murphy et al., 2012).

The dendritic cell acts as a bridge between the innate and adaptive immune system by presenting antigenic peptides produced from phagocytosis of a pathogen to T-cells. These antigenic peptide fragments are presented by proteins known as MHC molecules, which are on the surface of antigen-presenting cells, in the case of class II MHC molecules, or all nucleated cells, in the case of class I MHC molecules. The MHC, or major histocompatibility complex, is a large cluster of genes that encodes proteins involved in antigen presentation to T-cells. The MHC is highly polymorphic, such that class I and class II MHC molecules exist in many allelic forms within a population, and the receptor on T-cells (TCR; T-cell Receptor) can only recognize an antigenic peptide in the context of a particular MHC allele; i.e., T-cell recognition of antigen is "MHC-restricted" (Neefjes et al., 2011).

In cell mediated immunity, naïve T-cells are activated by an antigen presenting cell (most commonly dendritic cells) expressing MHC molecules and co-stimulatory molecules B7.1 and B7.2. Upon activation, the T-cells produce IL-2, leading to proliferation and differentiation of antigen-specific T-cells. Class I MHC molecules present peptides derived from proteins synthesized within the cell to CD8+ T-

lymphocytes, which are then activated to kill the cells displaying aforementioned peptide-MHC complexes. Class II MHC proteins present peptides derived from proteins degraded in endocytic vesicles to CD4+T-lymphocytes (T-helper cells); these cells then differentiate to become specialized effector cells, T_H1, T_H2, T_H17 or T_{FH} (Murphy et al., 2012; Neefjes et al., 2011). While the main function of CD8+ T-cells is to kill virally-infected cells, the CD4+ T-cell subtypes are responsible for regulating many functions. CD4 T_H1 cells aid in activating infected macrophages and provide T-cell help to B-cells for antibody production. CD4 T_H2 cells aid B-cells in allergy and parasitic infections; T_{FH} cells, found primarily in the lymph nodes and the tonsils, aid in B-cell isotype switching and antibody production; lastly CD4 T_H17 and CD4 regulatory T-cells act in juxtaposition to one another, with T_H17 cells promoting the neutrophil response thus increasing inflammatory signaling, versus suppression of T-cell responses by CD4 Treg cells (Crotty, 2011).

Unlike T-cell mediated immunity, where cytotoxic lymphocytes can only eliminate infected cells, the humoral immune system has the potential to both eliminate infected cells and prevent infection by neutralizing the free pathogen. After an antigen binds to the B-Cell Receptor of a naïve B-cell and is stimulated by a CD4 T-helper cell, the B-cell will proliferate and can differentiate into plasma cells. Plasma cells are the cell line of defense for the humoral immune system, producing a soluble form of the B-cell receptor known as an antibody.

Antibodies

Antibodies can be found in nearly all body fluids, or humours, including milk, tears, bile, and saliva; however, they are most prevalent in blood serum (Murphy et al., 2012). Direct evidence of antibodies in serum first were reported by Kabat and Tiselus in 1939, in electrophoresis experiments of serum from immunized rabbits. In the experiment, rabbits were immunized with ovalbumin (OVA) and later blood was drawn and serum prepared. The serum was then aliquoted into two fractions; one sample was left untreated, while the other was incubated with OVA and then centrifuged to remove any aggregated immune complexes. Electrophoresis of the serum confirmed that it can be separated into four distinguishable serum fractions corresponding to serum albumin, and three unknown fractions of α, β, γ globulins. When the electrophoresis profiles of the treated and untreated serum were compared, Kabat and Tiselus noticed a significant decrease in the γ-globulin peak in the treated serum sample (Tiselius and Kabat, 1939). Therefore, they deduced that the γ-globulin fraction must be the one containing the serum antibodies, which was then coined immuno-globulin to differentiate this fraction of proteins from any other protein in the serum (Tiselius and Kabat, 1938; Tiselius and Kabat, 1939). Later, immunoglobulins were further classified into five major classes: IgA, IgD, IgE, IgG and IgM, with IgG being most abundant in the body (Murphy et al., 2012).

The basic organization of an antibody is a Y-shaped structure consisting of four peptide chains, two light chains (kappa or lambda), and two heavy chains with each chain approximately 25 kilodaltons (kDa) and between 50 -70kDa in molecular weight respectively (Figure 5). Each light chain is linked to a heavy chain by a disulfide bond at

the c-terminus of the light chain, and by non-covalent interaction to form a heterodimer. Within every antibody two identical heavy-light chain heterodimers form a “dimer of heterodimers” linked by a series of disulfide bonds between the two heavy chains (Murphy et al., 2012; Pieper et al., 2013).

All immunoglobulin subtypes share a common structure, and can be distinguished from one another through the constant domains of their heavy chains. IgG, the most abundant antibody in the body also has the most basic structure. The structures of both the heavy and light chains reveal a series of domains known for a signature immunoglobulin fold consisting of two β-sheets connected via hydrophobic bonds and a inter-disulfide bond. Each light chain has two immunoglobulin domains, and the heavy chain of IgGs contains five (Edelman, 1973; Marx, 1975).

The first Ig-domain on both heavy and light chain arm is a highly variable region conferring the antigen specificity of the antibody known as the VH or VL, respectively. It is in these variable regions that all differences found in specificity of the antibody can be traced to variations in the amino acid sequences within the specific regions of variable domains known as the complementarity-determining regions (CDRs). The CDRs of both the heavy and light chains form a surface at the tip of the antibody that is complementary to the antigen it is specific for. There are three CDR regions in each heavy and light variable domain (CDR1, CDR2, CDR3). The remaining regions of the variable domains are less variable and lie between the CDRs, and are known as the framework regions (FR1-4). Named for their utility, structurally, these regions form the framework of the variable domains while the CDRs form three loops joining the beta strands (Chang et al., 1985; Colman et al., 1974).

The remaining three domains of the IgG heavy chain and one domain of the light chain are relatively invariable in amino acid sequence and are known as constant regions C_H1-3 and C_L, respectively. After the digestion of an IgG with papain, a proteolytic enzyme, the product is three fragments: two identical "arms" containing the antigen binding sites, termed the Fraction antigen binding fragments or Fab Fragments (V_H-C_H1/V_LC_L), and a third fragment of similar molecular weight to the Fab fragments (50 kDa) that lacked antigen binding capabilities but crystallized readily during storage of the proteins, dubbed the Fc fragment, which was later found to be a dimer of C_H2-C_H3 domains of the heavy chains (Marx, 1975) (Figure 5). The Fc fragment joins the two Fab arms through a short flexible linker known as the hinge region. This overall Y-shaped dimeric antibody structure leads to two identical antigen binding sites on each immunoglobulin monomer, both with the ability to bind to two of the same antigen on a given surface resulting in an increase in apparent affinity of the antibody to the antigen known as avidity. The concept of avidity, important to antibody function (Murphy et al., 2012), will be discussed later in this chapter.

The generation of antibody diversity is primarily though VDJ recombination. During VDJ recombination, the variable region of the heavy chain is encoded by three separate gene segments: V(variable), D (diversity), and J (joining), with the V_H gene segment encoding amino acids 1-94 and the J_H segment encoding for amino acids 98-113 while the D_H gene segment joins the two larger segments encoding for amino acids 95-97 (Tonegawa, 1983). These gene segments are located on chromosome 14 and are referred to as the heavy chain multigene family, which has been found to have 39 V_H segments followed by the D locus containing 23 functional D_H segments and 6 J_H segments.

Downstream to VDJ fragments are a series of genes that encode the different constant regions of the immunoglobulin classes.

A similar process occurs for the light chains of antibodies, with the kappa and lambda light chain loci found on chromosome 2 and 22, respectively. Unlike the heavy chain, the variable domain of the light chain is encoded by two gene segments (V and J). In the kappa chain family there are 85 V_κ segments upstream to four functional J_κ fragments and 1 Constant C_κ gene fragment. The lambda gene locus is slightly different as there are 30 V_λ segments upstream to four functional J_λ fragments and four Constant C_λ gene fragments. While the limited variable fragments in the lambda compared to the kappa may lead to reduced diversity of the lambda V_L domains, it makes up for it with the four function C_λ gene segments, allowing for four different λ-chain subtypes to be produced (Murphy et al., 2012).

During B-cell maturation in the bone marrow, the heavy chain gene rearrangements occur first, followed by light chain gene rearrangement, and the result of both leads to each B-cell containing two genes encoding for both a fully functional heavy and light variable region. At this point, the B cell is now mature and committed to produce the specific antibody composed of a heavy and light chain variable domains assembled through gene rearrangements.

The diversity of the antibody is derived from a number of factors in the bone marrow including through the combinatorial pairing of various germ-line gene segments, heavy and light chain pairings, and nucleotide additions. Once the B-cell leaves the bone marrow, a process known as affinity maturation can occur to add even greater diversity to the antibody repertoire. After the naïve mature B cell encounters an antigen, the T-cell-

dependent B cell response is initiated. The B cell travels to sites known as the germinal centers in secondary lymphoid organs such as the lymph nodes and the spleen. It is here that affinity maturation can occur through two different but related processes: somatic hypermutation and clonal selection.

During somatic hypermutation (SHM), the B cell already primed by the antigen is stimulated to proliferate and during this process the BCR locus undergoes somatic mutation at a rate approximately 10^5 greater than normal mutation rate (Maul and Gearhart, 2010). This process of SHM is catalyzed by an enzyme, activation induced deaminase (AID), which converts cytosine to uracil. Each mutation is typically a single nucleotide substitution, and usually occurs within mutation "hotspots," characteristically in the CDR regions of the variable domains and less often within the framework regions (Peled et al., 2008; Victora and Mesin, 2014; Victora and Nussenzweig, 2012). In addition to SHM, clonal selection occurs in the germinal center with the help of T_{FH} cells and follicular dendritic cells that reside there. It is here that follicular dendritic cells present the antigen to the germinal B cells and stimulation through cross-talk of T_{FH} cells, and allow for rounds of positive selection of B cells with high affinity to the antigen (Victora and Mesin, 2014; Victora and Nussenzweig, 2012). At the end of this entire process, the B cell can now become either a memory B cell, or a plasma cell expressing fully matured antibodies with higher affinities to the antigen and a longer life span than the plasma cells at the start of the infection (Dörner and Radbruch, 2007; Kurosaki et al., 2015).

Antibody Mediated Effector Functions

Once mature, antibodies are effective in sequestering the pathogen via three distinct pathways, activation of complement, opsonization, and neutralization. In the classical complement pathway, antibodies, typically IgM or IgG, play a key role in catalyzing the complement pathway by forming antigen-antibody complexes, leading to a conformational change in the antibody and exposing a receptor for the first complement protein to bind. This binding event then leads to the standard cascade of events in the complement system leading to the formation of a pore in the microbe, resulting in lysis and engulfment of the pathogen. Neither truly part of the innate or adaptive system, complement straddles the line between each and plays an important role in the elimination of a pathogen (Murphy et al., 2012; Pieper et al., 2013).

Opsonization occurs when antibodies target a pathogen that can replicate outside of the host cell and coat the surface of the microbe. The aggregation of the antibodies on the surface then trigger phagocytosis from macrophages and neutrophils. Similarly, when antibodies are bound to a pathogen it can initiate effector functions through Fc-mediated recruitment of NK and CD8+ T- Cells resulting of direct killing of the antigen, this process is known as Antibody mediated cellular-cytotoxicity (ADCC) (Murphy et al., 2012; Pieper et al., 2013).

Lastly, and possibly the most efficient way that antibodies can eradicate an infection is through neutralization of the pathogen. This is particularly useful for viruses attempting to gain entry to a cell for replication. Antibodies can effectively neutralize viruses by either blocking the cellular receptors needed for the virus to bind to the cell, or through disruption of the fusion mechanism on the virus (Corti and Lanzavecchia, 2013;

Dörner and Radbruch, 2007). There are two different models to address how neutralization of viruses may occur. The first, known as the occupancy model, assumes that the antibodies, similarly to their role in opsonization, merely occupy and coat the viral surface of the antibody, making it difficult for the virus to approach the cell (Burton et al., 2000; Klasse and Sattentau, 2002; Parren et al., 2000), In the alternative model, known as the critical binding site model, antibodies hinder fusion by binding to the necessary sites for binding to the host (Parren et al., 2000).

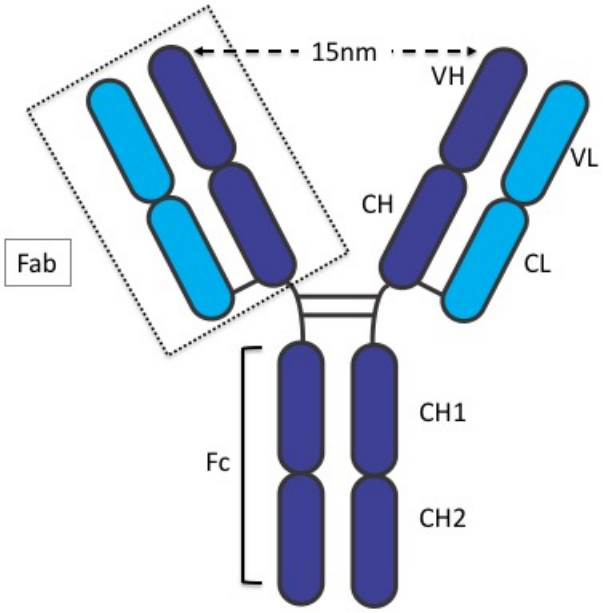

Figure 5. The IgG Structure.

The antibody is composed of two Fab regions consisting of the entire light chain (VLCL) and the VHCH1 domains of the heavy chain, a region known as an Fc, which is a dimer of heavy chain domains CH2-CH3. The antigen binding sites are located at the tip of the Fab regions at the interface between VH and VL. The maximum distance between these two antigen binding sites is approximately 15nm.

Broadly Neutralizing Antibodies against HIV

The HIV Envelope spike contains the only sites on the HIV virion that can be targeted by neutralizing antibodies. The virus employs various well-characterized mechanisms in order to evade the immune response against the trimer spike, such as rapid mutation and glycan shielding that make it difficult to boost an effective antibody response. In fact, only 15% of HIV-infected individuals develop neutralizing antibodies against heterologous HIV-1 strains, leaving the majority of the HIV-infected population with a handicapped immune response. Looking at the numbers closer, the situation appears even more bleak, with only 1% of HIV-positive individuals capable of developing broad and potent neutralizing antibody responses (Sather et al., 2012). Moreover, despite being able to produce these broad and potent neutralizing antibodies, these antibodies are no longer effective against the viral strains circulating in the patients' body (Doria-Rose et al., 2009; Euler et al., 2010; van Gils et al., 2009; van Gils and Sanders, 2013).

The first anti-HIV broadly neutralizing antibody was isolated from a phage display library derived from the bone marrow of an asymptomatic HIV+ patient in 1994 (Burton et al., 1994). The antibody, b12, was found to bind the CD4 binding site of gp120 and was broadly neutralizing against a panel of HIV-1 isolates (Burton et al., 1994). The isolation of b12 gave hope to the HIV field that other broadly neutralizing antibodies could be found, and soon after, a handful of more broadly neutralizing antibodies were isolated. Among these were 2F5 and 4E10, both broadly neutralizing antibodies specific for the MPER region of gp41, and 2G12, a carbohydrate-binding antibody, specific to the high mannose patch of glycans on gp120 (Buchacher et al.,

1994; Purtscher et al., 1994; Stiegler et al., 2001; Trkola et al., 1996). Despite being described as broadly neutralizing antibodies, these early antibodies had limited potency and breadth but were found to protect against SIV in non-human primate models and found to delay viral rebound after anti-retroviral cessation in patients (Ferrantelli et al., 2004; Hessell, 2007; Hessell et al., 2009; Hofmann-Lehmann et al., 2001; Mascola, 1997, 1999, 2000; Trkola et al., 2005)

Technological advancements in single B cell cloning methods (Scheid et al., 2009a)led to the discovery of dozens of new broadly neutralizing antibodies (McCoy et al., 2012; Pejchal et al., 2011; Scheid et al., 2009b; Scheid et al., 2011a; Sok et al., 2014; Walker et al., 2011; Wu et al., 2010a). Discovery of this new generation of broadly neutralizing antibodies was only made possible through development of a new single B cell cloning technique that allowed for identification and enrichment of memory B cells from HIV-infected patients (Scheid et al., 2009a). In addition to expanding the library of broadly neutralizing antibodies, it was also found that this generation of broadly neutralizing antibodies also aided in defining and identifying new and different sites of vulnerability on the HIV envelope spike. The major epitopes of these new broadly neutralizing antibodies include previously described epitopes (Figure 6) such as the CD4 binding site (CD4bs) (Diskin et al., 2011b; Scheid et al., 2011a; Wu et al., 2010a); the MPER region of gp41 (Huang et al., 2012b); as well as new epitopes such as the quaternary epitope at the apex of the trimer defined by a glycan at Asn160 of gp120 (Julien et al., 2013a; McLellan et al., 2011; Walker et al., 2011; Walker et al., 2009a) the V3 loop including Asn332 and other glycans on the gp120 outer domain (Garces et al., 2014; Julien et al., 2013a; Kong et al., 2013; Mouquet et al., 2012b; Walker et al., 2011),

and epitopes spanning interface of gp41 and gp120 (Blattner et al., 2014; Huang et al., 2014; Scharf et al., 2014; Scharf et al., 2015). Other epitopes on the env trimer that induce neutralizing antibodies include the CD4-induced (CD4i) site, whose footprint is the partial co-receptor binding site (Diskin et al., 2010; Kwong et al., 1998).

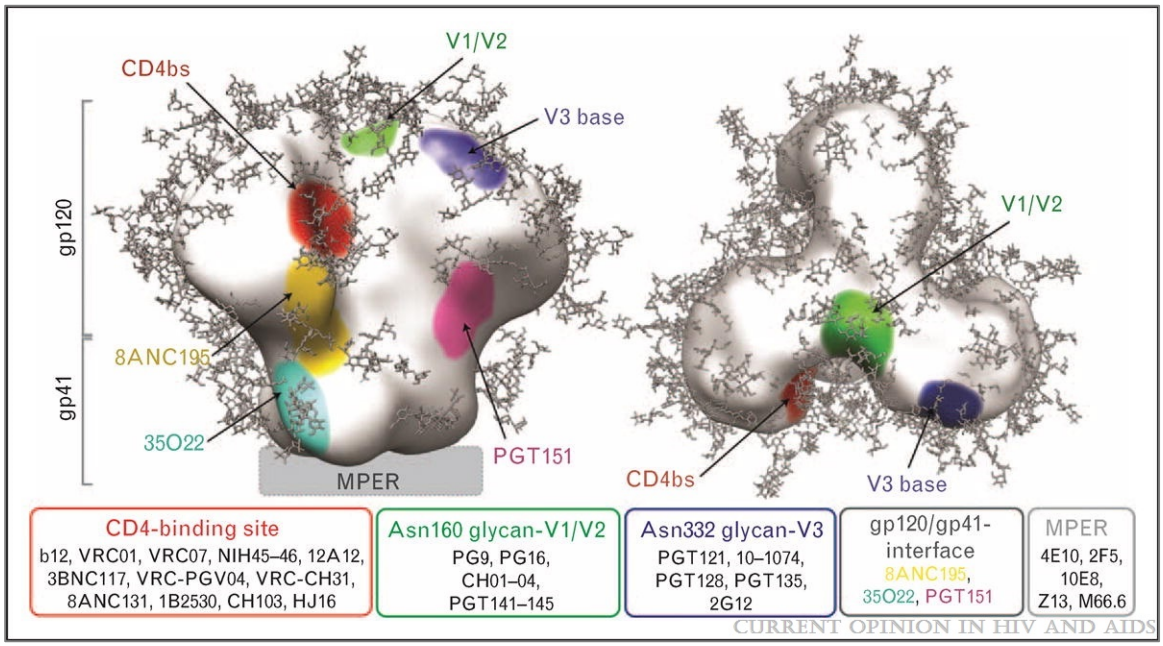

Figure 6. Location of bNAb epitopes on HIV-1 Env trimer. The approximate location of epitopes (shown only once per trimer) are highlighted on a surface representation of Env derived from electron microscopy, structure EMD-5782 [1▪]: CD4-binding site Ab epitope (red), V1/V2 loop/Asn160 Ab epitope (green), V3 loop/Asn332 Ab epitope (blue), 8ANC195 epitope (yellow), 35O22 epitope (cyan), PGT151 epitope (pink), MPER epitope (gray). N-linked glycans shown as grey sticks were added to all potential N-linked glycosylation sites present in the coordinates for BG505 SOSIP Env (PDB 4NCO) [2▪] using Glyprot [3]. Representative bNAbs targeting each epitope are listed (Sievers et al., 2015).

Figure borrowed from: Sievers, Stuart A.; Scharf, Louise; West, Anthony P. Jr; Bjorkman, Pamela J. Current Opinion in HIV and AIDS. 10(3):151-159, May 2015.

Limitations of Broadly Neutralizing Antibodies against HIV

Despite the discovery of these extremely broad and potent neutralizing antibodies, clinical trials and animal studies have shown that the use of a single broadly neutralizing antibody as a treatment to HIV+ individuals is not enough for sterilizing protection from the virus (Caskey et al., 2015; Diskin et al., 2013a; Diskin et al., 2013b; Horwitz et al., 2013; Klein et al., 2012a; Klein et al., 2012b; Klein et al., 2014a).

Combination therapy using a minimum of three antibodies was found to be required to suppress viremia in a humanized mouse model (Klein et al., 2012b). One reason for this may be elucidated by delving deeper into the natural envelope landscape of the HIV virion. The first images of intact HIV virion by electron tomography revealed a small number of Env trimers on the surface of the HIV virions (Zhu et al., 2003; Zhu et al., 2006), consistent with earlier biochemical studies of purified HIV (Chertova et al., 2002b). The cryoEM images demonstrated relatively few spikes on the virion surface, with an average of 14±7 on any given virion (Zhu et al., 2003; Zhu et al., 2006). Nearest neighbor analysis of the HIV envelope spikes on intact HIV virions revealed that the separation between most spikes on HIV virions exceeds the 15nm separation between the two antigen-combining sites of a typical antibody (Figure 7) (Zhu et al., 2006).

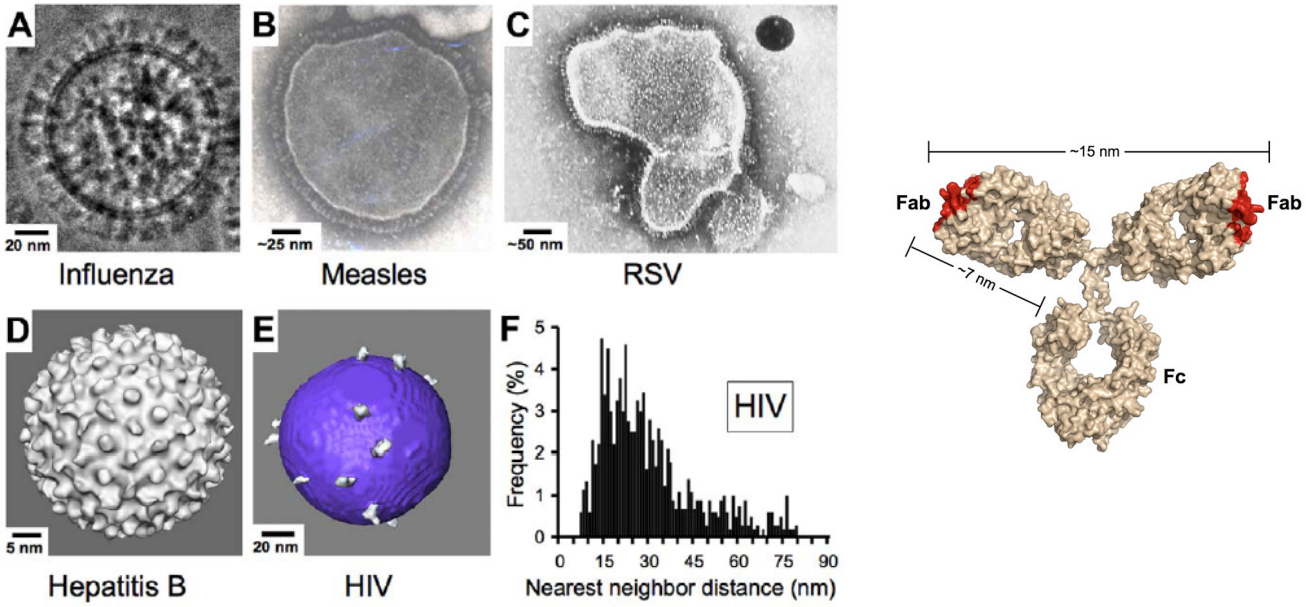

Figure 7. Comparison of enveloped virus and contributions of spike density to nearest neighbor distances for HIV.

A. Influenza type A virus
B. Measles virus
C. Respiratory Syncytial virus
D. Hepatitis B virus
E. HIV-1 virus
F. Distribution of nearest neighbor distances between HIV spikes derived from 40 HIV virions imaged through cryo-ET. Average number of spikes on surface ~14.
G. IgG Antibody. The maximum distance between the two antigen binding sites is roughly 15nm.

Figure adapted from Klein, J. S. and P. J. Bjorkman (2010). "Few and far between: how HIV may be evading antibody avidity." PLoS Pathog **6**(5): e1000908.

In a novel hypothesis first described in the Bjorkman lab in 2010 by Joshua Klein, the ability for HIV to escape from and poor efficacy of broadly neutralizing antibodies to treat infection was hypothesized to be due to the sparse landscape of env trimers on the surface of HIV virions (Klein and Bjorkman, 2010). Klein and Bjorkman postulated that large inter-spike distances creates a barrier for an antibody to bind bivalently to virions by crosslinking between adjacent spikes (Klein and Bjorkman, 2010). By contrast, for viruses in which we are able to mount an effective humoral response, such as hepatitis B, measles, and influenza, viral spikes cover the surface the of the virion, lending to numerous epitopes for an antibody to bind bivalently (Figure 7). It was therefore suggested that most anti-HIV antibodies bind monovalently to HIV virions; i.e., using only one Fab arm (Klein and Bjorkman, 2010), which would not allow anti-HIV antibodies to take advantage of avidity effects to overcome the reduced binding affinity that would result from mutations in HIV Env.

Antibody Affinity vs. Avidity

Antibody affinity can be described as the binding strength between a monovalent antigen and the antigen-binding site of one Fab arm (Eisen and Siskind, 1964; Pauling et al., 1944). The affinity of an antibody-antigen interaction can be described as the equilibrium constant $K_D = k_d / k_a = [Ab][Ag]/[Ab:Ag]$, where [Ab], [Ag] and [Ab:Ag] are the concentrations of the antibody, antigen, and the complex, respectively, and k_a and k_d are the association and disassociation rate constants (Mattes, 2004). A high affinity can typically be described as having a fast association rate with a slow dissociation rate. However, as stated, this definition only describes a monovalent interaction with one Fab

arm and a single antigen. In the case of an IgG in which there are two available antigen binding sites, binding to an antigens tethered to a surface such as a viral membrane, the functional affinity changes due to the ability of an antibody to bind bivalently. The change in functional, or apparent affinity, is known as avidity. Once the first Fab is able to bind to the antigen on the surface, the second Fab binding will likely occur if there are many epitopes on the surface that are within reach for the antibody to bind (Karush, 1976). Thus the ability to bind bivalently is dependent on geometric factors such as spaces of the tethered antigen, in this case, the viral spikes.

Therefore, in the case of neutralizing antibodies against HIV, even when the affinity of an individual Fab is high, because of the low density of spikes on the viral surface, its apparent affinity, or avidity, will be much lower than if the spikes were available at high density on the surface. Another means by which IgG antibodies could bind HIV virions with avidity would be through bivalent binding achieved by simultaneous binding of both Fabs to the adjacent epitopes within the same Env trimer. However, the distribution of antibody epitopes on the HIV Env trimer, combined with the architecture of IgG antibodies, suggests that most or all anti-HIV antibodies cannot use both Fabs to bind a single Env trimer (Klein and Bjorkman, 2010). The inability to bind with avidity leaves anti-HIV antibodies vulnerable to substitutions in HIV Env that are produced as a result of the high mutation rate of HIV reverse transcriptase; i.e., anti-HIV antibodies cannot generally use avidity effects to overcome the reduced binding affinities resulting from Env mutation (Klein and Bjorkman, 2010).

The work described in the subsequent chapters attempts to overcome HIV's evasion strategy of low spike density through the design of novel antibody architectures.

Chapter 2 will describe early attempts to design a bivalent reagent of HIV, making only modest improvements to the original antibody against HIV, but later repurposed as a potent reagent against SIV. Chapter 3 will describe a novel strategy using double-stranded DNA as a molecular ruler to measure distances between epitopes on a single envelope spike to produce antibody reagents capable of bivalent binding via intra-spike crosslinking. Chapter 4 will discuss new protein linkers that can be utilized to substitute for the DNA linkers in promising candidates found in Chapter 3. Chapter 5 will delve deeper into preliminary research converter the optimal bivalent reagent to an all protein-based therapeutic. Additionally, I will discuss some early work in investigating how cancer therapeutics can teach us how to make better HIV immunotherapies in Chapter 6.

References

Alkhatib, G. B., Edward A. . (2007). HIV coreceptors: from discovery and designation to new paradigms and promise. *European Journal of Medicine, 12*(9), 375-384.

Altfeld, M., & Gale, M., Jr. (2015). Innate immunity against HIV-1 infection. *Nat Immunol, 16*(6), 554-562. doi:10.1038/ni.3157

Baltimore, D. (1970). RNA-dependent DNA polymerase in virions of RNA tumour viruses. *Nature, 226*(5252), 1209-1211.

Blattner, C., Lee, J. H., Sliepen, K., Derking, R., Falkowska, E., de la Pena, A. T., . . . Ward, A. B. (2014). Structural delineation of a quaternary, cleavage-dependent epitope at the gp41-gp120 interface on intact HIV-1 Env trimers. *Immunity, 40*(5), 669-680. doi:10.1016/j.immuni.2014.04.008

Boffey, P. M. (1986, January 14, 1986). AIDS IN THE FUTURE: EXPERTS SAY DEATHS WILL CLIMB SHARPLY. *The New York Times*.

Boggiano, C., & Littman, D. R. (2007). HIV's vagina travelogue. *Immunity, 26*(2), 145-147. doi:10.1016/j.immuni.2007.02.001

Briggs, J. A., & Krausslich, H. G. (2011). The molecular architecture of HIV. *J Mol Biol, 410*(4), 491-500. doi:10.1016/j.jmb.2011.04.021

Buchacher, A., Predl, R., Strutzenberger, K., Steinfellner, W., Trkola, A., Purtscher, M., . . . et al. (1994). Generation of human monoclonal antibodies against HIV-1 proteins; electrofusion and Epstein-Barr virus transformation for peripheral blood lymphocyte immortalization. *AIDS Res Hum Retroviruses, 10*(4), 359-369.

Buonaguro, L., Tornesello, M. L., & Buonaguro, F. M. (2007). Human immunodeficiency virus type 1 subtype distribution in the worldwide epidemic: pathogenetic and therapeutic implications. *J Virol, 81*(19), 10209-10219. doi:10.1128/JVI.00872-07

Burton, D. R., Pyati, J., Koduri, R., Sharp, S. J., Thornton, G. B., Paul, W. H. I. P., . . . Barbas, C. F. (1994). Efficient Neutralization of Primary Isolates of HIV-1 by a Recombinant Human Monoclonal Antibody. *Science, 266*(5187), 1024-1027.

Burton, D. R., Williamson, R. A., & Parren, P. W. (2000). Antibody and virus: binding and neutralization. *Virology, 270*(1), 1-3. doi:10.1006/viro.2000.0239

Capon, D. J., & Ward, R. H. R. (1991). The CD4-gpl20 Interaction and Aids Pathogenesis. *Annual Review of Immunology, 9*(1), 649-678. doi:10.1146/annurev.iy.09.040191.003245

Caskey, M., Klein, F., Lorenzi, J. C. C., Seaman, M. S., West Jr, A. P., Buckley, N., . . . Nussenzweig, M. C. (2015). Viraemia suppressed in HIV-1-infected humans by broadly neutralizing antibody 3BNC117. *Nature, 522*(7557), 487-491. doi:10.1038/nature14411

CDC, C. f. D. C. a. P. (2012). *Estimated HIV incidence among adults and adolescents in the United States, 2007-2010.* . Retrieved from Atlanta, GA:

Chan, D. C., Fass, D., Berger, J. M., & Kim, P. S. (1997). Core structure of gp41 from the HIV envelope glycoprotein. *Cell, 89*(2), 263-273.

Chan, D. C., & Kim, P. S. (1998). HIV entry and its inhibition. *Cell, 93*(5), 681-684.

Chang, C. H., Short, M. T., Westholm, F. A., Stevens, F. J., Wang, B. C., Furey, W., Jr., . . . Schiffer, M. (1985). Novel arrangement of immunoglobulin variable domains: X-

ray crystallographic analysis of the lambda-chain dimer Bence-Jones protein Loc. *Biochemistry, 24*(18), 4890-4897.

Chertova, E., Bess, J. W., Jr., Crise, B. J., Sowder, I. R., Schaden, T. M., Hilburn, J. M., . . . Arthur, L. O. (2002). Envelope glycoprotein incorporation, not shedding of surface envelope glycoprotein (gp120/SU), Is the primary determinant of SU content of purified human immunodeficiency virus type 1 and simian immunodeficiency virus. *J Virol, 76*(11), 5315-5325.

Coffin, J., & Swanstrom, R. (2013). HIV pathogenesis: dynamics and genetics of viral populations and infected cells. *Cold Spring Harb Perspect Med, 3*(1), a012526. doi:10.1101/cshperspect.a012526

Colman, P. M., Epp, O., Fehlhammer, H., Bode, W., Schiffer, M., Lattman, E. E., . . . Palm, W. (1974). X-ray studies on antibody fragments. *FEBS Lett, 44*(2), 194-199.

Cook, L. B., Melamed, A., Niederer, H., Valganon, M., Laydon, D., Foroni, L., . . . Bangham, C. R. (2014). The role of HTLV-1 clonality, proviral structure, and genomic integration site in adult T-cell leukemia/lymphoma. *Blood, 123*(25), 3925-3931. doi:10.1182/blood-2014-02-553602

Corti, D., & Lanzavecchia, A. (2013). Broadly neutralizing antiviral antibodies. *Annu Rev Immunol, 31*, 705-742. doi:10.1146/annurev-immunol-032712-095916

Crotty, S. (2011). Follicular helper CD4 T cells (TFH). *Annu Rev Immunol, 29*, 621-663. doi:10.1146/annurev-immunol-031210-101400

Diskin, R., Klein, F., Horwitz, J. A., Halper-Stromberg, A., Sather, D. N., Marcovecchio, P. M., . . . Bjorkman, P. J. (2013). Restricting HIV-1 pathways for escape using

rationally designed anti–HIV-1 antibodies. *The Journal of Experimental Medicine, 210*(6), 1235-1249.

Diskin, R., Marcovecchio, P. M., & Bjorkman, P. J. (2010). Structure of a clade C HIV-1 gp120 bound to CD4 and CD4-induced antibody reveals anti-CD4 polyreactivity. *Nat Struct Mol Biol, 17*(5), 608-613.

Diskin, R., Scheid, J. F., Marcovecchio, P. M., West, A. P., Klein, F., Gao, H., . . . Bjorkman, P. J. (2011). Increasing the Potency and Breadth of an HIV Antibody by using Structure-Based Rational Design. *Science (New York, N.Y.), 334*(6060), 1289-1293. doi:10.1126/science.1213782

Do Kwon, Y., Pancera, M., Acharya, P., Georgiev, I. S., Crooks, E. T., Gorman, J., . . . Kwong, P. D. (2015). Crystal structure, conformational fixation and entry-related interactions of mature ligand-free HIV-1 Env. *Nat Struct Mol Biol, 22*(7), 522-531. doi:10.1038/nsmb.3051

Doria-Rose, N. A., Klein, R. M., Manion, M. M., O'Dell, S., Phogat, A., Chakrabarti, B., . . . Connors, M. (2009). Frequency and Phenotype of Human Immunodeficiency Virus Envelope-Specific B Cells from Patients with Broadly Cross-Neutralizing Antibodies. *Journal of Virology, 83*(1), 188-199.

Dörner, T., & Radbruch, A. (2007). Antibodies and B Cell Memory in Viral Immunity. *Immunity, 27*(3), 384-392. doi:10.1016/j.immuni.2007.09.002

Edelman, G. M. (1973). Antibody structure and molecular immunology. *Science, 180*(4088), 830-840.

Eisen, H. N., & Siskind, G. W. (1964). Variations in Affinities of Antibodies during the Immune Response*. *Biochemistry, 3*(7), 996-1008. doi:10.1021/bi00895a027

Euler, Z., van Gils, M. J., Bunnik, E. M., Phung, P., Schweighardt, B., Wrin, T., & Schuitemaker, H. (2010). Cross-Reactive Neutralizing Humoral Immunity Does Not Protect from HIV Type 1 Disease Progression. *Journal of Infectious Diseases, 201*(7), 1045-1053.

A FAILURE LED TO DRUG AGAINST AIDS. (1986, September 20, 1986). *The New York Times*

Feinberg, M. B., Baltimore, D., & Frankel, A. D. (1991). The role of Tat in the human immunodeficiency virus life cycle indicates a primary effect on transcriptional elongation. *Proc Natl Acad Sci U S A, 88*(9), 4045-4049.

Felber, B. K., Drysdale, C. M., & Pavlakis, G. N. (1990). Feedback regulation of human immunodeficiency virus type 1 expression by the Rev protein. *J Virol, 64*(8), 3734-3741.

Ferrantelli, F., Rasmussen, R. A., Buckley, K. A., Li, P. L., Wang, T., Montefiori, D. C., . . . Ruprecht, R. M. (2004). Complete protection of neonatal rhesus macaques against oral exposure to pathogenic simian-human immunodeficiency virus by human anti-HIV monoclonal antibodies. *J Infect Dis, 189*(12), 2167-2173. doi:10.1086/420833

Fischl, M. A., Richman, D. D., Grieco, M. H., Gottlieb, M. S., Volberding, P. A., Laskin, O. L., . . . et al. (1987). The efficacy of azidothymidine (AZT) in the treatment of

patients with AIDS and AIDS-related complex. A double-blind, placebo-controlled trial. *N Engl J Med, 317*(4), 185-191. doi:10.1056/NEJM198707233170401

Flint, S. J., Enquist, L. W., Racaniello, V. R., & Skalka, A. M. (2008). *Principles of Virology*: ASM Press.

Freed, E. O., & Mouland, A. J. (2006). The cell biology of HIV-1 and other retroviruses. *Retrovirology, 3*, 77. doi:10.1186/1742-4690-3-77

Gallo, R., & Montagnier, L. (2003). PERSPECTIVE: The Discovery of HIV as the Cause of AIDS *The New England Journal of Medicine, 349*(2), 2283-2285.

Gallo, R. C. (2005). The discovery of the first human retrovirus: HTLV-1 and HTLV-2. *Retrovirology, 2*, 17. doi:10.1186/1742-4690-2-17

Ganser-Pornillos, B., Yeager, M., & Sundquist, W. I. (2008). The Structural Biology of HIV Assembly. *Current opinion in structural biology, 18*(2), 203. doi:10.1016/j.sbi.2008.02.001

Garces, F., Lee, Jeong H., de Val, N., Torrents de la Pena, A., Kong, L., Puchades, C., . . . Wilson, Ian A. (2015). Affinity Maturation of a Potent Family of HIV Antibodies Is Primarily Focused on Accommodating or Avoiding Glycans. *Immunity, 43*(6), 1053-1063. doi:10.1016/j.immuni.2015.11.007

Garces, F., Sok, D., Kong, L., McBride, R., Kim, Helen J., Saye-Francisco, Karen F., . . . Wilson, Ian A. (2014). Structural Evolution of Glycan Recognition by a Family of Potent HIV Antibodies. *Cell, 159*(1), 69-79.

Geijtenbeek, T. B., Kwon, D. S., Torensma, R., van Vliet, S. J., van Duijnhoven, G. C., Middel, J., . . . van Kooyk, Y. (2000). DC-SIGN, a dendritic cell-specific HIV-1-binding protein that enhances trans-infection of T cells. *Cell, 100*(5), 587-597.

Go, E. P., Liao, H. X., Alam, S. M., Hua, D., Haynes, B. F., & Desaire, H. (2013). Characterization of host-cell line specific glycosylation profiles of early transmitted/founder HIV-1 gp120 envelope proteins. *J Proteome Res, 12*(3), 1223-1234. doi:10.1021/pr300870t

Graham, B. S. (2002). Clinical Trials of HIV Vaccines. *Annual Review of Medicine, 53*, 207-221.

Haase, A. T. (1999). Population Biology of HIV-1 Infection: Viral and CD4+ T Cell Demographics and Dynamics in Lymphatic Tissues. *Annual Review of Immunology, 17*, 625-656.

Harris, A., Borgnia, M. J., Shi, D., Bartesaghi, A., He, H., Pejchal, R., . . . Subramaniam, S. (2011). Trimeric HIV-1 glycoprotein gp140 immunogens and native HIV-1 envelope glycoproteins display the same closed and open quaternary molecular architectures. *Proc Natl Acad Sci U S A, 108*(28), 11440-11445. doi:10.1073/pnas.1101414108

Harrison, S. C. (2015). Viral membrane fusion. *Virology, 479-480*, 498-507. doi:10.1016/j.virol.2015.03.043

Hessell, A. J. (2007). Fc receptor but not complement binding is important in antibody protection against HIV. *Nature, 449*, 101-104.

Hessell, A. J., Poignard, P., Hunter, M., Hangartner, L., Tehrani, D. M., Bleeker, W. K., . . . Burton, D. R. (2009). Effective, low-titer antibody protection against low-dose repeated mucosal SHIV challenge in macaques. *Nat Med, 15*(8), 951-954.

HIV Transmission. (2015, 12/14/2015). *HIV basics.* Retrieved from http://www.cdc.gov/hiv/basics/transmission.html

Hofmann-Lehmann, R., Vlasak, J., Rasmussen, R. A., Smith, B. A., Baba, T. W., Liska, V., . . . Ruprecht, R. M. (2001). Postnatal passive immunization of neonatal macaques with a triple combination of human monoclonal antibodies against oral simian-human immunodeficiency virus challenge. *J Virol, 75*(16), 7470-7480. doi:10.1128/JVI.75.16.7470-7480.2001

Horwitz, J. A., Halper-Stromberg, A., Mouquet, H., Gitlin, A. D., Tretiakova, A., Eisenreich, T. R., . . . Nussenzweig, M. C. (2013). HIV-1 suppression and durable control by combining single broadly neutralizing antibodies and antiretroviral drugs in humanized mice. *Proceedings of the National Academy of Sciences, 110*(41), 16538-16543.

Huang, J., Kang, B. H., Pancera, M., Lee, J. H., Tong, T., Feng, Y., . . . Connors, M. (2014). Broad and potent HIV-1 neutralization by a human antibody that binds the gp41-gp120 interface. *Nature, 515*(7525), 138-142. doi:10.1038/nature13601

Huang, J., Ofek, G., Laub, L., Louder, M. K., Doria-Rose, N. A., Longo, N. S., . . . Connors, M. (2012). Broad and potent neutralization of HIV-1 by a gp41-specific human antibody. *Nature, 491*(7424), 406-412.

Hutchinson, J. F. (2001). The Biology and Evolution of HIV. *Annual Review of Anthropology, 30*, 85-108.

Jowett, J. B., Planelles, V., Poon, B., Shah, N. P., Chen, M. L., & Chen, I. S. (1995). The human immunodeficiency virus type 1 vpr gene arrests infected T cells in the G2 + M phase of the cell cycle. *J Virol, 69*(10), 6304-6313.

Julien, J.-P., Sok, D., Khayat, R., Lee, J. H., Doores, K. J., Walker, L. M., . . . Wilson, I. A. (2013). Broadly Neutralizing Antibody PGT121 Allosterically Modulates CD4 Binding via Recognition of the HIV-1 gp120 V3 Base and Multiple Surrounding Glycans. *PLoS Pathog, 9*(5), e1003342. doi:10.1371/journal.ppat.1003342

Julien, J. P., Cupo, A., Sok, D., Stanfield, R. L., Lyumkis, D., Deller, M. C., . . . Wilson, I. A. (2013). Crystal structure of a soluble cleaved HIV-1 envelope trimer. *Science, 342*(6165), 1477-1483. doi:10.1126/science.1245625

Karush, F. (1976). Multivalent binding and functional affinity. *Contemp Top Mol Immunol, 5*, 217-228.

Klasse, P. J., Depetris, R. S., Pejchal, R., Julien, J. P., Khayat, R., Lee, J. H., . . . Moore, J. P. (2013). Influences on trimerization and aggregation of soluble, cleaved HIV-1 SOSIP envelope glycoprotein. *J Virol, 87*(17), 9873-9885. doi:10.1128/JVI.01226-13

Klasse, P. J., & Sattentau, Q. J. (2002). Occupancy and mechanism in antibody-mediated neutralization of animal viruses. *J Gen Virol, 83*(Pt 9), 2091-2108. doi:10.1099/0022-1317-83-9-2091

Klein, F., Gaebler, C., Mouquet, H., Sather, D. N., Lehmann, C., Scheid, J. F., . . . Nussenzweig, M. C. (2012). Broad neutralization by a combination of antibodies recognizing the CD4 binding site and a new conformational epitope on the HIV-1 envelope protein. *The Journal of Experimental Medicine, 209*(8), 1469-1479.

Klein, F., Halper-Stromberg, A., Horwitz, J. A., Gruell, H., Scheid, J. F., Bournazos, S., . . . Nussenzweig, M. C. (2012). HIV therapy by a combination of broadly neutralizing antibodies in humanized mice. *Nature, 492*(7427), 118-122.

Klein, F., Nogueira, L., Nishimura, Y., Phad, G., West, A. P., Halper-Stromberg, A., . . . Nussenzweig, M. C. (2014). Enhanced HIV-1 immunotherapy by commonly arising antibodies that target virus escape variants. *The Journal of Experimental Medicine, 211*(12), 2361-2372.

Klein, J. S., & Bjorkman, P. J. (2010). Few and far between: how HIV may be evading antibody avidity. *PLoS Pathog, 6*(5), e1000908. doi:10.1371/journal.ppat.1000908

Kong, L., Lee, J. H., Doores, K. J., Murin, C. D., Julien, J.-P., McBride, R., . . . Wilson, I. A. (2013). Supersite of immune vulnerability on the glycosylated face of HIV-1 envelope glycoprotein gp120. *Nat Struct Mol Biol, 20*(7), 796-803. doi:10.1038/nsmb.2594

Kurosaki, T., Kometani, K., & Ise, W. (2015). Memory B cells. *Nat Rev Immunol, 15*(3), 149-159. doi:10.1038/nri3802

Kwong, P. D., Doyle, M. L., Casper, D. J., Cicala, C., Leavitt, S. A., Majeed, S., . . . Arthos, J. (2002). HIV-1 evades antibody-mediated neutralization through conformational

masking of receptor-binding sites. *Nature, 420*(6916), 678-682. doi:10.1038/nature01188

Kwong, P. D., Wyatt, R., Robinson, J., Sweet, R. W., Sodroski, J., & Hendrickson, W. A. (1998). Structure of an HIV gp120 envelope glycoprotein in complex with the CD4 receptor and a neutralizing human antibody. *Nature, 393*(6686), 648-659. doi:10.1038/31405

Labrijn, A. F., Poignard, P., Raja, A., Zwick, M. B., Delgado, K., Franti, M., . . . Burton, D. R. (2003). Access of antibody molecules to the conserved coreceptor binding site on glycoprotein gp120 is sterically restricted on primary human immunodeficiency virus type 1. *J Virol, 77*(19), 10557-10565.

Lake, J.-a., Carr, J., Feng, F., Mundy, L., Burrell, C., & Li, P. (2003). The role of Vif during HIV-1 infection: interaction with novel host cellular factors. *Journal of Clinical Virology, 26*(2), 143-152. doi:10.1016/S1386-6532(02)00113-0

Lama, J., Mangasarian, A., & Trono, D. (2001). Cell-surface expression of CD4 reduces HIV-1 infectivity by blocking Env incorporation in a Nef- and Vpu-inhibitable manner. *Current Biology, 9*(12), 622-631. doi:10.1016/S0960-9822(99)80284-X

Lawrence K. Altman, M. D. (1981, July 3, 1981). Rare Cancer Seen in 41 Homosexuals. *The New York Times*.

Levy, J. A. (1993). Pathogenesis of human immunodeficiency virus infection. *Microbiol Rev, 57*(1), 183-289.

Liu, J., Bartesaghi, A., Borgnia, M. J., Sapiro, G., & Subramaniam, S. (2008). Molecular architecture of native HIV-1 gp120 trimers. *Nature, 455*(7209), 109-113. doi:10.1038/nature07159

Lyumkis, D., Julien, J. P., de Val, N., Cupo, A., Potter, C. S., Klasse, P. J., . . . Ward, A. B. (2013). Cryo-EM structure of a fully glycosylated soluble cleaved HIV-1 envelope trimer. *Science, 342*(6165), 1484-1490. doi:10.1126/science.1245627

Magadán, J. G., Pérez-Victoria, F. J., Sougrat, R., Ye, Y., Strebel, K., & Bonifacino, J. S. (2010). Multilayered Mechanism of CD4 Downregulation by HIV-1 Vpu Involving Distinct ER Retention and ERAD Targeting Steps. *PLoS Pathog, 6*(4), e1000869. doi:10.1371/journal.ppat.1000869

Marx, J. L. (1975). Antibody structure: now in three dimensions. *Science, 189*(4208), 1075-1114. doi:10.1126/science.189.4208.1075

Mascola, J. R. (1997). Potent and synergistic neutralization of human immunodeficiency virus (HIV) type 1 primary isolates by hyperimmune anti-HIV immunoglobulin combined with monoclonal antibodies 2F5 and 2G12. *J. Virol., 71*, 7198-7206.

Mascola, J. R. (1999). Protection of macaques against pathogenic simian/human immunodeficiency virus 89.6PD by passive transfer of neutralizing antibodies. *J. Virol., 73*, 4009-4018.

Mascola, J. R. (2000). Protection of macaques against vaginal transmission of a pathogenic HIV-1/SIV chimeric virus by passive infusion of neutralizing antibodies. *Nat. Med., 6*, 207-210.

Mascola, J. R., & Montefiori, D. C. (2010). The role of antibodies in HIV vaccines. *Annu Rev Immunol, 28*, 413-444. doi:10.1146/annurev-immunol-030409-101256

Mattes, M. J. (2004). Binding parameters of antibodies: pseudo-affinity and other misconceptions. *Cancer Immunology, Immunotherapy, 54*(6), 513-516. doi:10.1007/s00262-004-0644-3

Maul, R. W., & Gearhart, P. J. (2010). AID and somatic hypermutation. *Adv Immunol, 105*, 159-191. doi:10.1016/S0065-2776(10)05006-6

McCoy, L. E., Quigley, A. F., Strokappe, N. M., Bulmer-Thomas, B., Seaman, M. S., Mortier, D., . . . Weiss, R. A. (2012). Potent and broad neutralization of HIV-1 by a llama antibody elicited by immunization. *The Journal of Experimental Medicine, 209*(6), 1091-1103.

McLellan, J. S., Pancera, M., Carrico, C., Gorman, J., Julien, J.-P., Khayat, R., . . . Kwong, P. D. (2011). Structure of HIV-1 gp120 V1/V2 domain with broadly neutralizing antibody PG9. *Nature, 480*(7377), 336-343.

McMichael, A. J. (2006). HIV vaccines. *Annu Rev Immunol, 24*, 227-255. doi:10.1146/annurev.immunol.24.021605.090605

McNatt, M. W., Zang, T., & Bieniasz, P. D. (2013). Vpu Binds Directly to Tetherin and Displaces It from Nascent Virions. *PLoS Pathog, 9*(4), e1003299. doi:10.1371/journal.ppat.1003299

Medzhitov, R. (2007). Recognition of microorganisms and activation of the immune response. *Nature, 449*(7164), 819-826. doi:10.1038/nature06246

Medzhitov, R., & Janeway, C., Jr. (2000). Innate immunity. *N Engl J Med, 343*(5), 338-344. doi:10.1056/NEJM200008033430506

Mehellou, Y., & De Clercq, E. (2010). Twenty-six years of anti-HIV drug discovery: where do we stand and where do we go? *J Med Chem, 53*(2), 521-538. doi:10.1021/jm900492g

Michael S. Gottlieb, M., **Schroff, R.**, **Schanker, H. M.**, **Weisman, J. D.**, **Fan, P. T.**, **Wolf, R.**, & **Saxon, A.** (1981). Pneumocystis carinii pneumonia and mucosal candidiasis in previously healthy homosexual men: evidence of a new acquired cellular immunodeficiency. *The New England Journal of Medicine, 305*(24), 1425-1431.

Moir, S., Chun, T. W., & Fauci, A. S. (2011). Pathogenic mechanisms of HIV disease. *Annu Rev Pathol, 6*, 223-248. doi:10.1146/annurev-pathol-011110-130254

Moody, M. A., Santra, S., Vandergrift, N. A., Sutherland, L. L., Gurley, T. C., Drinker, M. S., . . . Haynes, B. F. (2014). Toll-like receptor 7/8 (TLR7/8) and TLR9 agonists cooperate to enhance HIV-1 envelope antibody responses in rhesus macaques. *J Virol, 88*(6), 3329-3339. doi:10.1128/JVI.03309-13

Moore, J. P., & Sodroski, J. (1996). Antibody cross-competition analysis of the human immunodeficiency virus type 1 gp120 exterior envelope glycoprotein. *J Virol, 70*(3), 1863-1872.

Mouquet, H., Scharf, L., Euler, Z., Liu, Y., Eden, C., Scheid, J. F., . . . Bjorkman, P. J. (2012). Complex-type N-glycan recognition by potent broadly neutralizing HIV antibodies. *Proceedings of the National Academy of Sciences, 109*(47), E3268-E3277.

Murphy, K., Travers, P., Walport, M., & Janeway, C. (2012). *Janeway's immunobiology*. New York: Garland Science.

Neefjes, J., Jongsma, M. L., Paul, P., & Bakke, O. (2011). Towards a systems understanding of MHC class I and MHC class II antigen presentation. *Nat Rev Immunol, 11*(12), 823-836. doi:10.1038/nri3084

Ostertag, W., Roesler, G., Krieg, C. J., Kind, J., Cole, T., Crozier, T., . . . Dube, S. (1974). Induction of endogenous virus and of thymidine kinase by bromodeoxyuridine in cell cultures transformed by Friend virus. *Proc Natl Acad Sci U S A, 71*(12), 4980-4985.

Palella, F. J., Jr., Delaney, K. M., Moorman, A. C., Loveless, M. O., Fuhrer, J., Satten, G. A., . . . Holmberg, S. D. (1998). Declining morbidity and mortality among patients with advanced human immunodeficiency virus infection. HIV Outpatient Study Investigators. *N Engl J Med, 338*(13), 853-860. doi:10.1056/NEJM199803263381301

Pancera, M., Zhou, T., Druz, A., Georgiev, I. S., Soto, C., Gorman, J., . . . Kwong, P. D. (2014). Structure and immune recognition of trimeric pre-fusion HIV-1 Env. *Nature, 514*(7523), 455-461. doi:10.1038/nature13808

Pantophlet, R., & Burton, D. R. (2006). GP120: target for neutralizing HIV-1 antibodies. *Annu Rev Immunol, 24*, 739-769. doi:10.1146/annurev.immunol.24.021605.090557

Parkin, N. T., Chamorro, M., & Varmus, H. E. (1992). Human immunodeficiency virus type 1 gag-pol frameshifting is dependent on downstream mRNA secondary structure: demonstration by expression in vivo. *J Virol, 66*(8), 5147-5151.

Parren, P. W., Poignard, P., Ditzel, H. J., Williamson, R. A., & Burton, D. R. (2000). Antibodies in human infectious disease. *Immunol Res, 21*(2-3), 265-278. doi:10.1385/IR:21:2-3:265

Pauling, L., Pressman, D., & Grossberg, A. L. (1944). The Serological Properties of Simple Substances. VII. A Quantitative Theory of the Inhibition by Haptens of the Precipitation of Heterogeneous Antisera with Antigens, and Comparison with Experimental Results for Polyhaptenic Simple Substances and for Azoproteins. *Journal of the American Chemical Society, 66*(5), 784-792. doi:10.1021/ja01233a039

Paxton, W., Connor, R. I., & Landau, N. R. (1993). Incorporation of Vpr into human immunodeficiency virus type 1 virions: requirement for the p6 region of gag and mutational analysis. *J Virol, 67*(12), 7229-7237.

Pejchal, R., Doores, K. J., Walker, L. M., Khayat, R., Huang, P.-S., Wang, S.-K., . . . Wilson, I. A. (2011). A potent and broad neutralizing antibody recognizes and penetrates the HIV glycan shield. *Science (New York, N.Y.), 334*(6059), 1097-1103. doi:10.1126/science.1213256

Peled, J. U., Kuang, F. L., Iglesias-Ussel, M. D., Roa, S., Kalis, S. L., Goodman, M. F., & Scharff, M. D. (2008). The Biochemistry of Somatic Hypermutation. *Annual*

Review of Immunology, 26(1), 481-511. doi:10.1146/annurev.immunol.26.021607.090236

Perelson, A. S., Neumann, A. U., Markowitz, M., Leonard, J. M., & Ho, D. D. (1996). HIV-1 dynamics in vivo: virion clearance rate, infected cell life-span, and viral generation time. *Science, 271*(5255), 1582-1586.

Pettit, S. C., Everitt, L. E., Choudhury, S., Dunn, B. M., & Kaplan, A. H. (2004). Initial cleavage of the human immunodeficiency virus type 1 GagPol precursor by its activated protease occurs by an intramolecular mechanism. *J Virol, 78*(16), 8477-8485. doi:10.1128/JVI.78.16.8477-8485.2004

Picker, L. J., Hansen, S. G., & Lifson, J. D. (2012). New paradigms for HIV/AIDS vaccine development. *Annu Rev Med, 63*, 95-111. doi:10.1146/annurev-med-042010-085643

Pieper, K., Grimbacher, B., & Eibel, H. (2013). B-cell biology and development. *Journal of Allergy and Clinical Immunology, 131*(4), 959-971. doi:10.1016/j.jaci.2013.01.046

Pritchard, L. K., Harvey, D. J., Bonomelli, C., Crispin, M., & Doores, K. J. (2015). Cell- and Protein-Directed Glycosylation of Native Cleaved HIV-1 Envelope. *J Virol, 89*(17), 8932-8944. doi:10.1128/JVI.01190-15

Purtscher, M., Trkola, A., Gruber, G., Buchacher, A., Predl, R., Steindl, F., . . . et al. (1994). A broadly neutralizing human monoclonal antibody against gp41 of human immunodeficiency virus type 1. *AIDS Res Hum Retroviruses, 10*(12), 1651-1658.

Rizzuto, C. D., Wyatt, R., Hernandez-Ramos, N., Sun, Y., Kwong, P. D., Hendrickson, W. A., & Sodroski, J. (1998). A conserved HIV gp120 glycoprotein structure involved in chemokine receptor binding. *Science, 280*(5371), 1949-1953.

Ross, T. M., Oran, A. E., & Cullen, B. R. (1999). Inhibition of HIV-1 progeny virion release by cell-surface CD4 is relieved by expression of the viral Nef protein. *Current Biology, 9*(12), 613-621. doi:10.1016/S0960-9822(99)80283-8

Sanders, R. W., Derking, R., Cupo, A., Julien, J. P., Yasmeen, A., de Val, N., . . . Moore, J. P. (2013). A next-generation cleaved, soluble HIV-1 Env trimer, BG505 SOSIP.664 gp140, expresses multiple epitopes for broadly neutralizing but not non-neutralizing antibodies. *PLoS Pathog, 9*(9), e1003618. doi:10.1371/journal.ppat.1003618

Sanders, R. W., Vesanen, M., Schuelke, N., Master, A., Schiffner, L., Kalyanaraman, R., . . . Moore, J. P. (2002). Stabilization of the soluble, cleaved, trimeric form of the envelope glycoprotein complex of human immunodeficiency virus type 1. *J Virol, 76*(17), 8875-8889.

Sather, D. N., Carbonetti, S., Kehayia, J., Kraft, Z., Mikell, I., Scheid, J. F., . . . Stamatatos, L. (2012). Broadly Neutralizing Antibodies Developed by an HIV-Positive Elite Neutralizer Exact a Replication Fitness Cost on the Contemporaneous Virus. *Journal of Virology, 86*(23), 12676-12685.

Sattentau, Q. J., & Moore, J. P. (1991). Conformational changes induced in the human immunodeficiency virus envelope glycoprotein by soluble CD4 binding. *J Exp Med, 174*(2), 407-415.

Scharf, L., Scheid, Johannes F., Lee, Jeong H., West, Anthony P., Jr., Chen, C., Gao, H., . . . Bjorkman, Pamela J. (2014). Antibody 8ANC195 Reveals a Site of Broad Vulnerability on the HIV-1 Envelope Spike. *Cell Reports, 7*(3), 785-795. doi:10.1016/j.celrep.2014.04.001

Scharf, L., Wang, H., Gao, H., Chen, S., McDowall, A. W., & Bjorkman, P. J. (2015). Broadly Neutralizing Antibody 8ANC195 Recognizes Closed and Open States of HIV-1 Env. *Cell, 162*(6), 1379-1390. doi:10.1016/j.cell.2015.08.035

Scheid, J., Mouquet, H., Feldhahn, N., Walker, B., Pereyra, F., Cutrell, E., . . . Nussenzweig, M. C. (2009). A method for identification of HIV gp140 binding memory B cells in human blood. *Journal of immunological methods, 343*(2), 65-67. doi:10.1016/j.jim.2008.11.012

Scheid, J. F., Mouquet, H., Feldhahn, N., Seaman, M. S., Velinzon, K., Pietzsch, J., . . . Nussenzweig, M. C. (2009). Broad diversity of neutralizing antibodies isolated from memory B cells in HIV-infected individuals. *Nature, 458*(7238), 636-640.

Scheid, J. F., Mouquet, H., Ueberheide, B., Diskin, R., Klein, F., Oliveira, T. Y. K., . . . Nussenzweig, M. C. (2011). Sequence and Structural Convergence of Broad and Potent HIV Antibodies That Mimic CD4 Binding. *Science (New York, N.Y.), 333*(6049), 1633-1637. doi:10.1126/science.1207227

Schulke, N., Vesanen, M. S., Sanders, R. W., Zhu, P., Lu, M., Anselma, D. J., . . . Olson, W. C. (2002). Oligomeric and conformational properties of a proteolytically mature, disulfide-stabilized human immunodeficiency virus type 1 gp140 envelope glycoprotein. *J Virol, 76*(15), 7760-7776.

Sharp, P. M., & Hahn, B. H. (2011). Origins of HIV and the AIDS pandemic. *Cold Spring Harb Perspect Med, 1*(1), a006841. doi:10.1101/cshperspect.a006841

Sievers, S. A., Scharf, L., West, A. P., Jr., & Bjorkman, P. J. (2015). Antibody engineering for increased potency, breadth and half-life. *Current Opinion in HIV and AIDS, 10*(3).

Simon, V., Ho, D. D., & Abdool Karim, Q. (2006). HIV/AIDS epidemiology, pathogenesis, prevention, and treatment. *The Lancet, 368*(9534), 489-504. doi:10.1016/s0140-6736(06)69157-5

Sok, D., van Gils, M. J., Pauthner, M., Julien, J.-P., Saye-Francisco, K. L., Hsueh, J., . . . Burton, D. R. (2014). Recombinant HIV envelope trimer selects for quaternary-dependent antibodies targeting the trimer apex. *Proceedings of the National Academy of Sciences, 111*(49), 17624-17629.

Solis, M., Nakhaei, P., Jalalirad, M., Lacoste, J., Douville, R., Arguello, M., . . . Hiscott, J. (2011). RIG-I-mediated antiviral signaling is inhibited in HIV-1 infection by a protease-mediated sequestration of RIG-I. *J Virol, 85*(3), 1224-1236. doi:10.1128/JVI.01635-10

Starcich, B. R., Hahn, B. H., Shaw, G. M., McNeely, P. D., Modrow, S., Wolf, H., . . . et al. (1986). Identification and characterization of conserved and variable regions in the envelope gene of HTLV-III/LAV, the retrovirus of AIDS. *Cell, 45*(5), 637-648.

Stiegler, G., Kunert, R., Purtscher, M., Wolbank, S., Voglauer, R., Steindl, F., & Katinger, H. (2001). A potent cross-clade neutralizing human monoclonal antibody against

a novel epitope on gp41 of human immunodeficiency virus type 1. *AIDS Res Hum Retroviruses, 17*(18), 1757-1765. doi:10.1089/08892220152741450

Stopak, K., de Noronha, C., Yonemoto, W., & Greene, W. C. (2003). HIV-1 Vif Blocks the Antiviral Activity of APOBEC3G by Impairing Both Its Translation and Intracellular Stability. *Molecular Cell, 12*(3), 591-601. doi:10.1016/S1097-2765(03)00353-8

Tamamis, P., & Floudas, C. A. (2014). Molecular recognition of CCR5 by an HIV-1 gp120 V3 loop. *PLoS One, 9*(4), e95767. doi:10.1371/journal.pone.0095767

Tiselius, A., & Kabat, E. A. (1938). ELECTROPHORESIS OF IMMUNE SERUM. *Science, 87*(2262), 416-417.

Tiselius, A., & Kabat, E. A. (1939). An Electrophoretic Study of Immune Sera and Purified Antibody Preparations. *J Exp Med, 69*(1), 119-131.

Tonegawa, S. (1983). Somatic generation of antibody diversity. *Nature, 302*(5909), 575-581.

Tran, E. E., Borgnia, M. J., Kuybeda, O., Schauder, D. M., Bartesaghi, A., Frank, G. A., . . . Subramaniam, S. (2012). Structural mechanism of trimeric HIV-1 envelope glycoprotein activation. *PLoS Pathog, 8*(7), e1002797. doi:10.1371/journal.ppat.1002797

Trkola, A., Kuster, H., Rusert, P., Joos, B., Fischer, M., Leemann, C., . . . Gunthard, H. F. (2005). Delay of HIV-1 rebound after cessation of antiretroviral therapy through passive transfer of human neutralizing antibodies. *Nat Med, 11*(6), 615-622.

Trkola, A., Purtscher, M., Muster, T., Ballaun, C., Buchacher, A., Sullivan, N., . . . Katinger, H. (1996). Human monoclonal antibody 2G12 defines a distinctive neutralization

epitope on the gp120 glycoprotein of human immunodeficiency virus type 1. *Journal of Virology, 70*(2), 1100-1108.

UNAIDS. (2015). *UNAIDS Facts Sheet 2015*.

UNAIDS, & Sabin, K. (Eds.). (2015). *UNAIDS Report: How AIDS changed everything*. Switzerland: UNAIDS.

van Gils, M. J., Euler, Z., Schweighardt, B., Wrin, T., & Schuitemaker, H. (2009). Prevalence of cross-reactive HIV-1-neutralizing activity in HIV-1-infected patients with rapid or slow disease progression. *AIDS, 23*(18).

van Gils, M. J., & Sanders, R. W. (2013). Broadly neutralizing antibodies against HIV-1: Templates for a vaccine. *Virology, 435*(1), 46-56.

Victora, G. D., & Mesin, L. (2014). Clonal and cellular dynamics in germinal centers. *Curr Opin Immunol, 28*, 90-96. doi:10.1016/j.coi.2014.02.010

Victora, G. D., & Nussenzweig, M. C. (2012). Germinal Centers. *Annual Review of Immunology, 30*(1), 429-457. doi:10.1146/annurev-immunol-020711-075032

Walker, L. M., Huber, M., Doores, K. J., Falkowska, E., Pejchal, R., Julien, J.-P., . . . Poignard, P. (2011). Broad neutralization coverage of HIV by multiple highly potent antibodies. *Nature, 477*(7365), 466-470.

Walker, L. M., Phogat, S. K., Chan-Hui, P.-Y., Wagner, D., Phung, P., Goss, J. L., . . . Burton, D. R. (2009). Broad and Potent Neutralizing Antibodies from an African Donor Reveal a New HIV-1 Vaccine Target. *Science (New York, N.Y.), 326*(5950), 285-289. doi:10.1126/science.1178746

Waters, L., Mandalia, S., Randell, P., Wildfire, A., Gazzard, B., & Moyle, G. (2008). The Impact of HIV Tropism on Decreases in CD4 Cell Count, Clinical Progression, and Subsequent Response to a First Antiretroviral Therapy Regimen. *Clinical Infectious Diseases, 46*(10), 1617-1623.

Watkins, D. I. (2008, November 2008). The Vaccine Search Goes On. *Scientific American,* 69-77.

Weissenhorn, W., Dessen, A., Harrison, S. C., Skehel, J. J., & Wiley, D. C. (1997). Atomic structure of the ectodomain from HIV-1 gp41. *Nature, 387*(6631), 426-430. doi:10.1038/387426a0

West, Anthony P., Jr., Scharf, L., Scheid, Johannes F., Klein, F., Bjorkman, Pamela J., & Nussenzweig, Michel C. (2014). Structural Insights on the Role of Antibodies in HIV-1 Vaccine and Therapy. *Cell, 156*(4), 633-648. doi:10.1016/j.cell.2014.01.052

Wu, X., Yang, Z.-Y., Li, Y., Hogerkorp, C.-M., Schief, W. R., Seaman, M. S., . . . Mascola, J. R. (2010). Rational Design of Envelope Identifies Broadly Neutralizing Human Monoclonal Antibodies to HIV-1. *Science (New York, N.Y.), 329*(5993), 856-861. doi:10.1126/science.1187659

Wu, Y. (2015). *STRUCTURAL CHARACTERIZATIONS OF THE DIMERIC ANTI-HIV ANTIBODY 2G12 AND THE HIV-2 ENVELOPE GLYCOPROTEIN.* (Doctoral Dissertation (Ph.D)), California Institute of Technology, Pasadena, CA. (CaltechTHESIS:05212015-194407438)

Wyatt, R., Kwong, P. D., Desjardins, E., Sweet, R. W., Robinson, J., Hendrickson, W. A., & Sodroski, J. G. (1998). The antigenic structure of the HIV gp120 envelope glycoprotein. *Nature, 393*(6686), 705-711. doi:10.1038/31514

Zhu, P., Chertova, E., Bess, J., Lifson, J. D., Arthur, L. O., Liu, J., . . . Roux, K. H. (2003). Electron tomography analysis of envelope glycoprotein trimers on HIV and simian immunodeficiency virus virions. *Proceedings of the National Academy of Sciences, 100*(26), 15812-15817.

Zhu, P., Liu, J., Bess, J., Jr., Chertova, E., Lifson, J. D., Grise, H., . . . Roux, K. H. (2006). Distribution and three-dimensional structure of AIDS virus envelope spikes. *Nature, 441*(7095), 847-852. doi:10.1038/nature04817

Zhu, T., Korber, B. T., Nahmias, A. J., Hooper, E., Sharp, P. M., & Ho, D. D. (1998). An African HIV-1 sequence from 1959 and implications for the origin of the epidemic. *Nature, 391*(6667), 594-597.

Chapter Two

Investigating the use of CD4-CD4i antibody reagents to clear SIV in Chimpanzees

This chapter describes the characterization of an antibody-based reagent for the treatment of an endangered population of chimpanzees infected with SIV in Tanzania. My contribution to this work involved the repurposing and redesign of a reagent from previous research that I had done prior to beginning as a graduate student at Caltech. I designed and performed initial characterization of the second generation reagents that were later tested for use against SIV. This work was a collaboration with Anthony West and Alysia Ahmed in the Bjorkman lab, Hannah Barbian and other members of Beatrice Hahn's lab at UPENN, and Michael Farzan at HMS. Portions of this chapter have been published as Barbian, H. J., Decker, J.M., Bibollet-Ruche, F., **Galimidi, R.P** et al. (2015). "Neutralization properties of simian immunodeficiency viruses infecting chimpanzees and gorillas." MBio **6**(2).

Abstract

Like HIV-1 in humans, SIVcpz is pathogenic in wild-living chimpanzees and has a substantial negative impact on their health, reproduction, and life span. While HIV-1 infection can be controlled by anti-retroviral therapy, treating wild-living chimpanzees is not feasible. However, it might be possible to curb ongoing transmission of SIVcpz in select communities using AAV-mediated antibody gene transfer approaches to reduce viral load in infected chimpanzees. This would require the availability of antibodies that can neutralize SIVcpz with both breadth and potency. To screen for such antibodies, we generated a panel of genetically diverse infectious molecular clones of SIVcpz and SIVgor (n=12) from fecal consensus sequences. Testing sera from a small number of long-term HIV-1 infected (captive) chimpanzees, we failed to detect cross-reactive neutralizing antibodies. However, analysis of over 50 monoclonal antibodies known to potently neutralize diverse strains of HIV-1 identified reagents that also had potent anti-SIVcpz activity in TZM-bl cells. All of these reagents were composed of the D1/D2 domain of human CD4 linked to a natural antibody or the Fc region of an antibody. Synthesis of modified CD4-based antibodies revealed that potency could be further increased with the addition of a CCR5 mimetic or fusion (T20) peptide to the Fc portion of the reagent. In contrast to broadly cross-reactive neutralizing antibodies such as VRC01, PG9, and PGT121, which had minimal activity against SIVcpz, these reagents (CD4-218.3-E51-E3, CD4-218.3-E51-YE3, and CD4-218.3-E51-T20), neutralized all 12 SIVcpz and SIVgor strains in TZM-bl cells with IC50 titers ranging from 0.02 to 8.8 ug/ml. These same constructs were also capable of blocking SIVcpz replication in

primary chimpanzee CD4+ T cells. We have thus identified monoclonal antibody-like reagents that neutralize a panel of divergent SIVcpz strains with both breadth and potency. Used in combination, these reagents might prove useful for vector-mediated antibody gene transfer approaches aimed at protecting select chimpanzee communities against the spread of SIVcpz infection in the wild.

Introduction

Human immunodeficiency virus type 1 (HIV-1) derived from the chimpanzee simian immunodeficiency virus (SIVcpz) (Sharp and Hahn, 2011). Prior to the late 2000's, SIVcpz was thought to have a non-pathogenic phenotype and resemble natural SIV infection of other non-human primates (Keele et al., 2009). This original notion was based off limited data from two studies where one chimpanzee was infected naturally with SIVcpz, and two primates challenged with SIVcpz. Unlike HIV-1 in humans, these studies showed that the chimpanzees did not present signatures of HIV infection such as loss of T-cell function and decline in CD4+ T cells (Keele et al., 2009). However, through long-term studies following chimpanzees at the Gombe National Park in Tanzania this hypothesis was proved false. Similarly to HIV-1, recent studies of the wild living chimpanzees in this area have shown that SIVcpz infection is pathogenic and associated with AIDS-like disease including CD4+ T-cell depletion and similar morbidity and mortality rates (Keele et al., 2009; Rudicell et al., 2010).

The Gombe National Park located in western Tanzania spans twenty square miles of forest and is home to the Gombe Stream Research Center, founded in 1965 by Jane Goodall. Within the park are three separate chimpanzee communities known as Kalande, Kasekela, and Mitumba (Goodall, 1983). Our basic understanding of primates is largely due to Goodall's work with these communities, as each member has been under continuous observation for at least thirty years. The two largest communities the Kasekela and Mitumba, have been studied extensively by a research team led by Jane Goodall, and information regarding their social structure, individual life histories, and

reproductive and social behavior is well documented (Goodall, 1983; Keele et al., 2009). The chimpanzees in this area have become increasingly more endangered due to human population growth and deforestation in the area, and chimpanzees living in this area have become increasing more isolated (Keele et al., 2009; Thaxton, 2006). In addition, all three chimpanzee communities have a growing number of SIVcpz infected individuals (Keele et al., 2009).

Similar to HIV-1, sexual contact and mating within the community is the most common form of SIVcpz, as well as mother to infant SIVcpz transmission through breast milk has also been seen (Keele et al., 2009; Rudicell et al., 2010). SIVcpz infected individuals have been studied post-mortem and found to have exhibited severe lymphopenia, follicular hyalinization in the spleen, and liver and muscle atrophy, as well as destruction of the gut associated lymphoid tissues (GALT); these findings all agree with the hallmark symptoms of an AIDS-like illness (Keele et al., 2009). SIVcpz infection also has been shown to lead to a 10-16 fold increase risk of death compared to uninfected cohorts (Keele et al., 2009; Rudicell et al., 2010). Efforts from the scientific community have been made to intervene and attempt to save this declining community (Barbian et al., 2015; Rudicell et al., 2010).

Since these primate communities live in the wild, typical anti-retroviral therapy such as HAART, where constant administration of the drug is needed, would not be a realistic option. One potential option would be gene delivery of an antibody based reagent through the use of Adeno-Associated virus (AAV) as a gene-therapy vector. AAV, a non-virulent commensal virus found ubiquitously in humans, is a member of the parvoviridae family has been used in primate and human clinical trials and has been

shown to be tolerated and relatively safe (Balazs et al., 2012; Balazs and West, 2013; Gardner et al., 2015). Efforts to further reduce immunogenicity are described in Appendix A of this thesis. Broadly neutralizing antibodies have been shown to protect against a chimeric simian-human immunodeficiency virus (SHIV) in non-human primates (Barouch et al., 2013; Gardner et al., 2015; Shingai et al., 2013). The goal of this study was to develop an antibody based reagent that can be delivered through AAV to SIVcpz infected chimpanzees in the wild (Figure 1).

Since SIV and HIV both utilize CD4 as well as co-receptor binding to gain entry into the host cell, and because of the high sequence similarity between human and simian CD4 was observed (Figure 2), our collaborators at UPENN performed a screen of CD4 binding site antibodies in an in-vitro neutralization assay against a panel of HIV, SIVcpz and SIVgor strains (Barbian et al., 2015). Unfortunately, none of the CD4bs antibodies were able to neutralize the SIV strains despite showing great potency against HIV (Figure 3) (Barbian et al., 2015).

Previous published work from the Bjorkman lab described a new class anti-HIV reagents composed of the first two domains of CD4 linked to the N-terminus of an IgG that recognizes the CD4 induced co-receptor binding site of the HIV envelope trimer (West et al., 2010). We found that these bivalent reagents were expressed well, and were relatively stable under typical storage conditions. These reagents also showed great promise as therapeutic reagent demonstrating broad neutralization capabilities against a panel of HIV-1 isolates equal to or greater than many broadly neutralizing antibodies at the time (West et al., 2010).

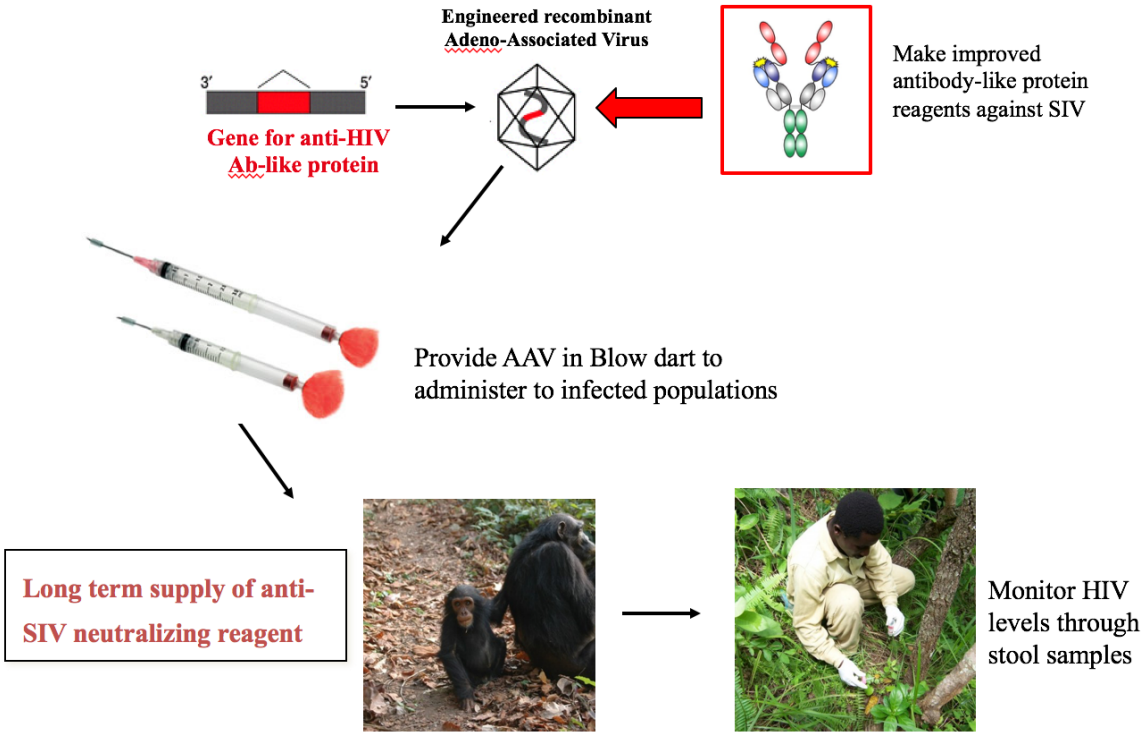

Figure 1. Schematic of experimental outline for administration of AAV expressing anti-SIV antibody reagents in the wild.

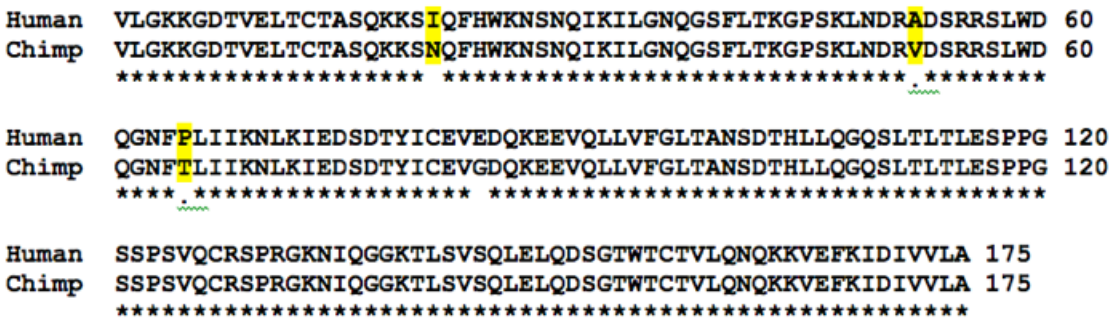

Figure 2. Amino acid sequence comparison of human and chimpanzee CD4 domains 1-2. Amino acid sequences of CD4 from human and chimpanzees show a 98% sequence identity between the two proteins. Amino acid differences are highlighted in yellow.

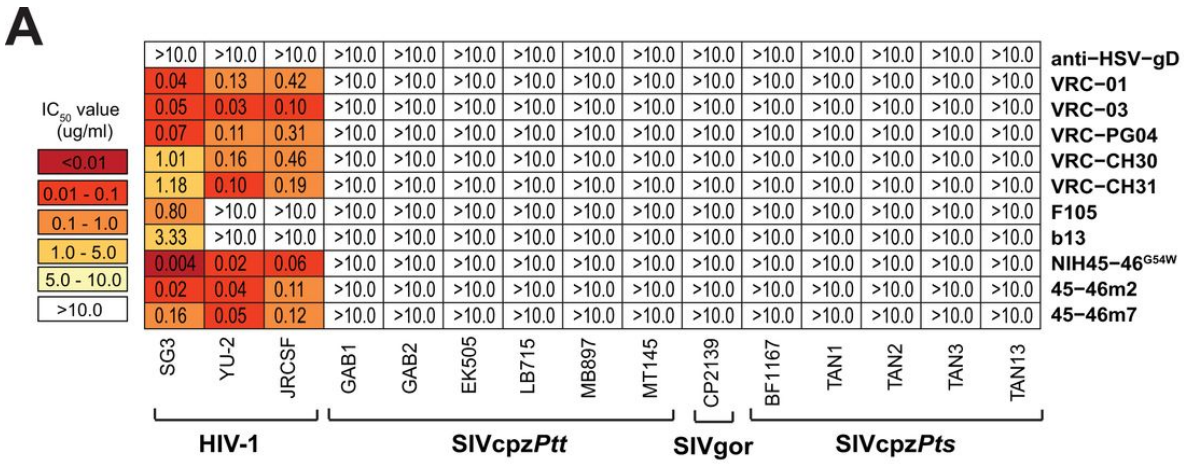

Figure 3.* Neutralizing capacity of CD4 binding site (CD4bs) antibodies. (A) The ability of CD4bs monoclonal antibodies (listed on the right) to neutralize HIV-1, SIVcpz, and SIVgor strains (listed on the bottom) is shown. Numbers indicate IC_{50}s (in micrograms per milliliter) in TZM-bl cells, averaged from three different experiments, with a heat map indicating the relative neutralization potency. The highest antibody concentration was 10 µg/ml. A herpes virus antibody (anti-HSV-gD) was used as a negative control.

*Adapted from Figure 2 of Barbian, H. J., Decker, J.M., Bibollet-Ruche, F., **Galimidi, R.P** et al. (2015). "Neutralization properties of simian immunodeficiency viruses infecting chimpanzees and gorillas." MBio **6**(2).

Our contribution to this SIVcpz study was the development of second generation reagents based on the CD4-CD4i antibody architecture in a deliverable AAV format. Because of the high sequence similarity between domains 1-2 of human and chimpanzee CD4, we believed that our previously designed reagents may be effective against chimpanzee SIV strains (Figure 4).

Second generation CD4-CD4i antibody reagents were designed to containing different protein linkers (Table 1; and described in greater detail in Chapter 4) in an attempt to see if rigidity and length of the linker contributed to potency. CD4-CD4i Antibody-peptide fusion constructs were designed to include CCR5-mimetic peptides at the C-terminus of the Fc. These CCR5-mimetics had been previously shown to inhibit HIV-1 infection in vitro (Chiang et al., 2012; Kwong et al., 2011).

Lastly, a CD4-CD4i antibody fusion construct was designed to include the FDA approved entry-inhibitor Fuzeon at the C-terminus of the Fc region. Fuzeon, or T-20, is a synthetic peptide corresponding to the HR-2 domain of gp41 was found to inhibit fusion through disruption of the gp41 conformational changes associated with membrane fusion (Kilby et al., 1998). T-20 was the first of a novel class of anti-retroviral drugs used in combination therapy for the treatment of HIV-1 infection (Harris et al., 2012). Due to bioavailability and the known short half-life of peptide drugs, T-20 must be administered twice daily through subcutaneous injection. However effective, due to its complicated synthesis process, prescribed dosage, and limited availability, T-20 regimens currently cost an estimated $25,000 per person per year (Harris et al., 2012). Currently, because HAART treatment has been found to be so effective, T-20 is only taken by patients who

are infected with multi-drug resistant forms of HIV-1 (Harris et al., 2012). We proposed that the fusion of T-20 to the CD4i based reagents could enhance neutralization of HIV-1 In addition, a lower effective dose would be needed for this reagent due to its multivalency and the incorporation of an Fc would increase the half-life in-vivo through FcRn mediated antibody recycling (Murphy et al., 2012).

Figure 4 depicts schematics for all of the second generation reagents designed.

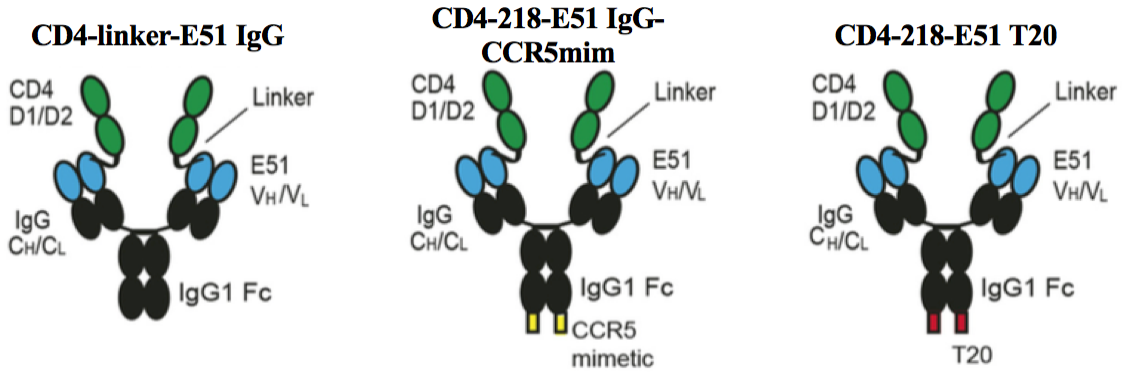

Figure 4. Schematic of antibody based reagents

Materials and Methods

Materials. Genes encoding the variable regions (variable heavy and variable light, V_H and V_L, or the intact light chain V_L-C_L, where C_L refers to the constant light domain) of the E51Ab were synthesized (BlueHeron Biotechnologies or Integrated DNA Technologies). Intact IgG genes were constructed by subcloning the relevant variable sequences onto a human IgG1 sequence.

CD4-IgG heavy chain constructs (denoted by the prefix $CD4_{HC\text{-}}$) by fusing the DNA encoding the CD4 hydrophobic leader sequence and first two domains (D1-D2; residues 1 to 182 of the mature CD4 protein) first to a $(Gly_4Ser)7$ (noted as GS7) linker sequence flanked by restriction sites NgOMIV and NheI, to the N-terminus of the mature E51 IgG sequence. Various other synthetic linkers (Table 1) were used, and were swapped out of the plasmid through restriction digest cloning. Oligos corresponding to CCR5 and gp41 mimetic peptides were synthesized and pieced together through sticky end PCR and cloned into the CD4-CD4i construct through restriction digest cloning.

Protein expression and purification.

All other constructs were subcloned into the mammalian expression vector pTT5 (NRC Biotechnology Research Institute), and the corresponding proteins were expressed transiently in suspension HEK 293-6E cells (NRC Biotechnology Research Institute) using 25-kDa linear polyethylenimine (PEI) (Polysciences) as described previously (West et al., 2010). The heavy chain and light chain vectors were mixed at a 1:1 ratio by mass. Cell culture supernatants were collected six days post transfection. Supernatants were passed over protein A resin (Thermo Fisher Scientific), eluted using pH 3.0 citrate buffer,

and then immediately neutralized. All reagents were then subjected to size exclusion chromatography in 20 mM Tris (pH 8.0)-150 mM NaCl using a Superdex 200 16/60 or 10/30 column (GE Healthcare). Final yields of purified reagents are given in Table S1 in the supplemental material.

In vitro neutralization assays. A previously described pseudovirus neutralization assay that measures the reduction in luciferase reporter gene expression in the presence of a potential inhibitor following a single round of pseudovirus infection in TZM-bl cells was used to evaluate the neutralization potencies of the reagents. Pseudoviruses were generated by cotransfection of HEK 293T cells with an Env expression plasmid and a replication-defective backbone plasmid. Neutralization assays were performed either by our laboratory or by the Hahn lab as described (Barbian et al., 2015). Briefly, for all assays done in-house, each sample was tested in triplicate (our assays) or duplicate (CAVD assays), with 200 infectious viral units per well incubated with a threefold dilution series and with 75 μg/ml DEAE-dextran. After a 1-h incubation at 37°C, 10,000 TZM-bl cells were added to each well and incubated for 2 days. Cells were then lysed and assayed for luciferase expression using BriteLite plus (PerkinElmer) and a Victor3 luminometer (PerkinElmer). Percentage neutralization was determined by calculating the difference in luminescence between test wells (cells plus virus plus reagent) and cell control wells (cells only), dividing this value by the difference between the virus control wells (cells plus virus) and cell control wells, subtracting from 1, and multiplying by 100. Nonlinear regression analysis was used to calculate concentrations at which half-maximal inhibition was observed (IC_{50}s).

Linker ID	Linker Composition
L1	GlySer-polyPro(Glyc)-polyPro(Glyc)-polyPro(Glyc)
L3	GlySer-polyPro-GlySer(Glyc)-polyPro
L5	GlySer-polyPro-b2m-polyPro
L7	polyPro-b2m-GlySer-b2m-GlySer
L8	GlySer-polyPro-b2m-GlySer-b2m-polyPro
L14	GlySer-polyPro-ZAG-polyPro
L17	GlySer-GlySer-ZAG-GlySer-ZAG-polyPro
218	GSTSGSGKPGSGEGSTKGGSTSGSGKPGSGEGSTKGG STSGSGKPGSGEGSTKG
(G4S)7	GGGGSGGGGSGGGGSGGGGSGGGGSGGGGSGGGGS

Table 1. Description of structured linker designs. $(Gly_4Ser)_n$=Gly-Gly-Gly-Gly-Ser sequence with n number of repeats; GlySer = (N-term: $AGS(GGS)_3$; Middle: $(GGS)_4$; C-term: $(GGS)_3GAS]_2S$); GlySer(Glyc)=Gly-Gly-Ser sequence with an embedded potential N-linked glycosylation site (Asn-Ser-Ser); polyPro=proline-rich hinge sequence from IgA1; polyPro(Glyc)=proline-rich hinge sequence from IgA1 with an embedded potential N-linked glycosylation site (Asn-Ser-Ser); β2m=β-2-microglobulin; Ub=ubiquitin; ZAG=Zn-α2-glycoprotein

Results

Linkage between CD4 domain and CD4i antibody effects neutralization potency. CD4-CD4i antibody reagents containing linkers of various length, glycosylation, and flexibility were tested against a panel of HIV and SIV strains (Table 1). An antibody against a herpes viral protein (gD) was used as a control in order to determine if the parental antibody was instrumental at all in neutralization. In general, CD4-CD4i constructs neutralized viral strains more effectively than sCD4 alone. Contribution of the E51 antibody can be seen when comparing data against anti-gD reagents.

Interestingly, previously published CD4-GS7-E51 IgG was among the worst neutralizers in this assay, despite previous data proving otherwise. This raises questions about the stability of the protein. CD4-E51 reagents containing L7 and L8 linkers displayed the weakest capacity to neutralize viral strains effectively only neutralizing 1 viral strain each. Both L7 and L8 linkers were designed to be more rigid, each containing two copies of the beta-2 microglobulin (b2m) protein. L5, a similar linker containing only one copy of b2m performed much better neutralizing 8 out of the 10 strains tested. The most promising linkers by far were those with the shorter flexible linkers, L1 and 218 respectively, suggesting that the ability to orient rather than distance is preferred.

Moreover, the stability of these linkered reagents must be revisited. The most promising linker 218 showed signs of degradation 1 month post production after storage in Phosphate Buffered Saline solution at 4°C (Figure 5). Edman Sequencing of a similar reagent containing a 218 linker showed cleavage is occurring within the linker itself and not at the junction sites (data not shown).

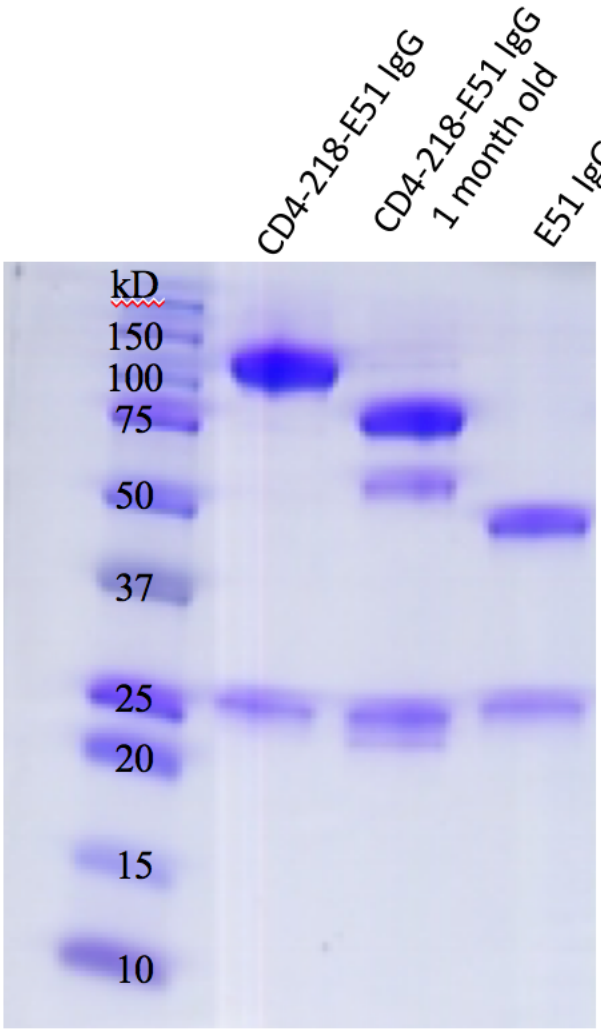

Figure 5. SDS Page analysis shows proteolytic cleavage of 218 linker over time. Freshly prepared CD4-218-E51 IgG was compared to a prep of the same reagent expressed and purified one month earlier. The gel clearly shows proteolytic cleavage within the linker.

		IC_{50} ug/ml												
Virus	**Virus Group**	**sCD4**	**E51 IgG**	**anti-GD IgG**	**CD4 GS7 anti-GD IgG**	**CD4 GS7 E51 IgG**	**CD4 218 E51 IgG**	**CD4 L1 E51 IgG**	**CD4 L3 E51 IgG**	**CD4 L5 E51 IgG**	**CD4 L7 E51 IgG**	**CD4 L8 E51 IgG**	**CD4 L14 E51 IgG**	**CD4 L17 E51 IgG**
SG3	**HIV-1**	**0.17**	> 10	> 10	0.98	0.2	0.01	0.04	0.02	0.03	0.49	2.79	0.01	0.09
YU-2	**HIV-1**	1	> 10	> 10	> 10	> 10	0.05	0.07	0.06	0.14	> 10	> 10	0.2	0.49
JRCSF	**HIV-1**	> 10	> 10	> 10	> 10	> 10	0.9	5.86	2.21	4.53	> 10	> 10	8.46	> 10
EK505	**SIVcpz*Ptt***	> 10	> 10	> 10	> 10	> 10	3.77	10.53	6.73	> 10	> 10	> 10	> 10	> 10
GAB-1	**SIVcpz*Ptt***	0.16	> 10	> 10	4.1	4.21	0.09	0.17	0.07	0.16	9.7	> 10	0.2	0.01
GAB-2	**SIVcpz*Ptt***	0.57	> 10	> 10	9.02	> 10	0.24	0.54	0.29	0.54	> 10	> 10	0.62	1.45
LB715	**SIVcpz*Ptt***	6.63	> 10	> 10	8.68	> 10	1.02	3.39	2.43	3.49	> 10	> 10	4.9	> 10
MB897	**SIVcpz*Ptt***	> 10	> 10	> 10	> 10	> 10	8.01	> 10	> 10	> 10	> 10	> 10	> 10	> 10
MT145	**SIVcpz*Ptt***	1.67	> 10	> 10	> 10	> 10	0.34	0.87	0.42	0.87	> 10	> 10	1.04	3.52
BF1167	**SIVcpz*Pts***	> 10	> 10	> 10	> 10	> 10	0.25	3.13	1.82	4.15	> 10	> 10	7.25	> 10
TAN-1	**SIVcpz*Pts***	> 10	> 10	> 10	> 10	> 10	4.82	> 10	NT	NT	> 10	> 10	> 10	> 10
TAN-2	**SIVcpz*Pts***	2.68	> 10	> 10	> 10	> 10	0.16	0.35	NT	NT	> 10	> 10	0.54	1.62
TAN-3	**SIVcpz*Pts***	3	> 10	> 10	8.58	> 10	1.05	4.54	NT	NT	> 10	> 10	7.18	> 10
TAN-13	**SIVcpz*Pts***	2.81	> 10	> 10	> 10	> 10	0.24	0.86	NT	NT	> 10	> 10	1.17	3.37
SIVgor	**SIVgor**	4.94	> 10	> 10	> 10	> 10	0.48	0.96	NT	NT	> 10	> 10	2.24	5.24

<1 ug/ml	1-3 ug/ml	3-7 ug/ml	7-10 ug/ml	>10 ug/ml

Table 2. Second Generation CD4-CD4i Broadly neutralizing antibody reagents potently neutralize SIV strains found in chimpanzees (SIVcpz) and gorillas (SIVgor).

The addition of a C-terminal fusion inhibitor seemed to only modestly improve the overall reagent. (Table 3). The greatest improvements were found with the CCR5 mimetic peptide Y3. The addition of T-20 peptide as well as Y3 allowed for neutralization of previously resistant strains, suggesting the functionality of the peptide.

Discussion

Through this study we designed potent broadly neutralizing antibody reagents capable of neutralizing both HIV and SIV strains. This work provides a promising new avenue for CD4-CD4i antibody reagents. Further investigation to optimize the linker between the CD4 D1-D2 domains and the CD4i antibody as linker choice was an important determinate in predicting neutralization activity.

Virus	Virus Group	IC_{50} ug/ml CD4 218 E51 IgG	CD4 218 E51 IgG -E3	CD4 218 E51 IgG-Y3	CD4 218 E51 IgG-T20
SG3	**HIV-1**	0.15	0.25	0.07	0.44
YU-2	**HIV-1**	0.72	1.11	0.53	1.28
JRCSF	**HIV-1**	NT	NT	5.89	NT
EK505	**SIVcpz*Ptt***	NT	NT	8.83	0.84
GAB-1	**SIVcpz*Ptt***	0.82	0.35	0.15	0.59
GAB-2	**SIVcpz*Ptt***	3.70	2.61	1.24	3.08
LB715	**SIVcpz*Ptt***	3.88	7.19	0.44	2.29
MB897	**SIVcpz*Ptt***	7.02	NT	2.94	7.75
MT145	**SIVcpz*Ptt***	2.10	2.00	0.08	1.69
BF1167	**SIVcpz*Pts***	1.95	2.26	0.80	1.22
TAN-1	**SIVcpz*Pts***	3.91	7.82	1.57	1.61
TAN-2	**SIVcpz*Pts***	1.59	2.69	0.68	1.73
TAN-3	**SIVcpz*Pts***	1.66	1.84	0.66	1.08
TAN-13	**SIVcpz*Pts***	1.96	2.92	0.60	0.55
SIVgor	**SIVgor**	1.34	4.28	0.98	0.86

<1 ug/ml	1-3 ug/ml	3-7 ug/ml	7-10 ug/ml	>10 ug/ml

Table 3. Linkage between CD4 domain and CD4i antibody effects neutralization potency. In-vitro neutralization assay data of CD4-LINKER-CD4i Antibody reagents. Numbers indicate $IC_{50\ in}$ microgram per milliliter. Heat map indicates relative neutralization ability with warmer colors indicating greater neutralization potency.

References:

Balazs, A. B., Chen, J., Hong, C. M., Rao, D. S., Yang, L., & Baltimore, D. (2012). Antibody-based protection against HIV infection by vectored immunoprophylaxis. *Nature, 481*(7379), 81-84. doi:10.1038/nature10660

Balazs, A. B., & West, A. P., Jr. (2013). Antibody gene transfer for HIV immunoprophylaxis. *Nat Immunol, 14*(1), 1-5. doi:10.1038/ni.2480

Barbian, H. J., Decker, J. M., Bibollet-Ruche, F., Galimidi, R. P., West, A. P., Jr., Learn, G. H., . . . Hahn, B. H. (2015). Neutralization properties of simian immunodeficiency viruses infecting chimpanzees and gorillas. *MBio, 6*(2). doi:10.1128/mBio.00296-15

Barouch, D. H., Whitney, J. B., Moldt, B., Klein, F., Oliveira, T. Y., Liu, J., . . . Burton, D. R. (2013). Therapeutic Efficacy of Potent Neutralizing HIV-1-Specific Monoclonal Antibodies in SHIV-Infected Rhesus Monkeys. *Nature, 503*(7475), 224-228. doi:10.1038/nature12744

Chiang, J. J., Gardner, M. R., Quinlan, B. D., Dorfman, T., Choe, H., & Farzan, M. (2012). Enhanced Recognition and Neutralization of HIV-1 by Antibody-Derived CCR5-Mimetic Peptide Variants. *Journal of Virology, 86*(22), 12417-12421.

Gardner, M. R., Kattenhorn, L. M., Kondur, H. R., von Schaewen, M., Dorfman, T., Chiang, J. J., . . . Farzan, M. (2015). AAV-expressed eCD4-Ig provides durable protection from multiple SHIV challenges. *Nature, 519*(7541), 87-91. doi:10.1038/nature14264

Goodall, J. (1983). Population Dynamics during a 15 Year Period in one Community of Free-living Chimpanzees in the Gombe National Park, Tanzania. *Zeitschrift für Tierpsychologie, 61*(1), 1-60. doi:10.1111/j.1439-0310.1983.tb01324.x

Harris, M., Nosyk, B., Harrigan, R., Lima, V. D., Cohen, C., & Montaner, J. (2012). Cost-Effectiveness of Antiretroviral Therapy for Multidrug-Resistant HIV: Past, Present, and Future. *AIDS Research and Treatment, 2012*, 595762. doi:10.1155/2012/595762

Keele, B. F., Jones, J. H., Terio, K. A., Estes, J. D., Rudicell, R. S., Wilson, M. L., . . . Hahn, B. H. (2009). Increased mortality and AIDS-like immunopathology in wild chimpanzees infected with SIVcpz. *Nature, 460*(7254), 515-519. doi:10.1038/nature08200

Kilby, J. M., Hopkins, S., Venetta, T. M., DiMassimo, B., Cloud, G. A., Lee, J. Y., . . . Saag, M. S. (1998). Potent suppression of HIV-1 replication in humans by T-20, a peptide inhibitor of gp41-mediated virus entry. *Nat Med, 4*(11), 1302-1307.

Kwong, J. A., Dorfman, T., Quinlan, B. D., Chiang, J. J., Ahmed, A. A., Choe, H., & Farzan, M. (2011). A Tyrosine-Sulfated CCR5-Mimetic Peptide Promotes Conformational Transitions in the HIV-1 Envelope Glycoprotein. *Journal of Virology, 85*(15), 7563-7571.

Murphy, K., Travers, P., Walport, M., & Janeway, C. (2012). *Janeway's immunobiology*. New York: Garland Science.

Rudicell, R. S., Holland Jones, J., Wroblewski, E. E., Learn, G. H., Li, Y., Robertson, J. D., . . . Wilson, M. L. (2010). Impact of Simian Immunodeficiency Virus

Infection on Chimpanzee Population Dynamics. *PLoS Pathog, 6*(9), e1001116. doi:10.1371/journal.ppat.1001116

Sharp, P. M., & Hahn, B. H. (2011). Origins of HIV and the AIDS pandemic. *Cold Spring Harb Perspect Med, 1*(1), a006841. doi:10.1101/cshperspect.a006841

Shingai, M., Nishimura, Y., Klein, F., Mouquet, H., Donau, O. K., Plishka, R., . . . Martin, M. A. (2013). Antibody-mediated immunotherapy of macaques chronically infected with SHIV suppresses viraemia. *Nature, advance online publication*. doi:10.1038/nature12746

Thaxton, M. (2006). Why the Chimpanzees of Gombe National Park are in Jeopardy. Retrieved from http://www.prb.org/Publications/Articles/2006/WhytheChimpanzeesofGombeNationalParkAreinJeopardy.aspx

West, A. P., Jr., Galimidi, R. P., Foglesong, C. P., Gnanapragasam, P. N., Klein, J. S., & Bjorkman, P. J. (2010). Evaluation of CD4-CD4i antibody architectures yields potent, broadly cross-reactive anti-human immunodeficiency virus reagents. *J Virol, 84*(1), 261-269. doi:10.1128/JVI.01528-09

Chapter Three

Intra-spike crosslinking overcomes antibody evasion by HIV-1

This chapter describes the development of a series of broadly neutralizing antibody-based reagents capable of intraspike cross-linking on an HIV envelope spike. These bivalent engineered reagents bind with high-avidity leading to >100 fold average increased neutralization potencies. These data further validate a hypothesis first described in Pamela Bjorkman's lab suggesting that the low spike density on HIV-1 virions evolved to facilitate antibody evasion. Here we also describe a novel molecular tool to measure distances on a virtually sub-nanometer scale.

This work was published as:

Galimidi, R. P., Klein, J. S., Politzer, M. S., Bai, S., Seaman, M. S., Nussenzweig, M. C., et al. (2015). Intra-spike crosslinking overcomes antibody evasion by HIV-1. *Cell*, *160*(3), 433–446. http://doi.org/10.1016/j.cell.2015.01.016

SUMMARY

Antibodies developed during HIV-1 infection lose efficacy as the viral spike mutates. We postulated that anti-HIV-1 antibodies primarily bind monovalently because HIV's low spike density impedes bivalent binding through inter-spike crosslinking, and the spike structure prohibits bivalent binding through intra-spike crosslinking. Monovalent binding reduces avidity and potency, thus expanding the range of mutations permitting antibody evasion. To test this idea, we engineered antibody-based molecules capable of bivalent binding through intra-spike crosslinking. We used DNA as a "molecular ruler" to measure intra-epitope distances on virion-bound spikes and construct intra-spike crosslinking molecules. Optimal bivalent reagents exhibited up to 2.5 orders-of-magnitude increased potency (>100-fold average increases across virus panels) and identified conformational states of virion-bound spikes. The demonstration that intra-spike crosslinking lowers the concentration of antibodies required for neutralization supports the hypothesis that low spike densities facilitate antibody evasion and the use of molecules capable of intra-spike crosslinking for therapy or passive protection.

INTRODUCTION

The HIV-1 envelope (Env) spike trimer, a trimer of gp120 and gp41 subunits, is the only target of neutralizing antibodies. The spike utilizes antibody-evasion strategies including mutation, glycan shielding, and conformational masking (West et al., 2014). While important, these features are not unique to HIV-1: other viruses employing these strategies elicit IgG antibody responses that provide sterilizing immunity or viral clearance. A potentially unique antibody-evasion strategy for HIV-1 involves hindering IgGs from using both antigen-binding fragments (Fabs) to bind bivalently to spikes (Klein and Bjorkman, 2010; Mouquet et al., 2010). This is accomplished by the small number and low density of Env spikes (Chertova et al., 2002a; Liu et al., 2008; Zhu et al., 2006), which prevent most IgGs from inter-spike crosslinking (bivalent binding between spikes), and the architecture of the Env trimer, which impedes intra-spike crosslinking (bivalent binding within a spike trimer) (Klein et al., 2009a; Luftig et al., 2006).

On a typical virus with closely-spaced envelope spikes, an IgG antibody can bind using both Fabs to crosslink neighboring spikes, leading to a nearly irreversible antibody-antigen interaction (Mattes, 2005). Avidity effects from bivalent binding of IgG antibodies have been shown to be critical for neutralization of many viruses, including polio and influenza (Icenogle et al., 1983; Schofield et al., 1997). By contrast, the small number of spikes (~14) present on the surface of HIV-1 (Chertova et al., 2002a; Liu et al., 2008; Zhu et al., 2006) impedes simultaneous engagement of both antibody combining sites (Klein and Bjorkman, 2010; Mouquet et al., 2010): most spikes are separated by distances that far exceed the ~15 nm reach of the two Fab arms of an IgG

(Liu et al., 2008; Zhu et al., 2006) (Figure 1A). Inter-spike crosslinking might still be possible if spikes could freely diffuse within the viral membrane. However, cryo-electron tomography of HIV-1 (Zhu et al., 2006) and evidence for interactions between the cytoplasmic tail of gp41 and the matrix protein of HIV (Bhatia et al., 2009; Crooks et al., 2008; Yu et al., 1992) suggest that a virion's spike distribution is likely to be relatively static over time scales relevant to neutralization. Taken together, the mechanisms to hinder inter- and intra-spike crosslinking imply that most anti-HIV-1 IgGs bind monovalently to virions.

It seems an unlikely coincidence that HIV-1, among the most adept of viruses at evading antibody-mediated neutralization, has an unusually low density of surface envelope spikes with restricted mobility as well as an unusually high mutation rate. We speculated that HIV-1 evolved a low spike density to hinder bivalent binding by antibodies(Klein and Bjorkman, 2010) and postulated that the combination of predominantly monovalent IgG binding and HIV-1's rapid mutation rate creates an additional effective antibody evasion strategy (Klein and Bjorkman, 2010). If the affinity between an IgG Fab and a viral spike is high enough, monovalent IgG binding to a virion should not, in and of itself, hinder or prevent viral neutralization. Thus affinity-matured anti-Env IgGs raised against a particular strain of virus can effectively neutralize autologous virus (Klein et al., 2013; West et al., 2014). However, upon mutation of an antibody epitope on Env, the low affinity of the monovalent Fab-antigen interaction would result in either complete loss of neutralization or neutralization only at very high concentrations. These concepts are illustrated by comparisons of binding and neutralization for variants of IgG and Fab forms of palivizumab, a neutralizing IgG

against respiratory syncytial virus (RSV) (Wu et al., 2005), a virus with a high density of Env spikes (Liljeroos et al., 2013). Palivizumab Fabs with fast off-rates/low affinities exhibited 2-3 log improvements in neutralization potencies when converted to bivalent IgGs and the potencies of the IgGs were not affected by mutations that increased the off-rates of their corresponding monovalent Fabs by >100-fold (Wu et al., 2005), illustrating the importance of avidity for IgGs with weak or moderate affinity Fabs. However, high affinity/slow off-rate palivizumab Fabs were equally as potent as their IgG counterparts, which could bind bivalently to RSV through inter-spike crosslinking. In the palivizumab example, binding and neutralization potencies were evaluated for a single strain of virus and antibodies. In the case of HIV-1, we are interested in the effects of mutations in the virus on binding of the same antibody, but the effects of mutation are expected to be similar. Thus we postulate that avidity effects through bivalent binding can serve as a buffer to dampen the effects of viral mutations on neutralization potencies of IgGs.

This line of reasoning suggests that bivalent HIV-1 binders would be optimal for passive prevention or immunotherapy, but because inter-spike distances are not constant even on a single virion, it is not possible to engineer reagents that could consistently accomplish inter-spike crosslinking. In contrast, reagents that can bind bivalently to a single trimeric spike would function independently of both spike density and distribution (Pace et al., 2013). To test the idea that intra-spike crosslinking results in increased neutralization potency, we used molecular rulers to map epitopes on virion-bound HIV-1 spikes and created new molecules designed to synergize through bivalent interactions within single Env trimers (Figure 1A). We developed methods to produce multiple combinations of Env-binders separated by different distances by attaching broadly

neutralizing antibody (bNAb) Fabs to variable-length double-stranded DNA (dsDNA) (Figure 1B; Figure S1). We chose dsDNA as a linker because its long persistence length (460-500 Å (Bednar et al., 1995) compared with ~30 Å for peptides (Zhou, 2004)) permits its use as a molecular ruler with 3.4 Å/basepair (bp) increments. Here we show that homo- and hetero-diFabs joined by optimal-length dsDNA bridges can achieve neutralization potency increases of 2-3 orders of magnitude and provide evidence that the synergy results from intra-spike crosslinking. Upon determining the optimal distances between Env trimer-bound Fabs, we show that it is possible to convert the dsDNA bridge to a protein linker to create a protein-based reagent with similar synergistic properties. These results illustrate the importance of avidity in antibody-pathogen interactions, elucidate mechanisms by which HIV-1 evades the host immune system, and are relevant to the choice of potential protein therapeutics to be delivered to prevent or treat HIV-1 infections.

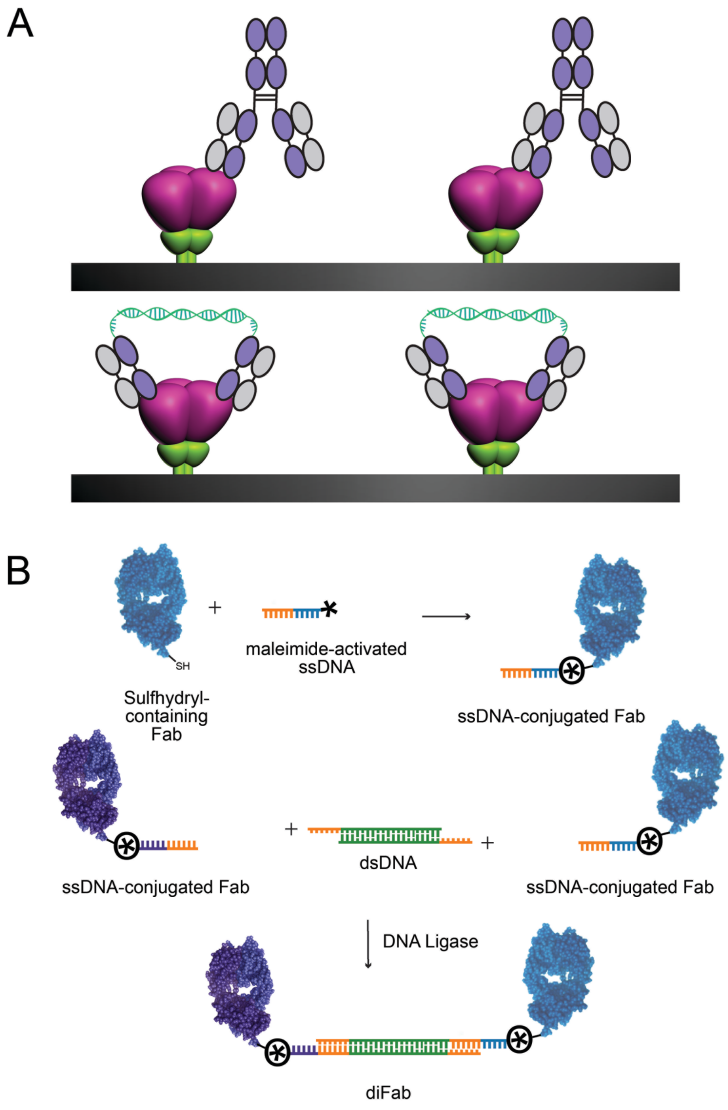

Figure 1. IgG and diFab reagents binding to viral spikes. (**A**) Top: IgG binding monovalently to spikes on HIV-1 surfaces, which include a small number (~14) and low density of Env (Chertova et al., 2002a; Liu et al., 2008; Zhu et al., 2006)**.** Bottom: Homo-diFab reagent binding bivalently to HIV-1 Env by intra-spike crosslinking. Schematic representations of Env adapted from figures in (Liu et al., 2008). (**B**) Schematic of method used to produce homo- and hetero-diFabs. See also Figure S1.

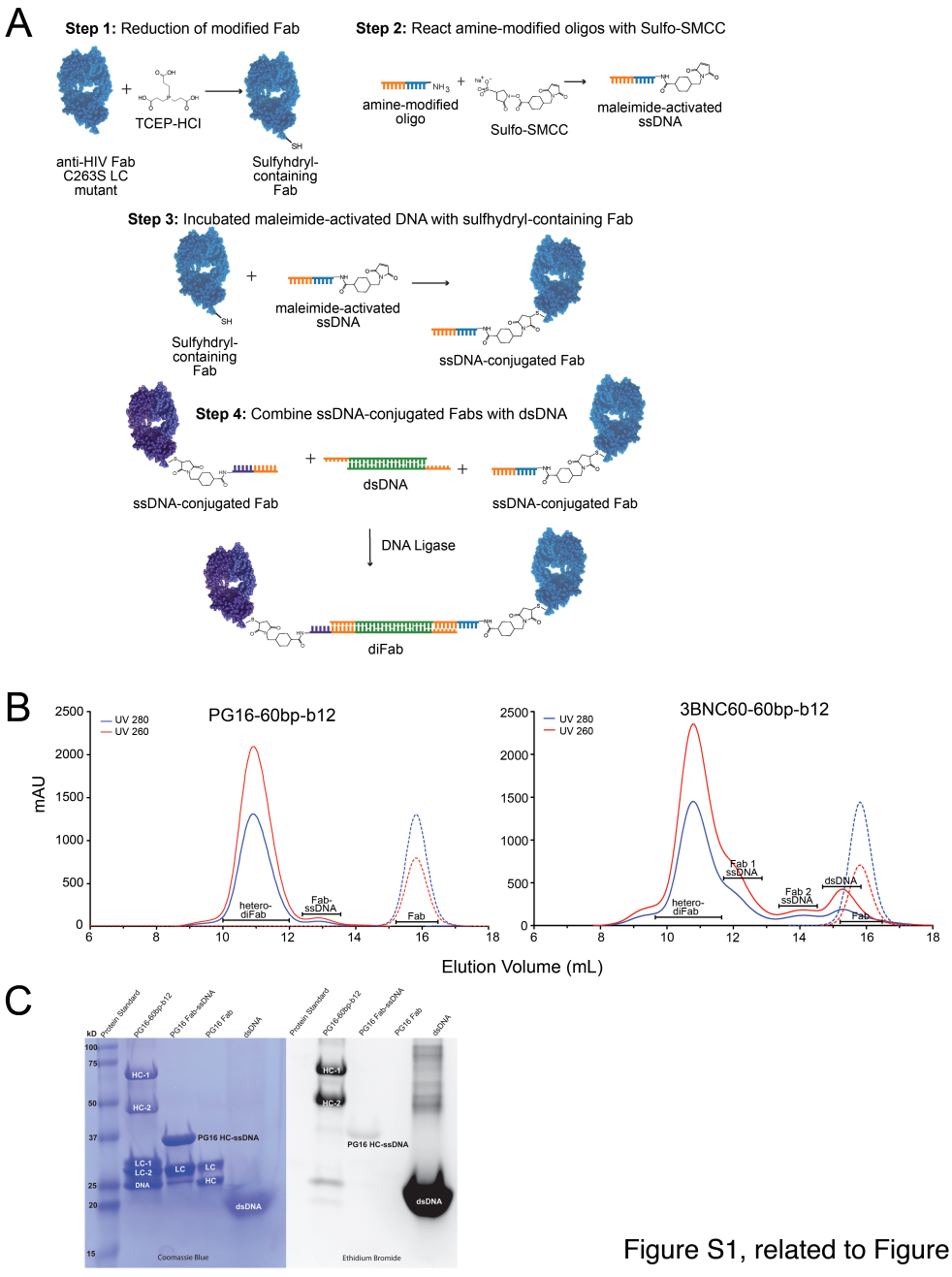

Figure S1, related to Figure 1

Supplemental Figure 1. Production of Fabs connected with dsDNA linkers, is related to Figure 1 by showing details in the production and characterization of homo- and hetero-diFabs.

RESULTS

Homo-diFabs exhibit length-dependent avidity effects consistent with intra-spike crosslinking

Fabs were modified to contain a free thiol and then conjugated to maleimide-activated single-stranded DNA (ssDNA) (Figure 1B). Different lengths of dsDNA (designed to lack secondary structures (Zadeh et al., 2011) (Supplementary Experimental Procedures) were annealed with and ligated to the ssDNA-Fab conjugates to create homo- or hetero-diFabs, in which the two Fabs were the same or different, respectively. Dynamic light scattering confirmed that conjugates with longer DNA bridges were more extended (Figure 2A), supporting the use of dsDNA as a ruler. Inter-Fab distances calculated from dsDNA lengths were regarded as approximate because the DNA linkers included short regions of ssDNA (persistence length 22 Å) (Chi et al., 2013) to permit orientational flexibility.

We first determined the optimal dsDNA linker for a homo-diFab constructed from 3BNC60, a bNAb against the CD4 binding site (CD4bs) on the gp120 subunit of Env (Scheid et al., 2011b), by evaluating homo-diFabs with different dsDNA lengths using *in vitro* neutralization assays. The 50% inhibitory concentrations (IC_{50}s) against HIV-1 strain 6535.3 depended on the dsDNA length, with the most potent homo-diFab containing a bridge of 62bp (211 Å) (Figure 2B; Figure S2). This length is close to the predicted distance (~198 Å) between the C-termini of adjacent 3BNC60 Fabs bound to the open structure of an HIV-1 trimer (Merk and Subramaniam, 2013) (Figure 3, Figure S3). Bridge lengths of ~60bp also exhibited the best potencies for 3BNC60 homo-diFabs against DU172 HIV-1 and for homo-diFabs constructed from VRC01 (Wu et al., 2010b),

a related CD4bs bNAb (Figure S2). The ~100-fold increased potency of 3BNC60-62bp-3BNC60 compared with 3BNC60 IgG against HIV-1 6535.3 (Figure 2B) suggested synergy resulting from avidity effects due to bivalent binding. The bivalent interaction likely resulted from intra-spike crosslinking rather than inter-spike crosslinking since the latter should not manifest with a sharp length-dependence because inter-spike distances are variable within and between virions (Liu et al., 2008; Zhu et al., 2006).

To formally assess the extent to which inter-spike crosslinking could contribute to synergy, we evaluated homo-diFabs constructed from the V1V2 loop-specific bNAb PG16 (Walker et al., 2009b), which cannot crosslink within a single spike because only one anti-V1V2 Fab binds per Env trimer (Julien et al., 2013c). PG16 homo-diFabs with different dsDNA bridges did not exhibit length-dependent neutralization profiles against strain 6535.3 (Figure 2B) and other viral strains (Figure S2D). However, increased potencies were observed for PG16 homo-diFabs with ≥ 70bp or 80bp (≥248 Å or 272 Å) bridges, perhaps reflecting increased inter-spike crosslinking with longer separation distances (Figure 2B; Figure S2D).

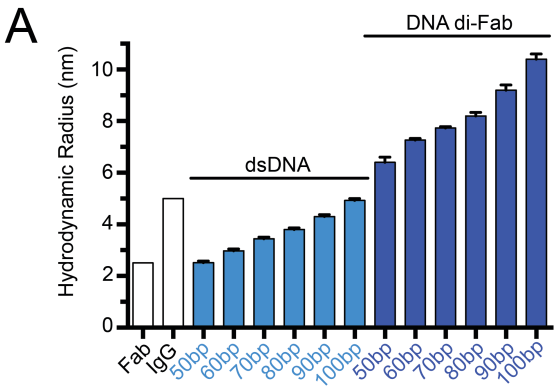

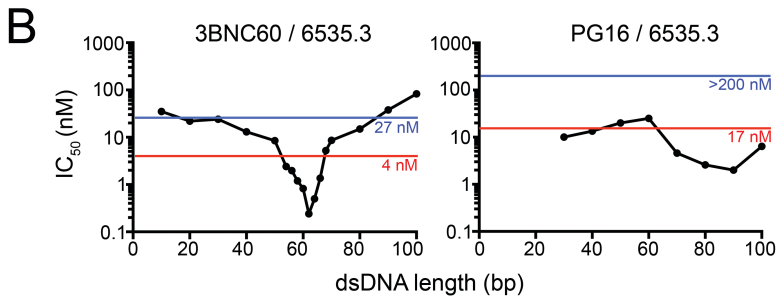

C

			IC$_{50}$ (nM)									
Virus	Clade	Tier	dsDNA	b12-60bp-b12	b12 Fab	b12 IgG	3BNC60-62bp-3BNC60	3BNC60 Fab	3BNC60 IgG	PG16-60bp-PG16	PG16 Fab	PG16 IgG
6535.3	B	1B	>1000	2.7 **(22x)**	360	60	0.24 **(17x)**	27	4.0	7.8 **(2x)**	>200	17
SC422661.8	B	2	>1000	0.55 **(5x)**	9.5	3.0	0.02 **(15x)**	1.0	0.3	1.3 **(4x)**	65.0	4.7
PVO.4	B	3	>1000	>70 **(1x)**	4700	700	0.01 **(10x)**	1.3	0.1	10 **(2x)**	150	16
TRO.11	B	2	>1000	8.9 **(>79x)**	7600	700	0.01 **(20x)**	1.3	0.2	7.8 **(1x)**	>200	6.5
TRJO4551.58	B	3	>1000	>70 **(1x)**	7900	700	0.03 **(<3x)**	4.8	<0.1	0.70 **(3x)**	64	2.1
CAAN5342.A2	B	2	>1000	35 **(20x)**	6800	700	0.16 **(22x)**	6.2	3.6	8.7 **(1x)**	65	6.0
THRO4156.18	B	2	>1000	2.7 **(4x)**	100	10	0.43 **(8x)**	23	3.5	4.9 **(0.5x)**	>200	2.7
RHPA4259.7	B	2	>1000	0.48 **(1x)**	6.0	0.73	0.007 **(43x)**	1.5	0.3	0.07 **(1x)**	1.5	<0.1
Du156.12	C	2	>1000	0.21 **(23x)**	150	4.8	0.03 **(10x)**	9.4	0.3	<0.04 **(1x)**	0.8	<0.1
Du172.17	C	2	>1000	0.35 **(28x)**	100	10	1.0 **(16x)**	210	16	<0.04 **(1x)**	2.6	<0.1
Du422.1	C	2	>1000	0.03 **(67x)**	60	2.0	42 **(>8x)**	>200	>330	<0.04 **(>7x)**	1.0	0.3
ZM197M.PB7	C	1B	>1000	4.9 **(126x)**	1000	620	0.11 **(34x)**	15	3.8	0.42 **(6x)**	5.5	2.4
ZM214M.PL15	C	1B	>1000	3.8 **(11x)**	380	43	0.07 **(24x)**	6.9	1.7	>70 **(1x)**	>200	>330
ZM233M.PB6	C	2	>1000	16 **(44x)**	4500	700	0.08 **(17x)**	14	1.4	<0.04 **(1x)**	<0.1	<0.1
ZM249M.PL1	C	2	>1000	1.1 **(21x)**	240	23	0.01 **(30x)**	2.7	0.3	<0.04 **(1x)**	0.4	<0.1
ZM53M.PB12	C	2	>1000	3.4 **(56x)**	890	190	0.11 **(12x)**	5.2	1.3	<0.04 **(1x)**	1.0	<0.1
ZM109F.PB4	C	1B	>1000	67 **(10x)**	3400	700	0.05 **(6x)**	39	0.3	0.14 **(214x)**	6.7	30
ZM135M.PL10a	C	2	>1000	46 **(15x)**	5900	700	0.03 **(13x)**	3.7	0.4	>70 **(1x)**	>200	>330
CAP45.2.00.G3	C	2	>1000	0.35 **(10x)**	40	3.4	0.3 **(167x)**	>200	50	<0.04 **(1x)**	<0.1	<0.1
CAP210.2.00.E8	C	2	>1000	5.7 **(9x)**	70	50	1.5 **(39x)**	>200	59	0.14 **(1x)**	11.0	<0.1
Q842.d12	A	2	>1000	7.1 **(99x)**	4200	700	0.001 **(90x)**	0.21	0.09	<0.04 **(1x)**	<0.1	<0.1
Q259.d2.17	A	2	>1000	48 **(15x)**	7500	700	0.007 **(4x)**	3.7	0.03	<0.04 **(1x)**	0.61	<0.1
3718.v3.c11	A	2	>1000	<0.04 **(>3100x)**	690	126	12.6 **(>26x)**	>200	>330	<0.04 **(1x)**	<0.1	<0.1
0330.v4.c3	A	2	>1000	60 **(12x)**	5600	700	0.007 **(29x)**	0.62	0.2	<0.04 **(1x)**	<0.1	<0.1
3415.v1.c1	A	2	>1000	2.3 **(23x)**	200	53	0.04 **(22x)**	4.6	0.9	0.07 **(1x)**	1.22	<0.1
Geometric Mean IC$_{50}$ (nM)				3.6			0.08			0.42		
Arithmetic Mean IC$_{50}$ (nM)				18			2.3			2.7		
Mean Fold Improvement Over IgG (Geometric)				**22**			**19**			**2.8**		
Mean Fold Improvement Over IgG (Arithmetic)				**18**			**14**			**2.1**		

>100x	50-100x	30-49x	10-29x	2-9x	≤2x

Figure 2. Characterization of homo-diFabs.

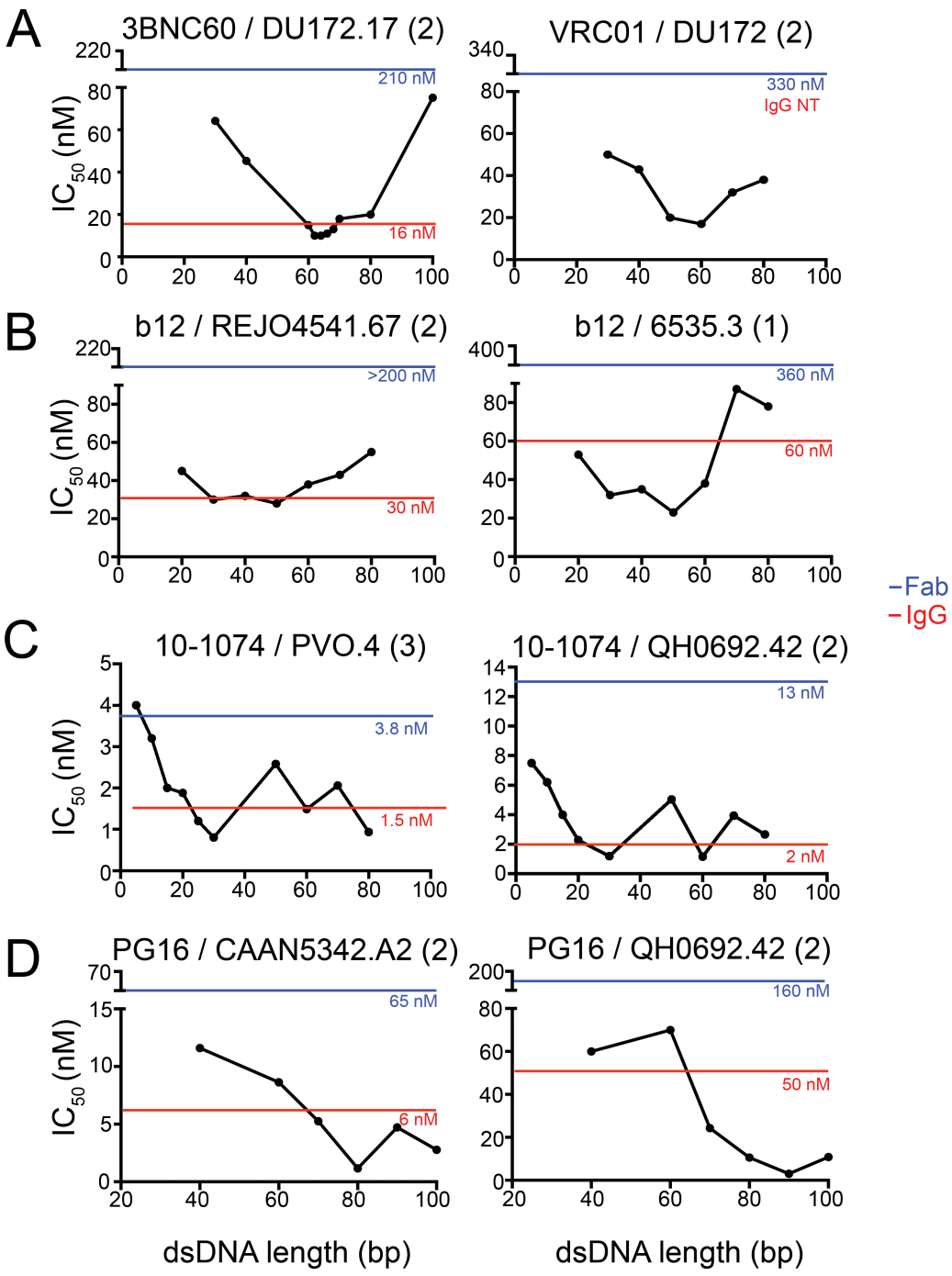

Supplemental Figure 2.

Figure 2. Characterization of homo-diFabs. (**A**) Dynamic light scattering measurements of hydrodynamic radii for IgG and Fab proteins, different lengths of dsDNA alone, and di-Fabs with different dsDNA linkers. (**B**) Effects of dsDNA bridge length on neutralization potencies of 3BNC60 and PG16 homo-diFabs against the Tier 1B HIV-1 strain 6535.3. Neutralization IC_{50}s are plotted against the length of the dsDNA linker. IC_{50}s for the parent IgG and Fab are indicated as red and blue lines, respectively. (**C**) Neutralization of primary HIV-1 strains by b12 and PG16 homo-diFabs, each constructed with a 60bp dsDNA bridge. IC_{50}s are reported for the homo-diFabs, the parental Fabs and IgGs, and dsDNA alone. As a measure of potential synergy, the molar ratio of the IC_{50} values for the IgG and the homo-diFab is listed for each strain in parentheses beside the IC_{50} for the homo-diFab. See also Figure S2.

Supplemental Figure 2. Effects of dsDNA bridge length on neutralization potencies of homo-diFabs, is related to Figure 2 by showing length dependence plots for additional homo-diFab reagents.

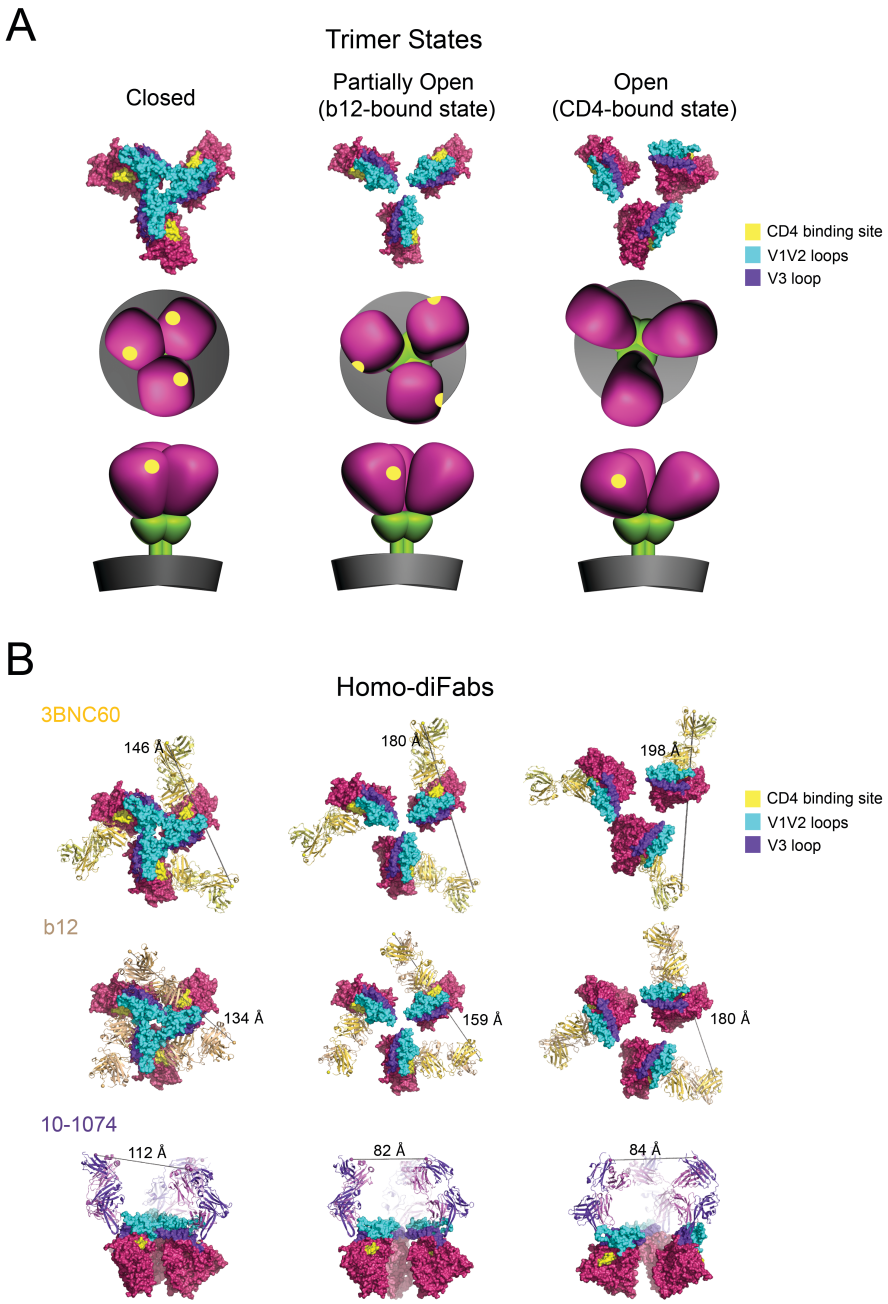

Figure 3. Comparison of intra-spike distances for three conformations found for virion-associated HIV-1 Env spike trimers.

Figure 3. Comparison of intra-spike distances for three conformations found for virion-associated HIV-1 Env spike trimers. (**A**) Three conformations of Env trimers shown as surface representations (top row: gp120 coordinates only) and schematically (bottom two rows). Schematic representations of Env trimers adapted from figures in (Liu et al., 2008). Env spikes are shown as seen from above (top and middle rows) and the side (bottom row). V1V2 loops are cyan, V3 loops are purple, the CD4 binding site is yellow, the remainder of gp120 is maroon, gp41 is green, and the membrane bilayer is gray. The closed structure (PDB code 4NCO) was observed for unliganded trimers (Liu et al., 2008) and trimers associated with Fabs from potent VRC01-like (PVL) antibodies (Lyumkis et al., 2013; Merk and Subramaniam, 2013). The open structure was observed for trimers associated with CD4 or the Fab from the CD4-induced antibody 17b (Merk and Subramaniam, 2013; Tran et al., 2012) (coordinates obtained from S. Subramaniam). The partially-open structure was observed for trimers associated with the Fab from b12 (Liu et al., 2008; Merk and Subramaniam, 2013) (PDB code 3DNL). (**B**) Measured distances between homo-diFabs bound to HIV-1 trimer structures. Fabs from the indicated bNAbs shown bound to the gp120 portions of Env in the three conformation shown in panel A. Fabs are shown as ribbons; gp120 subunits are shown as surface representations with V1V2 loops in cyan, V3 in purple, the CD4 binding site in yellow, and the remainder of gp120 in maroon. The distance between the $Cys233_{heavy\ chain}$ carbon-

atoms of adjacent bound Fabs is indicated by a gray line as an approximation of an optimal length for a dsDNA bridge attached to $Cys233_{heavy\ chain}$. Assuming three-fold symmetry of trimers, only one distance is possible for bound 3BNC60, b12, and 10-1074 homo-diFabs. See also Figure S3.

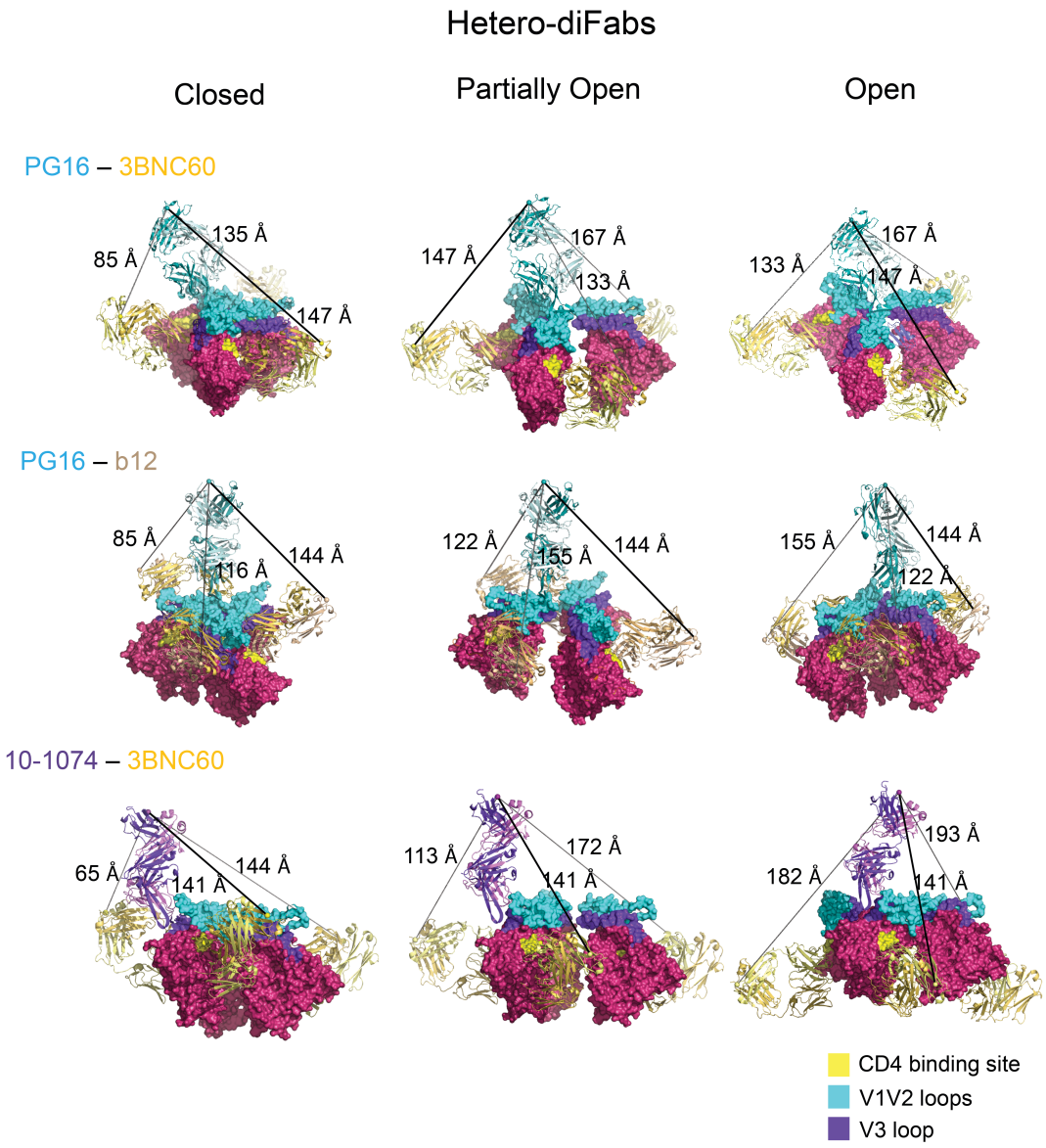

Supplemental Figure 3. Measured distances between hetero-diFabs bound to HIV-1 trimer structures, is related to Figure 3 by showing additional distance measurements between Fabs on trimer structures.

Comparison of homo-diFabs that can or cannot exhibit intra-spike crosslinking

To evaluate the potential for intra-spike crosslinking across different viral strains, we compared homo-diFabs designed to be capable (b12 and 3BNC60) or incapable (PG16) of intra-spike crosslinking (Figure 2C). To minimize inter-spike crosslinking, the homo-diFabs were constructed with 60–62bp bridges. The b12-60bp-b12 homo-diFab exhibited increased potency compared with b12 IgG in 21 of 25 strains in a cross-clade panel of primary HIV-1, with potency increases ≥10-fold for 16 strains and a geometric mean potency increase of 22-fold. 3BNC60-62bp-3BNC60 showed even more consistent synergy, being more potent than 3BNC60 IgG against all 25 strains tested, with ≥10-fold increases for 20 strains and a mean increase of 19-fold. By contrast, the PG16-60bp-PG16 homo-diFab showed potency increases compared with PG16 IgG against only six strains, with relatively small (2- to 7-fold) increases in five strains and an overall 2.8-fold mean potency change.

Hetero-diFabs exhibit dramatic potency increases consistent with intra-spike crosslinking

To determine whether heterotypic bivalent binding can produce synergy and to measure distances between epitopes, we used dsDNA to link Fabs recognizing different epitopes on gp120. We first evaluated hetero-diFabs constructed with Fabs from V1V2 (PG16 or PG9) (Walker et al., 2009b) and CD4bs (b12 or 3BNC60) (Roben et al., 1994; Scheid et al., 2011b) bNAbs linked with 60bp dsDNA bridges. PG16-60bp-b12 hetero-diFabs were evaluated in neutralization assays against HIV-1 strains SC4226618 (more sensitive to b12 than PG16) and CAP210 (more sensitive to PG16 than b12). According to the model

being tested, in the absence of synergistic binding; i.e., when only one Fab can bind to a spike at a time, a hetero-diFab would be no more potent than a non-covalent mixture of the dsDNA and the two Fabs against each viral strain, whereas synergistic binding would result in avidity effects exhibited by increased potency of the hetero-diFab. For both viral strains, the PG16-60bp-b12 hetero-diFab was ~10-fold more potent than the mixture of Fabs plus dsDNA or the more potent of the two Fabs alone (Figure 4; Figure S4). To more systematically explore potential synergy, we evaluated PG16-60bp-b12 against a 25-member panel of HIV-1 strains, finding synergistic effects (between 2- and 145-fold more potent than the corresponding non-covalent mixture for most strains; geometric mean improvement of 4.7-fold) (Table S1). When Fabs from PG16 or PG9 were combined with a more potent CD4bs-recognizing bNAb (3BNC60), the resulting hetero-diFabs exhibited greater synergy – several examples of >150-fold improvement for PG16-60bp-3BNC60 and PG9-60bp-3BNC60 and geometric mean potency improvements of 29- and 68-fold, respectively (Figure 4, Tables S2,S3). Other hetero-diFabs, constructed with combinations of Fabs recognizing the CD4bs (3BNC60 (Scheid et al., 2011b)), the gp120 V3 loop (10-1074 (Mouquet et al., 2012a)), and a gp41 epitope (10E8 (Huang et al., 2012a)), also showed synergistic effects (Figure 4, Table S4), and a 3BNC60-60bp-b12 hetero-diFab exhibited up to 660-fold synergy and a geometric mean potency increase of 90-fold (Figure 4, Table S5). In contrast, analogous IgG heterodimers, constructed with two different Fabs linked to a single Fc (Schaefer et al., 2011), did not show synergy when evaluated against the same viruses, demonstrating that synergistic effects required optimal separation distances that permitted each Fab to achieve its specific binding orientation (Figure S4; Tables S1-S5). We conclude that hetero-diFabs

can achieve synergy through simultaneous recognition of two different epitopes on the same HIV-1 Env trimer.

To more precisely define optimal intra-epitope separation distances, we evaluated hetero-diFabs with different bridge lengths, finding length-dependent synergy effects. For example, PG16–3BNC60 hetero-diFabs with 40bp and 50bp dsDNA bridges showed improved neutralization potencies when compared to the 60bp (204 Å) version, achieving ≥100-fold potency increases against over half of the tested strains and geometric mean improvements of 98- and 107-fold, respectively (Figure 4, Table S4). The 40bp and 50bp bridges (136 Å and 170 Å, respectively) corresponded to the approximate separation distances between PG16 and 3BNC60 Fabs when bound to the same gp120 within a trimer (147 Å) or to neighboring protomers within open or partially-open trimers (167 Å) (Figure S3). In a second length dependency example, 10-1074-40bp-3BNC60 was more potent than 10-1074-60bp-3BNC60 (Figure 4, Table S4). The ~136 Å distance between the two Fabs in 10-1074-40bp-3BNC60 corresponded to the approximate separation between these Fabs bound to the same gp120 (141 Å), while 60bp more closely approximated Fabs bound to neighboring protomers on an open trimer (193 Å) (Figure S3). The 40bp and 50bp versions of 10E8–3BNC60 showed consistent synergy (Figure 4, Table S4); however, the lack of structural information concerning 10E8 binding to Env trimer hindered interpretation of 10E8-containing hetero-diFabs.

Virus	Clade	Tier	IC_{50} (nM) PG16-40bp-3BNC60	PG16-50bp-3BNC60	PG16-60bp-3BNC60	PG9-60bp-3BNC60	3BNC60-60bp-b12
6535.3	B	1B	0.31 **(351x)**	0.23 **(474x)**	0.66 **(165x)**	<0.03 **(>767x)**	0.22 **(>172x)**
SC422661.8	B	2	0.021 **(86x)**	0.01 **(180x)**	0.05 **(36x)**	<0.03 **(>47x)**	<0.04 **(>30x)**
PVO.4	B	3	0.04 **(40x)**	0.03 **(53x)**	0.04 **(40x)**	<0.03 **(>40x)**	0.04 **(50x)**
TRO.11	B	2	0.03 **(67x)**	0.03 **(67x)**	0.05 **(40x)**	<0.03 **(>40x)**	<0.04 **(>55x)**
TRJO4551.58	B	3	0.04 **(145x)**	0.03 **(193x)**	0.1 **(58x)**	<0.03 **(>187x)**	<0.04 **(>165x)**
CAAN5342.A2	B	2	0.22 **(118x)**	0.17 **(153x)**	0.5 **(52x)**	200 **(0.08x)**	0.3 **(72x)**
THRO4156.18	B	2	0.59 **(80x)**	0.38 **(124x)**	1.2 **(39x)**	22 **(1x)**	0.52 **(23x)**
RHPA4259.7	B	2	0.007 **(200x)**	0.007 **(200x)**	0.02 **(70x)**	<0.03 **(>20x)**	<0.04 **(>70x)**
Du156.12	C	2	0.007 **(114x)**	0.007 **(114x)**	0.04 **(20x)**	<0.03 **(>53x)**	<0.04 **(>205x)**
Du172.17	C	2	0.06 **(70x)**	0.06 **(70x)**	0.36 **(12x)**	<0.03 **(>273x)**	0.22 **(117x)**
Du422.1	C	2	0.36 **(14x)**	0.41 **(12x)**	0.25 **(20x)**	<0.03 **(>160x)**	0.15 **(13x)**
ZM197M.PB7	C	1B	0.06 **(107x)**	0.06 **(107x)**	0.18 **(35x)**	19 **(0.5x)**	0.22 **(91x)**
ZM214M.PL15	C	1B	0.001 **(9000x)**	0.002 **(4500x)**	0.007 **(1280x)**	78 **(0.1x)**	0.15 **(81x)**
ZM233M.PB6	C	2	0.001 **(100x)**	0.001 **(100x)**	0.007 **(14x)**	<0.03 **(>3x)**	0.07 **(320x)**
ZM249M.PL1	C	2	0.01 **(60x)**	0.01 **(60x)**	0.03 **(20x)**	<0.03 **(>27x)**	<0.04 **(>155x)**
ZM53M.PB12	C	2	0.04 **(25x)**	0.03 **(33x)**	0.13 **(8x)**	<0.03 **(>33x)**	0.07 **(149x)**
ZM109F.PB4	C	1B	0.03 **(133x)**	0.03 **(133x)**	0.12 **(33x)**	<0.03 **(>280x)**	0.07 **(660x)**
ZM135M.PL10a	C	2	0.06 **(83x)**	0.06 **(83x)**	0.14 **(36x)**	<0.03 **(>140x)**	0.07 **(69x)**
CAP45.2.00.G3	C	2	<0.0007 **(>143x)**	<0.0007 **(>143x)**	0.003 **(33x)**	<0.03 **(>3x)**	0.07 **(29x)**
CAP210.2.00.E8	C	2	0.05 **(52x)**	0.02 **(130x)**	0.11 **(24x)**	<0.03 **(>140x)**	1.3 **(>154x)**
Q842.d12	A	2	0.001 **(200x)**	0.001 **(200x)**	0.007 **(29x)**	<0.03 **(>7x)**	<0.04 **(>15x)**
Q259.d2.17	A	2	0.01 **(80x)**	0.01 **(80x)**	0.03 **(27x)**	<0.03 **(>33x)**	<0.04 **(>110x)**
3718.v3.c11	A	2	0.03 **(13x)**	0.03 **(13x)**	0.12 **(3x)**	<0.03 **(>27x)**	5.67 **(35x)**
0330.v4.c3	A	2	0.002 **(50x)**	0.001 **(100x)**	0.007 **(14x)**	<0.03 **(>7x)**	<0.04 **(>40x)**
3415.v1.c1	A	2	0.01 **(120x)**	0.01 **(120x)**	0.05 **(24x)**	<0.03 **(>67x)**	0.07 **(94x)**
Geometric Mean IC_{50} (nM)			0.022	0.020	0.075	0.038	0.091
Arithmetic Mean IC_{50} (nM)			0.083	0.068	0.24	0.050	0.36
Mean Fold Improvement Over Mixture (Geometric)			**98**	**107**	**29**	**68**	**90**
Mean Fold Improvement Over Mixture (Arithmetic)			**120**	**145**	**42**	**121**	**74**

Virus	Clade	Tier	IC_{50} (nM) 10-1074-40bp-3BNC60	10-1074-60bp-3BNC60	10E8-40bp-3BNC60	10E8-50bp-3BNC60	10E8-60bp-3BNC60
QH-0692	B	2	NT	NT	1.2 **(34x)**	1.4 **(30x)**	1.3 **(32x)**
CAAN5342.A2	B	2	NT	NT	7.3 **(>46x)**	10**(>32x)**	25 **(>13x)**
THRO4156.18	B	2	24 **(2.5x)**	19 **(3x)**	NT	NT	NT
Du172.17	C	2	0.64 **(19x)**	4.0 **(3x)**	NT	NT	NT
Du422.1	C	2	NT	NT	2.2 **(8x)**	3.6 **(5x)**	5.0 **(3x)**
CAP45.2.00.G3	C	2	40 **(11x)**	260 **(2x)**	11 **(2x)**	15 **(1x)**	17 **(1x)**
CAP210.2.00.E8	C	2	56. **(11x)**	79 **(8x)**	NT	NT	NT
T250-4	AG	2	NT	NT	0.92 **(53x)**	0.66 **(74x)**	12 **(4x)**
Geometric Mean IC_{50} (nM)			14	35	2.9	3.5	8
Arithmetic Mean IC_{50} (nM)			30	90	4.5	6.1	12
Mean Fold Improvement Over Mixture (Geometric)			**8.70**	**3.30**	**16**	**13**	**5.8**
Mean Fold Improvement Over Mixture (Arithmetic)			**9.3**	**3.1**	**20**	**15**	**7.6**

>100x	50-100x	30-49x	10-29x	2-9x	≤2x	NT

Figure 4. Synergistic dsDNA-based hetero-diFabs. Neutralization of primary HIV-1 strains by hetero-diFabs. IC_{50}s are reported for the hetero-diFabs. See Tables S1-S5 for IC_{50}s of parental Fabs and IgGs, dsDNA alone, and the non-covalent mixtures of Fabs and dsDNA. As a measure of potential synergy of each hetero-diFab, the molar ratio of the IC_{50} values for the non-covalent mixture and the hetero-diFab is listed for each strain in parentheses beside the IC_{50} for the hetero-diFab. NT = not tested. See also Figure S4.

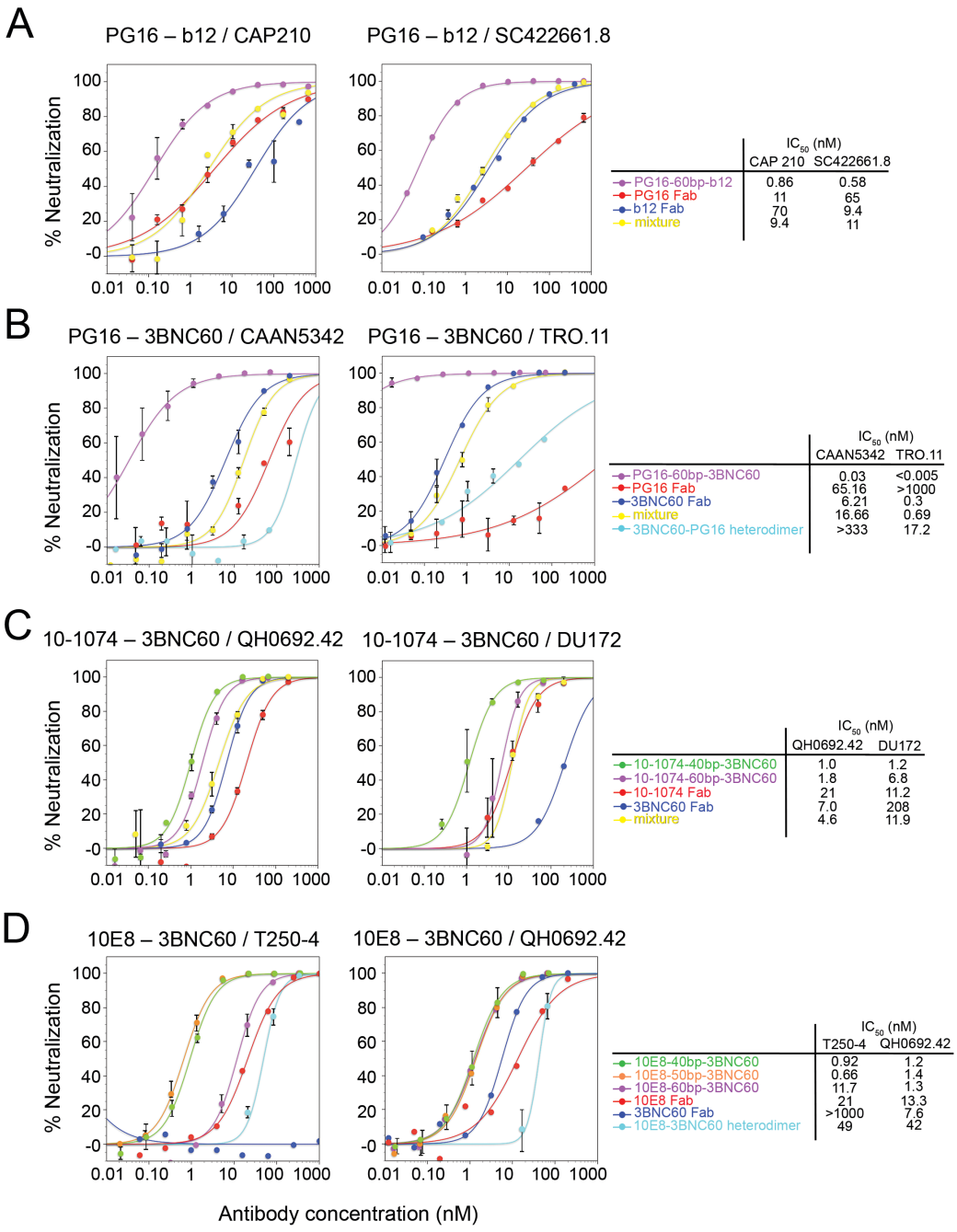

Supplemental Figure 4. Examples of neutralization data for hetero-diFabs, is related to Figure 4 by showing example neutralization curves for data shown in Figure 4.

			IC_{50} (nM)						
Virus	Clade	Tier	dsDNA	PG16-60bp-b12	Mix of PG16, b12, dsDNA	PG16 Fab	PG16 IgG	b12 Fab	b12 IgG
6535.3	B	1B	>1000	1.1 **(145x)**	160	>200	17	360	60
SC422661.8	B	2	>1000	0.28 **(15x)**	4.2	65.0	4.7	9.5	3.0
PVO.4	B	3	>1000	15 **(>13x)**	>200	150	16	4700	700
TRO.11	B	2	>1000	18 **(0.8x)**	15	>200	6.5	7600	700
TRJO4551.58	B	3	>1000	8.5 **(10x)**	85	64	2.1	7900	700
CAAN5342.A2	B	2	>1000	28 **(3x)**	87	65	6.0	6800	700
THRO4156.18	B	2	>1000	3.1 **(11x)**	35	>200	2.7	100	10
RHPA4259.7	B	2	>1000	0.28 **(4x)**	1.0	1.5	<0.1	6.0	0.73
Du156.12	C	2	>1000	0.07 **(11x)**	0.8	0.8	<0.1	150	4.8
Du172.17	C	2	>1000	0.14 **(16x)**	2.2	2.6	<0.1	100	10
Du422.1	C	2	>1000	<0.04 **(>17x)**	0.6	1.0	0.3	60	2.0
ZM197M.PB7	C	1B	>1000	2.8 **(1x)**	3.8	5.5	2.4	1000	620
ZM214M.PL15	C	1B	>1000	11 **(>18x)**	>200	>200	>330	380	43
ZM233M.PB6	C	2	>1000	<0.04 **(1x)**	<0.10	<0.1	<0.1	4500	700
ZM249M.PL1	C	2	>1000	0.21 **(2x)**	0.4	0.4	<0.1	240	23
ZM53M.PB12	C	2	>1000	0.70 **(2x)**	1.2	1.0	<0.1	890	190
ZM109F.PB4	C	1B	>1000	1.5 **(4x)**	6.4	6.7	30	3400	700
ZM135M.PL10a	C	2	>1000	68 **(>3x)**	>200	>200	>330	5900	700
CAP45.2.00.G3	C	2	>1000	<0.04 **(>1x)**	<0.10	<0.1	<0.1	40	3.4
CAP210.2.00.E8	C	2	>1000	0.56 **(4x)**	2.2	11.0	<0.1	70	50
Q842.d12	A	2	>1000	0.21 **(0.5x)**	<0.10	<0.1	<0.1	4200	700
Q259.d2.17	A	2	>1000	0.42 **(2x)**	0.8	0.61	<0.1	7500	700
3718.v3.c11	A	2	>1000	0.56 **(3x)**	2.0	<0.1	<0.1	690	126
0330.v4.c3	A	2	>1000	0.14 **(1x)**	<0.10	<0.1	<0.1	5600	700
3415.v1.c1	A	2	>1000	0.42 **(3x)**	1.4	1.22	<0.1	200	53
Geometric Mean IC_{50} (nM)				1.1					
Arithmetic Mean IC_{50} (nM)				7.0					
Mean Fold Improvement Over Mixture (Geometric)				**4.7**					
Mean Fold Improvement Over Mixture (Arithmetic)				**6.3**					

>100x	50-100x	30-49x	10-29x	2-9x	≤2x

Table S1. IC_{50} values for neutralization of primary HIV-1 strains by PG16-60bp-b12 hetero-diFab, related to Figure 4. IC_{50}s are reported for the hetero-diFab, the parental Fabs and IgGs, the dsDNA bridge alone, and a non-covalent mixture of the Fabs and the dsDNA bridge. As a measure of potential synergy of the hetero-diFab, the molar ratio of the IC_{50} values for the non-covalent mixture and the hetero-diFab is listed for each strain in parentheses beside the IC_{50} for the hetero-diFab.

			IC_{50} (nM)									
Virus	Clade	Tier	dsDNA	PG16-40bp-3BNC60	PG16-50bp-3BNC60	PG16-60bp-3BNC60	PG16-3BNC60 heterodimer	Mix of PG16, 3BNC60, dsDNA	PG16 Fab	PG16 IgG	3BNC60 Fab	3BNC60 IgG
6535.3	B	1B	>1000	0.31 **(351x)**	0.23 **(474x)**	0.66 **(165x)**		109	>200	17	27	4.0
SC422661.8	B	2	>1000	0.021 **(86x)**	0.01 **(180x)**	0.05 **(36x)**		1.8	65.0	4.7	1.0	0.3
PVO.4	B	3	>1000	0.04 **(40x)**	0.03 **(53x)**	0.04 **(40x)**		1.6	150	16	1.3	0.1
TRO.11	B	2	>1000	0.03 **(67x)**	0.03 **(67x)**	0.05 **(40x)**	2.6	2.0	>200	6.5	1.3	0.2
TRJO4551.58	B	3	>1000	0.04 **(145x)**	0.03 **(193x)**	0.1 **(58x)**		5.8	64	2.1	4.8	<0.1
CAAN5342.A2	B	2	>1000	0.22 **(118x)**	0.17 **(153x)**	0.5 **(52x)**	42.6	26	65	6.0	6.2	3.6
THRO4156.18	B	2	>1000	0.59 **(80x)**	0.38 **(124x)**	1.2 **(39x)**	>10	47	>200	2.7	23	3.5
RHPA4259.7	B	2	>1000	0.007 **(200x)**	0.007 **(200x)**	0.02 **(70x)**		1.4	1.5	<0.1	1.5	0.3
Du156.12	C	2	>1000	0.007 **(114x)**	0.007 **(114x)**	0.04 **(20x)**		0.8	0.8	<0.1	9.4	0.3
Du172.17	C	2	>1000	0.06 **(70x)**	0.06 **(70x)**	0.36 **(12x)**		4.2	2.6	<0.1	210	16
Du422.1	C	2	>1000	0.36 **(14x)**	0.41 **(12x)**	0.25 **(20x)**		5.0	1.0	0.3	>200	>330
ZM197M.PB7	C	1B	>1000	0.06 **(107x)**	0.06 **(107x)**	0.18 **(35x)**		6.4	5.5	2.4	15	3.8
ZM214M.PL15	C	1B	>1000	0.001 **(9000x)**	0.002 **(4500x)**	0.007 **(1280x)**	2.4	9.0	>200	>330	6.9	1.7
ZM233M.PB6	C	2	>1000	0.001 **(100x)**	0.001 **(100x)**	0.007 **(14x)**		0.1	<0.1	<0.1	14	1.4
ZM249M.PL1	C	2	>1000	0.01 **(60x)**	0.01 **(60x)**	0.03 **(20x)**		0.6	0.4	<0.1	2.7	0.3
ZM53M.PB12	C	2	>1000	0.04 **(25x)**	0.03 **(33x)**	0.13 **(8x)**		1.0	1.0	<0.1	5.2	1.3
ZM109F.PB4	C	1B	>1000	0.03 **(133x)**	0.03 **(133x)**	0.12 **(33x)**		4.0	6.7	30	39	0.3
ZM135M.PL10a	C	2	>1000	0.06 **(83x)**	0.06 **(83x)**	0.14 **(36x)**		5.0	>200	>330	3.7	0.4
CAP45.2.00.G3	C	2	>1000	<0.0007 **(>143x)**	<0.0007 **(>143x)**	0.003 **(33x)**		0.1	<0.1	<0.1	>200	50
CAP210.2.00.E8	C	2	>1000	0.05 **(52x)**	0.02 **(130x)**	0.11 **(24x)**		2.6	11.0	<0.1	>200	59
Q842.d12	A	2	>1000	0.001 **(200x)**	0.001 **(200x)**	0.007 **(29x)**		0.2	<0.1	<0.1	0.21	0.09
Q259.d2.17	A	2	>1000	0.01 **(80x)**	0.01 **(80x)**	0.03 **(27x)**		0.8	0.61	<0.1	3.7	0.03
3718.v3.c11	A	2	>1000	0.03 **(13x)**	0.03 **(13x)**	0.12 **(3x)**		0.4	<0.1	<0.1	>200	>330
0330.v4.c3	A	2	>1000	0.002 **(50x)**	0.001 **(100x)**	0.007 **(14x)**		0.1	<0.1	<0.1	0.62	0.2
3415.v1.c1	A	2	>1000	0.01 **(120x)**	0.01 **(120x)**	0.05 **(24x)**		1.2	1.22	<0.1	4.6	0.9
Geometric Mean IC_{50} (nM)				0.022	0.020	0.075						
Arithmetic Mean IC_{50} (nM)				0.083	0.068	0.24						
Mean Fold Improvement Over Mixture (Geometric)				**98**	**107**	**29**						
Mean Fold Improvement Over Mixture (Arithmetic)				**120**	**145**	**42**						

>100x	50-100x	30-49x	10-29x	2-9x	≤2x

Table S2. IC_{50} values for neutralization of primary HIV-1 strains by PG16-3BNC60 hetero-diFabs, related to Figure 4. IC_{50}s are reported for the hetero-diFab, the parental Fabs and IgGs, the dsDNA bridge alone, and a non-covalent mixture of the Fabs and the dsDNA bridge. As a measure of potential synergy of the hetero-diFab, the molar ratio of the IC_{50} values for the non-covalent mixture and the hetero-diFab is listed for each strain in parentheses beside the IC_{50} for the hetero-diFab.

			IC_{50} (nM)							
Virus	Clade	Tier	dsDNA	PG9-60bp-3BNC60	PG9-3BNC60 heterodimer	Mix of PG9, 3BNC60, dsDNA	PG9 Fab	PG9 IgG	3BNC60 Fab	3BNC60 IgG
6535.3	B	1B	>1000	<0.03 **(>767x)**		23	18	4.0	27	4.0
SC422661.8	B	2	>1000	<0.03 **(>47x)**		1.4	14	6.9	1.0	0.3
PVO.4	B	3	>1000	<0.03 **(>40x)**	40	1.2	59	57	1.3	0.1
TRO.11	B	2	>1000	<0.03 **(>40x)**	2.6	1.2	54	71	1.3	0.2
TRJO4551.58	B	3	>1000	<0.03 **(>187x)**		5.6	32	7.6	4.8	<0.1
CAAN5342.A2	B	2	>1000	0.07 **(229x)**	>10	16	25	26	6.2	3.6
THRO4156.18	B	2	>1000	0.21 **(152x)**	>10	32	<0.1	110	23	3.5
RHPA4259.7	B	2	>1000	<0.03 **(>20x)**		0.6	0.2	<0.1	1.5	0.3
Du156.12	C	2	>1000	<0.03 **(>53x)**		1.6	0.6	0.3	9.4	0.3
Du172.17	C	2	>1000	<0.03 **(>273x)**		8.2	2.2	3.1	210	16
Du422.1	C	2	>1000	<0.03 **(>160x)**	9.3	4.8	0.6	1.8	>200	>330
ZM197M.PB7	C	1B	>1000	0.07 **(143x)**		10	5.4	5.1	15	3.8
ZM214M.PL15	C	1B	>1000	0.21 **(39x)**	16	8.2	>200	>330	6.9	1.7
ZM233M.PB6	C	2	>1000	<0.03 **(>3x)**		<0.1	<0.1	<0.1	14	1.4
ZM249M.PL1	C	2	>1000	<0.03 **(>27x)**		0.8	0.2	0.3	2.7	0.3
ZM53M.PB12	C	2	>1000	<0.03 **(>33x)**	0.63	1.0	0.4	0.5	5.2	1.3
ZM109F.PB4	C	1B	>1000	<0.03 **(>280x)**		8.4	6.8	2.1	39	0.3
ZM135M.PL10a	C	2	>1000	<0.03 **(>140x)**		4.2	160	>330	3.7	0.4
CAP45.2.00.G3	C	2	>1000	<0.03 **(>3x)**		<0.1	<0.1	<0.1	>200	50
CAP210.2.00.E8	C	2	>1000	<0.03 **(>140x)**		4.2	1.6	2.0	>200	59
Q842.d12	A	2	>1000	<0.03 **(>7x)**		0.2	<0.1	<0.1	0.21	0.09
Q259.d2.17	A	2	>1000	<0.03 **(>33x)**		1.0	0.4	0.2	3.7	0.03
3718.v3.c11	A	2	>1000	<0.03 **(>27x)**		0.8	<0.1	<0.1	>200	>330
0330.v4.c3	A	2	>1000	<0.03 **(>7x)**		0.2	<0.1	<0.1	0.62	0.2
3415.v1.c1	A	2	>1000	<0.03 **(>67x)**		2.0	1.0	1.2	4.6	0.9
Geometric Mean IC_{50} (nM)				0.038						
Arithmetic Mean IC_{50} (nM)				0.049						
Mean Fold Improvement Over Mixture (Geometric)				**68**						
Mean Fold Improvement Over Mixture (Arithmetic)				**121**						

>100x	50-100x	30-49x	10-29x	2-9x	≤2x

Table S3. **IC_{50} values for neutralization of primary HIV-1 strains by PG9-60bp-3BNC60 hetero-diFab, related to Figure 4.** IC_{50}s are reported for the hetero-diFab, the parental Fabs and IgGs, the dsDNA bridge alone, and a non-covalent mixture of the Fabs and the dsDNA bridge. As a measure of potential synergy of the hetero-diFab, the molar ratio of the IC_{50} values for the non-covalent mixture and the hetero-diFab is listed for each strain in parentheses beside the IC_{50} for the hetero-diFab.

			IC_{50} (nM)								
Virus	Clade	Tier	dsDNA	10-1074-40bp-3BNC60	10-1074-60bp-3BNC60	mix 10-1074, 3BNC60, dsDNA	10-1074-3BNC60 heterodimer	10-1074 Fab	10-1074 IgG	3BNC60 Fab	3BNC60 IgG
THRO4156.18	B	2	>1000	24 **(2.5x)**	19 **(3x)**	62	68	>1000	>330	71	3.5
Du172.17	C	2	>1000	0.64 **(19x)**	4.0 **(3x)**	12	22	11.24	0.81	210	16
CAP45.2.00.G3	C	2	>1000	40 **(11x)**	260 **(2x)**	430	>330	NT	>330	>1000	50
CAP210.2.00.E8	C	2	>5000	56. **(11x)**	79 **(8x)**	620	>330	>1000	>330	>1000	59
Geometric Mean IC_{50} (nM)				14	35						
Arithmetic Mean IC_{50} (nM)				30	90						
Mean Fold Improvement Over Mixture (Geometric)				**8.70**	**3.30**						
Mean Fold Improvement Over Mixture (Arithmetic)				**9.3**	**3.1**						

			IC_{50} (nM)								
Virus	Clade	Tier	dsDNA	10E8-40bp-3BNC60	10E8-50bp-3BNC60	10E8-60bp-3BNC60	10E8-3BNC60 heterodimer	10E8 Fab	10E8 IgG	3BNC60 Fab	3BNC60 IgG
CAAN5342.A2	B	2	>1000	7.3 **(>46x)**	10**(>32x)**	25 **(>13x)**	>330	>550	8.3	12	3.8
QH-0692	B	2	>1000	1.2 **(34x)**	1.4 **(30x)**	1.3 **(32x)**	42	13	3.1	7.6	0.93
Du422.1	C	2	>1000	2.2 **(8x)**	3.6 **(5x)**	5.0 **(3x)**	17	4.5	3.5	>1000	>330
CAP45.2.00.G3	C	2	>1000	11 **(2x)**	15 **(1x)**	17 **(1x)**	19	20	2.4	>1000	50
T250-4	AG	2	>1000	0.92 **(53x)**	0.66 **(74x)**	12 **(4x)**	49	21	1.4	>1000	NT
Geometric Mean IC_{50} (nM)				2.9	3.5	8					
Arithmetic Mean IC_{50} (nM)				4.5	6.1	12					
Mean Fold Improvement Over Heterodimer (Geometric)				**16**	**13**	**5.8**					
Mean Fold Improvement Over Heterodimer (Arithmetic)				**20**	**15**	**7.6**					

>100x	50-100x	30-49x	10-29x	2-9x	≤2x

Table S4. **IC_{50} values for neutralization of primary HIV-1 strains by 10-1074-3BNC60 and 10E8-3BNC60 heterodi-Fabs, related to Figure 4.** IC_{50}s are reported for the hetero-diFab, the parental Fabs and IgGs, the dsDNA bridge alone, and a non-covalent mixture of the Fabs and the dsDNA bridge. As a measure of potential synergy of the hetero-diFab, the molar ratio of the IC_{50} values for the non-covalent mixture and the hetero-diFab is listed for each strain in parentheses beside the IC_{50} for the hetero-diFab.

			IC_{50} (nM)						
Virus	Clade	Tier	dsDNA	3BNC60-60bp-b12	Mix of 3BNC60, b12, dsDNA	3BNC60 Fab	3BNC60 IgG	b12 Fab	b12 IgG
6535.3	B	1B	>1000	0.22 **(>172x)**	38	27	4.0	360	60
SC422661.8	B	2	>1000	<0.04 **(>30x)**	1.2	1.0	0.3	30	1.9
PVO.4	B	3	>1000	0.04 **(50x)**	2.0	1.3	0.1	4700	>330
TRO.11	B	2	>1000	<0.04 **(>55x)**	2.2	1.3	0.2	7600	>330
TRJO4551.58	B	3	>1000	<0.04 **(>165x)**	6.6	4.8	<0.1	7900	>330
CAAN5342.A2	B	2	>1000	0.3 **(72x)**	21.6	6.2	3.6	6800	>330
THRO4156.18	B	2	>1000	0.52 **(23x)**	11.8	23	3.5	100	5.2
RHPA4259.7	B	2	>1000	<0.04 **(>70x)**	2.8	1.5	0.3	6.0	0.73
Du156.12	C	2	>1000	<0.04 **(>205x)**	8.2	9.4	0.3	150	4.8
Du172.17	C	2	>1000	0.22 **(117x)**	25.8	210	16	100	3.7
Du422.1	C	2	>1000	0.15 **(13x)**	2.0	>200	>330	60	2.0
ZM197M.PB7	C	1B	>1000	0.22 **(91x)**	20	15	3.8	1000	100
ZM214M.PL15	C	1B	>1000	0.15 **(81x)**	12.2	6.9	1.7	380	43
ZM233M.PB6	C	2	>1000	0.07 **(320x)**	22.4	14	1.4	4500	>330
ZM249M.PL1	C	2	>1000	<0.04 **(>155x)**	6.2	2.7	0.3	240	23
ZM53M.PB12	C	2	>1000	0.07 **(149x)**	10.4	5.2	1.3	890	190
ZM109F.PB4	C	1B	>1000	0.07 **(660x)**	46.2	39	0.3	3400	>330
ZM135M.PL10a	C	2	>1000	0.07 **(69x)**	4.8	3.7	0.4	5900	>330
CAP45.2.00.G3	C	2	>1000	0.07 **(29x)**	2.0	>200	50	40	3.4
CAP210.2.00.E8	C	2	>1000	1.3 **(>154x)**	>200	>200	59	1680	160
Q842.d12	A	2	>1000	<0.04 **(>15x)**	0.60	0.21	0.09	4200	>330
Q259.d2.17	A	2	>1000	<0.04 **(>110x)**	4.40	3.7	0.03	7500	>330
3718.v3.c11	A	2	>1000	5.67 **(35x)**	>200	>200	>330	690	126
0330.v4.c3	A	2	>1000	<0.04 **(>40x)**	1.60	0.62	0.2	5600	>330
3415.v1.c1	A	2	>1000	0.07 **(94x)**	6.60	4.6	0.9	200	53
Geometric Mean IC_{50} (nM)				0.091					
Arithmetic Mean IC_{50} (nM)				0.360					
Mean Fold Improvement Over Mixture (Geometric)				**90**					
Mean Fold Improvement Over Mixture (Arithmetic)				**74**					

>100x	50-100x	30-49x	10-29x	2-9x	≤2x

Table S5. IC_{50} values for neutralization of primary HIV-1 strains by 3BNC60-60bp-b12 hetero-diFab, related to Figure 4. IC_{50}s are reported for the hetero-diFab, the parental Fabs and IgGs, the dsDNA bridge alone, and a non-covalent mixture of the Fabs and the dsDNA bridge. As a measure of potential synergy of the hetero-diFab, the molar ratio of the IC_{50} values for the non-covalent mixture and the hetero-diFab is listed for each strain in parentheses beside the IC_{50} for the hetero-diFab.

A hetero-diFab constructed with a protein linker exhibits synergistic potency increases

Bivalent molecules involving dsDNA linkers were effective for demonstrating synergistic neutralization, but a protein reagent would be preferable as an anti-HIV-1 therapeutic. We recently described a series of protein linkers of various lengths and rigidities (Klein et al., 2014b) that can mimic the properties of different lengths of dsDNA. Thus we can substitute a comparable protein linker for an optimal dsDNA bridge to create a protein reagent capable of simultaneous binding to two different epitopes on a single HIV-1 spike trimer. As a proof-of-principle example, we used sortase-catalyzed protein ligation and click chemistry (Witte et al., 2013) to construct a bivalent reagent analogous to PG16-40bp-3BNC60 by substituting the dsDNA linker with 12 domains of a designed tetratricopeptide-repeat (TPR) protein (Kajander et al., 2007a) (Figure 5A; Figure S5). We chose a TPR linker because tandem repeats of TPR domains form a rigid rod-like structure whose length corresponds predictably with the number of repeats, with each domain contributing ~10 Å (Kajander et al., 2007a). PG16 Fab was expressed with a C-terminal sortase signal, and the C-terminus of the 3BNC60 Fab was modified to include twelve TPR repeats and a sortase signal. The tagged Fabs were covalently attached to peptides containing click handles using sortase-catalyzed ligation, and then incubated to allow the click reaction to form PG16 Fab linked to 3BNC60 Fab by twelve TPR repeats (PG16-TPR12-3BNC60). Together with the remnants of the click handles, the linker would occupy ~131 Å, approximately the same length as the dsDNA linker in PG16-40bp-3BNC60 reagent (Figure 5A; Figure S5). The protein-based molecule, PG16-

TPR12-3BNC60, exhibited between 11- and >200-fold synergy against 12 primary HIV-1 strains (Figure 5B; 33-fold geometric mean increased potency).

Simulations of the effects of avidity on IgG binding to tethered antigens

To better understand the effects of avidity arising from bivalent binding of IgGs to antigens tethered to a surface such as a viral membrane, we used modeling software to simulate the saturation of surface-bound antigens by monovalent Fabs and bivalent IgGs. We chose a 1 hour incubation time based upon conditions under which in vitro neutralization assays are conducted (Montefiori, 2005). We varied the density of the tethered antigens, the concentrations of Fab or IgG, and investigated a range of intrinsic association and dissociation rate constants for the binding interaction. The fraction of antigen bound by a Fab or IgG was calculated as a function of on- and off-rates (k_a and k_d), whose ratio (k_d/k_a) is equal to the affinity (K_D, or equilibrium dissociation constant). We compared saturation by Fabs (top row), IgGs in which only monovalent binding was permitted (center row), and IgGs that bound bivalently through crosslinking of neighboring antigens (bottom row) (Figure 6A). As expected, saturation by Fabs and IgGs was nearly identical for monovalent binding conditions (Figure 6A, first two rows). By contrast, across a range of input concentrations, there were k_a and k_d combinations for IgGs binding bivalently that exhibited saturation binding under conditions in which monovalent Fabs and IgGs binding monovalently did not (Figure 6A, bottom row). Thus, consistent with experimental results in the palivizumab/RSV system (Wu et al., 2005), the simulations suggested that bivalency through crosslinking can rescue binding of IgGs whose Fabs exhibit weak binding affinities as a result of fast dissociation rate constants,

whereas IgGs whose Fabs exhibit high affinities because of slow dissociation rates did not display strong avidity enhancement.

The simulations also demonstrate that the effects of avidity on binding are a complicated mixture of kinetics, input concentration, and incubation time. At any particular concentration, the threshold at which avidity is observed is controlled by kinetics rather than affinity because different combinations of kinetic constants yield the same K_D. The kinetic threshold at which avidity effects are observed varies depending on the difference between the input concentration and the K_D. For concentrations near or below the K_D, there is a kinetic threshold such that for on- and off-rates slower than ~10^3 $M^{-1}s^{-1}$ and ~10^{-5} s^{-1}, respectively, avidity enhancement is not observed (Figure 6A). The binding reactions are also affected by the length of incubation, such that the lower the input concentration, the longer it takes to reach saturation (Figure 6B).

We note that the simulations model binding interactions only, whereas our homo- and hetero-diFabs were evaluated for their ability to enhance neutralization of viral infectivity, a process more complicated than binding. For example, neutralization mechanisms may involve conformational changes in Env that were not accounted for in our binding simulation. In addition, kinetics constants for antibody-mediated neutralization of HIV-1 are not known, nor is the fraction of Env spikes on a virion that are required for neutralization or for fusion. In any case, it appears that the kinetic properties of the bNAb Fab components in our reagents were appropriate to realize avidity-enhanced neutralization since hetero-diFab reagents displayed ~100-fold mean improved neutralization potencies. The data therefore support the hypothesis that intra-

spike crosslinking by anti-HIV-1 binding molecules represents a valid strategy for increasing potency and resistance to HIV-1 Env mutations.

A

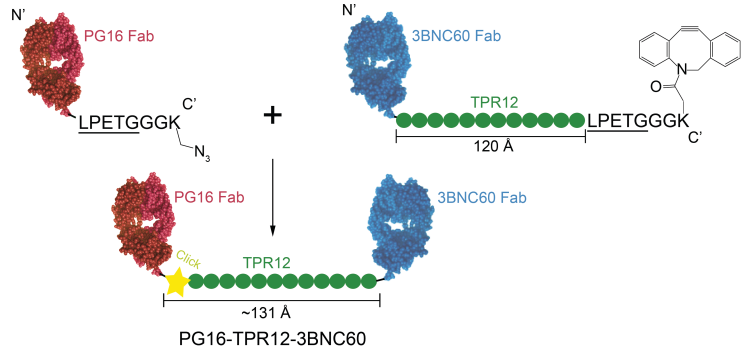

PG16-TPR12-3BNC60

B

Virus	Clade	Tier	IC50 (nM) TPR12	PG16 Fab	3BNC60 Fab-TPR12	PG16- TPR12-3BNC60
6535.3	B	1B	>1000	750	28	0.9 **(30x)**
SC422661.8	B	2	600	>1000	1.8	0.1 **(15x)**
TRO.11	B	2	600	>1000	1.0	0.09 **(11x)**
CAAN5342.A2	B	2	600	400	10	0.7 **(14x)**
THRO4156.18	B	2	>1000	910	38	0.6 **(59x)**
RHPA4259.7	B	2	600	300	0.6	0.05 **(11x)**
Du172.17	C	2	600	2.7	150	0.1 **(27x)**
Du422.1	C	2	600	36	360	0.3 **(116x)**
ZM197M.PB7	C	1B	210	640	11	0.9 **(12x)**
ZM109F.PB4	C	1B	600	>1000	25	0.4 **(59x)**
ZM53M.PB12	C	2	600	4.2	7.5	0.02 **(209x)**
CAP210.2.00.E8	C	2	>1000	9.5	290	0.1 **(73x)**
Geometric Mean IC50 (nM)						0.21
Arithmetic Mean IC50 (nM)						0.37
Mean Fold Improvement Over Best Component (Geometric)						**33**
Mean Fold Improvement Over Best Component (Arithmetic)						**38**

>100x	50-100x	30-49x	10-29x	2-9x	≤2x

Figure 5. Synergistic protein-based hetero-diFab. (**A**) Schematic representation of PG16-TPR12-3BNC60 (not to scale). Approximate lengths are indicated (120 Å for the TRP12 linker plus ~11 Å for the fused click handles). (**B**) Neutralization of primary HIV-1 strains. IC_{50}s are reported for PG16-TPR12-3BNC60, the parental components of the reagent (PG16 Fab and 3BNC60 Fab-TPR12), and TPR12 alone. As a measure of potential synergy of PG16-TPR12-3BNC60, the molar ratio of the IC_{50} values for the most potent component and PG16-TPR12-3BNC60 is listed for each strain in parentheses beside the IC_{50} for PG16-TPR12-3BNC60. See also Figure S5

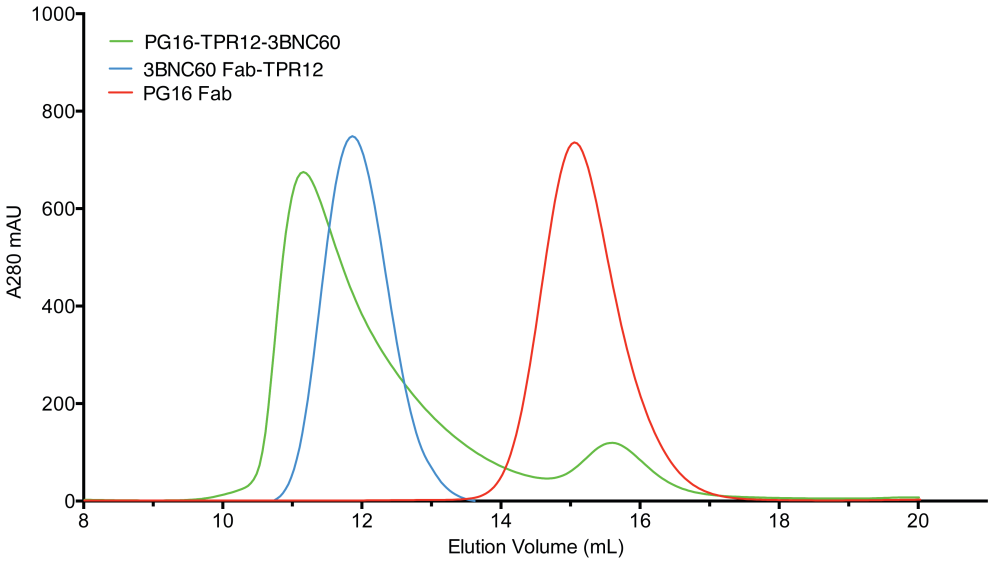

Figure S5. Size exclusion chromatography profiles for PG16-TPR12-3BNC60, related to Figure 5

SEC runs from which PG16-TPR12-3BNC60 was isolated from fractions 10.3 mL – 11.8 mL. SEC profiles are shown for 3BNC60 Fab-TPR12 and PG16 Fab for comparison. Fractions were assayed by 10% SDS-PAGE (data not shown).

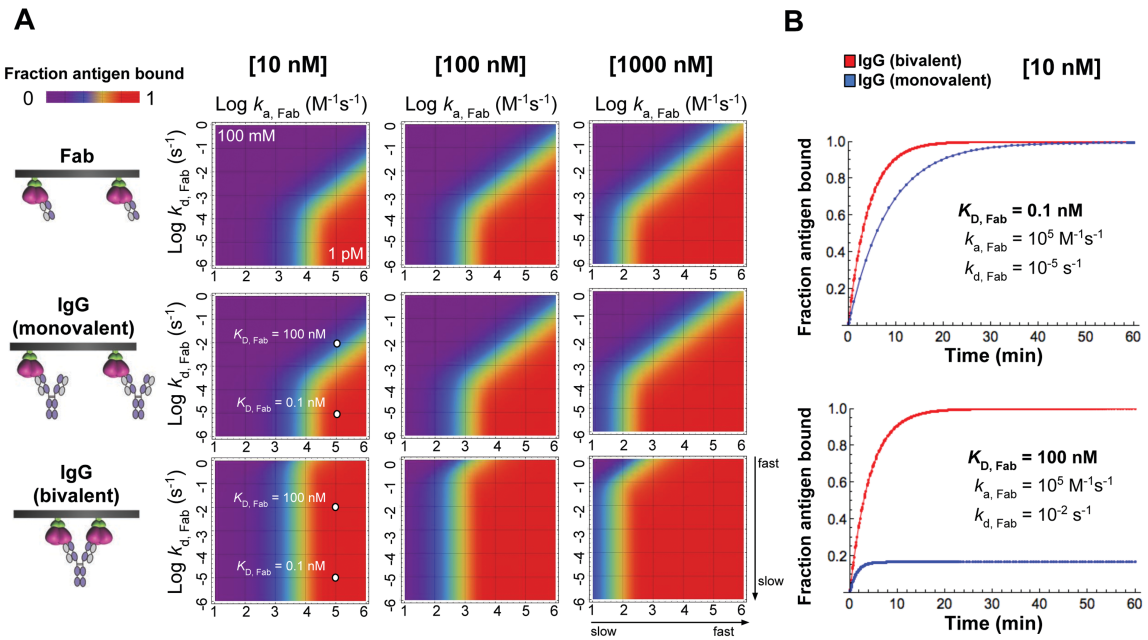

Figure 6. Simulations of avidity effects due to bivalent binding of IgG to a tethered antigen. (**A**) The fraction of tethered antigen bound by different concentrations of IgG or Fab after 1 hour shown as a heat map (cooler colors representing a lower percentage bound and warmer colors representing a higher percentage bound) as a function of kinetic constants for the IgG-antigen or Fab-antigen interaction. The fraction of antigen bound by a Fab or IgG was calculated as a function of k_a and k_d. The intrinsic affinities are strongest in the lower right corner (1 pM) and weakest in the upper left corner (100 mM) of each graph. For IgG, binding was forced to 100% monovalent binding (middle row) or 100% bivalent binding (bottom row). Saturation by Fabs and IgGs was nearly identical for monovalent binding conditions because the binding kinetics of IgGs would be enhanced by at most 2-fold. Comparisons of the simulations for bivalent binding (bottom row) and monovalent binding (top two panels) showed regions of saturation binding resulting from avidity effects. (**B**) The fraction of antigen bound as a function of time for

IgGs binding to surface-tethered antigens at an input concentration of 10 nM. When the dissociation rate constant of the Fab portion of the IgG is slow (top panel) and the input concentration is approximately 100-fold higher than the affinity of the Fab, IgGs can reach saturation binding after an hour whether binding monovalently or bivalently to the surface – therefore avidity effects are not apparent after an hour. However, weakening the affinity of the Fab by making the dissociation rate 1000-fold faster (bottom panel) prevents saturation when binding monovalently, but has no affect on saturation when binding bivalently – thus avidity effects are apparent throughout the incubation.

DISCUSSION

We engineered new HIV-1 spike-binding molecules designed to bind bivalently to demonstrate the importance of avidity effects in antibody efficacy in HIV-1 neutralization and to establish that lack of bivalent binding by physiologic IgGs is an additional antibody evasion strategy utilized by HIV-1.

The importance for HIV-1 in maintaining a low spike density to avoid inter-spike crosslinking by IgGs was suggested by the relatively small improvements in neutralization potencies of intact anti-HIV-1 IgGs compared with their Fab counterparts (Klein and Bjorkman, 2010) and by the discovery that polyreactivity increased the apparent affinity of anti-HIV-1 antibodies through a mechanism of heteroligation (Mouquet et al., 2010). Comparison of the neutralization potencies of IgGs versus Fabs in the current study provides further support for the observation that anti-HIV-1 IgGs generally exhibit relatively small increased potencies compared to Fabs. To quantify potential avidity effects, we previously defined the molar neutralization ratio (MNR) for IgG versus Fab forms of an antibody as IC_{50} Fab (nM)/IC_{50} IgG (nM). In the absence of avidity or other advantages of the IgG compared with the Fab (e.g., increased size), the ratio would be 2.0 (Klein and Bjorkman, 2010). In the current study, the mean MNR for PG16, an IgG that cannot exhibit intra-spike crosslinking (Julien et al., 2013c), was 8.0 (data from Figure 2C), similar to the 10.5 mean MNR in a previous study (West et al., 2012). These values are lower than MNRs observed for IgGs against densely-packed viruses, which can be over 1000, but are consistent with a limited amount of inter-spike crosslinking by anti-HIV-1 IgGs whose epitopes on neighboring spikes are accessible to simultaneous engagement of the combining sites of the two Fabs of an IgG, which are

separated by ~150 Å (Klein and Bjorkman, 2010). Our current results suggested that inter-spike crosslinking can be increased by creating homo-diFabs with 70bp–100bp dsDNA linkers (Figure 2B, Figure S2D). These linkers would separate the combining sites of the Fabs by ≥240–340 Å, distances that should enhance inter-spike crosslinking.

Indirect evidence for the hypothesis that HIV-1 evolved a low spike density to avoid inter-spike crosslinking IgGs comes from studies of a cytoplasmic tail deletion in the simian immunodeficiency virus (SIV) spike trimer. Cytoplasmic tail deletion has been suggested to increase the number of spikes per virion (Zingler and Littman, 1993) and/or the spike mobility in the virion bilayer (Crooks et al., 2008), both of which could enhance inter-spike crosslinking. Although tail-deleted mutant viruses can be produced in vitro, propagation of the virus in macaques favors viruses containing the full-length envelope spike (Zingler and Littman, 1993). These findings are consistent with the idea that an intact host immune system selects against those viruses that facilitate the ability of host IgGs to bind bivalently through inter-spike crosslinking.

Here we present a method to create potential intra-spike crosslinking antibody-based molecules using dsDNA- and protein-based linkers, and demonstrate that these reagents can exhibit up to three orders of magnitude increases in neutralization potency. We argue that the optimized versions of our new molecules achieve potency increases through intra-spike, rather than inter-spike, crosslinking because (*i*) distances measured between epitopes on virion-bound spike trimers corresponded to approximate intra-epitope distances on HIV-1 spike trimer structures, and (*ii*) increases in inter-spike crosslinking by homotypic and heterotypic reagents should not exhibit sharp linker length-dependent neutralization potencies since distances between spikes vary within a

single virion and between virions. The latter point is valid even if HIV-1 spikes are clustered on mature virions, as suggested by fluorescence nanoscopy (Chojnacki et al., 2012), but not cryoelectron microscopy (Liu et al., 2008; Zhu et al., 2006). Whether HIV-1 spikes cluster upon encountering a target cell to form an entry claw (Sougrat et al., 2007) is not relevant to the mechanism of action of our reagents, since neutralization assays are conducted by incubating potential inhibitors with virions prior to addition of target cells (Montefiori, 2005), a mechanism that is also presumably relevant for most in vivo interactions of antibody and antibody-like inhibitors. Because avidity effects require recognition of two or more antigens tethered to the same surface, another potential action of our reagents, inter-virion crosslinking, would not result in avidity effects by analogy to the lack of avidity enhancement for an IgG binding two soluble antigens, one per Fab. In this respect, we note that although IgAs are capable of inter-virion crosslinking (Stieh et al., 2014), conversion of IgG bNAbs to IgAs did not result in potency increases (Kunert et al., 2004; Wolbank et al., 2003).

The use of dsDNA- and protein-based molecular rules to measure inter-epitope distances presented here can be used to probe conformations of virion-bound Env trimers. By contrast, EM and X-ray structures (Bartesaghi et al., 2013; Julien et al., 2013b; Lyumkis et al., 2013; Pancera et al., 2014b) cannot capture dynamic information concerning Env conformations during neutralization. Single-molecule fluorescence resonance energy transfer (smFRET) measurements suggested that Env trimers on the surface of HIV-1 virions transition between different conformations (Munro et al., 2014), and spike trimers have been visualized by EM in different conformations: the closed structure of unliganded trimers and trimers associated with VRC01-like bNAbs

(Bartesaghi et al., 2013; Liu et al., 2008; Lyumkis et al., 2013) (also observed in Fab-bound crystal structures (Julien et al., 2013b; Pancera et al., 2014b)), a CD4- and/or 17b-bound open structure (Liu et al., 2008; Tran et al., 2012), and a partially-open b12-bound structure (Liu et al., 2008) (Figure 3A). Homo- and hetero-diFabs joined by different lengths of dsDNA bridges offer a new methodology to probe Env trimer conformational states on virions and potentially to address strain-specific conformational differences.

Homo-diFabs constructed from VRC01-like bNAbs showed greatest potency when binding to epitopes separated by distances most closely approximating the open structure (Liu et al., 2008; Tran et al., 2012), rather than the closed structure observed for soluble and virion-associated spike trimers bound to VRC01-like Fabs (Bartesaghi et al., 2013; Liu et al., 2008; Lyumkis et al., 2013) (Figure 2B, 3; Figure S3-S4). These results suggest that optimal intra-spike crosslinking molecules can inhibit a different state than recognized by monovalent Fabs binding to spike trimers in static EM and X-ray structures (Bartesaghi et al., 2013; Liu et al., 2008; Lyumkis et al., 2013; Merk and Subramaniam, 2013; Tran et al., 2012). If so, one Fab of a homo-diFab could first bind to its epitope on a closed trimer, allowing the second Fab to latch on to a transiently-populated open form of that trimer. Alternatively, binding of the first Fab may trap the trimer into a conformation, allowing increased accessibility of the second Fab, or both Fabs could bind simultaneously to a transiently-appearing open trimer. Interestingly, the distance dependence of two CD4bs antibodies, 3BNC60 and b12, was more strongly pronounced for a Tier 1B HIV-1 strain, 6535.3, than for Tier 2 or 3 strains against which the homo-diFabs were tested (Figure 2B, Figure S2). Tier categorization of HIV-1 strains refers to the sensitivity of a strain to antibody neutralization, with Tier 1 strains being

more sensitive in general to antibodies than Tier 2 or 3 strains (Seaman et al., 2010). The differences in length dependence for CD4bs homo-diFabs may reflect differences in conformational variability within Env trimers from different tiers, with Tier 1 Env perhaps more easily able to adopt the open conformations likely recognized by the CD4bs antibodies with optimal bridge lengths.

For the PG16-3BNC60 hetero-diFabs, the optimal 40bp and 50bp bridge lengths (136 Å and 170 Å, respectively) corresponded to the approximate separation distances between PG16 and 3BNC60 Fabs when bound to the same gp120 within a trimer (147 Å) or to neighboring protomers within open or partially-open trimers (167 Å) (Figure S3). In a second hetero-diFab bridge length dependency example, 10-1074-40bp-3BNC60 was more potent than 10-1074-60bp-3BNC60 (Figure 4, Table S4). The ~136 Å distance between the two Fabs in 10-1074-40bp-3BNC60 corresponded to the approximate separation between these Fabs bound to the same gp120 (141 Å), while 60bp more closely approximated Fabs bound to neighboring protomers on an open trimer (193 Å) (Figure S3). In general, it is more difficult to deduce information about Env trimer conformations recognized by hetero-diFabs because the intra-epitope distance is the same in the three conformations for Fabs binding to the same gp120 subunit within an Env trimer (Figure S3), and length-dependence data for some of the hetero-diFabs, e.g., 10-1074-40bp-3BNC60, was consistent with binding to a single gp120 within an Env trimer as well as to adjacent gp120s (Figure S2). However, whether binding to the same or to adjacent protomers within the spike trimer, the increased synergy of optimal hetero-diFabs suggested a mechanism in which the more potent/tighter-binding Fab of the

hetero-diFab initially bound to the viral spike, thereby allowing the second Fab, even when only weakly neutralizing on its own, to attach.

In summary, our results demonstrated that optimal length homo- and hetero-diFabs are capable of synergistic effects that increased neutralization potencies, and in some cases, allowed neutralization of viral strains resistant to conventional IgGs. These results are consistent with the hypothesis that most anti-HIV-1 IgGs bind monovalently to single Env spikes, which leaves them vulnerable to Env mutations that weaken monovalent interactions but would still permit bivalent interactions (Klein and Bjorkman, 2010). The demonstration that anti-HIV-1 reagents designed to be capable of intra-spike binding with avidity can more potently and broadly neutralize HIV-1 than conventional anti-spike IgGs is relevant to the choice of anti-HIV-1 proteins or genes to be delivered passively to prevent infection or suppress active infections. Bi-specific antibodies that simultaneously bind to HIV-1 Env and to CD4 or CCR5 host receptors on the target cell represent a conceptually distinct method to increase the potency and breadth of anti-HIV-1 reagents (Pace et al., 2013). In contrast to these reagents, antibodies that achieve synergy via bivalent binding to Env by intra-spike crosslinking offer significant advantages for passive delivery; for example, neutralizing antibodies against HIV-1 Env protect more effectively in vivo than antibodies against CD4 (Pegu et al., 2014), and anti-self antibodies such as anti-CD4 IgGs have short half-lives in vivo (Bruno and Jacobson, 2010). We propose that the ideal therapeutic molecule would utilize avidity achieved by intra-spike crosslinking to reduce the concentration required for sterilizing immunity and render the low spike density of HIV-1 irrelevant to its efficacy. Moreover, analogous to

using several drugs or antibodies during anti-retroviral therapy, simultaneous binding to different HIV-1 epitopes should reduce or abrogate sensitivity to Env mutations.

EXPERIMENTAL PROCEDURES

Expression and purification of Fabs

Genes encoding IgG light chain genes were modified by site-directed mutagenesis to replace $Cys263_{Light\ Chain}$, the C-terminal cysteine that forms a disulfide bond with $Cys233_{Heavy\ Chain}$, with a serine. Modified light chain genes and genes encoding 6x-His- or StrepII-tagged Fab heavy chains (V_H–C_H1–tag) were subcloned separately into the pTT5 mammalian expression vector (NRC Biotechnology Research Institute). Fabs were expressed by transient transfection in HEK 293-6E (NRC Biotechnology Research Institute) cells as described (Diskin et al., 2011a) and purified from supernatants by Ni-NTA or StrepII affinity chromatography followed by size exclusion chromatography in PBS pH 7.4 using a Superdex 200 10/300 or Superdex 200 16/600 column (Amersham Biosciences).

IgG heterodimers

Bispecific IgGs were constructed using "knobs-into-holes" mutations (Thr366Trp on one heavy chain, and Thr366Ser, Leu368Ala, and Tyr407Val on the other heavy chain (Atwell et al., 1997)) to promote Fc heterodimerization, and crossover of the heavy and light chain domains of one half of the bispecific IgG to prevent light chain mispairing (Schaefer et al., 2011). Heterodimerizing leucine zipper sequences (O'Shea et al., 1993) followed by either a 6x-His or Strep II tag sequence (Schmidt and Skerra, 2007) were added to the C-termini of the heavy chains. The V_H domain on one heavy chain of each heterodimer was replaced by the V_L domain, and the corresponding light chain was

constructed with the V_H domain joined to the C_L domain as described (Schaefer et al., 2011). Heterodimeric IgGs were expressed by transient transfection and isolated from supernatants by Protein A chromatography followed by Strep II and Ni-NTA chromatography. Heterodimers were further purified by size exclusion chromatography using a Superdex 200 10/300 or 16/600 column (Amersham Biosciences) equilibrated in PBS pH 7.4.

DNA conjugation to Fabs

The NUPACK server (Zadeh et al., 2011) was used to predict thermally-stable DNA sequences lacking secondary structures to make dsDNA bridges. Bridge and linker sequences are listed in table below.

DNA type	Linker Length (bp)	DNA sequence
Fab 1 ssoligo linker	32	5- /5AmMC6/TTT TTT TTT TTT CTT TGT TCT TAT TCT CTG CT-3
Fab 2 ssoligo linker	32	5- /5AmMC6/AAG AGA GAG AAA AGG AAG AAG GGA AGA AGA GG-3
10bp bridge and linker	10	5- /5AmMC6/TTT TTT TTT TTT GGA CGA AGT C-3
		5- /5AmMC6/AAG AGA GAG AAA GAC TTC GTC C -3
15bp bridge and linker	15	5- /5AmMC6/TTT TTT TTT TTT GGA CGA AGT CCA ACC -3
		5- /5AmMC6/AAG AGA GAG AAA GGT TGG ACT TCG TCC -3
20bp bridge and linker	20	5- /5AmMC6/TTT TTT TTT TTT CGT GGT CAT GAG CCG GGA CG -3
		5- /5AmMC6/AAG AGA GAG AAA CGT CCC GGC TCA TGA CCA CG -3
25bp bridge and linker	25	5- /5AmMC6/TTT TTT TTT TTT CGT GGT CAT GAG CCG GGA CGA AGT C -3
		5- /5AmMC6/AAG AGA GAG AAA GAC TTC GTC CCG GCT CAT GAC CAC G -3
30bp bridge and linker	30	5- /5AmMC6/TTT TTT TTT TTT CGT GGT CAT GAG CCG GGA CGA AGT CCA ACC -3
		5- /5AmMC6/AAG AGA GAG AAA GGT TGG ACT TCG TCC CGG CTC ATG ACC ACG -3
40bp bridge and linker	40	5- /5Phos/GAG GAC TAT CCG GCG CCG TCC CTC TTC TTC CCT TCT TCC T -3
		5- /5Phos/GAC GGC GCC GGA TAG TCC TCA GCA GAG AAT AAG AAC AAA G -3
50bp bridge and linker	50	5- /5Phos/TGG GCG ACT CGA CGG CGC CGG ATA GTC CTC AGC AGA GAA TAA GAA CAA AG -3
		5- /5Phos/GAG GAC TAT CCG GCG CCG TCG AGT CGC CCA CCT CTT CTT CCC TTC TTC CT -3
60bp bridge and linker	60	5- /5Phos/T TCT TTC TTT CCT CCT TCT CCC TCT TCT TCC CTT CTT CCT-3
		5- /5Phos/G AGA AGG AGG AAA GAA AGA AAG CAG AGA ATA AGA ACA AAG-3
70bp bridge and linker	70	5- /5Phos/TTT TTT TTT TTT CGT GGT CAT GAG CCG GGA CG -3
		5- /5Phos/AGC CTT ACT GGT GGT GCC ACT GGG CGA CTC GAC GGC GCC GGA TAG TCC TCA GCA GAG AAT AAG AAC AAA G -3
80bp bridge and linker	80	5- /5Phos/GAG GAC TAT CCG GCG CCG TCG AGT CGC CCA GTG GCA CCA CCA GTA AGG CTT ATC GCA TGT CCT CTT CTT CCC TTC TTC CT -3
		5- /5Phos/ACA TGC GAT AAG CCT TAC TGG TGG TGC CAC TGG GCG ACT CGA CGG CGC CGG ATA GTC CTC AGC AGA GAA TAA GAA CAA AG -3
90bp bridge and linker	90	5- /5Phos/GAG GAC TAT CCG GCG CCG TCG AGT CGC CCA GTG GCA CCA CCA GTA AGG CTT ATC GCA TGT AAG TTG CAC CCC TCT TCT TCC CTT CTT CCT -3
		5- /5Phos/GGT GCA ACT TAC ATG CGA TAA GCC TTA CTG GTG GTG CCA CTG GGC GAC TCG ACG GCG CCG GAT AGT CCT CAG CAG AGA ATA AGA ACA AAG-3
100bp bridge and linker	100	5- /5Phos/GAG GAC TAT CCG GCC CCG TCG AGT CGC CCA GTG GCA CCA CCA GTA AGG CTT ATC GCA TGT AAG TTG CAC CCC CAT CCT CCC CTC TTC TTC CCT TCT TCC T-3
		5- /5Phos/GGA GGA TGG GGG TGC AAC TTA CAT GCG ATA AGC CTT ACT GGT GGT GCC ACT GGG CGA CTC GAC GGG GCC GGA TAG TCC TCA GCA GAG AAT AAG AAC AAA G-3

DNA was conjugated to free thiol-containing Fabs using a modified version of a previously-described protocol (Hendrickson et al., 1995). Briefly, Fabs were reduced in a buffer containing 10mM TCEP-HCl pH 7-8 for two hours, and then buffer exchanged three times over Zeba desalting columns (Thermo Scientific). The percentage of reduced Fab was determined using Invitrogen's Measure-IT Thiol Assay. Concurrently, a 5-20 base ssDNA containing a 5' amino group (Integrated DNA Technologies, IDT-DNA) was incubated with a 100-fold molar excess of an amine-to-sulfhydryl crosslinker (Sulfo-SMCC; Thermo Scientific) for 30 minutes to form a maleimide-activated DNA strand, which was buffer exchanged as described above. The reduced Fab and activated ssDNA were incubated overnight, and the Fab-ssDNA conjugate was purified by Ni-NTA or StrepII affinity chromatography (GE Biosciences) to remove unreacted Fab and ssDNA.

ssDNA was synthesized, phosphorylated, and PAGE purified by Integrated DNA Technologies. For di-Fabs containing dsDNA bridges longer than 40bp, complementary ssDNAs were annealed by heating (95˚C) and cooling (room temperature) to create dsDNA containing overhangs complementary to the Fab-ssDNA conjugates. dsDNA was purified by size exclusion chromatography (Superdex 200 10/300) and incubated overnight with the corresponding tagged Fab-ssDNA conjugates. Homo- and hetero-diFab reagents were purified by Ni-NTA and StrepII affinity chromatography when appropriate to remove free DNA and excess Fab-ssDNA conjugates, treated with T4 DNA ligase (New England Biolabs), and purified again by size exclusion chromatography (Figure S1B). To make di-Fabs containing dsDNA bridge lengths less than 40bp, two complementary ssDNA-conjugated Fabs were incubated at 37˚C without

a dsDNA bridge and then purified as described above. Protein-DNA reagents were stable at 4°C for >6 months as assessed by SDS-PAGE.

Characterization of DNA-Fab reagents

Fractions from the center of an SEC elution peak were concentrated using Amicon Ultra-15 Centrifugal Filter Units (Millipore) (MW cutoff = 10 kDa) to a volume of 500 µL, and DLS measurements were performed on a DynaPro® NanoStar™ (Wyatt Technology) using the manufacturer's suggested settings. Hydrodynamic radii were determined as described (Dev and Surolia, 2006). Briefly, a nonlinear least squares fitting algorithm was used to fit the measured correlation function to obtain a decay rate. The decay rate was converted to the diffusion constant that can be interpreted as the hydrodynamic radius via the Stokes-Einstein equation.

Hetero-diFab with TPR linker

PG16-TPR12-3BNC60, a C-to-C linked hetero-diFab containing 12 consensus tetratricopeptide-repeat (TPR) domains (Kajander et al., 2007a) as a protein linker (Klein et al., 2014b), was prepared from modified PG16 and 3BNC60 Fabs using a combination of sortase-catalyzed peptide ligation and click chemistry (Witte et al., 2013). The C-terminus of the PG16 Fab heavy chain was modified to include the amino acid sequence GGGGASLPETGGLNDIFEAQKIEWHEHHHHHH, comprising a flexible linker, the recognition sequence for *S. aureus* Sortase A (underlined), a BirA tag, and a 6x-His tag. The C-terminus of The 3BNC60 Fab heavy chain C-terminus was modified to include a $(Gly_4Ser)_3$ linker followed by 12 tandem TPR domains and the amino acid sequence

ASGGGGSGGGGSGGGGSLPETGGHHHHHH, comprising a second $(Gly_4Ser)_3$ linker, the Sortase A recognition sequence (underlined), and a 6x-His tag. The Fabs were expressed in HEK-6E cells and purified with Ni-NTA and gel filtration chromatography as described above. Peptides (GGGK with C-terminal azide and cyclooctyne click handles) were synthesized by GenScript, and sortase-catalyzed peptide ligation was used to attach the azide-containing peptide to PG16 Fab and the cyclooctyne-containing peptide to the 3BNC60-TPR12 fusion protein as described (Guimaraes et al., 2013). Approximate yields after each sortase reaction were ~30%. Peptide-ligated PG16 and 3BNC60 Fabs were passed over a Ni-NTA column to remove His-tagged enzyme and Fabs that did not lose their His tags during the reaction, mixed at equimolar ratios, and the click reaction was accomplished by incubating overnight at 25˚C. The approximate yield for the click reaction was ~65%. The resulting PG16-TPR12-3BNC60 hetero-diFab was purified by size exclusion chromatography to remove unreacted Fabs for an overall yield of ~22%.

Measurements of intra-spike distances

To derive predicted distances between two adjacent Fab bound to HIV-1 Env, we superimposed Fabs bound to their epitopes on the structures of Env trimers in three different conformations: closed (a 4.7 Å crystal structure of a gp140 SOSIP trimer; PDB code 4NCO), open (a 9 Å EM structure of a SOSIP trimer–17b Fab complex (Tran et al., 2012); coordinates obtained from S. Subramaniam), partially-open (an ~20 Å EM structure of a viral spike bound to b12 Fab; PDB code 3DNL). The positions of the C_H1 and C_L domains in Fab structures used for docking were adjusted to create Fabs with the

average elbow bend angle found in a survey of human Fab structures (Stanfield et al., 2006). The V_H-V_L domains of the adjusted Fabs were then superimposed on crystal structures of Fab-gp120 or Fab-gp140 complexes (PDB codes 3NGB, 2NY7 and 4CNO for complexes with VRC01, b12 and PGT122 Fabs, respectively) or a PG16-epitope scaffold complex (PDB code 4DQO). The position on Env trimer of 10-1074, a clonal variant of the PGT121-PGT123 family (Mouquet et al., 2012a), was approximated using the 4CNO gp140–PGT122 structure. In other cases, related antibodies, e.g., PG9/PG16 and VRC01/3BNC117/3BNC60, were also assumed to bind similarly. The complex structures were superimposed on the Env trimer structures by aligning the common portions. The distance between the $Cys233_{heavy\ chain}$ carbon- atoms of adjacent Fabs was then measured using PyMol (Schrödinger, 2011) to approximate the length of dsDNA bridges attached to $Cys233_{heavy\ chain}$. Measurements derived using other EM structures for the closed and open trimers (PDB codes 3DNN, 3J5M and 3DNO) or using a recent 3.5 Å Env trimer crystal structure (Pancera et al., 2014b) resulted in differences of ≤10 Å for analogous distance measurements.

In vitro neutralization assays

Neutralization of pseudoviruses derived from primary HIV-1 isolates was monitored by the reduction of HIV-1 Tat-induced luciferase reporter gene expression in the presence of a single round of pseudovirus infection in TZM-bl cells as described (Montefiori, 2005). In some cases, DEAE-dextran, an additive used to enhance viral infection of target cells (Montefiori, 2005), led to false positive neutralization signals for dsDNA alone and for dsDNA-containing reagents, presumably because of interactions

between dextran and DNA (Maes et al., 1967). Dextran was eliminated from assays in which the dsDNA linker alone reduced infectivity, in which case the pseudovirus concentration was increased by 2.5-40–fold, allowing for comparable infectivity as in the presence of dextran.

Pseudoviruses were generated by co-transfecting HEK293T cells with vectors encoding Env and a replication-deficient HIV-1 backbone as described (Montefiori, 2005) or obtained from the Fraunhofer Institut IBMT (6535.3, CAAN5342, CAP45, CAP210.200.E8, DU172, DU422, QH-0692, THRO4156.18, TRO.11, ZM53, ZM214, ZM233, ZM249). Neutralization assays were preformed in-house (Figure 2-4) and by the Collaboration for AIDS Vaccine Discovery (CAVD) core neutralization facility for testing against a panel of isolates (Figure 2C; Tables S1-S5). Some of the in-house data were derived from neutralization assays that were prepared by a Freedom EVO® (Tecan) liquid handler. Reagents (prepared as 3-, 4-, or 5-fold dilution series; each concentration in duplicate or triplicate) were incubated with 250 (when DEAE-dextran was added) or >1000 viral infectious units at 37°C for one hour prior to incubation with reporter cells (10,000/well) for 48 hours. Luciferase levels were measured from a cell lysate using an Infinite 200 Pro microplate reader (Tecan) after addition of BrightGlo (Promega). Data were fit by Prism (GraphPad) using nonlinear regression to derive IC_{50} values. IC_{50}s derived from independent replicates of manual and robotic assays generally agreed within 2-4 fold. Average IC_{50} values reported in the figures and tables are geometric means calculated using the formula $(\prod a_i)^{(1/n)}$; $i = 1, 2, \ldots, n$. Geometric means are suitable statistics for data sets covering multiple orders of magnitude (Sheskin, 2004), as is the case for neutralization data across multiple viral strains. Fold improvements were

calculated as the ratio of the geometric mean IC_{50} values for the reagents being compared.

Simulation of Fab and IgG saturation of surface-bound antigens

Numerical analysis (Mathematica, v. 10) was used to simulate saturation of surface-bound antigens by monovalent Fabs (Equation 1), bivalent IgGs to unpaired antigen (*Ag*) (Equation 2), and paired antigen (*pAg*) (Equations 3,4), where "paired antigen" was defined as antigens that are spaced such that an IgG can bind two epitopes simultaneously (e.g., intra-spike crosslinking of two epitopes on the same viral spike or inter-spike crosslinking between two viral spikes). In the bivalent model (Equations 3,4), the surface concentrations of antigen and IgG-antigen complexes were approximated by the inverse of the volume of a sphere (V_s) with radius equal to the hydrodynamic radius of the molecule multiplied by Avogadro's number (N_a) as described previously (Müller et al., 1998).

Fab binding to antigen:

$$Fab + Ag \rightleftarrows Fab - Ag$$

$$\frac{d[Fab-Ag]}{dt} = k_a[Fab][Ag] - k_d[Fab - Ag] \quad [1]$$

IgG binding to unpaired antigen:

$$IgG + Ag \rightleftarrows IgG - Ag$$

$$\frac{d[IgG-Ag]}{dt} = 2k_a[IgG][Ag] - k_d[IgG - Ag] \quad [2]$$

IgG binding to paired antigen:

$$IgG + pAg \rightleftarrows IgG - pAg$$

$$IgG - pAg + pAg \rightleftarrows IgG - pAg_2$$

$$\frac{d[IgG-pAg]}{dt} = 2k_a[IgG][pAg] - k_d[IgG - pAg]\frac{1}{V_s\,N_a} - \frac{d[IgG-pAg_2]}{dt} \quad [3]$$

$$\frac{d[IgG-pAg_2]}{dt} = k_a[IgG - pAg]\frac{1}{V_s\,\square_a}[pAg]\frac{1}{V_s\,N_a} - 2k_d[IgG - pAg_2]\frac{1}{V_s\,N_a} \quad [4]$$

Author Contributions

R.P.G. and P.J.B. conceived the study, J.S.K. performed simulations to assess avidity effects; R.P.G. and M.S.P. prepared dsDNA-Fab reagents, R.P.G., M.S.P., J.S.K., S.B., and A.P.W. perfected methods to attach dsDNA to Fabs, R.P.G. and M.S.S. performed neutralization assays, R.P.G., A.P.W., and P.J.B. analyzed the data, and R.P.G., M.C.N, and P.J.B. wrote the paper with contributions from all coauthors.

Acknowledgements

We thank Martin Witte, Jessica Ingram, Chris Theile, and Hidde Ploegh for advice and help with sortase/click chemistry experiments, Sriram Subramaniam for helpful discussions, coordinates, and files to make schematic figures, David Baltimore, Bil Clemons, Ron Diskin, Jennifer Keeffe, Sarkis Mazmanian, Stuart Sievers, Louise Scharf, and Kai Zinn for suggestions, Jost Vielmetter and the Caltech Protein Expression Center for assistance with protein production and neutralization assay development, Priyanthi Gnanapragasam for doing in-house neutralization assays, the NIH AIDS Reagent Program, the Fraunhofer Institut IBMT, and Rene Mares for pseudoviruses, Erin Isaza, Siduo Jiang, and Jennifer Keeffe for reagents, Sonal N. Patel and Marta Murphy for help with figures. This work was supported by the Director's Pioneer Award [1DP1OD006961-01 to P.J.B.], National Institutes of Health HIVRAD [P01 Al100148 to P.J.B.], and Collaboration for AIDS Vaccine Discovery (CAVD) grants with support from the Bill and Melinda Gates Foundation [grant 38660 (P.J.B.) and grant 1032144 (M.S.S.). P.J.B. and M.C.N. are HHMI Investigators.

References

Bartesaghi, A., Merk, A., Borgnia, M.J., Milne, J.L., and Subramaniam, S. (2013). Prefusion structure of trimeric HIV-1 envelope glycoprotein determined by cryo-electron microscopy. Nat Struct Mol Biol *20*, 1352-1357.

Bednar, J., Furrer, P., Katritch, V., Stasiak, A.Z., Dubochet, J., and Stasiak, A. (1995). Determination of DNA persistence length by cryo-electron microscopy. Separation of the static and dynamic contributions to the apparent persistence length of DNA. J Mol Biol *254*, 579-594.

Bhatia, A.K., Kaushik, R., Campbell, N.A., Pontow, S.E., and Ratner, L. (2009). Mutation of critical serine residues in HIV-1 matrix result in an envelope incorporation defect which can be rescued by truncation of the gp41 cytoplasmic tail. Virology *384*, 233-241.

Bruno, C.J., and Jacobson, J.M. (2010). Ibalizumab: an anti-CD4 monoclonal antibody for the treatment of HIV-1 infection. The Journal of antimicrobial chemotherapy *65*, 1839-1841.

Chertova, E., Bess Jr, J.W., Jr., Crise, B.J., Sowder, I.R., Schaden, T.M., Hilburn, J.M., Hoxie, J.A., Benveniste, R.E., Lifson, J.D., Henderson, L.E.*, et al.* (2002). Envelope glycoprotein incorporation, not shedding of surface envelope glycoprotein (gp120/SU), Is the primary determinant of SU content of purified human immunodeficiency virus type 1 and simian immunodeficiency virus. J Virol *76*, 5315-5325.

Chi, Q., Wang, G., and Jiang, J. (2013). The persistence length and length per base of single-stranded DNA obtained from fluorescence correlation spectroscopy

measurements using mean field theory. Physica A: Statistical Mechanics and its Applications *392*, 1072-1079.

Chojnacki, J., Staudt, T., Glass, B., Bingen, P., Engelhardt, J., Anders, M., Schneider, J., Muller, B., Hell, S.W., and Krausslich, H.G. (2012). Maturation-dependent HIV-1 surface protein redistribution revealed by fluorescence nanoscopy. Science *338*, 524-528.

Crooks, E.T., Jiang, P., Franti, M., Wong, S., Zwick, M.B., Hoxie, J.A., Robinson, J.E., Moore, P.L., and Binley, J.M. (2008). Relationship of HIV-1 and SIV envelope glycoprotein trimer occupation and neutralization. Virology *377*, 364-378.

Dev, S., and Surolia, A. (2006). Dynamic light scattering study of peanut agglutinin: size, shape and urea denaturation. Journal of biosciences *31*, 551-556.

Diskin, R., Scheid, J.F., Marcovecchio, P.M., West, A.P., Jr., Klein, F., Gao, H., Gnanapragasam, P.N., Abadir, A., Seaman, M.S., Nussenzweig, M.C.*, et al.* (2011). Increasing the potency and breadth of an HIV antibody by using structure-based rational design. Science *334*, 1289-1293.

Guimaraes, C.P., Witte, M.D., Theile, C.S., Bozkurt, G., Kundrat, L., Blom, A.E., and Ploegh, H.L. (2013). Site-specific C-terminal and internal loop labeling of proteins using sortase-mediated reactions. Nat Protoc *8*, 1787-1799.

Hendrickson, E.R., Truby, T.M., Joerger, R.D., Majarian, W.R., and Ebersole, R.C. (1995). High sensitivity multianalyte immunoassay using covalent DNA-labeled antibodies and polymerase chain reaction. Nucleic Acids Res *23*, 522-529.

Huang, J., Ofek, G., Laub, L., Louder, M.K., Doria-Rose, N.A., Longo, N.S., Imamichi, H., Bailer, R.T., Chakrabarti, B., Sharma, S.K.*, et al.* (2012). Broad and potent neutralization of HIV-1 by a gp41-specific human antibody. Nature *491*, 406-412.

Icenogle, J., Shiwen, H., Duke, G., Gilbert, S., Rueckert, R., and Anderegg, J. (1983). Neutralization of poliovirus by a monoclonal antibody: kinetics and stoichiometry. Virology *127*, 412-425.

Julien, J.P., Cupo, A., Sok, D., Stanfield, R.L., Lyumkis, D., Deller, M.C., Klasse, P.J., Burton, D.R., Sanders, R.W., Moore, J.P.*, et al.* (2013a). Crystal structure of a soluble cleaved HIV-1 envelope trimer. Science *342*, 1477-1483.

Julien, J.P., Lee, J.H., Cupo, A., Murin, C.D., Derking, R., Hoffenberg, S., Caulfield, M.J., King, C.R., Marozsan, A.J., Klasse, P.J.*, et al.* (2013b). Asymmetric recognition of the HIV-1 trimer by broadly neutralizing antibody PG9. Proc Natl Acad Sci U S A *110*, 4351-4356.

Kajander, T., Cortajarena, A.L., Mochrie, S., and Regan, L. (2007). Structure and stability of designed TPR protein superhelices: unusual crystal packing and implications for natural TPR proteins. Acta Crystallographica Section D-Biological Crystallography *63*, 800-811.

Klein, F., Mouquet, H., Dosenovic, P., Scheid, J.F., Scharf, L., and Nussenzweig, M.C. (2013). Antibodies in HIV-1 vaccine development and therapy. Science *341*, 1199-1204.

Klein, J.S., and Bjorkman, P.J. (2010). Few and far between: how HIV may be evading antibody avidity. PLoS Pathog *6*, e1000908.

Klein, J.S., Gnanapragasam, P.N., Galimidi, R.P., Foglesong, C.P., West, A.P., Jr., and Bjorkman, P.J. (2009). Examination of the contributions of size and avidity to the neutralization mechanisms of the anti-HIV antibodies b12 and 4E10. Proc Natl Acad Sci USA *106*, 7385-7390.

Klein, J.S., Jiang, S., Galimidi, R.P., Keeffe, J.R., and Bjorkman, P.J. (2014). Design and characterization of structured protein linkers with differing flexibilities. Protein Engineering, Design, and Selection *27*, 325-330.

Kunert, R., Wolbank, S., Stiegler, G., Weik, R., and Katinger, H. (2004). Characterization of molecular features, antigen-binding, and in vitro properties of IgG and IgM variants of 4E10, an anti-HIV type 1 neutralizing monoclonal antibody. AIDS Res Hum Retroviruses *20*, 755-762.

Liljeroos, L., Krzyzaniak, M.A., Helenius, A., and Butcher, S.J. (2013). Architecture of respiratory syncytial virus revealed by electron cryotomography. Proc Natl Acad Sci U S A *110*, 11133-11138.

Liu, J., Bartesaghi, A., Borgnia, M.J., Sapiro, G., and Subramaniam, S. (2008). Molecular architecture of native HIV-1 gp120 trimers. Nature *455*, 109-113.

Luftig, M.A., Mattu, M., Di Giovine, P., Geleziunas, R., Hrin, R., Barbato, G., Bianchi, E., Miller, M.D., Pessi, A., and Carfi, A. (2006). Structural basis for HIV-1 neutralization by a gp41 fusion intermediate-directed antibody. Nat Struct Mol Biol *13*, 740-747.

Lyumkis, D., Julien, J.P., de Val, N., Cupo, A., Potter, C.S., Klasse, P.J., Burton, D.R., Sanders, R.W., Moore, J.P., Carragher, B.*, et al.* (2013). Cryo-EM structure of a

fully glycosylated soluble cleaved HIV-1 envelope trimer. Science *342*, 1484-1490.

Mattes, M.J. (2005). Binding parameters of antibodies: pseudo-affinity and other misconceptions. Cancer Immunol Immunother *54*, 513-516.

Merk, A., and Subramaniam, S. (2013). HIV-1 envelope glycoprotein structure. Curr Opin Struct Biol *23*, 268-276.

Montefiori, D.C. (2005). Evaluating neutralizing antibodies against HIV, SIV, and SHIV in luciferase reporter gene assays. Current protocols in immunology / edited by John E Coligan [et al *Chapter 12*, Unit 12 11.

Mouquet, H., Scharf, L., Euler, Z., Liu, Y., Eden, C., Scheid, J.F., Halper-Stromberg, A., Gnanapragasam, P.N., Spencer, D.I., Seaman, M.S.*, et al.* (2012). Complex-type N-glycan recognition by potent broadly neutralizing HIV antibodies. Proc Natl Acad Sci U S A *109*, E3268-3277.

Mouquet, H., Scheid, J.F., Zoller, M.J., Krogsgaard, M., Ott, R.G., Shukair, S., Artyomov, M.N., Pietzsch, J., Connors, M., Pereyra, F.*, et al.* (2010). Polyreactivity increases the apparent affinity of anti-HIV antibodies by heteroligation. Nature *467*, 591-595.

Munro, J.B., Gormann, J., Ma, X., Zhou, Z., Arthos, J., Burton, D.R., Koff, W.C., Courtner, J.R., Smith, A.B., 3rd, Kwong, P.D.*, et al.* (2014). Conformational dynamics of single HIV-1 envelope trimers on the surface of native virions. Science Xpress *published online 8 October 2014 [DOI:10.1126/science.1254426]*.

Pace, C.S., Song, R., Ochsenbauer, C., Andrews, C.D., Franco, D., Yu, J., Oren, D.A., Seaman, M.S., and Ho, D.D. (2013). Bispecific antibodies directed to CD4 domain 2 and HIV envelope exhibit exceptional breadth and picomolar potency against HIV-1. Proc Natl Acad Sci U S A *110*, 13540-13545.

Pancera, M., Zhou, T., Druz, A., Georgiev, I.S., Soto, C., Gorman, J., Huang, J., Acharya, P., Chuang, G.Y., Ofek, G.*, et al.* (2014). Structure and immune recognition of trimeric pre-fusion HIV-1 Env. Nature.

Pegu, A., Yang, Z.Y., Boyington, J.C., Wu, L., Ko, S.Y., Schmidt, S.D., McKee, K., Kong, W.P., Shi, W., Chen, X.*, et al.* (2014). Neutralizing antibodies to HIV-1 envelope protect more effectively in vivo than those to the CD4 receptor. Science translational medicine *6*, 243ra288.

Roben, P., Moore, J.P., Thali, M., Sodroski, J., Barbas, C.F., 3rd, and Burton, D.R. (1994). Recognition properties of a panel of human recombinant Fab fragments to the CD4 binding site of gp120 that show differing abilities to neutralize human immunodeficiency virus type 1. J Virol *68*, 4821-4828.

Schaefer, W., Regula, J.T., Bahner, M., Schanzer, J., Croasdale, R., Durr, H., Gassner, C., Georges, G., Kettenberger, H., Imhof-Jung, S.*, et al.* (2011). Immunoglobulin domain crossover as a generic approach for the production of bispecific IgG antibodies. Proc Natl Acad Sci U S A *108*, 11187-11192.

Scheid, J.F., Mouquet, H., Ueberheide, B., Diskin, R., Klein, F., Olivera, T.Y., Pietzsch, J., Fenyo, D., Abadir, A., Velinzon, K.*, et al.* (2011). Sequence and Structural Convergence of Broad and Potent HIV Antibodies That Mimic CD4 Binding. Science *333*, 1633-1637.

Schofield, D.J., Stephenson, J.R., and Dimmock, N.J. (1997). Variations in the neutralizing and haemagglutination-inhibiting activities of five influenza A virus-specific IgGs and their antibody fragments. J Gen Virol *78 (Pt 10)*, 2431-2439.

Schrödinger, L. (2011). The PyMOL Molecular Graphics System (The PyMOL Molecular Graphics System).

Seaman, M.S., Janes, H., Hawkins, N., Grandpre, L.E., Devoy, C., Giri, A., Coffey, R.T., Harris, L., Wood, B., Daniels, M.G.*, et al.* (2010). Tiered categorization of a diverse panel of HIV-1 Env pseudoviruses for assessment of neutralizing antibodies. J Virol *84*, 1439-1452.

Sougrat, R., Bartesaghi, A., Lifson, J.D., Bennett, A.E., Bess, J.W., Zabransky, D.J., and Subramaniam, S. (2007). Electron tomography of the contact between T cells and SIV/HIV-1: implications for viral entry. PLoS Pathog *3*, e63.

Stanfield, R.L., Zemla, A., Wilson, I.A., and Rupp, B. (2006). Antibody elbow angles are influenced by their light chain class. J Mol Biol *357*, 1566-1574.

Stieh, D.J., King, D.F., Klein, K., Liu, P., Shen, X., Hwang, K., Ferrari, G., Montefiori, D.C., Haynes, B., Pitisuttithum, P.*, et al.* (2014). Aggregate complexes of HIV-1 induced by multimeric antibodies. Retrovirology *11*, 78.

Tran, E.E., Borgnia, M.J., Kuybeda, O., Schauder, D.M., Bartesaghi, A., Frank, G.A., Sapiro, G., Milne, J.L., and Subramaniam, S. (2012). Structural mechanism of trimeric HIV-1 envelope glycoprotein activation. PLoS Pathog *8*, e1002797.

Walker, L.M., Phogat, S.K., Chan-Hui, P.Y., Wagner, D., Phung, P., Goss, J.L., Wrin, T., Simek, M.D., Fling, S., Mitcham, J.L.*, et al.* (2009). Broad and Potent

Neutralizing Antibodies from an African Donor Reveal a New HIV-1 Vaccine Target. Science *326*, 285-289.

West, A.P., Jr., Galimidi, R.P., Gnanapragasam, P.N., and Bjorkman, P.J. (2012). Single-chain Fv-based anti-HIV proteins: potential and limitations. J Virol *86*, 195-202.

West, A.P., Jr., Scharf, L., Scheid, J.F., Klein, F., Bjorkman, P.J., and Nussenzweig, M.C. (2014). Structural insights on the role of antibodies in HIV-1 vaccine and therapy. Cell *156*, 633-648.

Witte, M.D., Theile, C.S., Wu, T., Guimaraes, C.P., Blom, A.E., and Ploegh, H.L. (2013). Production of unnaturally linked chimeric proteins using a combination of sortase-catalyzed transpeptidation and click chemistry. Nat Protoc *8*, 1808-1819.

Wolbank, S., Kunert, R., Stiegler, G., and Katinger, H. (2003). Characterization of human class-switched polymeric (immunoglobulin M [IgM] and IgA) anti-human immunodeficiency virus type 1 antibodies 2F5 and 2G12. J Virol *77*, 4095-4103.

Wu, H., Pfarr, D.S., Tang, Y., An, L.L., Patel, N.K., Watkins, J.D., Huse, W.D., Kiener, P.A., and Young, J.F. (2005). Ultra-potent antibodies against respiratory syncytial virus: effects of binding kinetics and binding valence on viral neutralization. J Mol Biol *350*, 126-144.

Wu, X., Yang, Z.Y., Li, Y., Hogerkorp, C.M., Schief, W.R., Seaman, M.S., Zhou, T., Schmidt, S.D., Wu, L., Xu, L.*, et al.* (2010). Rational design of envelope identifies broadly neutralizing human monoclonal antibodies to HIV-1. Science *329*, 856-861.

Yu, X., Yuan, X., Matsuda, Z., Lee, T.H., and Essex, M. (1992). The matrix protein of human immunodeficiency virus type 1 is required for incorporation of viral envelope protein into mature virions. J Virol *66*, 4966-4971.

Zadeh, J.N., Steenberg, C.D., Bois, J.S., Wolfe, B.R., Pierce, M.B., Khan, A.R., Dirks, R.M., and Pierce, N.A. (2011). NUPACK: Analysis and design of nucleic acid systems. J Comput Chem *32*, 170-173.

Zhou, H.X. (2004). Polymer models of protein stability, folding, and interactions. Biochemistry *43*, 2141-2154.

Zhu, P., Liu, J., Bess, J., Jr., Chertova, E., Lifson, J.D., Grise, H., Ofek, G.A., Taylor, K.A., and Roux, K.H. (2006). Distribution and three-dimensional structure of AIDS virus envelope spikes. Nature *441*, 847-852.

Zingler, K., and Littman, D.R. (1993). Truncation of the cytoplasmic domain of the simian immunodeficiency virus envelope glycoprotein increases env incorporation into particles and fusogenicity and infectivity. J Virol *67*, 2824-2831.

Chapter Four

The design and characterization of structured protein linkers with differing flexibilities

This chapter describes the characterization of engineered protein linkers. This work was a collaboration between Joshua Klein, Siduo Jiang, Jennifer Keeffe, and myself. Joshua Klein, Siduo Jiang and I each contributed equally to this work. The conception and many of the initial designs of linkers were by Joshua Klein. Joshua also performed early experiments and analyzed initial data. Siduo Jiang cloned, expressed, and purified protein linker reagents, as well as performed experiments, analyzed data, and aided in the design of various protein linkers. My contribution to this work was the design of a subset of the structured linkers, and cloning, expression, and purification of linker reagents, and performance experiments; as well as analysis and characterization of the protein linkers. In addition, throughout Siduo Jiang's time as an undergraduate researcher in the lab, I was his primary mentor, and oversaw all of the work that was done.

This chapter was previously published as:

Klein, J. S.*, Jiang, S.*, **Galimidi, R. P.*** et al. (2014). "Design and characterization of structured protein linkers with differing flexibilities." Protein Eng Des Sel **27**(10): 325-330.

*These authors all contributed equally to this work.

Abstract

Engineered fusion proteins containing two or more functional polypeptides joined by a peptide or protein linker are important for many fields of biological research. The separation distance between functional units can impact epitope access and the ability to bind with avidity; thus the availability of a variety of linkers with different lengths and degrees of rigidity would be valuable for protein design efforts. Here, we report a series of designed structured protein linkers incorporating naturally-occurring protein domains and compare their properties to commonly-used Gly_4Ser repeat linkers. When incorporated into the hinge region of an immunoglobulin G (IgG) molecule, flexible Gly_4Ser repeats did not result in detectable extensions of the IgG antigen binding domains, in contrast to linkers including more rigid domains such as β2-microglobulin, Zn-α2-glycoprotein, and tetratricopeptide repeats (TPRs). This study adds an additional set of linkers with varying lengths and rigidities to the available linker repertoire, which may be useful for the construction of antibodies with enhanced binding properties or other fusion proteins.

Introduction

Fusion proteins are engineered biomolecules containing parts from two or more genes synthesized as a single multi-functional construct. These have been critical in many areas of biological research including affinity purification (Lichty et al., 2005) and protein stabilization for structure determination (Zou et al., 2012). Bi-specific fusion proteins have also been utilized as biopharmaceuticals, with an active drug domain fused to a carrier domain, allowing for the drug's proper transport (Chen et al., 2013). Such proteins have been designed to penetrate epithelial membranes including the blood brain barrier, as well as to target a specific cell population (Pardridge, 2010). Due to the modularity of protein domains in the generation of functional constructs, fusion proteins will likely have increasing importance in research and drug design.

The successful construction of fusion proteins relies on the proper choice of a protein linker as direct fusion of two domains can lead to compromised biological activity (Bai et al., 2005; Zhang et al., 2009). Several studies have utilized existing databases to compile and characterize linkers in naturally occurring multi-domain proteins (Argos, 1990; George and Heringa, 2002). These studies have yielded amino acid sequence propensities for natural linkers of various sizes and lengths, as well to information on rigidity and secondary structure. This information has helped the empirical design of linkers that are customized for particular applications.

Linkers can be classified into three groups: flexible, rigid, and cleavable (Chen et al., 2013). Flexible linkers are generally composed of small, non-polar or polar residues such as Gly, Ser, and Thr. The most common is the $(Gly_4Ser)_n$ linker (Gly-Gly-Gly-Gly-Ser)$_n$, where n indicates the number of repeats of the motif. Poly-glycine linkers have also

been evaluated, but the addition of a polar residue such as serine can reduce linker-protein interactions and preserve protein function. Due to their flexibility, these linkers are unstructured and thus provided limited domain separation in a previous study (Evers et al., 2006). As a result, more rigid linkers including poly-proline motifs (Schuler et al., 2005) and an all alpha-helical linker $A(EAAAK)_nA$ (Arai et al., 2001) have been developed.

We are interested in using relatively rigid protein linkers to separate anti-HIV binding proteins at distances that would permit bi- or multivalent binding to HIV Env glycoproteins with the objective of creating reagents capable of cross-linking epitopes within a single Env trimer (intra-spike crosslinking). Such reagents would take advantage of avidity effects to minimize HIV's ability to evade neutralizing antibodies by rapidly mutating to lower the affinity between the HIV epitopes and the antigen recognition fragment (Fab) of the antibody (Klein et al., 2009b). Although the architecture of the HIV spike trimer does not permit intra-spike cross-linking by most natural antibodies (Klein and Bjorkman, 2010; Zhu et al., 2006), it may be possible to create reagents capable of bivalent binding to an HIV Env trimer by fusing two identical reagents or two different reagents with an appropriate length linker. Here we report the design, construction, and characterization of a series of structured protein linkers incorporating both rigid and flexible domains that can be used to achieve a variety of different desired separations. The linkers were incorporated into the hinge region of an intact IgG antibody and evaluated for their relative lengths and rigidities by dynamic light scattering.

Methods

Plasmid construction and protein purification

Genes encoding designed linkers were synthesized (Blue Heron Bio) with restriction sites for the enzymes NheI (5' end) and either NgoMIV or HindIII (3' end). These sites were also introduced into the gene, encoding the heavy chain of the HIV-neutralizing antibody b12 (Roben et al., 1994) such that the insert would be located between hinge region residues His235 and Thr236. Constructs encoding the b12 heavy chain gene with a linker inserted in the hinge region were subcloned into the pTT5 mammalian expression vector. The b12-linker IgGs were expressed transiently in HEK-6E cells by co-transfecting the b12-linker heavy chain genes with the b12 light chain gene as described (Diskin et al., 2011a).

IgG-linker fusion constructs were purified by protein A affinity chromatography (GE Healthcare) followed by purification and analysis by size exclusion chromatography (SEC) using a Superdex 200 10/300 GL column (GE Healthcare) in phosphate-buffered saline, 0.05% w/v sodium azide, pH 7.4.

Dynamic light scattering (DLS)

Fractions corresponding to the center of the SEC elution peak were concentrated using Amicon Ultra-15 Centrifugal Filter Units (Millipore) with a molecular weight cutoff of 100 kDa to a volume of 80-400 uL and concentrations of 0.5-1 mg/mL. Concentration differences within this range were not observed to affect the hydrodynamic radius values determined by DLS (data not shown). Sample sizes ranging from 80-350 µL were loaded into a disposable cuvette, and measurements were performed on a DynaPro® NanoStar™ (Wyatt Technology) using the manufacturer's suggested settings. A fit of the second

order autocorrelation function to a globular protein model was used to derive the hydrodynamic radius.

Results and Discussion

Design and identity of designed linkers

In order to design potential structured linkers, we surveyed the Protein Data Bank (PDB) to find structures that were relatively elongated and rigid, or represented small globular proteins. We chose Zn-α2-glycoprotein (ZAG; PDB code: 1ZAG) as an example of a relatively elongated and rigid structure (Sanchez et al., 1999), and β2-microgloblin (β2m; PDB code: 1LDS) and ubiquitin (Ub; PDB code: 1UBQ) as examples of small globular proteins (Figure 1a). ZAG is a 31.5 kDa protein with a class I MHC heavy chain-like fold and a separation distance between the N- and C-termini of approximately 45 Å. β2m is a stable 12 kDa protein with an immunoglobulin constant region-like fold that forms a rigid structure with a separation distance between the N- and C-terminus of approximately 35 Å (Trinh et al., 2002). Likewise, Ub is a compact, stable 8.5 kDa protein with an N- and C-terminal separation distance of about 37 Å (Vijay-Kumar et al., 1987). In addition to the structured linkers chosen from the PDB, proline-rich linkers were designed from the hinge sequence from IgA1 (polyPro and polyPro(Glyc)). This glycosylated region confers rotational flexibility of the Fab relative to the Fc in the context of wildtype dimeric IgA1 (Bonner et al., 2008). In addition, glycosylation has been shown to potentially increase stability of polypeptide linkers (Imperiali and O'Connor, 1999). ZAG, β2m, and Ub proteins were joined in various combinations with short linker

regions, either $(Gly_2Ser)_n$ repeats, glycosylated proline-rich sequences (polypro(Glyc)), or unglycosylated proline-rich sequences (polypro), to create linkers L1 – L12 (Table 1).

We also created linkers using tetratricopeptide repeat domains (TPRs; PDB code: 2AVP; L13-L16; Table 1; Figure 1a) (Kajander et al., 2007b) that are found in natural proteins such as HSP70/90 (Scheufler et al., 2000). These domains are optimal for use as potential structured linkers because the length of a set of tandem TPR domains corresponds predictably with the number of repeats. Each repeat consists of 34 amino acids with a defined sequence motif that forms two α-helices (D'Andrea and Regan, 2003). Seven to eight TPRs form a complete superhelical turn with a pitch of about 72 Å. For our TPR linkers, we used a consensus sequence defined by the amino acid of the greatest global propensity in the natural database of the TPR domains at each position, which was shown to form a stable superhelix and was therefore named the consensus TPR sequence or cTPR (Main et al., 2003).

Finally, for comparison, we constructed a series of $(Gly_4Ser)_n$ linkers (L17 – L24; Table 1) in order to determine the effect of increasing the number of flexible Gly_4Ser repeats on the hydrodynamic radius of the IgG. The complete sequence of each linker is given in Table 2.

As a scaffold for comparing the designed structured linkers, we inserted each into the hinge region of an intact IgG antibody (the anti-HIV antibody b12) (Roben et al., 1994). We chose the hinge region of an IgG, which encompasses the amino acids between the C-terminus of the heavy chain portion of the antigen-binding fragment (Fab) and the N-terminus of the Fc, to insert the linkers because it can tolerate large protein

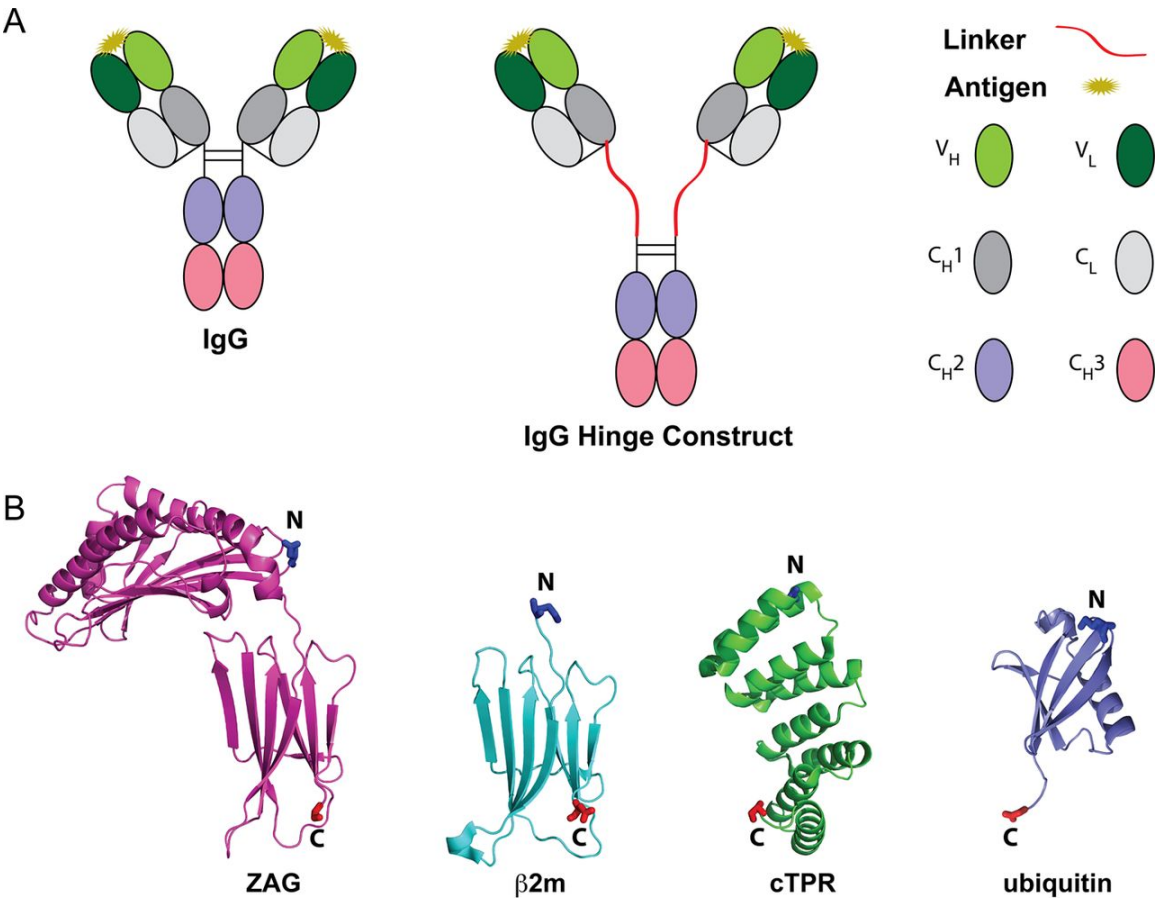

Figure 1. (A) Schematic of wildtype IgG (left) and IgG with a designed linker in its hinge region (middle). IgG domains are color coded as shown in the right panel. **(B)** Ribbon diagrams for domains used in structured linkers shown to scale (pdb codes: ZAG (1ZAG), β2m (1LDS), cTPR (2FO7), ubiquitin (1UBQ)). The cTPR structure shown contains 8 tandem repeats. N- and C-terminal residues are shown as sticks, color-coded blue for the N-terminus and red for the C-terminus.

Linker	Name	Description
L1	GPcPcPc	GlySer-polyPro(Glyc)-polyPro(Glyc)-polyPro(Glyc)
L2	GPPcP	GlySer-polyPro-polyPro(Glyc)-polyPro
L3	GPGcP	GlySer-polyPro-GlySer(Glyc)-polyPro
L4	GPPP	GlySer-polyPro-polyPro-polyPro
L5	GPbP	GlySer-polyPro-β2m-polyPro
L6	GPbG	GlySer-polyPro-β2m-GlySer
L7	PbGbG	polyPro-β2m-GlySer-β2m-GlySer
L8	GPbGbP	GlySer-polyPro-β2m-GlySer-β2m-polyPro
L9	GPUG	GlySer-polyPro-Ub-GlySer
L10	GPZP	GlySer-polyPro-ZAG-polyPro
L11	GGZGZP	GlySer-GlySer-ZAG-GlySer-ZAG-polyPro
L12	GcGcP	GlySer(Glyc)- GlySer(Glyc)-polyPro
L13	cTPR3	$(G_4S)_3$-cTPR3-$(G_4S)_3$
L14	cTPR6	$(G_4S)_3$-cTPR6-$(G_4S)_3$
L15	cTPR9	$(G_4S)_3$-cTPR9-$(G_4S)_3$
L16	cTPR12	$(G_4S)_3$-cTPR12-$(G_4S)_3$
L17	GS1	$(G_4S)_1$
L18	GS2	$(G_4S)_2$
L19	GS3	$(G_4S)_3$
L20	GS5	$(G_4S)_5$
L21	GS6	$(G_4S)_6$
L22	GS7	$(G_4S)_7$
L23	GS8	$(G_4S)_8$
L24	GS9	$(G_4S)_9$

Table 1. Description of structured linker designs. $(Gly_4Ser)_n$=Gly-Gly-Gly-Gly-Ser sequence with n number of repeats; GlySer = (N-term: $AGS(GGS)_3$; Middle: $(GGS)_4$; C-term: $(GGS)_3GAS]_2S$); GlySer(Glyc)=Gly-Gly-Ser sequence with an embedded potential N-linked glycosylation site (Asn-Ser-Ser); polyPro=proline-rich hinge sequence from IgA1; polyPro(Glyc)=proline-rich hinge sequence from IgA1 with an embedded potential N-linked glycosylation site (Asn-Ser-Ser); β2m=β-2-microglobulin; Ub=ubiquitin; ZAG=Zn-α2-glycoprotein; cTPRX=consensus tetratricopeptide repeat sequence with X number of repeats.

insertions (Redpath *et al.,* 1998). In addition, extension in the hinge region could potentially increase the separation distance of the Fab arms (Figure 1b).

Characterization of the IgGs containing structured linkers

The b12 IgG proteins containing linkers L1 – L24 were expressed by transient transfection in HEK 293-6E mammalian cells and purified by affinity and size exclusion chromatography. Visualization by SDS-PAGE for IgGs containing the L1 – L8 linkers showed that all proteins were purified to >95% homogeneity (Figure 2). Under reducing conditions, two heavy chain bands were observed for b12-L1, which contained a linker containing three potential N-linked glycosylation sites, indicating the presence of multiple glycosylated isoforms. An overlay of the chromatograms derived from SEC showed that the IgGs containing the L1 – L8 structured linkers all exhibited a decrease in retention volume relative to wild type IgG, consistent with the expected increases in the radius of gyration (R_g) of each of the constructs due to the addition of a structured linker (Figure 3).

We next derived the hydrodynamic radii using dynamic light scattering (DLS) for wildtype b12 and the b12 proteins containing designed linkers. DLS measures fluctuations in the intensity of scattered light of a protein solution over time, which can be used to calculate an autocorrelation function of intensity (Nobbmann et al., 2007). Typical monodisperse samples (including our hinge-linked antibodies) generate an exponential decay in the autocorrelation. A least squares fit can be performed to calculate the decay constant, which directly relates to the diffusion coefficient. The diffusion coefficient is then inversely related to the characteristic hydrodynamic radius R_H, which

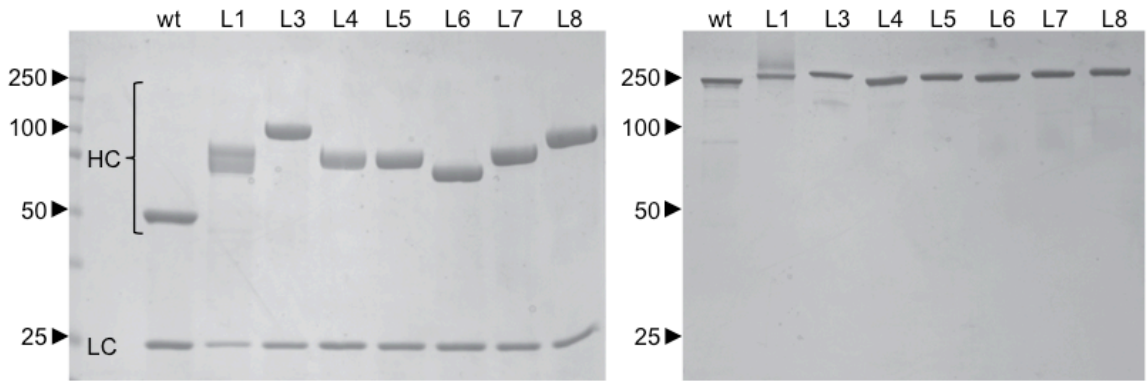

Figure 2. SDS-PAGE analysis of b12 IgG-structured linker proteins run under reducing (left) and non-reducing (right) conditions.

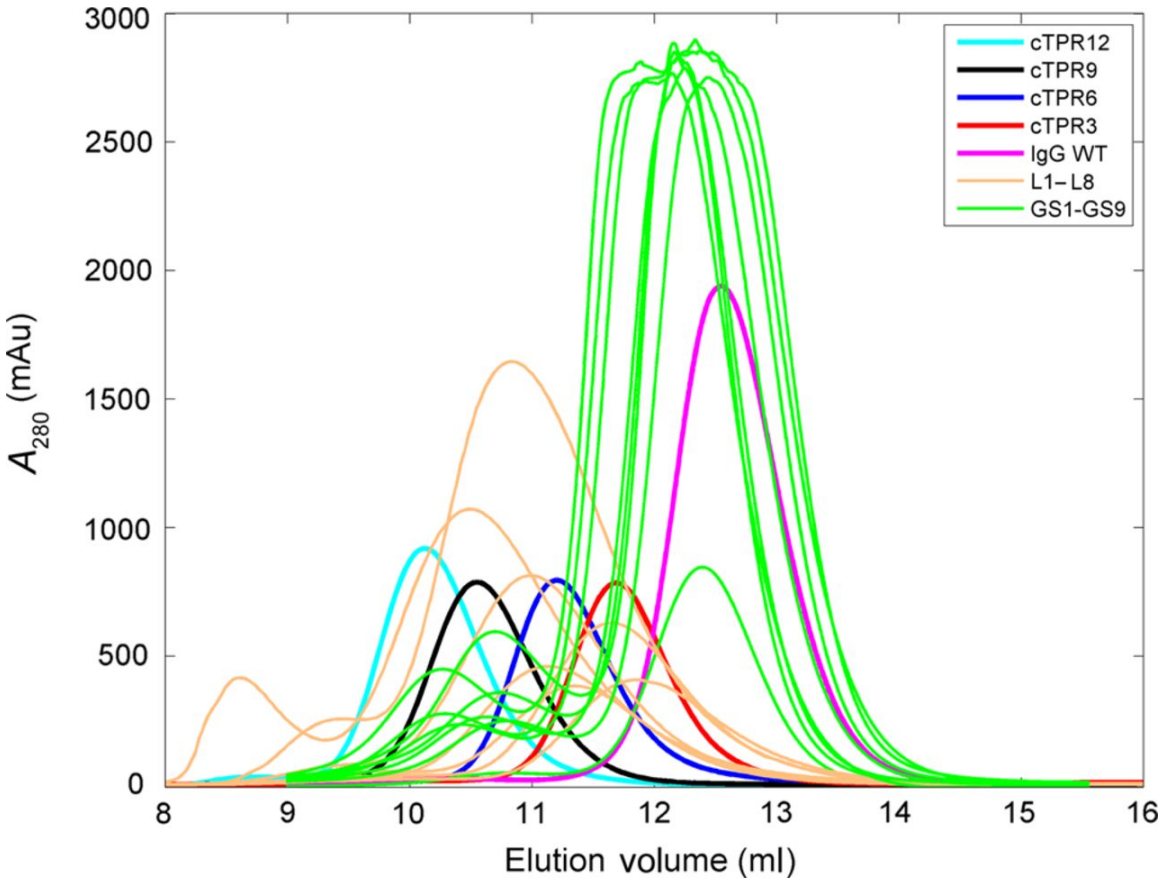

Figure 3. Overlay of size exclusion chromatograms for IgGs containing flexible and structured protein linkers. Structured linkers (L1-L8) exhibited larger decreases in retention volume with respect to wildtype compared to Gly_4Ser linkers, which exhibited little to no decrease depending on the number of repeats. Structured cTPR linkers also exhibited consistent decreases in retention volume as a function of the number of repeats.

reflects the radius of a hypothetical solid sphere that would diffuse at the same rate as the protein. The R_H value is not a direct measurement of the length that the linker contributes to the size of the IgG. However, comparative analysis can yield rank order differences for the relative lengths and rigidity of the various linkers. For example, if the separation between the IgG Fc and Fab domains were increased by the addition of a designed hinge linker, we would expect an observable increase in the R_H of the fusion construct compared to the parental b12 IgG due to increased size of the diffusion sphere.

The hydrodynamic radii were measured by DLS for each of the b12 IgG-linker fusion proteins and compared with an internal wildtype b12 IgG control (Figure 4). By comparing constructs containing elongated or small protein domain linkers, cTPR repeat linkers, and flexible $(Gly_4Ser)_n$ linkers of various lengths (L17 – L24), we could directly compare the effects of incorporating different lengths of flexible versus structured proteins linkers.

We observed a consistent trend for the R_H values between glycosylated and non-glycosylated linkers (L1, L2, L3, L12 vs. L4). The incorporation of three potential N-linked glycosylation sites in proline-rich linkers derived from the hinge region of IgA1 (L1) appeared to increase the R_H relative to constructs containing similar linker sequences with only one (L2) or no (L4) N-linked glycosylation sites, possibly through stabilization of the folded state and leading the linker to adopt a more extended conformation (Shental-Bechor and Levy, 2008). While the addition of only a single potential N-linked glycosylation site did not seem to affect the diffusion rate of proline-rich linkers (compare L2 and L4), a single potential N-linked glycosylation in the GGSG-NSS-GSGG region of a combination proline-rich and Gly_2Ser linker (L3) increased its

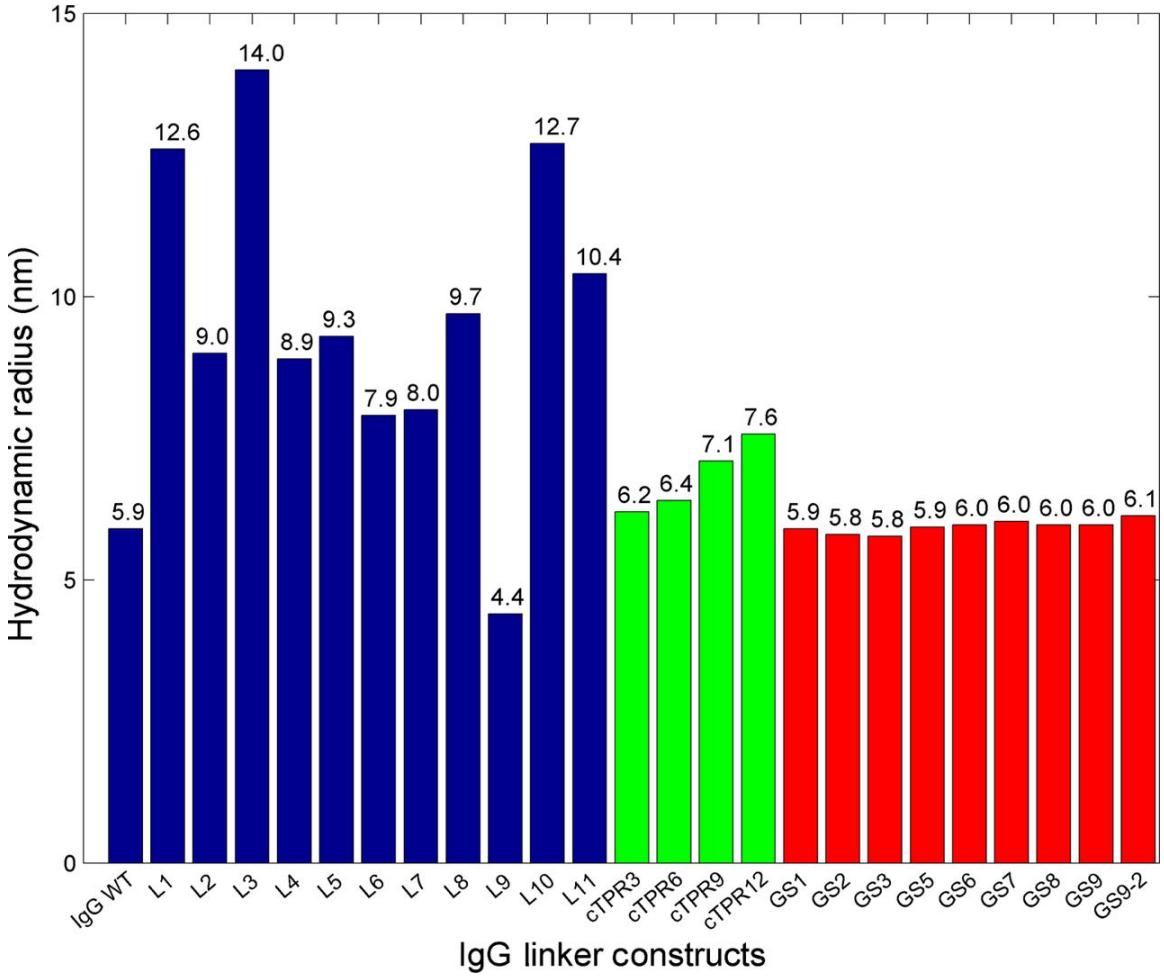

Figure 4. Comparative analysis by DLS of the hydrodynamic radii (R_H) of designed linkers in the context of the b12 IgG.

R_H beyond the R_H of a proline-rich linker with three potential N-linked glycosylation sites (L1). These data are consistent with the observation that N-linked glycosylation confers rigidity in the backbone of a flexible linker (Liu et al., 2000), suggesting these reagents contained linkers with a more extended conformation. Thus incorporating potential N-linked glycosylation sites within flexible linkers may be a general method to increase linker rigidity.

Adding a single β2m domain to a linker increased the R_H of the b12-linker protein to a similar degree as a proline-rich repeat relative to IgG (compare L5 to L2, L4, and IgG), suggesting that the structured β2m domain provided similar bulk and separation to the polyPro repeat. However, adding a second tandem β2m repeat separated from the first with a $(Gly_2Ser)_4$ sequence, did not increase the R_H appreciably (compare L8 and L5; L7 and L6). These results suggested that coupling a flexible Gly-Ser linker with the rigid β2m domain partially diminished the separation between Fc and Fab regions provided by β2m alone. A similar observation was made for hinge constructs containing ZAG (L10 and L11). A linker containing ZAG alone increased the hydrodynamic radius of the b12-linker protein compared to IgG and more than the IgG–proline-rich linker (compare L10 to L2 and L4). However, replacement of the proline-rich domain by ZAG that was flanked at both termini by a $(G_2S)_4$ peptide resulted in a decrease in hydrodynamic radius (compare L10 and L11).

We also investigated ubiquitin as a structured linker (L9). However, initial characterization by SDS-PAGE showed degradation at the linker site (data not shown). In addition, DLS measurements revealed that a purified sample of b12-L9 had a smaller R_H

than IgG similar to a Fab or Fc region alone, further suggesting ubiquitin-specific degradation (Figure 4).

cTPR linker series

cTPR constructs were generated with 3, 6, 9, or 12 tandem repeats. All cTPR linkers were flanked by $(Gly_4Ser)_3$ sequences (Table 2). The constructs exhibited a consistent decrease in elution volume on SEC as a function of the repeat length (Figure 3). These constructs also predictably increased the R_H of the linked IgG with increased number of tandem repeats (Figure 4). The hydrodynamic radius of the cTPR12 construct corresponded to approximately the size of L4, which contained a proline-rich linker. These data suggested that, unlike with repeated domains of the structured linkers, the increase in separation between the Fab and Fc correlated predictably with the number of cTPR repeats despite the presence of Gly_4Ser peptides flanking the N- and C-termini.

$(Gly_4Ser)_n$ linker series

In order to compare our structured linkers to the typical unstructured Gly-Ser linkers commonly used in protein design and engineering, we constructed, expressed, and purified eight IgG-$(G_4S)_n$ variants. In contrast to the SEC profiles for the structured linker constructs, there were only small differences in elution volume for the IgGs including Gly_4Ser linkers (L17 – L24). These differences often did not correlate with molecular mass as IgG-GS9, the IgG with the largest linker, eluted at approximately the same volume as wildtype IgG, which eluted after some of the constructs with shorter linkers (Figure 3).

Unlike proline-rich linkers and rigid linkers consisting of natural protein domains such as β2m, Gly_4Ser linkers that did not contain a potential N-linked glycosylation site did not detectably increase the hydrodynamic radius of the IgG, suggesting that these linkers did not provide increased separation between the Fab and Fc domains (Figure 4). These results were consistent with the observation that Gly_4Ser linkers did not provide significant separation between the joined domains in the context of other fusion proteins (Arai et al., 2001). Measurements of IgG-GS9 from two preparations showed only a slight difference in R_H (0.1 nm), indicating that these measurements were quite robust and relatively small differences in R_H may be significant.

Optimized linkers are important for the construction of multifunctional fusion proteins, in terms of both immunogenicity and conformational dynamics. Different linker compositions can alter their effective length and rigidity. In this study, we used SEC and DLS to characterize designed linkers in the context of an IgG to determine whether these linkers could increase the distance between the antigen binding fragments. We found that flexible Gly_4Ser linkers did not increase the R_H of fused reagents, suggesting that these linkers did not provide increased separation between the Fab and Fc domains even with up to nine Gly_4Ser repeats, in agreement with previous studies (Arai et al., 2001). By contrast, the structured helical cTPR linkers provided consistent increases in R_H and SEC elution volume as a function of repeat number, indicating that these repeats can be used to increase the separation distance between two proteins or domains. Our other designed linkers, including those containing naturally occurring proteins such as β2m and ZAG, yielded increases in the observed R_H by as much as twice the R_H of a naturally-occurring IgG. The systematic characterization of the lengths and rigidity properties of the

structured protein linkers and a range of $(Gly_4Ser)_n$ linkers reported here provide a new set of tools to the available linker repertoire for engineering fusion proteins.

Table 2. Complete sequences of designed linkers. Linkers L1-L21 were inserted into the hinge region of b12 IgG between residues His235 and Thr236. Linkers L22-L24 were inserted into the same hinge between residues Cys231 and Asp232.

Linker	Name	Complete Sequence
L1	GPcPcPc	AGSGGSGGSGGSPVPSTPPTNSSSTPPTPSPSPVPSTPPTNSSSTPPTPSPSPVPSTPPTNSSSTPPTPSPSAS
L2	GPPcP	AGSGGSGGSGGSPVPSTPPTPSPSTPPTPSPSPVPSTPPTNSSSTPPTPSPSPVPSTPPTPSPSTPPTPSPSAS
L3	GPGcP	AGSGGSGGSGGSPVPSTPPTPSPSTPPTPSPSGGSGNSSGSGGSPVPSTPPTPSPSTPPTPSPSAS
L4	GPPP	AGSGGSGGSGGSPVPSTPPTPSPSTPPTPSPSPVPSTPPTPSPSTPPTPSPSPVPSTPPTPSPSTPPTPSPSAS
L5	GPbP	AGSGGSGGSGGSPVPSTPPTPSPSTPPTPSPSIQRTPKIQVYSRHPAENGKSNFLNCYVSGFHPSDIEVDLLKNGERIEKVEHSDLSFSKDWSFYLLYYTEFTPTEKDEYACRVNHVTLSQPKIVKWDRDPVPSTPPTPSPSTPPTPSPSAS
L6	GPbG	AGSGGSGGSGGSPVPSTPPTPSPSTPPTPSPSIQRTPKIQVYSRHPAENGKSNFLNCYVSGFHPSDIEVDLLKNGERIEKVEHSDLSFSKDWSFYLLYYTEFTPTEKDEYACRVNHVTLSQPKIVKWDRDGGSGGSGGSGGSAS
L7	PbGbG	AGPVPSTPPTPSPSTPPTPSPSIQRTPKIQVYSRHPAENGKSNFLNCYVSGFHPSDIEVDLLKNGERIEKVEHSDLSFSKDWSFYLLYYTEFTPTEKDEYACRVNHVTLSQPKIVKWDRDGGSGGSGGSGGSIQRTPKIQVYSRHPAENGKSNFLNCYVSGFHPSDIEVDLLKNGERIEKVEHSDLSFSKDWSFYLLYYTEFTPTEKDEYACRVNHVTLSQPKIVKWDRDGGSGGSGGSGAS
L8	GPbGbP	AGSGGSGGSGGSPVPSTPPTPSPSTPPTPSPSIQRTPKIQVYSRHPAENGKSNFLNCYVSGFHPSDIEVDLLKNGERIEKVEHSDLSFSKDWSFYLLYYTEFTPTEKDEYACRVNHVTLSQPKIVKWDRDGGSGGSGGSGGSIQRTPKIQVYSRHPAENGKSNFLNCYVSGFHPSDIEVDLLKNGERIEKVEHSDLSFSKDWSFYLLYYTEFTPTEKDEYACRVNHVTLSQPKIVKWDRDPVPSTPPTPSPSTPPTPSPSAS
L9	GPUG	AGSGGSGGSGGSPVPSTPPTPSPSTPPTPSPSQIFVKTLTGKTITLEVEPSDTIENVKAKIQDKEGIPPDQQRLIFAGKQLEDGRTLSDYNIQKESTLHLVLRLRGGGGSGGSGGSGGSAS

L10	GPZP	AGSGGSGGSGGSPVPSTPPTPSPSTPPTPSPSDGRYSLTYIYTGLSKHVEDVPAFQAL GSLNDLQFFRYNSKDRKSQPMGLWRQVEGMEDWKQDSQLQKAREDIFMETLKDI VEYYNDSNGSHVLQGRFGCEIENNRSSGAFWKYYYDGKDYIEFNKEIPAWVPFDPA AQITKQKWEAEPVYVQRAKAYLEEECPATLRKYLKYSKNILDRQDPPSVVVTSHQAP GEKKKLKCLAYDFYPGKIDVHWTRAGEVQEPELRGDVLHNGNGTYQSWVVVAVPP QDTAPYSCHVQHSSLAQPLVVPWEASPVPSTPPTPSPSTPPTPSAS
L11	GGZGZP	AGSGGSGGSGGSGGSGGSGGSGGSDGRYSLTYIYTGLSKHVEDVPAFQALGSLNDL QFFRYNSKDRKSQPMGLWRQVEGMEDWKQDSQLQKAREDIFMETLKDIVEYYND SNGSHVLQGRFGCEIENNRSSGAFWKYYYDGKDYIEFNKEIPAWVPFDPAAQITKQ KWEAEPVYVQRAKAYLEEECPATLRKYLKYSKNILDRQDPPSVVVTSHQAPGEKKKL KCLAYDFYPGKIDVHWTRAGEVQEPELRGDVLHNGNGTYQSWVVVAVPPQDTAP YSCHVQHSSLAQPLVVPWEASGGSGGSGGSGGSDGRYSLTYIYTGLSKHVEDVPAF QALGSLNDLQFFRYNSKDRKSQPMGLWRQVEGMEDWKQDSQLQKAREDIFMET LKDIVEYYNDSNGSHVLQGRFGCEIENNRSSGAFWKYYYDGKDYIEFNKEIPAWVPF DPAAQITKQKWEAEPVYVQRAKAYLEEECPATLRKYLKYSKNILDRQDPPSVVVTSH QAPGEKKKLKCLAYDFYPGKIDVHWTRAGEVQEPELRGDVLHNGNGTYQSWVVV AVPPQDTAPYSCHVQHSSLAQPLVVPWEASPVPSTPPTPSPSTPPTPSPSAS
L12	GcGcP	AGSGNSSGSGGSGGSGNSSGSGGSPVPSTPPTPSPSTPPTPSPSAS
L13	cTPR3	KLSGGGGSGGGGSGGGGSAEAWYNLGNAYYKQGDYQKAIEYYQKALELDPNNAE AWYNLGNAYYKQGDYQKAIEYYQKALELDPNNAEAWYNLGNAYYKQGDYQKAIE DYQKALELDPNNLQRSAGGGGSGGGGSGGGGAS
L14	cTPR6	KLSGGGGSGGGGSGGGGSAEAWYNLGNAYYKQGDYQKAIEYYQKALELDPNNAE AWYNLGNAYYKQGDYQKAIEYYQKALELDPNNAEAWYNLGNAYYKQGDYQKAIE DYQKALELDPNNLQAEAWKNLGNAYYKQGDYQKAIEYYQKALELDPNNASAWYNL GNAYYKQGDYQKAIEYYQKALELDPNNAKAWYRRGNAYYKQGDYQKAIEDYQKAL ELDPNNRSRSAGGGGSGGGGSGGGGAS
L15	cTPR9	KLSGGGGSGGGGSGGGGSAEAWYNLGNAYYKQGDYQKAIEYYQKALELDPNNAE AWYNLGNAYYKQGDYQKAIEYYQKALELDPNNAEAWYNLGNAYYKQGDYQKAIE DYQKALELDPNNLQAEAWKNLGNAYYKQGDYQKAIEYYQKALELDPNNASAWYNL GNAYYKQGDYQKAIEYYQKALELDPNNAKAWYRRGNAYYKQGDYQKAIEDYQKAL ELDPNNRSAEAWYNLGNAYYKQGDYQKAIEYYQKALELDPNNAEAWYNLGNAYYK QGDYQKAIEYYQKALELDPNNAEAWYNLGNAYYKQGDYQKAIEDYQKALELDPNN LQRSAGGGGSGGGGSGGGGAS

L16	cTPR12	KLSGGGGSGGGGSGGGGSAEAWYNLGNAYYKQGDYQKAIEYYQKALELDPNNAE AWYNLGNAYYKQGDYQKAIEYYQKALELDPNNAEAWYNLGNAYYKQGDYQKAIE DYQKALELDPNNLQAEAWKNLGNAYYKQGDYQKAIEYYQKALELDPNNASAWYNL GNAYYKQGDYQKAIEYYQKALELDPNNAKAWYRRGNAYYKQGDYQKAIEDYQKAL ELDPNNRSAEAWYNLGNAYYKQGDYQKAIEYYQKALELDPNNAEAWYNLGNAYYK QGDYQKAIEYYQKALELDPNNAEAWYNLGNAYYKQGDYQKAIEDYQKALELDPNN LQAEAWKNLGNAYYKQGDYQKAIEYYQKALELDPNNASAWYNLGNAYYKQGDYQ KAIEYYQKALELDPNNAKAWYRRGNAYYKQGDYQKAIEDYQKALELDPNNRSAGG GGSGGGGSGGGGAS
L17	GS1	GGGGSAS
L18	GS2	GGGGSGGGGSAS
L19	GS3	GGGGSGGGGSGGGGSAS
L20	GS5	GGGGSGGGGSGGGGSGGGGSGGGGSAS
L21	GS6	GGGGSGGGGSGGGGSGGGGSGGGGSGGGGSAS
L22	GS7	AGGGSGGGGSGGGGSGGGGSGGGGSGGGGSGGGGSAS
L23	GS8	AGGGSGGGGSGGGGSGGGGSGGGGSGGGGSGGGGSGGGGSAS
L24	GS9	AGGGSGGGGSGGGGSGGGGSGGGGSGGGGSGGGGSGGGGSGGGGSAS

Conflict of Interest

The authors declare that they have no competing financial interests.

Funding information

This work was supported by a grant from the Bill and Melinda Gates Foundation through the Grand Challenges in Global Health Initiative, the Director's Pioneer Award [1DP1OD006961-01 to P.J.B.], and the National Institutes of Health HIVRAD [P01 Al100148 to P.J.B.].

Acknowledgements

We thank Maria Politzer for assistance with sub-cloning and plasmid preparations and the Caltech Protein Expression Center for producing antibody-linker constructs.

References

Arai R., Ueda H., Kitayama A., Kamiya N. and Nagamune T. (2001) Design of the linkers which effectively separate domains of a bifunctional fusion protein. *Protein Eng,* **14**, 529-532.

Argos P. (1990) An investigation of oligopeptides linking domains in protein tertiary structures and possible candidates for general gene fusion. *Journal of molecular biology,* **211**, 943-958.

Bai Y., Ann D.K. and Shen W.-C. (2005) Recombinant granulocyte colony-stimulating factor-transferrin fusion protein as an oral myelopoietic agent. *Proceedings of the National Academy of Sciences of the United States of America,* **102**, 7292-7296.

Bonner A., Furtado P.B., Almogren A., Kerr M.A. and Perkins S.J. (2008) Implications of the near-planar solution structure of human myeloma dimeric IgA1 for mucosal immunity and IgA nephropathy. *Journal of immunology,* **180**, 1008-1018. F

Chen X., Zaro J.L. and Shen W.C. (2013) Fusion protein linkers: property, design and functionality. *Advanced drug delivery reviews,* **65**, 1357-1369.

D'Andrea L.D. and Regan L. (2003) TPR proteins: the versatile helix. *Trends in biochemical sciences,* **28**, 655-662..

Diskin R., Scheid J.F., Marcovecchio P.M., West A.P., Jr., Klein F., Gao H., Gnanapragasam P.N., Abadir A., Seaman M.S., Nussenzweig M.C. *et al.* (2011) Increasing the potency and breadth of an HIV antibody by using structure-based rational design. *Science,* **334**, 1289-1293.

Evers T.H., van Dongen E.M., Faesen A.C., Meijer E.W. and Merkx M. (2006) Quantitative understanding of the energy transfer between fluorescent proteins connected via flexible peptide linkers. *Biochemistry,* **45**, 13183-13192.

George R.A. and Heringa J. (2002) An analysis of protein domain linkers: their classification and role in protein folding. *Protein Eng,* **15**, 871-879.

Imperiali B. and O'Connor S.E. (1999) Effect of N-linked glycosylation on glycopeptide and glycoprotein structure. *Current Opinion in Chemical Biology,* **3**, 643-649.

Kajander T., Cortajarena A.L., Mochrie S. and Regan L. (2007) Structure and stability of designed TPR protein superhelices: unusual crystal packing and implications for natural TPR proteins. *Acta crystallographica Section D, Biological crystallography,* **63**, 800-811. , doi: 10.1107/S0907444907024353.

Klein J.S. and Bjorkman P.J. (2010) Few and far between: how HIV may be evading antibody avidity. *PLoS pathogens,* **6**, e1000908.

Klein J.S., Gnanapragasam P.N., Galimidi R.P., Foglesong C.P., West A.P., Jr. and Bjorkman P.J. (2009) Examination of the contributions of size and avidity to the neutralization mechanisms of the anti-HIV antibodies b12 and 4E10. *Proceedings of the National Academy of Sciences of the United States of America,* **106**, 7385-7390.

Lichty J.J., Malecki J.L., Agnew H.D., Michelson-Horowitz D.J. and Tan S. (2005) Comparison of affinity tags for protein purification. *Protein expression and purification,* **41**, 98-105.

Liu H.L., Doleyres Y., Coutinho P.M., Ford C. and Reilly P.J. (2000) Replacement and deletion mutations in the catalytic domain and belt region of Aspergillus awamori glucoamylase to enhance thermostability. *Protein Eng,* **13**, 655-659.

Main E.R., Jackson S.E. and Regan L. (2003) The folding and design of repeat proteins: reaching a consensus. *Current opinion in structural biology,* **13**, 482-489.

Nobbmann U., Connah M., Fish B., Varley P., Gee C., Mulot S., Chen J., Zhou L., Lu Y., Shen F. *et al.* (2007) Dynamic light scattering as a relative tool for assessing the molecular integrity and stability of monoclonal antibodies. *Biotechnology & genetic engineering reviews,* **24**, 117-128.

Pardridge W.M. (2010) Biopharmaceutical drug targeting to the brain. *Journal of drug targeting,* **18**, 157-167.

Redpath S., Michaelsen T.E., Sandle I., Clark M.R. (1998) The Influence of the hinge region length in binding of human IgG to human Fc gamma receptors. *Human Immunology,* **59**, 720-727.

Roben P., Moore J.P., Thali M., Sodroski J., Barbas C.F., 3rd and Burton D.R. (1994) Recognition properties of a panel of human recombinant Fab fragments to the CD4 binding site of gp120 that show differing abilities to neutralize human immunodeficiency virus type 1. *Journal of virology,* **68**, 4821-4828.

Sanchez L.M., Chirino A.J. and Bjorkman P. (1999) Crystal structure of human ZAG, a fat-depleting factor related to MHC molecules. *Science,* **283**, 1914-1919.

Scheufler C., Brinker A., Bourenkov G., Pegoraro S., Moroder L., Bartunik H., Hartl F.U. and Moarefi I. (2000) Structure of TPR domain-peptide complexes: critical

elements in the assembly of the Hsp70-Hsp90 multichaperone machine. *Cell,* **101**, 199-210.

Schuler B., Lipman E.A., Steinbach P.J., Kumke M. and Eaton W.A. (2005) Polyproline and the "spectroscopic ruler" revisited with single-molecule fluorescence. *Proceedings of the National Academy of Sciences of the United States of America,* **102**, 2754-2759.

Shental-Bechor D. and Levy Y. (2008) Effect of glycosylation on protein folding: a close look at thermodynamic stabilization. *Proceedings of the National Academy of Sciences of the United States of America,* **105**, 8256-8261.

Trinh C.H., Smith D.P., Kalverda A.P., Phillips S.E. and Radford S.E. (2002) Crystal structure of monomeric human beta-2-microglobulin reveals clues to its amyloidogenic properties. *Proceedings of the National Academy of Sciences of the United States of America,* **99**, 9771-9776.

Vijay-Kumar S., Bugg C.E. and Cook W.J. (1987) Structure of ubiquitin refined at 1.8 A resolution. *Journal of molecular biology,* **194**, 531-544. .

Zhang J., Yun J., Shang Z., Zhang X. and Pan B. (2009) Design and optimization of a linker for fusion protein construction. *Progress in Natural Science,* **19**, 1197-1200.

Zhu P., Liu J., Bess J., Jr., Chertova E., Lifson J.D., Grise H., Ofek G.A., Taylor K.A. and Roux K.H. (2006) Distribution and three-dimensional structure of AIDS virus envelope spikes. *Nature,* **441**, 847-852. , doi: 10.1038/nature04817.

Zou Y., Weis W.I. and Kobilka B.K. (2012) N-terminal T4 lysozyme fusion facilitates crystallization of a G protein coupled receptor. *PloS one,* **7**, e46039.

Chapter Five

The use of cancer therapeutic technology to inspire next generation HIV reagents.

This chapter describes the rationale and preliminary data for the use of two different classes of immunotherapies typically used as cancer treatments to inspire new anti-HIV reagents. This work was conceived by myself, and experiments were done in collaboration with post-doc Alok Joglekar, and Caltech undergrad Erin Isaza. Technical support was provided by Devashish Joshi, Luke Klosterman, and Priyanthi Gnanapragasam.

Introduction

The use of combination highly active antiretroviral therapy (HAART) has significantly reduced the morbidity and mortality associated with HIV-1 infection and AIDS. Consistent and prolonged use of HAART has enabled patients to have a longer life expectancy (ARTCC, 2008). Despite this, when patients fail to comply with their ART regimen, the virus is able to replicate and drug resistant mutant variants develop (Dybul et al., 2002). HIV-infected individuals must commit to lifelong anti-retroviral treatment in order to keep this from occurring. In order to develop a curative therapeutic, it is important to understand the harbors of the virus that lie while under ART treatment. One source of viral rebound is the CD4+ memory T cell (Churchill et al., 2016; Dahabieh et al., 2015).

Early on in an HIV infection, the CCR5 tropic HIV virus targets the memory class of CD4+ T cells; these cells are long lived and can lie dormant while containing an integrated HIV provirus (Churchill et al., 2016; Dahabieh et al., 2015; Porter et al., 2011). Despite harboring the latent provirus, they do not express viral proteins or RNA to detectable levels, rendering them invisible to both ART therapy and the immune system (Marsden and Zack, 2015). Under incomplete compliance of ART therapy, this reservoir of HIV infected cells can become activated and produce new multidrug resistant virions. Thus, no HIV cure can be developed without complete eradication of the latent reservoir. Targeting the latent reservoir with the anti-cancer therapy anti-CTLA-4 was found to be promising, reducing the viral rebound frequency, but unfortunately it was unable to show complete eradication (Halper-Stromberg et al., 2014). Taking into account the current

efforts to purge the latent reservoir, the inability to control patient compliance and the insurmountable costs associated with HIV healthcare, it is necessary to explore non-traditional approaches to attempt to cure HIV infection.

Within the past thirty years, there has been enormous advances in cancer immunotherapy (Topalian et al., 2011). Many cancer immunotherapeutic methods seek to block regulatory pathways found to inhibit clearance of the tumor, or boost the endogenous immune response. Many of these approaches have been found to lead to successful remission of the cancer (Topalian et al., 2011). Since many of the fundamental mechanisms of immune escape are shared by HIV and cancer, HIV immunotherapy attempts can take a cue from the recent advances in cancer therapy in hopes of seeing similar advancements in HIV+ treatment. As the two fields emerge, we hope to find more effective reagents towards a functional cure for HIV.

In the following chapter, we will discuss preliminary data for ongoing investigations of two different anti-HIV therapies utilizing both our knowledge of broadly neutralizing antibodies and the successes in current cancer immunotherapies.

Part One: Use of Chimeric Antigen Receptors against HIV

Adoptive cell transfer and gene therapy approaches to modify T-cell specificity have shown to be effective in modulating the immune response against both cancer and viruses (Barrett et al., 2014; Kalos et al., 2011; Leen et al., 2006; Maude et al., 2014; Porter et al., 2011). The use of chimeric antigen receptors (CARs) is one such approach where an antigen binding motif, an antigen binding site of an antibody for example, is linked to the intracellular domain of the CD3-ζ chain (Roberts et al., 1994). The utility of this design is that it allows for CD8+ t-cell recognition without the restriction of the MHC. Typically, CARs are signal chain constructs composed of the variable domains of an IgG fused (scFv) either to a TCR constant domain or a T-receptor domain (Kalos et al., 2011). These reagents are beneficial because they allow for the specificity of an antibody with the cytotoxic effects of a T-cell. In addition, there has been success in optimizing the activation potential of CARs, with second and third generation CARs developed to include signaling molecules from costimulatory receptors such as CD28 or 4-1BB (Zhong et al., 2010).

Particularly encouraging are recent clinical trials for patients suffering from B-cell chronic lymphocytic leukemia (B-CLL) using a CAR containing a scFv against CD19 fused to TNF receptor, CD137 and CD3-ζ chain (Kalos et al., 2011). In this study, patients achieved complete remission of the leukemia (Kalos et al., 2011). However promising, the choice of antibody and target, as well as the addition of costimulatory modules, needs to be carefully chosen as it could lead to over activation and have adverse affects due to cytokine storms (Büning et al., 2010).

The notion of employing chimeric antigen receptors against HIV is not a new one. Prior to the discovery of HAART therapy, early successes in chimeric antigen receptors with cancer led HIV researchers to explore this as a potential treatment. Preliminary studies testing the efficacy of gene therapy against HIV used primary CD8+ T-cells stably expressing a CD4 molecule fused to a CD3-ζ chain (CD4ζ) showed specific lysis of a cell line expressing HIV env trimer (Roberts et al., 1994). Following this result three clinical trials testing the efficacy of the CD4ζ CAR expressed in autologous CD4+ and CD8+ T-cells from acute viremia or late stage chronic HIV infected patients on ART therapy (Scholler et al., 2012). In all three clinical trials, there was no significant difference in HIV viral load compared to the control placebo group (Deeks et al., 2002; Mitsuyasu et al., 2000). An additional concern with such CARs is whether the expression of CD4 on the surface of CD8+ T-cells would provide an additional target for HIV infection.

Despite disappointing effects on HIV clearance, these clinical trials provided data on the safety and expression of CD4ζ CARs in patients. In a longitudinal study following the patients from the CD4ζ CAR clinical trials determined that there were no significant adverse effects due to gene transfer with retroviral vectors over the ten years the patients have been monitored. Importantly, long term persistence of the functional CD4ζ CAR T-cells were observed with a half-life over 16 years (Scholler et al., 2012). These data suggest that with a more promising HIV binding motif, safe long term expression of functional chimeric antigen receptors is attainable.

CD4ζ CARs has resurfaced in two new studies showing greater success (Liu et al., 2015; Zhen et al., 2015). In the first study by Zhen et al., CD4ζ CAR was used in combination with two small hairpin RNA molecule specific for CCR5 and the LTR sequence of HIV and shown to suppress HIV replication in a humanized mouse model (Zhen et al., 2015). These "Triple CARs" when transduced into CD8+ T-cells, resulted in cells expressing CD4 and reduced CCR5 expression (Zhen et al., 2015). As expected, however, these cells were more susceptible to HIV infection compared to un-transduced cells. Interestingly, in the same study, when the TRIPLE CAR was transduced into hematopoietic cells, expression of the CAR was found on all lymphocytes lineages as well as on myeloid cells. Within the T-cell population, the transduction of the triple CAR resulted in downregulation of the endogenous TCR (Zhen et al., 2015). However, unlike the Roberts et al. study, the TRIPLE CAR showed moderate suppression of HIV in vivo (Zhen et al., 2015). While promising, the use of CD4 in the TRIPLE CAR continues to be problematic, by providing CD8+ T-cells as an additional target for HIV. Not discussed however, is whether the NK cell population was also susceptible to infection, CCR5 and CXCR4 are both found on NK cells (Berahovich et al., 2006).

A second study by Liu and colleagues, designed a bispecific CD4 based CAR containing the domains 1-2 of CD4 linked to the scFv of a CD4i antibody, 17b fused to the CD28 transmembrane domain and CD3ζ. Similarly to the Richards and Zhen studies, the CD4-17b CAR can successfully be detected on CD8+ T-cells, and demonstrated specific lysis of cells with HIV Env surface expression, and suppression of HIV spread in an in-vitro PBMC assay. Surprisingly, Liu et al. report that unlike the previous two studies, the HIV-1 infection was not observed on CD8+ T-cells transduced with the CD4-

17b CAR (Liu et al., 2015). However, careful examination of the flow cytometry results in the paper (Liu et al., 2015) show potential improper gating of the cell populations may have led to misreporting of the result. While it appears to be reduced infectivity compared to the CD4 CAR, a population of infected cells are present in the CD4-17b CAR that is not seen in the un-transduced control cells.

While promising, all three studies show a need for a redesign of the current CARs against HIV. Here I will describe preliminary data of a chimeric antigen receptor utilizing broadly neutralizing antibodies (BnAb) instead of CD4 as the HIV target binding motif.

Materials and Methods

Construction of chimeric antigen receptor

Genes encoding the hinge, transmembrane and cytoplasmic signaling domain of CD28 followed by 41-BB domain and CD3 zeta chains were synthesized (Figure 1). Broadly neutralizing CD4bs J3 camelid VHH (McCoy et al., 2012) linked by a (gly4ser)7 linker to an IgG Fc (CH2-CH3) containing G236R D265A L328R mutation remove FcγR function (Bournazos et al., 2014; Horton et al., 2008). The CAR gene was subcloned into both the mammalian expression plasmid PTT5 (NRC Biotechnology Research Institute), and a third generation lentiviral plasmid, pHAGE2 (Hao and Baltimore, 2009), previously described. The gene encoding the extracellular domain J3VHH-(gly4ser)7-Fc G236R D265A L328R was subcloned into PTT5 for initial characterization.

Protein expression and purification. J3VHH-(Gly4Ser)7-Fc G236R L328R was expressed transiently in suspension HEK 293-6E cells (NRC Biotechnology Research

Institute) using 25 kDa linear polyethylenimine (PEI) (Polysciences) for transfection as described (8). The supernatants were passed over protein A resin (Thermo Fisher Scientific), eluted using pH 3.0 citrate buffer, and then immediately neutralized and subsequently purified by size exclusion chromatography using a Superdex 200 10/300 GL column.

In vitro neutralization assays

A previously-described pseudovirus neutralization assay was used to evaluate the neutralization potencies of the reagents (Montefiori, 1996; Montefiori et al., 2001). Neutralization assays were performed in-house using the same protocol (Montefiori, 1996; Montefiori et al., 2001). In brief, pseudoviruses were generated by cotransfection of HEK 293T cells with an HIV-1 Env expression plasmid and a replication-defective backbone plasmid. Neutralization was determined by measuring the decrease in luciferase reporter gene expression in the presence of a potential inhibitor following a single round of pseudovirus infection in TZM-bl cells. Nonlinear regression analysis was used to calculate the concentrations at which half-maximal inhibition was observed (IC_{50} values).

Detection of CAR on transfected 293T cells.

J3-Fc CAR in PTT5 was transfected into HEK293T cells (Invitrogen) using lipofectamine (Invitrogen) as recommended. Three days' post transfection, CAR cells and mock transfected cells were harvested and stained with FITC-labeled anti-Fc antibody and run on flow cytometry.

Results

Design of BnAb chimeric antigen receptor

The VH domain of J3 (J3VHH), a CD4 binding site camelid antibody isolated from llamas shown to be broadly neutralizing against a large panel of HIV-1 isolates (McCoy et al., 2012), was chosen as the antigen binding motif for our first CAR design. The unique structure of camelid antibodies (McCoy et al., 2012) (Figure 1) made J3 an ideal choice, and the lack of light chain allowed for simple design without the need to use a scFv format. Unlike the previous versions of anti-HIV CARs (Liu et al., 2015; Roberts et al., 1994; Zhen et al., 2015), J3VHH is linked to an IgG1 Fc domain (Figure 1) to allow for efficient dimerization of CD28 and CD3 zeta chains, thereby leading to enhanced activation of the CD8+ T-cell and lysis of target cell (Lazar-Molnar et al., 2006; Rutledge et al., 1992).

Genes encoding the hinge, transmembrane, and cytoplasmic signaling domain of CD28 followed by 4-1BB domain and CD3 zeta chains were synthesized (Figure 1). Broadly neutralizing CD4bs J3 camelid VHH (McCoy et al., 2012) linked by a (Gly4Ser)7 linker to an IgG Fc (CH2-CH3) containing G236R L328R mutation remove FcγR function (Horton et al., 2008). The CAR gene was subcloned into both the mammalian expression plasmid PTT5 (NRC Biotechnology Research Institute), and a third generation lentiviral plasmid, pHAGE2 (Hao and Baltimore, 2009) previously described.

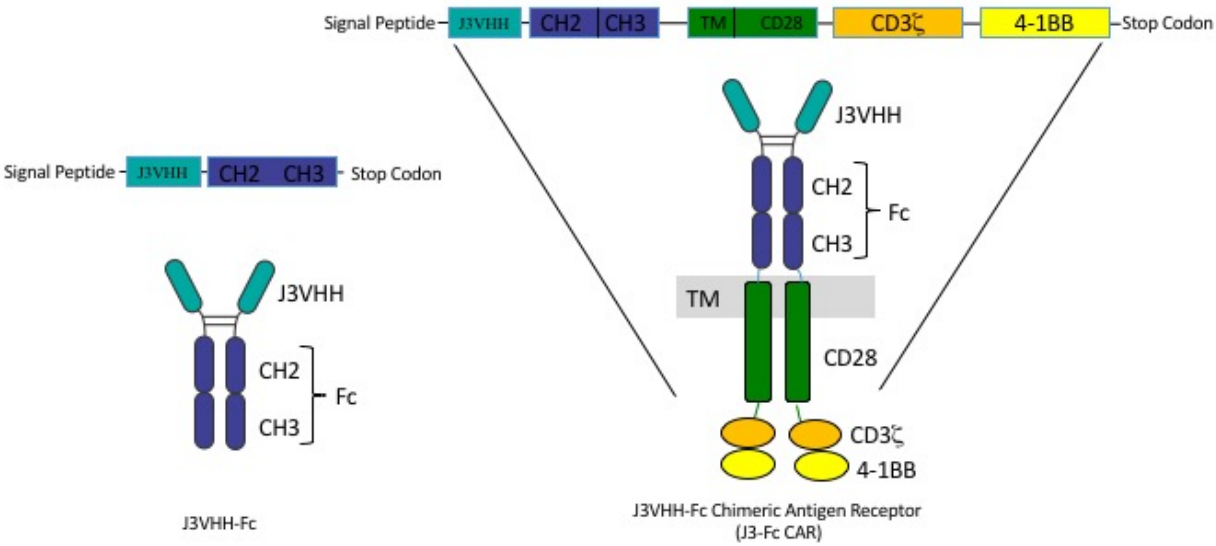

Figure 1. Design of Chimeric Antigen Receptor reagents. Organization of gene construction is shown by linear figure. Schematic under gene represents imagined protein construct. TM: Transmembrane domain.

J3VHH-(G4S)7-Fc Neutralizes HIV-1 strain YU2 in vitro

The extracellular domain of a chimeric antigen receptor is important for effective recognition of the antigen (Topalian et al., 2011). As a surrogate for a traditional binding assay, the soluble version of our CAR, containing J3VHH-(Gly4Ser)7-Fc, was tested it in an in-vitro neutralization assay to assess binding ability to HIV-1 isolate YU2. As anticipated, J3VHH-(Gly4Ser)7-Fc neutralized YU2 with an IC50 of <0.05 ug/ml (Figure 2). We suspect that this will lead to a highly specific potent CAR T-cell.

Detection of CAR on transfected 293T cells.

J3-Fc CAR in PTT5 was transfected into HEK293T cells (Invitrogen) using lipofectamine (Invitrogen) as recommended. Three days post transfection, CAR cells and mock transfected cells were harvested and stained with FITC-labeled anti-Fc antibody and run on flow cytometry. (Figure 2). Flow cytometry suggests efficient surface expression of the CAR in vitro; however, specificity of fully assembled CAR has yet to be tested. Current studies are underway to test CAR T-Cell binding to a fluorescently labelled soluble gp120.

Discussion and Future Directions

Thus far, we designed, cloned, and expressed a chimeric antigen receptor containing a broadly neutralizing antibody J3, as the antigen binding motif. We have demonstrated that the extracellular portion of the CAR, J3VHH-(Gly4Ser)7-Fc, can effectively neutralize HIV-1, and the CAR can be expressed and detected as a surface receptor on transfected 293T cells (Figure 2). The use of a broadly neutralizing antibody

that can bind HIV instead of CD4 was a purposeful attempt to reduce potential HIV infection of the CAR T-Cell. Future experiments using lentivirus transduced CD8+ T-cells will elucidate this further. Additional experiments include co-culturing experiments of HIV env expressing 293T cells with transduced J3-Fc CAR cells to assay CAR mediated lysis of infected cells. Future experiments could also include the transduction of hematopoietic stem cells and humanized mouse models.

Since most antigens expressed by human cancers are non-mutated surface receptors also found on normal cells (Houghton and Guevara-Patino, 2004), such as CD19 on B-cells (Porter et al., 2011), the consequence of an effective CAR therapy includes the elimination of all cells expressing the receptor. In the case of B-CLL, the CAR expressing anti-CD19 leads to the clearance of both leukemic and healthy B-cells in the patient (Barrett et al., 2014), leaving them with a reduced to no humoral immune system for the lifetime of the transduced cell. This makes chimeric antigen receptors an ideal candidate for HIV immunotherapy. Unlike in the case of B-CLL, HIV infected CD4+ T-cells express the HIV envelope trimer of its surface, making them easily decipherable from their uninfected counterparts (Ganser-Pornillos et al., 2008). Further, the use of BnAb CARs instead of previous CD4ζ iterations should avoid CAR mediated HIV infection (Liu et al., 2015; Zhen et al., 2015); however, this remains to be proven.

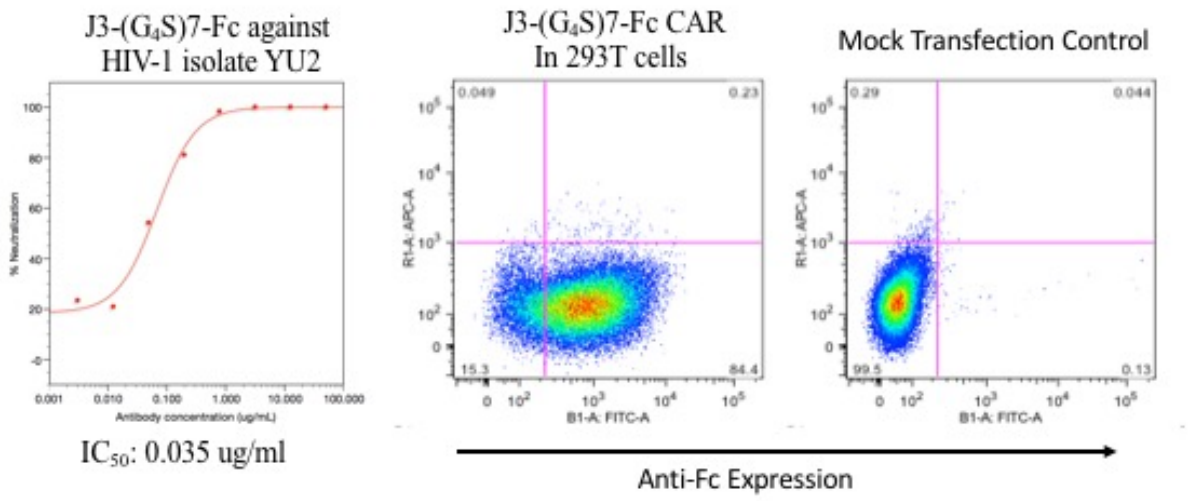

Figure 2. J3-Fc CAR can neutralize HIV in-vitro and is presented on the surface of transfected cells. Neutralization assay against YU-2 HIV Isolate showed potent neutralization with an IC_{50} of 0.035 ug/ml. J3-Fc CAR can be detected on the surface of 293T cells transfected with the CAR plasmid.

Part two: Elimination of latent reservoir using bispecific T-cell Engagers: BnAb BiTEremixes

Bi-specific antibody reagents have shown to be effective at redirecting T-cell targeting to tumor cells (Baeuerle and Reinhardt, 2009; Rossi et al., 2014; Wu et al., 2015). First described in 1985, hybrid antibodies were IgG based bispecific antibodies where one arm was targeted to the TCR of a CD8+ T-cell, while the other specific for an antigen located on the tumor cell but not the T-cell, was found to induce specific lysis of the target cell (Staerz et al., 1985). Currently, scFv bispecific reagents of a similar nature using anti-CD3 to stimulate the T-cell response has been used in clinical trials against various cancers at low effector cell: target ratios (Baeuerle and Reinhardt, 2009). These reagents, known as bispecific T-cell engagers (BiTEs) such as Blinatumomab (a BiTE specific for CD3 and CD19), have been assessed in Phase II clinical trials with great success in B-cell lymphoma (Baeuerle and Reinhardt, 2009); however, due to the extremely short half-life of these reagents, the BiTE was delivered through continuous intravenous infusion over a six week period. In some cases up to five cycles were delivered to a given patient (Baeuerle and Reinhardt, 2009).

Recently, it was considered whether the bispecific T-cell engagers could potentially activate the latent reservoir of HIV infected cells. Nabel and colleagues designed a bispecific a potent broadly neutralizing antibody Fab against the CD4 binding site linked to a scFv version anti-CD3 antibody, OKT3 (Pegu et al., 2015). A clonal variant of NIH-45-46, first discovered at Rockefeller University and later improved by introducing a G54W mutation within the heavy chain engineered in the Bjorkman Lab (Diskin et al., 2011b; Scheid et al., 2011a), was used in this study, and also contained the

G54W mutation known as VRC07 (Pegu et al., 2015). The reagent works two fold, first binding with the anti-CD3 arm, which allows activation of the latently infected memory T-cells. Next, a second BiTE binds to a nearby CD8+ T-cell, activating it, and then using the BnAb arm to tether it to newly activated memory cells. These reagents were also validated for safety in a non-human primate model.

While this reagent showed promise, with moderate capacity to activate latently infected T-cells and specificity to HIV env, it too has limitations based on its short half-life in vivo. Here I describe preliminary data for a new brand of BiTE reagents known as BiTEremixes, based on the earliest hybrid antibodies, that has multiple specificities and can target CD8+ T-cells with CD3 activation to infected cells with the broadly neutralizing antibody arm. Through the addition of an Fc we expect increased half-life compared to the scFv and Fab Bispecific iterations. We hope to show in on-going experiments its ability to activate the latent reservoir through CD3 activation on memory CD4+ T-cells. Next generation BiTEremixes will include NK cell activation through CD16 stimulation (Murphy et al., 2012).

Materials and Methods:

Cloning of desired BiTEremix constructs

Genes encoding the variable regions (VH and VL) of the murine OKT3 antibody were synthesized (Integrated DNA Technologies) based on sequences deposited to Genbank, accession numbers A22261 and A22259, respectively. Intact IgG genes were constructed by cloning the relevant variable domain on either human heavy or light chain via Gibson cloning techniques, forming murine/human chimeric OKT3 antibody. Similar methods

were used to clone IgG1 variants of broadly neutralizing antibodies 3BNC117, PGDM1400, 10-1074, 8ANC195, and J3. Every F405L IgG was mutated further to include a StrepII Tag, and K409R mutated to include a 6x his tag. The heavy chain of the chimera was mutated to include a single amino acid K409R mutation and a C-terminus 6x His Tag or F405L mutation with C-terminus StrepII tag through site directed mutagenesis to allow for the ability to produce heterodimers mimicking natural IgG4 Fab arm swapping, through a previously described technique called controlled Fab Arm Exchange (FAE) (Labrijn et al., 2013; Labrijn et al., 2014). Similar to the CAR design, QuikChange mutagenesis was performed on both heavy chain constructs to introduce G236R D265A L328R mutations and remove the FcγR function (Bournazos et al., 2014; Horton et al., 2008).

Protein expression and purification. Proteins were expressed transiently in suspension HEK 293-6E cells (NRC Biotechnology Research Institute) using 25 kDa linear polyethylenimine (PEI) (Polysciences) for transfection as described (8). When expressing heterodimeric constructs, the heavy chain (HC) and light chain (LC) plasmids were mixed at a 1:1 ratio by mass. Cell culture supernatants were collected six days post-transfection. All constructs supernatants were passed over protein A resin (Thermo Fisher Scientific), eluted using pH 3.0 citrate buffer, and then immediately neutralized. All reagents were purified by size exclusion chromatography using a Superdex 200 10/300 GL column.

2-Mercaptoethylamine–Mediated Controlled Fab-arm Exchange in Vitro. Equimolar amounts of OKT3 IgG1-F405L StrepII and BnAb IgG1-K409R His antibodies were

mixed and incubated with 2-mercaptoethylamine (2-MEA; Sigma) at a final concentration of 1 mg/mL per antibody. The final concentration of 2-MEA was 25-75 mM (the mixtures were typically incubated for 90 min at 37 °C or 5 h at 31 °C). Depending on the reaction volume, 2-MEA was removed by buffer-exchanging against PBS using Millipore 15ml 10-kDa MWCO conical concentrators, or Zebas desalting columns (1–5 mL; 7-kDa MWCO; Pierce). Samples were stored overnight at 4 °C to allow reoxidation of the disulfide bonds to occur.

Protein expression and purification of FAE heterodimers

Post reoxidation, FAE were purified via a dual tag purification technique to ensure 100% heterodimer in purified sample. His-Tagged proteins were purified using Ni-NTA chromatography and eluted using 300 mM imidazole. Post Ni-NTA purification proteins were purified over StrepII column (GE Healthcare) and eluted with 2.5mM desthiobiotin (sigma). Purified heterodimers are confirmed via size exclusion chromatography and SDS-PAGE analysis.

In-vitro neutralization assays

To ensure BnAb arm specificity in-vitro neutralization assays were performed as discussed earlier in this chapter.

Flow Cytometry

To confirm specificity of the OKT3 arm, T-cells were stained using a primary of the heterodimer OKT3/BnAb at a concentration of 1ug/ml for 1 hr. at 25°C. Cells were washed with PBS five times and secondary APC-labelled anti-human IgG.

Cellular Cytotoxicity Assay

The capacity to induce effector cell-dependent lysis of HIV infected cells was evaluated by the assay depicted in Figure 5. In Brief, GXR cells, a CD4 T-lymphoblast stable cell line immortalized with a GFP under a HIV LTR inducible promoter, are infected with replication competent HIV strains NL4-3 or YU2. When an active infection can be measured of over 25% infected cells, infected cells are split into a 24-well plate and conditions containing various BiTEremix reagents are added in the presence and absence of PBMCs enriched for CD8+ T-cells. The cultures are monitored for the % GFP every 24 hours for 3-5 days (Figure 6).

Additional experiments using suspension 293 6E-cells expressing HIV envelope-GFP instead of live HIV, as well as the use of a latenting infected cell line to see if the BiTEremix can activate the latent reservoir, are currently underway.

Results and Conclusions

Heterodimers containing Broadly Neutralizing Antibodies and OKT3 were efficiently produced through cFAE.

Heterodimer BiTEremix reagents containing one arm of OKT3 chimeric IgG of either 3BNC117, J3, 8ANC195, G52k5, PGDM1400, and 10-1074 IgG, See Schematic Fig 3.

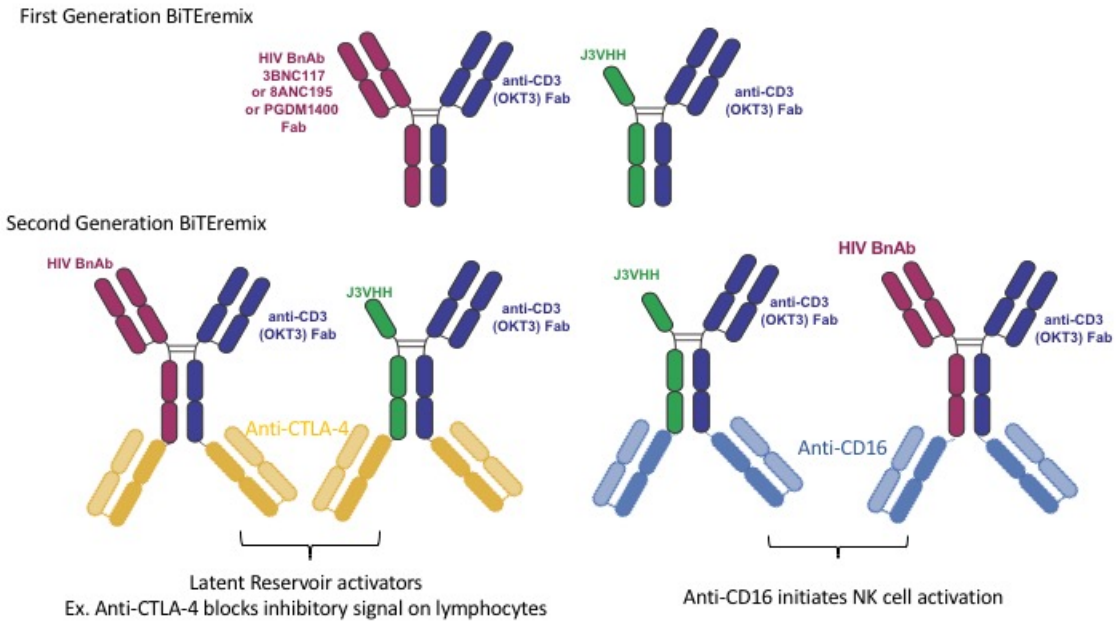

Figure 3. First and Second Generation BiTEremix reagents

These reagents were capable of neutralizing HIV and also showed CD3 specificity through Flow cytometry (Figure 4). The Fc regions that were mutated have either a F405L or K409R mutation, which under reducing conditions allows IgG1 based reagents to undergo IgG4 like arm exchange (Labrijn et al., 2013; Labrijn et al., 2014; Rispens et al., 2013; Schuurman et al., 2012) in the BiTEremix reagents. All cFAE IgGs are first expressed as homodimers and purified. Additional mutations in all of the cFAE BiTEremixes were made to introduce G236R L328R mutation remove FcγR function(Bournazos et al., 2014; Horton et al., 2008). We believe that this mutation would be necessary so as to not initiate Fc mediated antibody dependent cell cytotoxicity against the CD8+ T-cells.

Next generation BiTEremixes will include domains that can induce NK cell activation as well as other known latent reservoir activators such as the cancer immunotherapy, anti-CTLA-4, shown to block inhibitory signals on T-lymphocytes and activate the latent reservoir in an HIV humanized mouse model (Halper-Stromberg et al., 2014) (Figure 3). However, over-activation of lymphocytes could cause adverse effects and should be thoroughly investigated prior to therapy (Topalian et al., 2011).

OKT3/J3 was efficiently able to reduce HIV infection after 48 hours in culture

Due to a limitation of resources, thus far only one reagent, OKT3/J3 BiTEremix, has been tested in cytotoxicity assay. When compared to controls, OKT3/J3BiTEremix in the presence of CD8+ T-cells effectively showed a reduced HIV infection at 48-hour time point (Figures 5 and 6). Current efforts to repeat this experiment and test 293 expressing gp160 cell line are underway.

Put together, these preliminary data suggest that the OKT3/BnAb BiTEremix reagents are capable of recognizing both CD3 on the CD8+ T-cell as well as the HIV env on the surface of the infected cell.

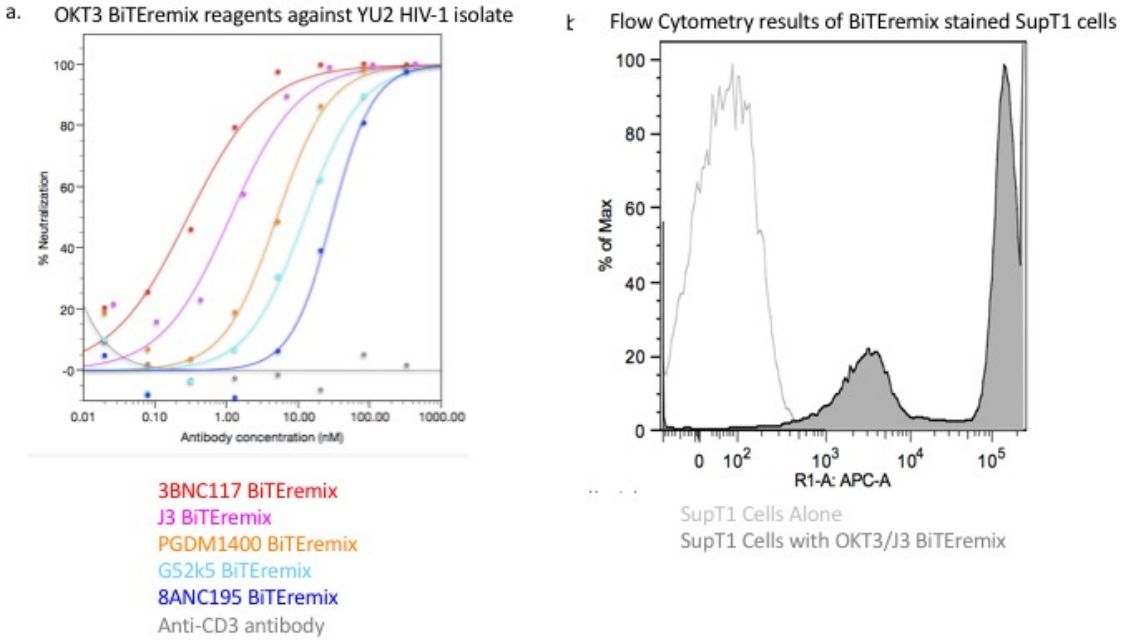

Figure 4. a. Neutralization data shows BiTEremix reagent is capable of neutralizing HIV with only one arm specific for the virus. As expected, OKT3 antibody arm shows no protection against HIV in the absence of CD8+ T-cells. Panel b. shows BiTEremix staining of SupT1 –T-lymphoblast cell line. Unshaded trace shows unstained SupT1 cells. Gray trace are cells stained with BiTEremix

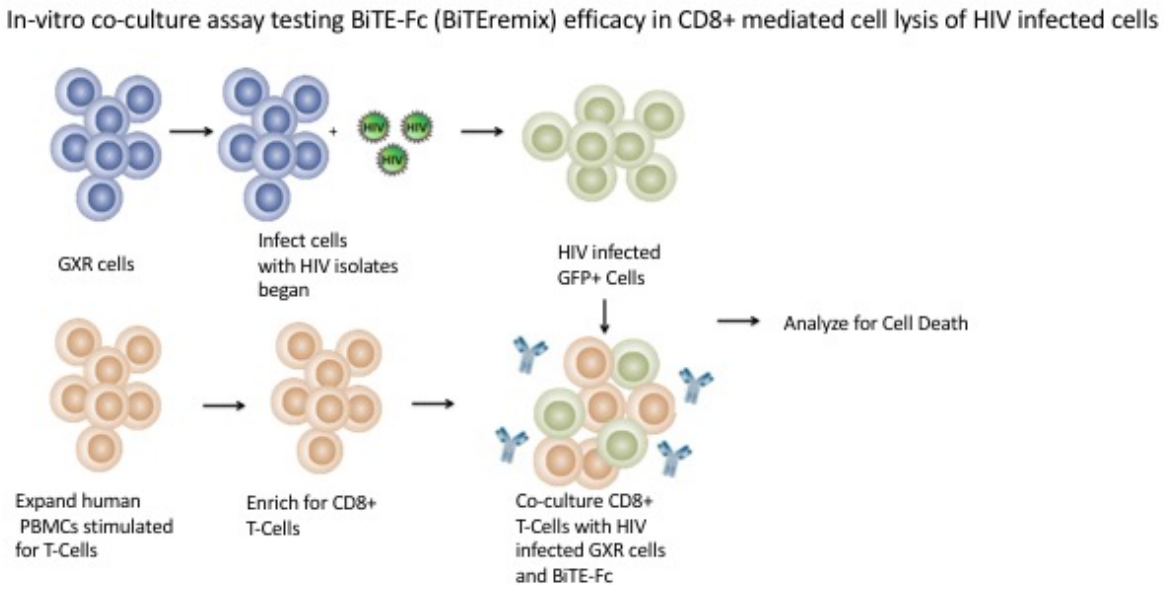

Figure 5. Experimental Set up for in-vitro Co-culture assays to test BiTEremix reagents.

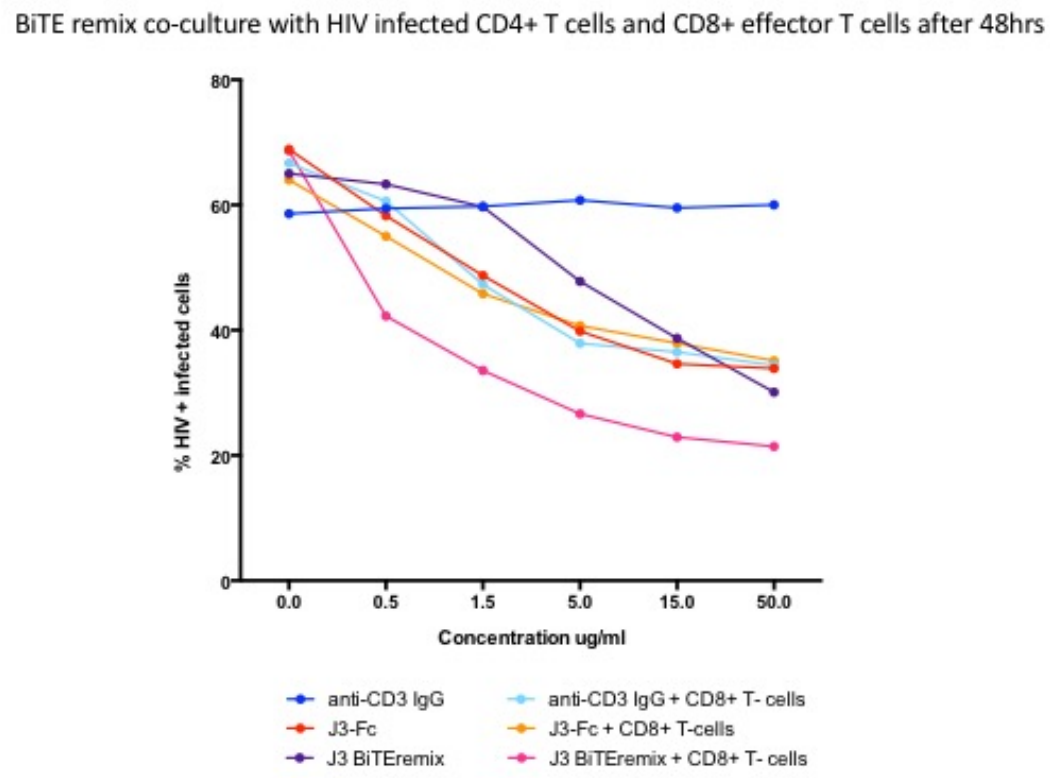

Figure 6. Co-culture experiments with HIV infected cells and OKT3/J3BiTEremix in the presence and absence of effect T-cells

References:

ARTCC. (2008). Life expectancy of individuals on combination antiretroviral therapy in high-income countries: a collaborative analysis of 14 cohort studies. *The Lancet, 372*(9635), 293-299. doi:10.1016/S0140-6736(08)61113-7

Baeuerle, P. A., & Reinhardt, C. (2009). Bispecific T-cell engaging antibodies for cancer therapy. *Cancer Res, 69*(12), 4941-4944. doi:10.1158/0008-5472.CAN-09-0547

Barrett, D. M., Singh, N., Porter, D. L., Grupp, S. A., & June, C. H. (2014). Chimeric Antigen Receptor Therapy for Cancer. *Annual Review of Medicine, 65*(1), 333-347. doi:10.1146/annurev-med-060512-150254

Berahovich, R. D., Lai, N. L., Wei, Z., Lanier, L. L., & Schall, T. J. (2006). Evidence for NK Cell Subsets Based on Chemokine Receptor Expression. *The Journal of Immunology, 177*(11), 7833-7840.

Bournazos, S., Klein, F., Pietzsch, J., Seaman, M. S., Nussenzweig, M. C., & Ravetch, J. V. (2014). Broadly neutralizing anti-HIV-1 antibodies require Fc effector functions for in vivo activity. *Cell, 158*(6), 1243-1253. doi:10.1016/j.cell.2014.08.023

Büning, H., Uckert, W., Cichutek, K., Hawkins, R. E., & Abken, H. (2010). Do CARs Need a Driver's License? Adoptive Cell Therapy with Chimeric Antigen Receptor-Redirected T Cells Has Caused Serious Adverse Events. *Human Gene Therapy, 21*(9), 1039-1042. doi:10.1089/hum.2010.131

Churchill, M. J., Deeks, S. G., Margolis, D. M., Siliciano, R. F., & Swanstrom, R. (2016). HIV reservoirs: what, where and how to target them. *Nat Rev Microbiol, 14*(1), 55-60. doi:10.1038/nrmicro.2015.5

Dahabieh, M. S., Battivelli, E., & Verdin, E. (2015). Understanding HIV latency: the road to an HIV cure. *Annu Rev Med, 66*, 407-421. doi:10.1146/annurev-med-092112-152941

Deeks, S. G., Wagner, B., Anton, P. A., Mitsuyasu, R. T., Scadden, D. T., Huang, C., . . . Hege, K. M. (2002). A phase II randomized study of HIV-specific T-cell gene therapy in subjects with undetectable plasma viremia on combination antiretroviral therapy. *Mol Ther, 5*(6), 788-797. doi:10.1006/mthe.2002.0611

Diskin, R., Scheid, J. F., Marcovecchio, P. M., West, A. P., Klein, F., Gao, H., . . . Bjorkman, P. J. (2011). Increasing the Potency and Breadth of an HIV Antibody by using Structure-Based Rational Design. *Science (New York, N.Y.), 334*(6060), 1289-1293. doi:10.1126/science.1213782

Dybul, M., Fauci, A. S., Bartlett, J. G., Kaplan, J. E., & Pau, A. K. (2002). Guidelines for Using Antiretroviral Agents among HIV-Infected Adults and Adolescents: The Panel on Clinical Practices for Treatment of HIV*. *Annals of Internal Medicine, 137*(5_Part_2), 381-433. doi:10.7326/0003-4819-137-5_Part_2-200209031-00001

Ganser-Pornillos, B., Yeager, M., & Sundquist, W. I. (2008). The Structural Biology of HIV Assembly. *Current opinion in structural biology, 18*(2), 203. doi:10.1016/j.sbi.2008.02.001

Halper-Stromberg, A., Lu, C. L., Klein, F., Horwitz, J. A., Bournazos, S., Nogueira, L., . . . Nussenzweig, M. C. (2014). Broadly neutralizing antibodies and viral inducers decrease rebound from HIV-1 latent reservoirs in humanized mice. *Cell, 158*(5), 989-999. doi:10.1016/j.cell.2014.07.043

Hao, S., & Baltimore, D. (2009). The stability of mRNA influences the temporal order of the induction of genes encoding inflammatory molecules. *Nature immunology, 10*(3), 281-288. doi:10.1038/ni.1699

Horton, H. M., Bernett, M. J., Pong, E., Peipp, M., Karki, S., Chu, S. Y., . . . Zhukovsky, E. A. (2008). Potent In vitro and In vivo Activity of an Fc-Engineered Anti-CD19 Monoclonal Antibody against Lymphoma and Leukemia. *Cancer Research, 68*(19), 8049-8057.

Houghton, A. N., & Guevara-Patino, J. A. (2004). Immune recognition of self in immunity against cancer. *J Clin Invest, 114*(4), 468-471. doi:10.1172/JCI22685

Kalos, M., Levine, B. L., Porter, D. L., Katz, S., Grupp, S. A., Bagg, A., & June, C. H. (2011). T Cells with Chimeric Antigen Receptors Have Potent Antitumor Effects and Can Establish Memory in Patients with Advanced Leukemia. *Science Translational Medicine, 3*(95), 95ra73-95ra73.

Labrijn, A. F., Meesters, J. I., de Goeij, B. E., van den Bremer, E. T., Neijssen, J., van Kampen, M. D., . . . Parren, P. W. (2013). Efficient generation of stable bispecific IgG1 by controlled Fab-arm exchange. *Proc Natl Acad Sci U S A, 110*(13), 5145-5150. doi:10.1073/pnas.1220145110

Labrijn, A. F., Meesters, J. I., Priem, P., de Jong, R. N., van den Bremer, E. T., van Kampen, M. D., . . . Parren, P. W. (2014). Controlled Fab-arm exchange for the generation of stable bispecific IgG1. *Nat Protoc, 9*(10), 2450-2463. doi:10.1038/nprot.2014.169

Lazar-Molnar, E., Almo, S. C., & Nathenson, S. G. (2006). The interchain disulfide linkage is not a prerequisite but enhances CD28 costimulatory function. *Cellular immunology, 244*(2), 125-129. doi:10.1016/j.cellimm.2007.02.014

Leen, A. M., Myers, G. D., Sili, U., Huls, M. H., Weiss, H., Leung, K. S., . . . Bollard, C. M. (2006). Monoculture-derived T lymphocytes specific for multiple viruses expand and produce clinically relevant effects in immunocompromised individuals. *Nat Med, 12*(10), 1160-1166. doi:10.1038/nm1475

Liu, L., Patel, B., Ghanem, M. H., Bundoc, V., Zheng, Z., Morgan, R. A., . . . Berger, E. A. (2015). Novel CD4-Based Bispecific Chimeric Antigen Receptor Designed for Enhanced Anti-HIV Potency and Absence of HIV Entry Receptor Activity. *J Virol, 89*(13), 6685-6694. doi:10.1128/JVI.00474-15

Marsden, M. D., & Zack, J. A. (2015). Double trouble: HIV latency and CTL escape. *Cell Host Microbe, 17*(2), 141-142. doi:10.1016/j.chom.2015.01.008

Maude, S. L., Frey, N., Shaw, P. A., Aplenc, R., Barrett, D. M., Bunin, N. J., . . . Grupp, S. A. (2014). Chimeric Antigen Receptor T Cells for Sustained Remissions in Leukemia. *New England Journal of Medicine, 371*(16), 1507-1517. doi:10.1056/NEJMoa1407222

McCoy, L. E., Quigley, A. F., Strokappe, N. M., Bulmer-Thomas, B., Seaman, M. S., Mortier, D., . . . Weiss, R. A. (2012). Potent and broad neutralization of HIV-1 by a llama antibody elicited by immunization. *The Journal of Experimental Medicine, 209*(6), 1091-1103.

Mitsuyasu, R. T., Anton, P. A., Deeks, S. G., Scadden, D. T., Connick, E., Downs, M. T., . . . Hege, K. M. (2000). Prolonged survival and tissue trafficking following

adoptive transfer of CD4zeta gene-modified autologous CD4(+) and CD8(+) T cells in human immunodeficiency virus-infected subjects. *Blood, 96*(3), 785-793.

Montefiori, D. C. (1996). Neutralizing and infection-enhancing antibody responses to human immunodeficiency virus type 1 in long-term nonprogressors. *J. Infect. Dis., 173*, 60-67.

Montefiori, D. C., Hill, T. S., Vo, H. T., Walker, B. D., & Rosenberg, E. S. (2001). Neutralizing antibodies associated with viremia control in a subset of individuals after treatment of acute human immunodeficiency virus type 1 infection. *J. Virol., 75*, 10200-10207.

Murphy, K., Travers, P., Walport, M., & Janeway, C. (2012). *Janeway's immunobiology*. New York: Garland Science.

Pegu, A., Asokan, M., Wu, L., Wang, K., Hataye, J., Casazza, J. P., . . . Nabel, G. J. (2015). Activation and lysis of human CD4 cells latently infected with HIV-1. *Nat Commun, 6*, 8447. doi:10.1038/ncomms9447

Porter, D. L., Levine, B. L., Kalos, M., Bagg, A., & June, C. H. (2011). Chimeric Antigen Receptor–Modified T Cells in Chronic Lymphoid Leukemia. *New England Journal of Medicine, 365*(8), 725-733. doi:10.1056/NEJMoa1103849

Rispens, T., Meesters, J., den Bleker, T. H., Ooijevaar-De Heer, P., Schuurman, J., Parren, P. W., . . . Aalberse, R. C. (2013). Fc-Fc interactions of human IgG4 require dissociation of heavy chains and are formed predominantly by the intra-chain hinge isomer. *Mol Immunol, 53*(1-2), 35-42. doi:10.1016/j.molimm.2012.06.012

Roberts, M. R., Qin, L., Zhang, D., Smith, D. H., Tran, A. C., Dull, T. J., . . . Finer, M. H. (1994). Targeting of human immunodeficiency virus-infected cells by CD8+ T lymphocytes armed with universal T-cell receptors. *Blood, 84*(9), 2878-2889.

Rossi, D. L., Rossi, E. A., Cardillo, T. M., Goldenberg, D. M., & Chang, C. H. (2014). A new class of bispecific antibodies to redirect T cells for cancer immunotherapy. *MAbs, 6*(2), 381-391. doi:10.4161/mabs.27385

Rutledge, T., Cosson, P., Manolios, N., Bonifacino, J. S., & Klausner, R. D. (1992). Transmembrane helical interactions: zeta chain dimerization and functional association with the T cell antigen receptor. *The EMBO Journal, 11*(9), 3245-3254.

Scheid, J. F., Mouquet, H., Ueberheide, B., Diskin, R., Klein, F., Oliveira, T. Y. K., . . . Nussenzweig, M. C. (2011). Sequence and Structural Convergence of Broad and Potent HIV Antibodies That Mimic CD4 Binding. *Science (New York, N.Y.), 333*(6049), 1633-1637. doi:10.1126/science.1207227

Scholler, J., Brady, T. L., Binder-Scholl, G., Hwang, W. T., Plesa, G., Hege, K. M., . . . June, C. H. (2012). Decade-long safety and function of retroviral-modified chimeric antigen receptor T cells. *Sci Transl Med, 4*(132), 132ra153. doi:10.1126/scitranslmed.3003761

Schuurman, J., Labrijn, A. F., & Parren, P. W. (2012). Fab-arm exchange: what's in a name? *MAbs, 4*(6), 636. doi:10.4161/mabs.22075

Staerz, U. D., Kanagawa, O., & Bevan, M. J. (1985). Hybrid antibodies can target sites for attack by T cells. *Nature, 314*(6012), 628-631.

Topalian, S. L., Weiner, G. J., & Pardoll, D. M. (2011). Cancer immunotherapy comes of age. *J Clin Oncol, 29*(36), 4828-4836. doi:10.1200/JCO.2011.38.0899

Wu, J., Fu, J., Zhang, M., & Liu, D. (2015). Blinatumomab: a bispecific T cell engager (BiTE) antibody against CD19/CD3 for refractory acute lymphoid leukemia. *J Hematol Oncol, 8*, 104. doi:10.1186/s13045-015-0195-4

Zhen, A., Kamata, M., Rezek, V., Rick, J., Levin, B., Kasparian, S., . . . Kitchen, S. G. (2015). HIV-specific Immunity Derived From Chimeric Antigen Receptor-engineered Stem Cells. *Mol Ther, 23*(8), 1358-1367. doi:10.1038/mt.2015.102

Zhong, X. S., Matsushita, M., Plotkin, J., Riviere, I., & Sadelain, M. (2010). Chimeric antigen receptors combining 4-1BB and CD28 signaling domains augment PI3kinase/AKT/Bcl-XL activation and CD8+ T cell-mediated tumor eradication. *Mol Ther, 18*(2), 413-420. doi:10.1038/mt.2009.210

Appendix A

Modifications to AAV viral vector to enhance transgene expression and to adhere to FDA regulations

This appendix describes the modification of Adeno-associated virus in order to address the difficulties of limited transgene size as well as potential oncogenic traits of the vehicle. The woodchuck post-transcriptional regulatory element (WPRE) in the viral vector has been implicated in oncogenesis. Modification of this element will aid in addressing both concerns. My contribution to this work was the design and characterization of the modified AAV vectors. This was done in the Baltimore Lab with helpful discussions with Alex Balazs.

Abstract:

Adeno-associated virus has been employed as a vehicle to deliver the anti-HIV antibodies in a current and future clinical trials. As recombinant AAV (rAAV) viral vectors become increasingly applied to human clinical trials, it is critical to continually evaluate the risks and limitations for its use. The difficulty in developing viral vectors for treatment is in being able to achieve the expression level and safety required in the clinical realm. Here I show work I have done to engineer novel rAAV serotype 8 viral vectors to address two major limitations that can affect the delivery of anti-HIV reagents in future clinical trials: the limited packaging capacity of the virus, and the potential immunogenicity of the virus. The woodchuck post-transcriptional regulatory element (WPRE) in the viral vector has been implicated in oncogenesis. Modification of this element will aid in addressing both concerns. Currently, this engineered improvements has been incorporated into an AAV viral vector being used for a clinical trial in 2016.

Introduction

In the past 10 years, the use of Adeno-Associated virus (AAV) vectors as a vehicle for gene therapy has rapidly increased (McLaughlin et al., 1988; Schnepp et al., 2009; Schultz and Chamberlain, 2008). Lack of pathogenicity makes AAV an attractive candidate for gene therapy applications in humans (Schnepp et al., 2009) . To date there are over twelve human serotypes of AAV and over one hundred non-human primate serotypes identified (Schnepp et al., 2009). AAV is a small non-enveloped virus belonging to the genus *Dependovirus* and requires genes of a helper virus such as adenovirus or herpes virus in order to propagate (Schultz and Chamberlain, 2008). The 4.7 kilobase DNA genome contains two open reading frames known as the cap region and the rep region (Schultz and Chamberlain, 2008). The cap region codes for three different proteins (VP1, VP2, and VP3), which comprise the icosahedral viral capsid and the rep region encodes for four proteins important to the replication of the virus (Schultz and Chamberlain, 2008). Flanking the genome are inverted terminal repeats or ITRs, which are required for the packaging of viral DNA into the capsid (McLaughlin et al., 1988) (Figure 1).

Adeno-associated viruses can be engineered for gene therapy where four separate plasmids contain ITRs flanking the gene of interest cassette, the cap, and rep genes, and adenoviral helper genes are co-transfected together to produce a viral vector. One limitation to AAV viral vectors is the restricted genome capacity of approximately five kilobases, which must include the promoter, gene of interest, and any enhancer elements desired (Grimm and Kay, 2003). Another limitation to AAV viral vectors is its potential

to exhibit oncogenic or immunogenic properties. Host immune responses can be generated against rAAV vector and its encoded transgene; the magnitude of these responses is dependent upon the transgene and serotype administered (Grimm and Kay, 2003) (Figure 1).

Previous research in the Baltimore lab revealed that recombinant adeno-associated virus (rAAV) expressing known broadly neutralizing antibodies can protect against HIV infection in a humanized mouse model (Balazs et al., 2013; Balazs et al., 2012; Balazs et al., 2014). As recombinant AAV viral vectors become increasingly applied to human clinical trials, it is critical to continually evaluate the risks and limitations for its use. Here I engineered rAAV serotype 8 viral vectors to address two major limitations for gene therapy applications: the limited packaging capacity of the virus, and the potential immunogenicity of the virus.

Modification of AAV viral vector

AAV has recently gained popularity as a viral vector for gene therapy because of its apparent lack of pathogenicity, ease in transducing various cell types, and the simplicity of its viral genome (Figure 1). The difficulty in developing viral vectors as vehicles for treatment is in being able to achieve the expectations required to bring the technology into clinical trials. An efficacious viral vector must be produced in high titers, exhibit long term expression of the transgene at high levels, cause little to no immune response, and results in minimal toxicity to the patient post transduction. As recombinant AAV

viral vectors are increasingly applied in human clinical trials, it is imperative to continually evaluate the risks of their use.

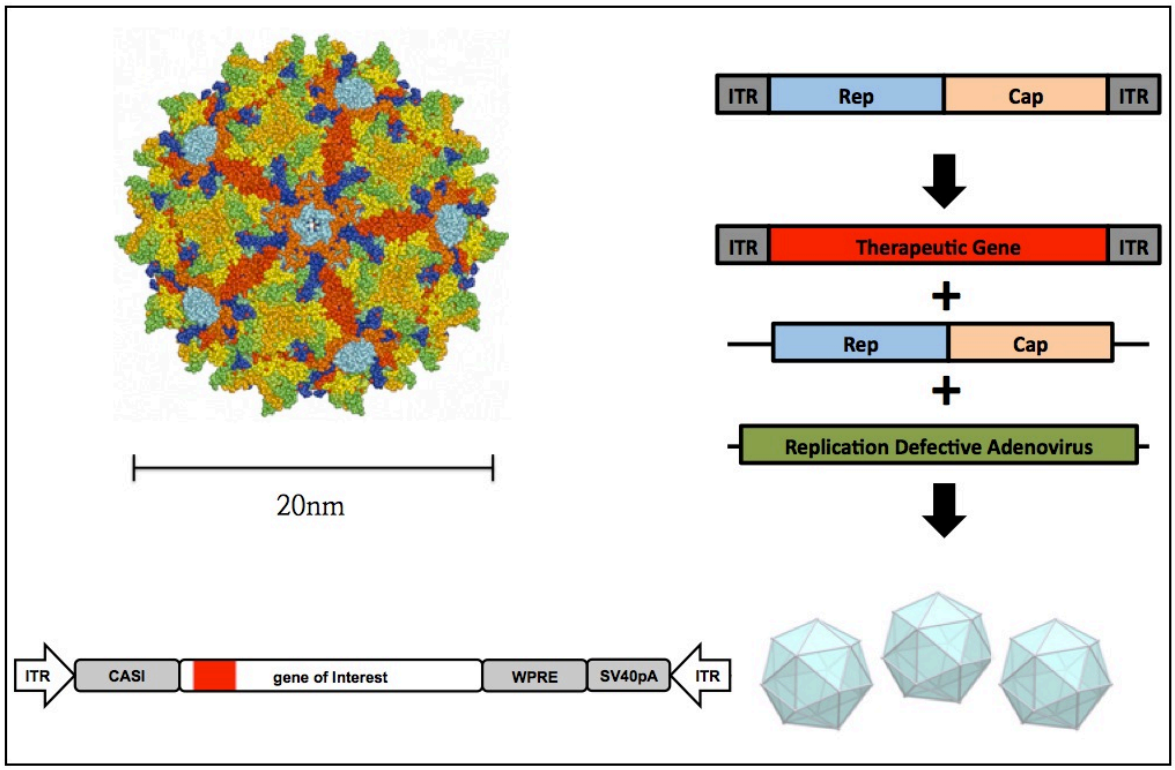

Figure 1. Adeno-associated virus and AAV viral vectors.

AAV is a small non-enveloped virus 20nm in diameter belonging to the genus *Dependovirus*. In order to propagate the virus requires genes of a helper virus such as adenovirus or herpes virus. The 4.7 kb genome is composed of the Rep and Cap genes flanked by ITR on either end. AAV gene therapy system requires a three plasmid system to form functional virions, 1. Plasmid containing therapeutic gene of interest is flanked by the ITRs; 2. Plasmid containing the Rep and Cap genes; 3. Replication defective adenovirus for helper genes. The therapeutic cassette is shown above. *Image courtesy of Alex Balazs.*

Results

Modification of AAV to increase transgene cassette size

A significant limitation of AAV gene therapy lies in the small packaging capacity of the virus (Monahan and Samulski, 2000). Until recently, the use of AAV viral vectors appeared unattainable because the wildtype viral genome of 4.7 kb can only withstand 900 bp of inserted genetic material for genes (of interest) to be delivered (Hermonat et al., 1997). Current versions of recombinant AAV (rAAV) remove the rep and cap genes from the viral vector and are supplied on a separate plasmid. The removal of these genes allows for the insertion of transgenes up to 2kb in size into the viral genome (Monahan and Samulski, 2000). While this is a great advancement from the first generation AAV viral vectors, there is opportunity for improvement to increase the capacity of the insert. Additional insert capacity can provide the opportunity to insert multiple therapeutic reagents along with a suicide gene into a single vector in order to improve the safety of the vector. Eliminating superfluous sequences in the viral vector and modification of the promoters and enhancers will be necessary in order to accomplish this.

A potential area in which the transgene cassette size can be expanded is the use of a minimal synthetic polyadenylation site. The addition of a poly(A) tail to RNA molecules is necessary for termination of transcription. In eukaryotes, the poly(A) tail protects the mRNA from enzymatic degradation in the cytoplasm. Levitt et al. describe the use of a synthetic polyadenylation site that uses the minimum sequences required for efficient polyadenylation (Levitt et al., 1989). Replacement of the SV40 late polyadenylation site with this minimal synthetic sequence was performed to allow for a 250 base pair cassette increase.

Modification of AAV to address FDA safety concerns for gene therapy

While recombinant AAV efficacy has been demonstrated in numerous gene therapy studies, it is important to assess the potential risks before beginning a clinical trial. During wild type infections AAV integrates into human chromosome 19 in over 50% of latently infected cell lines (Hermonat et al., 1997). However, the mechanism of the site-specific integration requires AAV rep proteins that are absent in the viral vector. Random integration of vector sequences has been demonstrated in recombinant AAV but at low frequency (~10%) in vivo (Hermonat et al., 1997). While this alludes to the low risk of activation of oncogenes and insertional mutagenesis through rAAV, one must not overlook the risks associated with engineering these viral vectors to become more effective. The use of stronger or less attenuated promoters such as Chicken Beta-Actin promoter (Xu et al., 2001) and inclusion of regulatory elements such as Woodchuck hepatitis posttranscriptional element (WPRE) (Loeb et al., 1999) can increase the potential oncogenic and immunogenic activity. Here I propose to increase the safety of the AAV viral vector through the elimination of the X-protein peptide within the WPRE element.

In an attempt to increase the cassette size of the AAV viral vector and reduce pathogenesis, I have designed, cloned, and tested AAV vectors containing truncated forms of the WPRE element. In particular, while it has been demonstrated that the WPRE gene has been greatly beneficial to the transgene expression in AAV (Loeb et al., 1999), the fragment also has the potential to express a 60 amino acid X-protein derived peptide known to be associated with liver pathogenesis (Loeb et al., 1999; Tu et al., 2001). The hepatitis B virus X protein is a transcriptional transactivator that has been implicated in

the development of HBV related hepatocellular carcinoma (Tu et al., 2001). Moreover, C-terminal truncations of the X protein have been shown to enhance the transforming ability of ras and myc oncogenes over the wildtype protein. This proves especially important in the modification of rAAV viruses. Truncations to eliminate and reduce the size of the X-protein were cloned and transfected to produce intact AAV virions.

AAV quantification and functional validation

Virus titer was determined by qPCR in comparison with an AAV standard and shown below (Graph 1). A vector containing no WPRE element was also included to provide a lower limit baseline of infectivity. Shortening the viral vectors did not appear to affect the overall ability to produce virions or infectivity when compared to the unmodified vector. The functional activity of the truncated mutant viruses was validated through an in vitro infection assays using 293T cells, and the concentration of the Luciferase expression in the cell supernatant measured. Genome copies (10^{11}) of each virus were added to each well and allowed to infect for 6 days.

AAV intramuscular injection and Imaging

Mice were anaesthetized by isofluorane inhalation and a single injection containing 10^{11} genome copies of each virus was administered into the gastrocnemius muscle. The mice were imaged for transgene expression at regular time points for x days following injection. To image, mice were anaesthetized by isofluorane inhalation and given D-luciferin (Gold Biotechnology) by intraperitoneal injection. I found that all of the modified viral vectors expressed Luciferase at equal to or greater levels than the standard

vector. Surprisingly, the most truncated virus, containing the synthetic poly-adenylation and the WPRE element with the X-protein deletion had over a two-fold increase in expression of the transgene (Graph 2).

Discussion

Modifications of AAV vector

I developed modifications of the WPRE element to remove the carcinogenic X-protein increased the safety of the viral vector, addressing the concerns of the Food and Drug Administration and researchers in the field. In addition, the removal increased the gene of interest cassette size by 200 base pairs and increased the expression of the transgene in vivo. Currently, in collaboration with Dr. David Baltimore, the NIH Vaccine Research Center led by Dr Gary Nabel is using this modification in the prototype AAV vector for an upcoming clinical trial.

Possible other applications for the AAV Technology

In addition, the modifications made in the current AAV vector show promise for other potential gene therapy strategies. The development of viral vectors with the ability to express transgenes of various sizes with little host response is necessary for the progress of the gene therapy field.

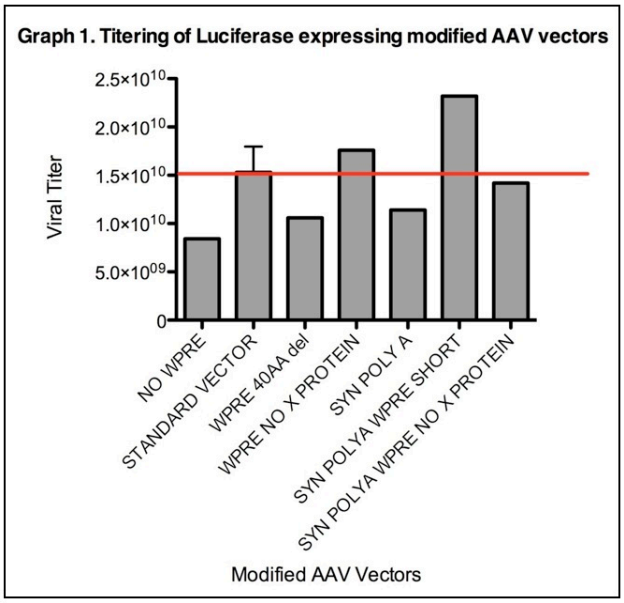

Figure 1. Viral titering of Luciferase expressing modified vector. Shortening the viral vectors did not appear to affect the overall ability to produce virions or infectivity when compared to the unmodified vector.

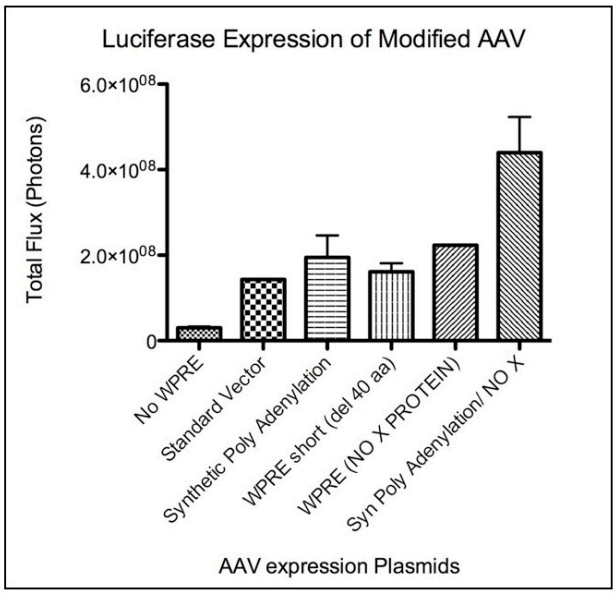

Figure 2. Transgene expression of Modified AAV.

All the modified viral vectors expressed Luciferase at equal to or greater levels than the standard vector. Modified vector containing the synthetic poly Adenylation and removal of X protein produced 2-fold more overall expression of the transgene.

References:

Balazs, A. B., Bloom, J. D., Hong, C. M., Rao, D. S., & Baltimore, D. (2013). Broad protection against influenza infection by vectored immunoprophylaxis in mice. *Nat Biotechnol, 31*(7), 647-652. doi:10.1038/nbt.2618

Balazs, A. B., Chen, J., Hong, C. M., Rao, D. S., Yang, L., & Baltimore, D. (2012). Antibody-based protection against HIV infection by vectored immunoprophylaxis. *Nature, 481*(7379), 81-84. doi:10.1038/nature10660

Balazs, A. B., Ouyang, Y., Hong, C. M., Chen, J., Nguyen, S. M., Rao, D. S., . . . Baltimore, D. (2014). Vectored immunoprophylaxis protects humanized mice from mucosal HIV transmission. *Nat Med, 20*(3), 296-300. doi:10.1038/nm.3471

Grimm, D., & Kay, M. A. (2003). From Virus Evolution to Vector Revolution: Use of Naturally Occurring Serotypes of Adeno-associated Virus (AAV) as Novel Vectors for Human Gene Therapy. *Current Gene Therapy, 3*(4), 281-304.

Hermonat, P. L., Quirk, J. G., Bishop, B. M., & Han, L. (1997). The packaging capacity of adeno-associated virus (AAV) and the potential for wild-type-plus AAV gene therapy vectors. *FEBS Lett, 407*(1), 78-84.

Levitt, N., Briggs, D., Gil, A., & Proudfoot, N. J. (1989). Definition of an efficient synthetic poly(A) site. *Genes Dev, 3*(7), 1019-1025.

Loeb, J. E., Cordier, W. S., Harris, M. E., Weitzman, M. D., & Hope, T. J. (1999). Enhanced expression of transgenes from adeno-associated virus vectors with the woodchuck hepatitis virus posttranscriptional regulatory element: implications for gene therapy. *Hum Gene Ther, 10*(14), 2295-2305. doi:10.1089/10430349950016942

McLaughlin, S. K., Collis, P., Hermonat, P. L., & Muzyczka, N. (1988). Adeno-associated virus general transduction vectors: analysis of proviral structures. *J Virol, 62*(6), 1963-1973.

Monahan, P. E., & Samulski, R. J. (2000). AAV vectors: is clinical success on the horizon? *Gene Ther, 7*(1), 24-30. doi:10.1038/sj.gt.3301109

Schnepp, B. C., Jensen, R. L., Clark, K. R., & Johnson, P. R. (2009). Infectious molecular clones of adeno-associated virus isolated directly from human tissues. *J. Virol., 83*, 1456-1464.

Schultz, B. R., & Chamberlain, J. S. (2008). Recombinant adeno-associated virus transduction and integration. *Mol Ther, 16*(7), 1189-1199. doi:10.1038/mt.2008.103

Tu, H., Bonura, C., Giannini, C., Mouly, H., Soussan, P., Kew, M., . . . Kremsdorf, D. (2001). Biological impact of natural COOH-terminal deletions of hepatitis B virus X protein in hepatocellular carcinoma tissues. *Cancer Res, 61*(21), 7803-7810.

Xu, L., Daly, T., Gao, C., Flotte, T. R., Song, S., Byrne, B. J., . . . Parker Ponder, K. (2001). CMV-beta-actin promoter directs higher expression from an adeno-associated viral vector in the liver than the cytomegalovirus or elongation factor 1 alpha promoter and results in therapeutic levels of human factor X in mice. *Hum Gene Ther, 12*(5), 563-573. doi:10.1089/104303401300042500

Appendix B

Potential and Limitations of Immunoadhesin Anti-HIV proteins

This chapter describes the strengths and weaknesses of a class of antibody based reagents for the use in immunotherapies against HIV. This work was done in collaboration with Anthony West, and Priyanthi Gnanapragasam. My contribution to this work was in aiding Anthony in initial construct design, cloning of DNA, protein purification, and preliminary characterization of the reagents. This work has been published as West, A. P., Jr., **Galimidi, R. P**, et al. (2012). "Single-chain Fv-based anti-HIV proteins: potential and limitations." J Virol **86**(1): 195-202.

Abstract

The existence of very potent, broadly neutralizing antibodies against human immunodeficiency virus type 1 (HIV-1) offers the potential for prophylaxis against HIV-1 infection by passive immunization or gene therapy. Both routes permit the delivery of modified forms of IgGs. Smaller reagents are favored when considering ease of tissue penetration and the limited capacities of gene therapy vectors. Immunoadhesin (single-chain fragment variable [scFv]-Fc) forms of IgGs are one class of relatively small reagent that has been explored for delivery by adeno-associated virus. Here we investigated the neutralization potencies of immunoadhesins compared to those of their parent IgGs. For the antibodies VRC01, PG9, and PG16, the immunoadhesins showed modestly reduced potencies, likely reflecting reduced affinities compared to those of the parent IgG, and the VRC01 immunoadhesin formed dimers and multimers with reduced neutralization potencies. Although scFv forms of neutralizing antibodies may exhibit affinity reductions, they provide a means of building reagents with multiple activities. Attachment of the VRC01 scFv to PG16 IgG yielded a bispecific reagent whose neutralization activity combined activities from both parent antibodies. Although the neutralization activity due to each component was partially reduced, the combined reagent is attractive since fewer strains escaped neutralization.

Introduction

Developing an effective human immunodeficiency virus type 1 (HIV-1) vaccine has been a great challenge for over 25 years. Results from the RV144 vaccine trial in Thailand suggested that a partial degree of protection from infection was achieved (32), but whether and how a more effective vaccine can be developed remain open questions (39, 40). Difficulties in making an effective vaccine result in part from the humoral immune response against HIV-1 in which the antibodies produced are generally strain-specific and can be quickly evaded by the rapidly mutating virus (43). Highly potent cross-strain anti-HIV antibodies have been isolated (5, 35, 41, 46 42, 45), but the unresolved problem is how to elicit these rare antibodies.

Although neutralizing antibodies have shown limited efficacy controlling an established HIV-1 infection (26, 31, 38), the observation that most new infections appear to be initiated by only one or a few viral particles (17, 33, 34) highlights the potential for antibodies to provide sterilizing immunity. Passive immunization studies with broadly neutralizing antibodies have demonstrated their ability to protect animals from an HIV/SIV chimera challenge (2, 11-13, 23, 24, 29, 30, 36). Hence, an alternative approach to prophylaxis is to deliver the genes for potent anti-HIV proteins to provide long lasting protection. A successful demonstration of this approach in rhesus macaques using adeno-associated virus (AAV) as the gene delivery vehicle has been achieved (15). AAV is an attractive vector due to its long- term gene expression and low toxicity (10). However, the use of AAV vectors imposes a size restriction on the gene delivered – expression from AAV vectors with genomes larger than 4900 bases is greatly attenuated (7). This can make it difficult to use AAV for delivery of large proteins such as IgG antibodies,

which include a heavy chain with four domains (the Fab heavy (VH) and constant heavy 1 (CH1) domains and the Fc CH2 and CH3 domains) and a light chain with two domains (the Fab variable light (VL) and constant light (CL) domains) (Fig. 1). Self-complementary AAV vectors are one means of achieving high expression levels (25), however size restrictions for these vectors prevent simultaneous incorporation of conventional antibody heavy and light chain genes.

To achieve high transduction levels, a smaller immunoglobulin architecture was used in the AAV-mediated gene therapy experiments in rhesus macaques (15): single-chain Fragment variable (scFv) units attached to a Fc domain (a scFv immunoadhesin comprising IgG VH, VL, CH2 and CH3 domains, hereafter referred to as an immunoadhesin or IA) (Fig. 1). A wide variety of Fc fusions have been developed over the last 20 years to take advantage of this architecture's key benefits: avidity provided by the homodimeric Fc, serum persistence provided by the Fc region due to FcRn-mediated protection from catabolism, and a size large enough to avoid filtration by the kidneys (14). A scFv unit, in which VH is fused to VL with a short linking region usually composed of glycines and serines, generally retains the antigen binding functionality of its parent Fab, although the scFv is only about 1/2 the size of an intact Fab. Although scFv-based reagents have been under development for many years, their overall potential as drugs remains uncertain (28).

Several broadly neutralizing and highly potent antibodies against HIV-1 have recently been isolated from infected individuals. Two such antibodies, PG9 and PG16, target a quaternary epitope involving the V1-V2 and V3 variables loops of gp120 (42). Another class of antibodies, typified by antibody VRC01, targets the CD4-binding site of gp120

(44). The efficacy of gene therapy reagents derived from these antibodies depends on a number of factors, including their potency, strain coverage, in vivo stability, effector function, and serum concentrations that can be achieved. To help inform decisions relating to the architecture of potential reagents, we systematically compared the potencies of IAs with their IgG and Fab counterparts. We also explored the potential to combine VCR01 and PG9/PG16 activities to produce a single reagent with two gp120 specificities.

MATERIALS AND METHODS

Materials. Sequences for all constructs are in Fig. S1 in the supplemental material. VRC01 IgG was expressed using plasmids VRC8551 & VRC8552 provided by Gary Nabel (Vaccine Research Center, NIH). VRC01 Fab was expressed using a truncated VRC8552 heavy chain gene sequence encoding a 7x-His tag and stop codon after the CH1 domain. VRC01 IgG-2A was expressed using plasmid VRC9715 which contains a picornavirus 2A peptide sequence (37) between the heavy and light chain genes. VRC01 IA was expressed using plasmid VRC9713 (provided by Gary Nabel), which encodes for an IA protein in which a VRC01 scFv (VH domain connected via a (Gly3Ser)4 linker to the VL domain) is fused to the Fc region from human IgG1. A VRC01 scFv gene was constructed by truncated the VRC01 IA gene by inserting a 6x- His tag and stop codon after the VL domain.

Genes encoding the variable regions (VH and VL) or the intact light chain (VL -CL) of PG9 and PG16 Abs were synthesized (BlueHeron Biotechnologies or Integrated DNA Technologies) based on sequences provided by Dennis Burton (The Scripps Research

Institute). Intact IgG genes were constructed by subcloning the relevant variable sequences onto a human IgG1 sequence. The designs of the PG9 and PG16 IAs were patterned after the rhesus IAs described in (15); thus PG9 IA was constructed as VH-(Gly4-Ser)3-VL-Fc, and PG16 IAs were constructed as VL-(Gly4-Ser)3-VH-Fc and VH-(Gly4-Ser)3-VL-Fc; for these IAs, the Fc sequence was that of human IgG2. PG9 and PG16 Fabs were expressed using truncated heavy chains with additional 7x-His tags. The PG9 and PG16 constructs were subcloned into the mammalian expression vector pTT5 (NRC Biotechnology Research Institute). The scFv genes for PG9 and PG16 were constructed by inserting a 6x-His tag and stop codon after the second variable domain.

VRC01scFv–PG16, VRC01scFv–ZAGα3–Fc, and VRC01scFv–E51 were constructed by combining the scFv gene from VRC01 IA with IgG heavy chain or Fc fusion constructs by PCR and enzymatic ligation techniques. All gene constructs were verified by complete sequencing.

Protein expression and purification. Proteins were expressed transiently in suspension HEK 293-6E cells (NRC Biotechnology Research Institute) using 25 kDa linear polyethylenimine (PEI) (Polysciences) for transfection as described (8). When expressing heterodimeric constructs, the heavy chain (HC) and light chain (LC) plasmids were mixed at a 1:1 ratio by mass. Cell culture supernatants were collected six days post-transfection. For Fc-containing constructs, supernatants were passed over protein A resin (Thermo Fisher Scientific), eluted using pH 3.0 citrate buffer, and then immediately neutralized. 7x-His tagged Fabs and scFvs were purified using Ni-NTA chromatography and eluted using 300 mM imidazole. All reagents tested in neutralization assays were purified by size exclusion chromatography using a Superdex 200 10/300 GL column.

In vitro neutralization assays. A previously-described pseudovirus neutralization assay was used to evaluate the neutralization potencies of the reagents (21, 27). Neutralization assays were performed either by the Collaboration for AIDS Vaccine Discovery (CAVD) core neutralization facility (Table 1 and Tables S1 and S2 in the supplemental material) or by our laboratory (Table 2) using the same protocol (21, 27). Briefly, pseudoviruses were generated by cotransfection of HEK 293T cells with an Env expression plasmid and a replication-defective backbone plasmid. Neutralization was determined by measuring the reduction in luciferase reporter gene expression in the presence of a potential inhibitor following a single round of pseudovirus infection in TZM-bl cells. Nonlinear regression analysis was used to calculate the concentrations at which half-maximal inhibition was observed (IC50 values).

Biosensor affinity measurements. A BIACORE 2000 biosensor system (GE Healthcare) was used to evaluate the interactions of VRC01 reagents with gp120. Approximately 750 response units (RUs) of Protein A was covalently immobilized on all flowcells of a CM5 biosensor chip using standard primary amine coupling chemistry (BIACORE manual). VRC01 IA, VRC01scFv –ZAGα3–Fc, and VRC01 IgG were then bound to three of the individual flow cells (~1400 RUs each), with the fourth flow cell serving as a blank. A concentration series of gp120 from strain Q259.d2.17 (expressed in baculovirus-infected insect cells as described (6)) was injected at room temperature in 10 mM Hepes with 150 mM NaCl, 3 mM EDTA and 0.005% surfactant P20 at pH 7.4. Equilibrium dissociation constants (KDs) were determined from kinetic constants derived from sensorgram data using simultaneous fitting to the association and dissociation phases of the interaction.

RESULTS

In order to compare the neutralization potencies of various antibody forms, we produced IgG, IA, and Fab forms of the anti-HIV antibodies PG9, PG16, and VRC01 (42, 44) (Fig. 1). We also produced the PG9 scFv, but were unable to express either the VRC01 or PG16 scFvs in isolation in sufficient quantities for testing. Proteins were expressed by transient transfection of mammalian cells, and purification was by Protein A or Ni-NTA chromatography followed by size exclusion chromatography. The size exclusion chromatography profiles of the PG9 and PG16 IAs revealed large peaks corresponding to the expected products (Fig. 2); i.e., a single Fc unit with two scFvs, which we will subsequently refer to as an IA monomer. During size exclusion chromatography of the VRC01 IA, however, both aggregated and apparently dimeric forms were observed in addition to the expected product (Fig. 2). These larger forms were a significant fraction of the material eluted from protein A chromatography, by contrast to the PG9 and PG16 IA purifications, in which only trace amounts of larger oligomers were observed.

The proteins were evaluated in an Env-pseudotyped HIV-1 neutralization assay against of panel of 30 strains (Table 1 and Table S1 in the supplemental material). As observed for other anti-HIV antibodies, the Fab forms were on average 5-10 fold less potent on a molar basis than the intact IgG (18). The 2A form of VRC01 IgG (translated from a single mRNA containing a picornavirus 2A peptide sequence (37) between the heavy and light chain genes) was equally as potent as VRC01 IgG. However, the IA forms of VRC01, PG9, and PG16 were less potent than the corresponding IgGs; the potencies were reduced overall by 5.9-fold (VRC01), 3.3-fold (PG9), and 15.5-fold

(PG16 IA, constructed as VL followed by VH). Two-tailed paired T-tests demonstrated that these differences were significant (P-values of 0.00045, 0.047, and 0.032). A PG16 IA constructed with VH followed by VL was also expressed and tested on a more limited number of strains; this reagent was also less potent than PG16 IgG (Table S2 in the supplemental material). Although the dimeric fraction of the VRC01 IA was active in neutralization, it was 2.3-fold less potent on a mass basis (P-value of 0.00012) than monomeric VRC01 IA (Table 1).

Potential reasons for the IAs to be less potent than their parent IgGs include (i) a shorter span between the two antigen combining sites; (ii) reduced stability of IAs versus IgGs in the assay media; and/or (iii) reduced affinity of the scFv antigen binding sites compared to Fab binding sites. To evaluate whether the shorter arm span of the IAs diminished their activity, we expressed a scFv-containing reagent with a combining site separation more similar to IgG by inserting an immunoglobulin constant region-like domain, the α3 domain from Zn-α2-glycoprotein (ZAG), between the scFv and Fc components to create VRC01scFv– ZAGα3–Fc (Fig. 1). The maximal separation between the VH-VL combining sites should be similar in VRC01scFv–ZAGα3–Fc and VRC01 IgG. To permit even greater separation, the VRC01 scFv was also attached to the N-terminus of the heavy chain of an unrelated IgG to create VRC01scFv–E51. The CD4-induced (CD4i) antibody E51 was chosen for this construct because E51 IgG expresses well and is weakly or non-neutralizing in the absence of CD4 (22), as observed for other CD4i antibodies (19). Neutralization assays using these reagents (Table 1) demonstrated an average IC50 similar to VRC01 IA, indicating that the arm span of VRC01scFv–based reagents had little impact on their neutralization potency.

We next tested whether differences in reagent stability (i.e., survival) under our neutralization assay conditions contributed to the differences we observed between IAs and IgGs by conducting assays with a 12 or 24 hour pre-incubation in assay media prior to adding pseudovirus. No trend toward diminished neutralization potency over time was observed (Table 2), demonstrating that differential stability in the assay media did not account for differences in potency.

A weaker antigen-binding affinity of the scFv in an IA versus the Fab in an IgG was suggested by the less potent neutralization observed for PG9 scFv compared to PG9 Fab (Table 1). The possibility of reduced antigen-binding affinity was directly tested by comparing the binding of gp120 to VRC01 IgG versus scFv-containing forms of VRC01. Purified gp120 from strain Q259.d2.17 was injected over protein A-immobilized VRC01 IgG, VRC01 IA, or VRC01scFv–ZAGα3–Fc in a surface plasmon resonance (SPR)-based binding assay (Fig. S2 in the supplemental material). The equilibrium dissociation constant (KD) derived for VRC01 IgG was 160 nM, compared with affinities of 590 nM and 570 nM for VRC01 IA and VRC01scFv– ZAGα3–Fc, respectively. The approximately 4-fold weaker affinity of the scFv-containing reagents was comparable to the 6-fold weaker neutralization IC50 of VRC01 IA compared to VRC01 IgG.

To explore the potential for combined reagents to provide greater neutralization breadth, we expressed a modified form of PG16 in which a VRC01 scFv was attached to the N-terminus of the PG16 light chain with a (Gly3-Ser)6 linker. The neutralization properties of VRC01scFv–PG16 are shown in Table 1. Inspection of the measured IC50s for strains that were resistant to either VRC01 or PG16 confirmed that both components in the combined reagent were active.

We assessed the potencies of each of the components in the bispecific VRC01scFv–PG16 reagent by a modeling procedure using the IC50 values for VRC01 IgG and PG16 IgG as follows: Assume the IC50s of the parent IgGs VRC01 and PG16 are v and p, respectively, for a given HIV-1 strain. Consider an idealized combined reagent in which both components functioned independently with no synergy or interference. In a very simplified picture of virus neutralization, reagent binding is equivalent to neutralization and the IC50 can be approximated by a single binding event with the same equilibrium dissociation constant. Solving the equilibrium equations for 50% binding/neutralization, we found the modeled IC50 was $\left(\sqrt{v^2+6vp+p^2}-v-p\right)/2$.. In the actual bispecific reagent, we anticipated the individual components would have reduced activity, i.e., $v_{reduced} = v_{eff} \times v$, where v_{eff} is >1, and $p_{reduced} = p_{eff} \times p$, where p_{eff} is >1. Assuming that v_{eff} and p_{eff} are constant across different strains, we solved for best-fit values of these parameters that minimized $\Sigma_{strains}(\log IC_{50\ observed} - \log IC_{50\ modeled})^2$. A fit assuming only one active antibody did not fit the data as well as a fit assuming that both components were active (Fig. S3 in the supplemental material).

Using our neutralization data for VRC01scFv–PG16 (Table 1), we derived values of 3.16 and 3.22 for veff and peff, thus the VRC01 scFv component possessed about 1/3 of the potency of VRC01 IgG, and the PG16 IgG portion possessed about 1/3 of the potency of unmodified PG16 IgG. On any given strain, the combined reagent was nearly always weaker than the stronger parent IgG. However, the combined reagent was superior on a mass basis to the weaker parent for 27 out of 30 strains (Fig. 3, bottom panel). In addition, the combined reagent neutralized more strains than either parent; e.g., using a IC50s < 5.0 μg/mL cutoff for neutralization, VRC01scFv–PG16 neutralized 90%

of the strains we tested, while VRC01 IgG neutralized 83%, and PG16 IgG neutralized 70% (Table 1 and Fig. 3, top panel). However, this depends on the neutralization threshold chosen. For IC50s <1.0 μg/mL, the combined reagent neutralized 67% of strains, while VRC01 and PG16 neutralized 77% and 60%, respectively.

DISCUSSION

Provision of prophylactic or therapeutic antibodies by direct injection or gene therapy permits consideration of a wide range of potential reagents building on initial discoveries of anti-HIV IgGs. Variations fall into three major categories: (i) those affecting the antigen binding site, (ii) choice of the overall architecture (e.g., IA versus IgG), and (iii) modulations of effector function. A thorough evaluation of the efficacies of the full range of potential reagents is a large task. A variety of selection strategies is available to screen variants in category (i), i.e., natural antibody repertoires and antigen binding site libraries. However, full exploration of the alternatives in categories (ii) and (iii) is limited by the need to produce purified, testable quantities of reagents and the screening limitations of evaluating effector function in complex cell- or animal-based assays. The present studies are intended to provide insight into the potential effects of architecture on reagent potency.

The size of a delivered reagent must be considered for gene therapy efforts involving AAV. In general, constructs approaching the size limit for packaging AAV suffer reduced expression level (7). Although the minimum serum or genital tract anti-HIV IgG concentration necessary for protection is not known, a rough estimate of 100 times the reagent's IC50 has been suggested (30). For broad strain coverage with reagents

such as VRC01, PG9, or PG16, this implies desired concentrations in the tens to hundreds of μg/mL. Early efforts using an AAV vector with separate promoters for heavy and light chains directing expression of anti-HIV IgG b12 yielded serum concentrations of only ~5 μg/mL (20). Alternative AAV/IgG constructs have permitted high-level IgG expression in other cases. For example, use of a single promoter with 2A self-processing peptide inserted between the antibody heavy and light chains permitted ~1 mg/mL IgG levels to be achieved with AAV-transduced liver expression (9). Nevertheless, the smaller size of IA constructs versus conventional IgG is attractive for gene therapy approaches in which vector capacity is severely limited – in particular, for self-complementary AAV vectors, which are more efficient at transduction than AAV vectors with a single stranded genome (25).

To more fully understand the potential trade-offs in vector and construct design, we compared the neutralization activities of IA versus IgG versions of three broadly neutralizing antibodies: PG9, PG16, and VRC01 (42, 44). We found that the PG9, PG16, and VRC01 IAs were several-fold less potent than their IgG forms. A reduced affinity of the scFv antigen-binding site is a likely contributing factor to this difference. Although some scFvs have affinities equivalent to the related Fab, it was noted in early studies that scFvs can exhibit up to 10-fold weaker binding (4). The weaker binding and neutralization by the VRC01 scFv-containing reagents is likely due to suboptimal geometry of the antigen binding site and/or steric interference by the Gly-Ser linker joining the VRC01 VH and VL domains. Steric interference from the scFv linker is consistent with the VRC01 Fab-gp120 crystal structure (45), in which the N-terminus of the Fab light chain is ~8 Å from the gp120 backbone. This relatively close distance

suggests that the Gly-Ser linker extending from the VL domain N-terminus could sterically interfere with antigen binding. It is possible that the scFvs in the reagents we tested were suboptimal – different designs might yield scFvs with affinities matching the corresponding Fabs. Thus, to achieve maximal efficacy it will be necessary to explore different architectures (VH–VL versus VL–VH) and different linker lengths for each scFv used in IAs.

A potential complication of scFv reagents is their tendency to dimerize or multimerize by 3-D domain swapping (3). The extent of dimerization of scFvs is variable, depending on linker length, antibody sequence, concentration, buffer conditions, and the presence or absence of antigen (1). The potential for IAs to form dimers or other oligomers as observed for VRC01 IA is a special concern for reagents that will be delivered by gene therapy, where it is not possible to remove higher order products once they are secreted from transduced cells. Multimeric forms of IAs may be less potent and potentially more immunogenic than the monomeric molecule; this may add to the immunogenicity of the artificial linker of IAs. AAV-mediated expression of IAs in rhesus macaques led to varying levels of IA- specific antibody response, which appeared correlated with reduced efficacy against viral challenge (15). The best means of addressing this possible complication is careful biophysical characterization of proposed gene therapy protein products.

In the recent rhesus macaque SIV challenge experiment, delivery of IAs was found to be superior to either scFv or whole IgG with respect to the serum concentrations that could be achieved (15). Although the IAs used in the challenge experiments exhibited neutralization IC50s well below 1.0 μg/mL, the Fabs from which

they were derived had IC50s that were 3-fold more potent on a mass basis (16). (The IC50s of the corresponding IgGs have not been reported). On a molar basis, the IAs were thus about 1.5-fold less potent than the Fab forms. This ratio is very similar to the average 1.2-fold and 1.5-fold weaker molar neutralization we observed for the VRC01 and PG16 IAs versus the corresponding Fabs (Table 1). In the rhesus challenge study, the IA potencies (IC50s of 0.01-0.02 μg/mL against the SIVmac316 challenge strain) were sufficient to provide protection. However, since anti-HIV IgGs are generally 6-30 fold more potent than their corresponding Fabs on a molar basis (18), the IAs evaluated here represent a significant trade-off necessitated by the lower serum IgG concentrations achievable (15) with currently available AAV technology.

While VRC01, PG9, and PG16 have very broad activities, each of these antibodies fails to neutralize 9 to 27% of HIV-1 strains (using a cutoff IC_{50} of 50 μg/ml; at 1 μg/ml, 28 to 49% of strains are not neutralized) (42, 44). For passive immunization or gene therapy applications, addressing the incomplete strain coverage requires delivering either multiple antibodies or a single reagent combining two or more activities. Here we investigated the feasibility of one such bispecific reagent, in which a VRC01 scFv was attached to PG16 IgG ($VRC01_{scFv}$-PG16). ***In vitro*** neutralization assays against a panel of HIV-1 strains demonstrated both VRC01 and PG16 activities. Although both potencies were reduced compared to those of the parental IgGs, $VRC01_{scFv}$-PG16 showed greater breadth, suggesting the potential for a bispecific reagent to provide complete or near-complete protection against HIV-1. Further development of such a reagent is possible, for example, given that the VRC01 scFv component of $VRC01_{scFv}$-PG16 had a reduced activity similar to that observed for the VRC01 IA, improvement of the scFv

portion could be attempted. The weaker activity of the PG16 component may result from steric factors from the scFv attached to the N terminus of the PG16 light chain. Switching the VRC01 scFv to the N terminus of the PG16 heavy chain did not improve PG16 activity (see Table S3 in the supplemental material). Changing the size or structure of the linker or switching to the C terminus of the heavy chain may permit greater PG16 activity. Although the reduced potencies of the individual components of a bispecific reagent might increase the risk that resistance to these neutralizing activities could develop, this concern is arguably secondary to providing breadth of coverage in the context of infection prophylaxis (versus treatment) since the goal of infection prophylaxis is to neutralize a small viral inoculum rather than to control an established infection.

The design of gene therapy reagents for HIV-1 prophylaxis potentially involves a variety of trade-offs, including breadth of reagent, potency, expression level, and minimization of potential for immunogenicity and other side effects. The newly discovered anti-HIV antibodies (42, 44) demonstrate that breadth and great potency can be achieved simultaneously. Our results suggest that careful optimization of reagent architecture and full biophysical characterization of the oligomeric states of potential protein reagents are important for fully exploiting the potential offered by genetic approaches to providing HIV-1 immunity. Direct conversion of IgGs to IAs will often entail a loss of potency due to weaker binding of the scFv compared to the Fab binding site and/or domain swapping to create scFv multimers, which can perhaps be avoided by screening many scFv designs. Whether this loss of potency is acceptable depends on relative ***in vivo*** serum levels of AAV-expressed IAs and IgGs. For prophylaxis against a wide variety of circulating HIV-1 strains, a delivered reagent will face strains where its

activity is far from maximal. In this situation, optimization of the reagent will be critical to provide robust protection.

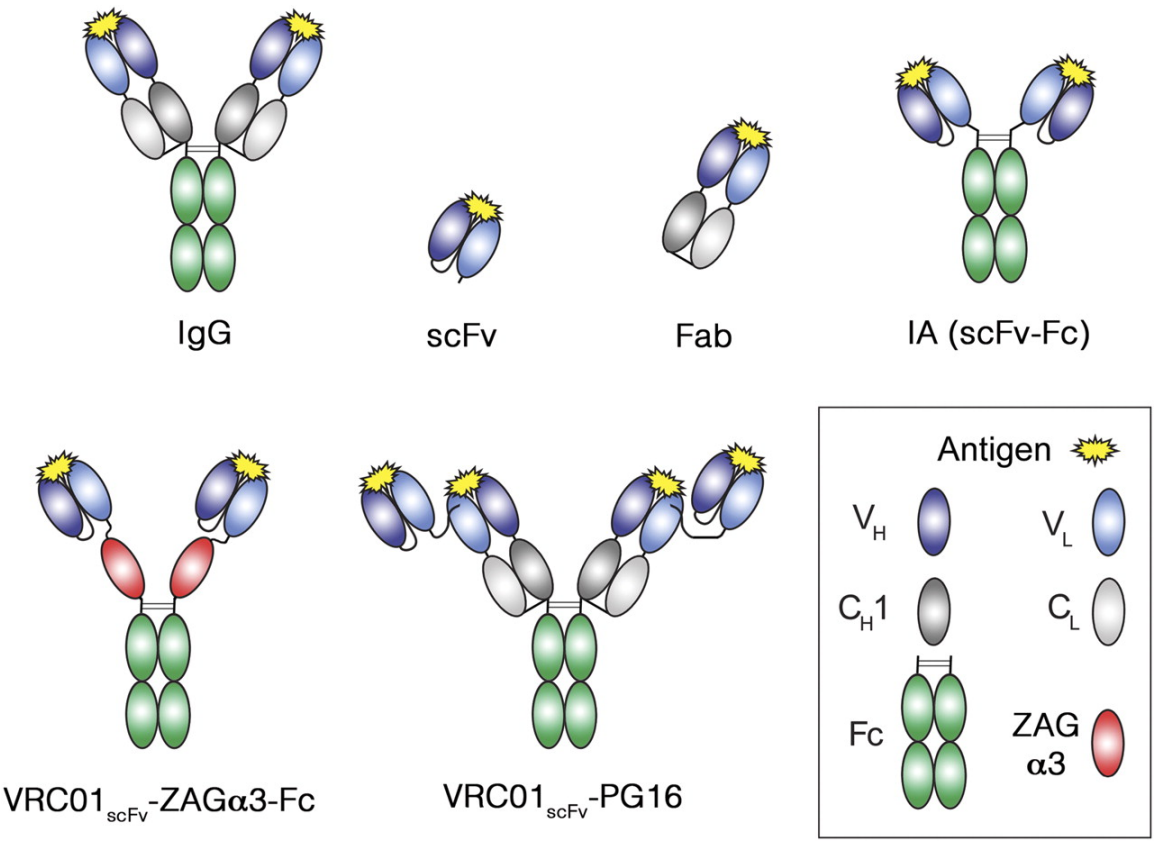

Figure 1. Schematic depiction of antibody reagent architectures. VH, variable domain of the IgG heavy chain (HC); VL, variable domain of the IgG light chain (LC); CH1, constant region 1 of the HC; CL, constant region of the LC; Fc, CH2 and CH3 domains of dimerized HCs; scFv, single-chain fragment variable (VH and VL domains of an IgG). The scFv shown is VH followed by VL; scFvs can also be constructed as VL followed by VH.

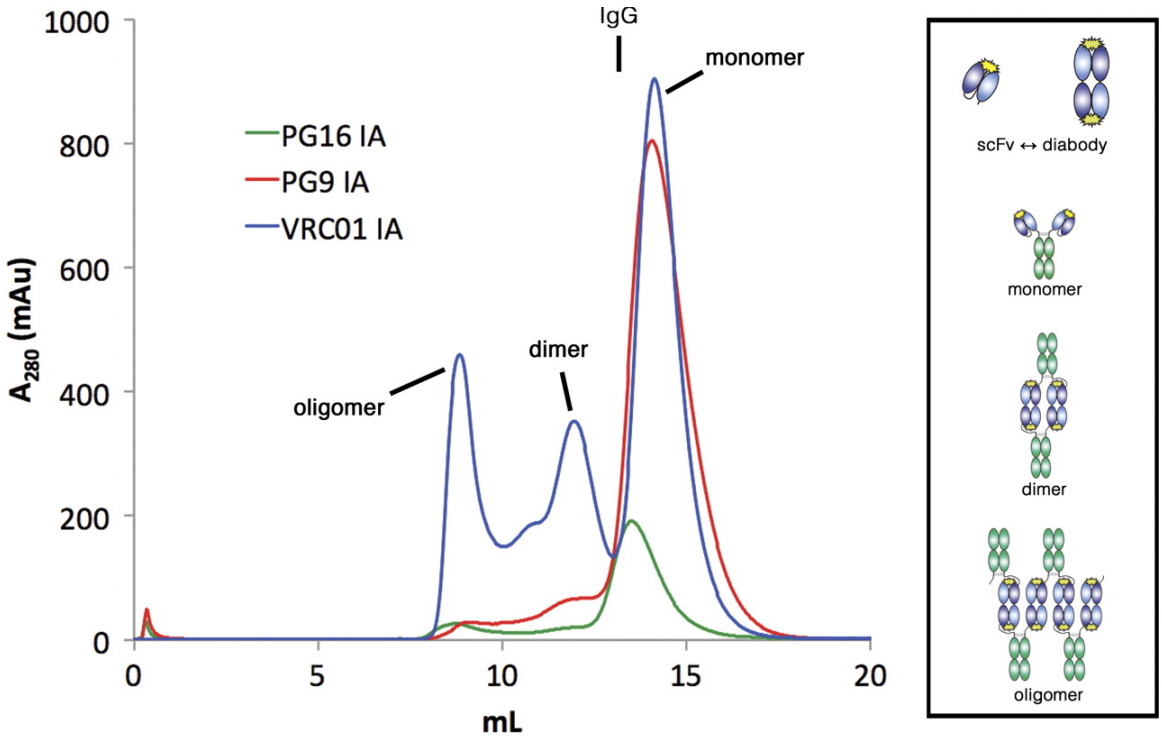

Figure 2. Size exclusion chromatography profiles of PG16, PG9, and VRC01 IAs. Protein A-purified IAs were injected over a Superdex 200 10/300 GL column. IgGs normally elute at ~13 ml (as indicated at the top of the figure), compared to the slightly smaller IA monomers, which elute at ~14.5 ml. (Data are shown for the VL-VH version of the PG16 IA; similar results were obtained for the VH-VL version.) Although the PG9 and PG16 IAs were predominantly monomeric, the VRC01 IA profile showed multimeric (presumably dimeric) and aggregate peaks in addition to the monomer. The tendency of scFv molecules to dimerize by 3-D domain swapping (shown schematically at the top in the box) may lead to the formation of dimeric and oligomeric forms of IAs (potential structures shown in the box).

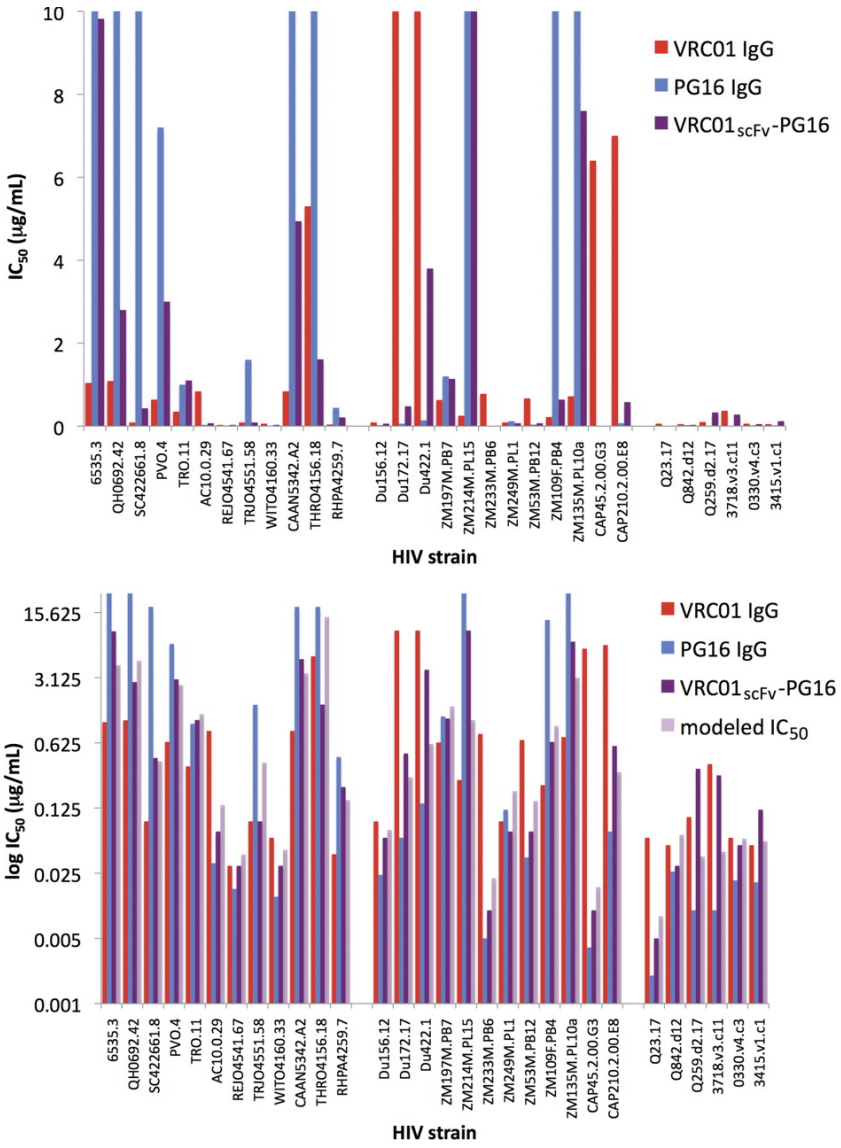

Figure 3. Histograms displaying IC50s (µg/ml) of VRC01 IgG (red), PG16 IgG (blue), and VRC01scFv-PG16 (purple) (top; linear scale) or VRC01 IgG (red), PG16 IgG (blue), VRC01scFv-PG16 (purple), and the modeled IC50s of VRC01scFv-PG16 (light purple) (bottom; logarithmic scale).

Single chain Fv-based anti-HIV proteins: Potential and Limitations

Anthony P. West, Jr., Rachel P. Galimidi, Priyanthi N. P. Gnanapragasam, and Pamela J. Bjorkman

Supplemental Tables S1-S3

Supplemental Figures S1-S3

Supplemental Table S1. IC_{50} values (g/mL) for IgG, Fab, IA, and scFv forms of VRC01, PG9, and PG16. IC_{50} values in nM are presented in Table 1.

µg/mL		VRC01						PG9				PG16			
Virus	Clade	IgG	IgG-2A	Fab	IA	IA dimer	VRC01$_{scFv}$-ZAGα3-Fc	VRC01$_{scFv}$-E51	IgG	Fab	IA	scFv	IgG	Fab	IA	VRC01$_{scFv}$-PG16
6535.3	B	1.04	1.22	1.94	>10	>10	>10	>10	0.6	8.63	0.18	85.9	42	86	0.2	9.82
QH0692.42	B	1.09	1.09	0.7	2.83	6	0.82	0.83	>100	>100	>100	>50	>100	>100	>100	2.80
SC422661.8	B	0.09	0.10	0.11	0.2	0.6	1.34	0.8	3	10.6	13.0	>100	18	42	20.82	0.43
PVO.4	B	0.64	0.67	0.51	2.05	5	2.87	4.65	12	25	>89	>50	13	13	>100	3.00
TRO.11	B	0.35	0.32	0.6	1.0	3	1	2.2	36	98.2	>100	>100	2.9	19	>100	1.10
AC10.0.29	B	0.84	0.74	0.8	1.99	6.7	3.99	7.31	0.08	0.3	>0.1	0.97	0.032	0.061	0.4	0.07
REJO4541.67	B	0.03	0.04	0.1	0.18	0.4	0.29	0.31	0.0	0.38	0.2	>3.0	0.02	1.29	5	0.03
TRJO4551.58	B	0.09	0.10	0.08	0.24	0.81	0.22	0.44	0.6	10.05	88.5	5.68	3.75	12	1.2	0.09
WITO4160.33	B	0.06	0.08	0.11	0.56	1.31	0.99	0.86	0.05	0.021	0.03	0.002	0.014	0.025	0.1	0.03
CAAN5342.A2	B	0.84	0.83	0.78	4.03	9.9	3.7	5.46	12	12	>5.0	>100	21	29	>100	4.94
THRO4156.18	B	5	5.04	3.4	8	9.96	9.47	7.88	41	76.68	>89	>100	13	98	>100	1.61
RHPA4259.7	B	0.04	0.04	0.1	0.10	0.29	0.1	0.22	27	76.26	>5.0	>50	0.505	2.6	42.2	0.21
Du156.12	C	0.09	0.06	0.06	0.41	1.66	0.57	0.52	0.05	0.141	>0.1	0.07	0.024	0.033	0.53	0.06
Du172.17	C	>10	>10	>30	>10	>10	>10	>10	0.49	0.47	1.0	6.23	0.06	0.0895	1.3	0.48
Du422.1	C	>10	>10	>30	>10	>10	>10	>10	0.43	0.4	>0.1	32	0.14	1.39	10.1	3.80
ZM197M.PB7	C	0.63	0.46	0.33	2.23	8.77	2	3.51	1.0	0.68	1.94	1.24	1.2	3.6	3.5	1.14
ZM214M.PL15	C	0.25	0.25	0.41	3.2	3.2	6.32	>10	230	>100	>100	>50	>100	>100	>100	>10
ZM233M.PB6	C	0.78	1.68	10.74	>10	>10	>10	>10	0.034	0.01	0.03	0.009	0.005	0.004	0.095	0.01
ZM249M.PL1	C	0.09	0.12	0.07	0.28	1	0.27	0.53	0.21	0.05	0.51	0.06	0.12	0.21	0.4	0.07
ZM53M.PB12	C	0.67	0.64	0.73	2.32	8	2.23	5.47	0.06	0.2	0.89	1.59	0.037	0.054	0.335	0.07
ZM109F.PB4	C	0.22	0.22	0.35	0.7	2	0.37	0.78	0.2	13	2.08	>34	20	>100	1.6	0.64
ZM135M.PL10a	C	0.72	0.77	1.97	1.35	4	3.22	5.26	>1.0	28.45	>5.0	>100	>100	>100	>100	7.60
CAP45.2.00.G3	C	6.4	3.4	>30	>10	>10	>10	>10	0.003	0.01	0.02	0.001	0.004	0.003	1.0	0.01
CAP210.2.00.E8	C	>7.0	>7.0	>30	>7.0	>7.0	>10	>10	0.47	0.31	1.95	14	0.07	0.69	5.51	0.58
Q23.17	A	0.06	0.08	0.21	0.24	0.7	0.39	0.39	0.01	<0.05	0.02	0.004	0.002	0.01	0.048	<0.005
Q842.d12	A	0.05	0.05	0.03	0.08	0.3	0.11	0.21	0.03	0.1	0.07	0.02	0.026	0.031	0.379	0.03
Q259.d2.17	A	0.10	0.05	5.12	4.23	6	>10	>10	0.22	<0.05	0.19	1	0.01	0.94	0.36	0.33
3718.v3.c11	A	0.37	0.37	6.18	9.4	10	>10	>10	0.07	0.1	0.25	0.07	0.01	0.102	2.55	0.28
0330.v4.c3	A	0.06	0.04	0.06	0.19	0.6	0.27	0.49	0.02	0.05	0.05	0.02	0.021	0.034	0.301	0.05
3415.v1.c1	A	0.05	0.04	0.05	0.22	0.74	0.23	0.51	0.08	0.09	0.47	0.2	0.02	0.114	2.38	0.12

Supplemental Table S2. IC_{50} values (nM) for PG16 IA (V_H-V_L) (opposite orientation to the PG16 IA (V_L-V_H) reagent in Table 1). †Due of the incomplete strain coverage of these data, a comparison of the mean potency with PG16 IgG is not given. ND = not determined.

		PG16			
Virus	Clade	IgG	Fab	IA (V_L-V_H)	IA (V_H-V_L)
6535.3	B	285	1800	1.9	650
QH0692.42	B	>680*	>2000	>930	>930
SC422661.8	B	120	850	200	>930
PVO.4	B	89.5	260	>930	>930
TRO.11	B	19.4	390	>930	620
AC10.0.29	B	0.22	1.2	3.7	ND
REJO4541.67	B	0.11	26	45	ND
TRJO4551.58	B	25.5	240	11	ND
WITO4160.33	B	0.095	0.51	1.4	<0.46
CAAN5342.A2	B	140	590	>930	200
THRO4156.18	B	85.5	2000	>930	ND
RHPA4259.7	B	3.4	53	>390	43
Du156.12	C	0.16	0.67	4.9	<0.46
Du172.17	C	0.41	2.6	12	0.65
Du422.1	C	0.95	28	94	61
ZM197M.PB7	C	8.1	73	33	ND
ZM214M.PL15	C	>680*	>2000	>930	ND
ZM233M.PB6	C	0.034	0.081	0.88	<0.46
ZM249M.PL1	C	0.81	4.3	3.7	ND
ZM53M.PB12	C	0.25	1.1	3.2	<0.46
ZM109F.PB4	C	134	>2000	15	ND
ZM135M.PL10a	C	>680*	>2000	>930	ND
CAP45.2.00.G3	C	0.027	0.061	9.0	ND
CAP210.2.00.E8	C	0.47	14	51	<0.46
Q23.17	A	0.014	0.20	0.45	<0.46
Q842.d12	A	0.18	0.63	3.5	<0.46
Q259.d2.17	A	0.068	19	3.4	ND
3718.v3.c11	A	0.068	2.1	24	1.0
0330.v4.c3	A	0.14	0.69	2.8	<0.46
3415.v1.c1	A	0.14	2.3	22	2.0
Geometric mean(*)		1.2	12.7	18.9	†
MNR			10.5	15.5	†

Supplemental Table S3. IC_{50} values (nM) for $VRC01_{scFv}$-PG16 reagents with the VRC01 scFv attached to the N-terminus of the PG16 light chain (the reagent shown in Table 1) or the N-terminus of the PG16 heavy chain.

		$VRC01_{scFv}$-PG16	
		scFv attached to:	
Virus	Clade	LC	HC
6535.3	B	48	7.1
QH0692.42	B	14	7.5
SC422661.8	B	2.1	3.4
PVO.4	B	15	13
TRO.11	B	5.4	3.9
AC10.0.29	B	0.34	1.1
REJO4541.67	B	0.15	0.10
TRJO4551.58	B	0.44	0.73
WITO4160.33	B	0.15	0.20
CAAN5342.A2	B	24	23
THRO4156.18	B	7.9	18
RHPA4259.7	B	1.0	0.73
Du156.12	C	0.29	0.44
Du172.17	C	2.3	8.3
Du422.1	C	19	21
ZM197M.PB7	C	5.6	4.7
ZM214M.PL15	C	>49	31
ZM233M.PB6	C	0.05	0.15
ZM249M.PL1	C	0.34	0.24
ZM53M.PB12	C	0.34	0.63
ZM109F.PB4	C	3.1	1.4
ZM135M.PL10a	C	37	8.6
CAP45.2.00.G3	C	0.05	0.05
CAP210.2.00.E8	C	2.8	16
Q23.17	A	<0.024	<0.05
Q842.d12	A	0.15	0.15
Q259.d2.17	A	1.6	1.7
3718.v3.c11	A	1.4	1.4
0330.v4.c3	A	0.24	0.34
3415.v1.c1	A	0.59	1.02
Geometric mean		1.40	1.56
Model fit for v_{eff}		3.16	1.80
Model fit for p_{eff}		3.22	9.24

Supplemental Figure. S1. DNA and amino acid sequences of constructs. In DNA sequences, surrounding non-coding sequences are shown in italics. For amino acid sequences, hydrophobic leader sequences are listed in the line above the sequence of the mature protein.

The following sequences are listed:

1) VRC01 IA (scFv(V_H-V_L)–Fc) – plasmid VRC9713 – from G. Nabel

2) PG9 IA (scFv(V_H-V_L)–Fc)

3) PG16 IA (scFv(V_L-V_H)–Fc)

4) PG16 IA (scFv(V_H-V_L)–Fc)

5) VRC01 HC–2A–LC plasmid VRC9715 – from G. Nabel

6) PG9 scFv-His_6 tagged

7) $VRC01_{scFv}$-E51 HC

8) $VRC01_{scFv}$-PG16 LC

9) $VRC01_{scFv}$-ZAG 3-Fc

10) VRC01 Fab HC (Fd)- His_7 tagged

11) PG9 Fab HC (Fd)- His_7 tagged

12) PG16 Fab HC (Fd)- His_7 tagged

13) $VRC01_{scFv}$–PG16 HC

1) VRC01 IA (VH-$(G_3S)_4$-VL-Fc (from hIgG1)) (plasmid VRC9713)

DNA:

*TCTAGACCACC*ATGGGATGGTCATGTATCATCCTTTTTCTAGTAGCAACTGCAA

CCGGTGTACATTCCCAGGTGCAGCTGGTGCAGTCTGGAGGTCAGATGAAGAA

GCCTGGCGAGTCGATGAGAATTTCTTGTCGGGCTTCTGGATATGAATTTATTG

ATTGTACGCTAAATTGGATTCGTCTGGCCCCCGGAAAAAGGCCTGAGTGGAT

GGGATGGCTGAAGCCTCGGGGGGGGGCCGTCAACTACGCACGTCCACTTCAG

GGCAGAGTGACCATGACTCGAGACGTTTATTCCGACACAGCCTTTTTGGAGCT

GCGCTCGTTGACAGTAGACGACACGGCCGTCTACTTTTGTACTAGGGGAAAA

AACTGTGATTACAATTGGGACTTCGAACACTGGGGCCGGGGCACCCCGGTCA

TCGTCTCATCAGGAGGGGGAAGCGGAGGGGGAAGCGGAGGGGGAAGCGGAG

GGGGATCCGAAATTGTGTTGACACAGTCTCCAGGCACCCTGTCTTTGTCTCCA

GGGGAAACAGCCATCATCTCTTGTCGGACCAGTCAGTATGGTTCCTTAGCCTG

GTATCAACAGAGGCCCGGCCAGGCCCCCAGGCTCGTCATCTATTCGGGCTCT

ACTCGGGCCGCTGGCATCCCAGACAGGTTCAGCGGCAGTCGGTGGGGGCCAG

ACTACAATCTCACCATCAGCAACCTGGAGTCGGGAGATTTTGGTGTTTATTAT

TGCCAGCAGTATGAATTTTTTGGCCAGGGGACCAAGGTCCAGGTCGACATTA

AAGAGCCCAAATCTTGTGACAAAACTCACACATGCCCACCGTGCCCAGCACC

TGAACTCCTGGGGGGGACCGTCAGTCTTCCTCTTCCCCCCAAAACCCAAGGAC

ACCCTCATGATCTCCCGGACCCCTGAGGTCACATGCGTGGTGGTGGACGTGA

GCCACGAAGACCCTGAGGTCAAGTTCAACTGGTACGTGGACGGCGTGGAGGT

GCATAATGCCAAGACAAAGCCGCGGGAGGAGCAGTACAACAGCACGTACCG

TGTGGTCAGCGTCCTCACCGTCCTGCACCAGGACTGGCTGAATGGCAAGGAG

TACAAGTGCAAGGTCTCCAACAAAGCCCTCCCAGCCCCCATCGAGAAAACCA

TCTCCAAAGCCAAAGGGCAGCCCCGAGAACCACAGGTGTACACCCTGCCCCC

ATCCCGGGATGAGCTGACCAAGAACCAGGTCAGCCTGACCTGCCTGGTCAAA

GGCTTCTATCCCAGCGACATCGCCGTGGAGTGGGAGAGCAATGGGCAGCCGG

AGAACAACTACAAGACCACGCCTCCCGTGCTGGACTCCGACGGCTCCTTCTT

CCTCTACAGCAAGCTCACCGTGGACAAGAGCAGGTGGCAGCAGGGGAACGT

CTTCTCATGCTCCGTGATGCATGAGGCTCTGCACAACCACTACACGCAGAAG

AGCCTCTCCCTGTCTCCGGGTAAATGA*TGA*

Protein:

MGWSCIILFLVATATGVHSQVQLVQSGGQMKKPGESMRISCRASGYEFIDCTLN

WIRLAPGKRPEWMGWLKPRGGAVNYARPLQGRVTMTRDVYSDTAFLELRSLT

VDDTAVYFCTRGKNCDYNWDFEHWGRGTPVIVSSGGGSGGGSGGGSGGGSEIV

LTQSPGTLSLSPGETAIISCRTSQYGSLAWYQQRPGQAPRLVIYSGSTRAAGIPDRF

SGSRWGPDYNLTISNLESGDFGVYYCQQYEFFGQGTKVQVDIKEPKSCDKTHTC

PPCPAPELLGGPSVFLFPPKPKDTLMISRTPEVTCVVVDVSHEDPEVKFNWYVDG

VEVHNAKTKPREEQYNSTYRVVSVLTVLHQDWLNGKEYKCKVSNKALPAPIEK

TISKAKGQPREPQVYTLPPSRDELTKNQVSLTCLVKGFYPSDIAVEWESNGQPEN

NYKTTPPVLDSDGSFFLYSKLTVDKSRWQQGNVFSCSVMHEALHNHYTQKSLSL

SPGK

2) PG9 IA (VH-(G_4S)$_3$-VL-Fc(from hIgG2))

DNA:

*GAATTCGCCGCCACC*ATGGAGTTTGGGCTGAGCTGGGTTTTCCTCGTTGCTTTC

TTAAGAGGTGTCCAGTGTCAGCGATTAGTGGAGTCTGGGGGAGGCGTGGTCC

AGCCTGGGTCGTCCCTGAGACTCTCCTGTGCAGCGTCCGGATTCGACTTCAGT

AGACAAGGCATGCACTGGGTCCGCCAGGCTCCAGGCCAGGGGCTGGAGTGG

GTGGCATTTATTAAATATGATGGAAGTGAGAAATATCATGCTGACTCCGTAT

GGGGCCGACTCAGCATCTCCAGAGACAATTCCAAGGATACGCTTTATCTCCA

AATGAATAGCCTGAGAGTCGAGGACACGGCTACATATTTTTGTGTGAGAGAG

GCTGGTGGGCCCGACTACCGTAATGGGTACAACTATTACGATTTCTATGATGG

TTATTATAACTACCACTATATGGACGTCTGGGGCAAAGGGACCACCGTGACA

GTCTCGAGCGCCTCCGGTGGCGGTGGCTCCGGAGGTGGTGGGAGCGGTGGCG

GCGGATCTCAGTCTGCCCTGACTCAGCCTGCCTCCGTGTCTGGGTCTCCTGGA

CAGTCGATCACCATCTCCTGCAATGGAACCAGCAATGATGTTGGTGGCTATG

AATCTGTCTCCTGGTACCAACAACATCCCGGCAAAGCCCCCAAAGTCGTGAT

TTATGATGTCAGTAAACGGCCCTCAGGGGTTTCTAATCGCTTCTCTGGCTCCA

AGTCCGGCAACACGGCCTCCCTGACCATCTCTGGGCTCCAGGCTGAGGACGA

GGGTGACTATTACTGCAAGTCTCTGACAAGCACGAGACGTCGGGTTTTCGGC

ACTGGGACCAAGCTGACCGTTCTAGAGCGCAAATGTTGTGTCGAGTGCCCAC

CGTGCCCAGCACCACCTGTGGCAGGACCGTCAGTCTTCCTCTTCCCCCCAAAA

CCCAAGGACACCCTCATGATCTCCCGGACCCCTGAGGTCACGTGCGTGGTGG

TGGACGTGAGCCACGAAGACCCCGAGGTCCAGTTCAACTGGTACGTGGACGG

CGTGGAGGTGCATAATGCCAAGACAAAGCCACGGGAGGAGCAGTTCAACAG

CACGTTCCGTGTGGTCAGCGTCCTCACCGTTGTGCACCAGGACTGGCTGAAC

GGCAAGGAGTACAAGTGCAAGGTCTCCAACAAAGGCCTCCCAGCCCCCATCG

AGAAAACCATCTCCAAAACCAAAGGGCAGCCCCGAGAACCACAGGTGTACA

CCCTGCCCCCATCCCGGGAGGAGATGACCAAGAACCAGGTCAGCCTGACCTG

CCTGGTCAAAGGCTTCTACCCCAGCGACATCGCCGTGGAGTGGGAGAGCAAT

GGGCAGCCGGAGAACAACTACAAGACCACACCTCCCATGCTGGACTCCGACG

GCTCCTTCTTCCTCTACAGCAAGCTCACCGTGGACAAGAGCAGGTGGCAGCA

GGGGAACGTCTTCTCATGCTCCGTGATGCATGAGGCTCTGCACAACCACTAC

ACGCAGAAGAGCCTCTCCCTGTCTCCGGGTAAATGA*GCGGCCGC*

Protein:

MEFGLSWVFLVAFLRGVQCQRLVESGGGVVQPGSSLRLSCAASGFDFSRQGMH

WVRQAPGQGLEWVAFIKYDGSEKYHADSVWGRLSISRDNSKDTLYLQMNSLRV

EDTATYFCVREAGGPDYRNGYNYYDFYDGYYNYHYMDVWGKGTTVTVSSAS

GGGGSGGGGSGGGGSQSALTQPASVSGSPGQSITISCNGTSNDVGGYESVSWYQ

QHPGKAPKVVIYDVSKRPSGVSNRFSGSKSGNTASLTISGLQAEDEGDYYCKSLT

STRRRVFGTGTKLTVLERKCCVECPPCPAPPVAGPSVFLFPPKPKDTLMISRTPEV

TCVVVDVSHEDPEVQFNWYVDGVEVHNAKTKPREEQFNSTFRVVSVLTVVHQD

WLNGKEYKCKVSNKGLPAPIEKTISKTKGQPREPQVYTLPPSREEMTKNQVSLTC

LVKGFYPSDIAVEWESNGQPENNYKTTPPMLDSDGSFFLYSKLTVDKSRWQQGN

VFSCSVMHEALHNHYTQKSLSLSPGK

3) PG16 IA (VL-$(G_4S)_3$-VH-Fc (from hIgG2))

DNA:

ATGGCCTGGGCTCTGCTATTCCTCACCCTCTTCACTCAGGGCACAGGGTCCTG

GGGCCAGTCTGCCCTGACTCAGCCTGCCTCCGTGTCTGGGTCTCCTGGACAGA

CGATCACCATCTCCTGCAATGGAACCAGCAGTGACGTTGGTGGATTTGACTCT

GTCTCCTGGTACCAACAATCCCCAGGGAAAGCCCCCAAAGTCATGGTTTTTG

ATGTCAGTCATCGGCCCTCAGGTATCTCTAATCGCTTCTCTGGCTCCAAGTCC

GGCAACACGGCCTCCCTGACCATCTCTGGGCTCCACATTGAGGACGAGGGCG

ATTATTTCTGCTCTTCACTGACAGACAGAAGCCATCGCATATTCGGCGGCGGG

ACCAAGGTGACCGTTCTAGGTGGCGGTGGCTCCGGAGGTGGTGGGAGCGGTG

GCGGCGGATCTCAGGAACAACTGGTGGAGTCTGGGGGAGGCGTGGTCCAGCC

GGGGGGGTCCCTGAGACTCTCCTGTTTAGCGTCTGGATTCACGTTTCACAAAT

ATGGCATGCACTGGGTCCGCCAGGCTCCAGGCAAGGGCCTGGAGTGGGTGGC

ACTCATCTCAGATGACGGAATGAGGAAATATCATTCAGACTCCATGTGGGGC

CGAGTCACCATCTCCAGAGACAATTCCAAGAACACTCTTTATCTGCAATTCAG

CAGCCTGAAAGTCGAAGACACGGCTATGTTCTTCTGTGCGAGAGAGGCTGGT

GGGCCAATCTGGCATGACGACGTCAAATATTACGATTTTAATGACGGCTACT

ACAACTACCACTACATGGACGTCTGGGGCAAGGGGACCACGGTCACCGTCTC

GAGCGCCTCCGAGCGCAAATGTTGTGTCGAGTGCCCACCGTGCCCAGCACCA

CCTGTGGCAGGACCGTCAGTCTTCCTCTTCCCCCCAAAACCCAAGGACACCCT

CATGATCTCCCGGACCCCTGAGGTCACGTGCGTGGTGGTGGACGTGAGCCAC

GAAGACCCCGAGGTCCAGTTCAACTGGTACGTGGACGGCGTGGAGGTGCATA

ATGCCAAGACAAAGCCACGGGAGGAGCAGTTCAACAGCACGTTCCGTGTGGT

CAGCGTCCTCACCGTTGTGCACCAGGACTGGCTGAACGGCAAGGAGTACAAG
TGCAAGGTCTCCAACAAAGGCCTCCCAGCCCCCATCGAGAAAACCATCTCCA
AAACCAAAGGGCAGCCCCGAGAACCACAGGTGTACACCCTGCCCCCATCCCG
GGAGGAGATGACCAAGAACCAGGTCAGCCTGACCTGCCTGGTCAAAGGCTTC
TACCCCAGCGACATCGCCGTGGAGTGGGAGAGCAATGGGCAGCCGGAGAAC
AACTACAAGACCACACCTCCCATGCTGGACTCCGACGGCTCCTTCTTCCTCTA
CAGCAAGCTCACCGTGGACAAGAGCAGGTGGCAGCAGGGGAACGTCTTCTC
ATGCTCCGTGATGCATGAGGCTCTGCACAACCACTACACGCAGAAGAGCCTC
TCCCTGTCTCCGGGTAAA

Protein:

MAWALLFLTLFTQGTGSWGQSALTQPASVSGSPGQTITISCNGTSSDVGGFDSVS
WYQQSPGKAPKVMVFDVSHRPSGISNRFSGSKSGNTASLTISGLHIEDEGDYFCS
SLTDRSHRIFGGGTKVTVLGGGGSGGGGSGGGGSQEQLVESGGGVVQPGGSLRL
SCLASGFTFHKYGMHWVRQAPGKGLEWVALISDDGMRKYHSDSMWGRVTISR
DNSKNTLYLQFSSLKVEDTAMFFCAREAGGPIWHDDVKYYDFNDGYYNYHYM
DVWGKGTTVTVSSASERKCCVECPPCPAPPVAGPSVFLFPPKPKDTLMISRTPEV
TCVVVDVSHEDPEVQFNWYVDGVEVHNAKTKPREEQFNSTFRVVSVLTVVHQD
WLNGKEYKCKVSNKGLPAPIEKTISKTKGQPREPQVYTLPPSREEMTKNQVSLTC
LVKGFYPSDIAVEWESNGQPENNYKTTPPMLDSDGSFFLYSKLTVDKSRWQQGN
VFSCSVMHEALHNHYTQKSLSLSPGK

4) PG16 IA (VH-$(G_4S)_3$-VL-Fc (from hIgG2))

DNA:

*GAATTCGCCGCCACC*ATGGAGTTTGGGCTGAGCTGGGTTTTCCTCGTTGCTTTC

TTAAGAGGTGTCCAGTGTCAGGAACAACTGGTGGAGTCTGGGGGAGGCGTGG

TCCAGCCGGGGGGGTCCCTGAGACTCTCCTGTTTAGCGTCTGGATTCACGTTT

CACAAATATGGCATGCACTGGGTCCGCCAGGCTCCAGGCAAGGGCCTGGAGT

GGGTGGCACTCATCTCAGATGACGGAATGAGGAAATATCATTCAGACTCCAT

GTGGGGCCGAGTCACCATCTCCAGAGACAATTCCAAGAACACTCTTTATCTG

CAATTCAGCAGCCTGAAAGTCGAAGACACGGCTATGTTCTTCTGTGCGAGAG

AGGCTGGTGGGCCAATCTGGCATGACGACGTCAAATATTACGATTTTAATGA

CGGCTACTACAACTACCACTACATGGACGTCTGGGGCAAGGGGACCACGGTC

ACCGTCTCGAGCGCCTCCGGTGGCGGTGGCTCCGGAGGTGGTGGGAGCGGTG

GCGGCGGATCTCAGTCTGCCCTGACTCAGCCTGCCTCCGTGTCTGGGTCTCCT

GGACAGACGATCACCATCTCCTGCAATGGAACCAGCAGTGACGTTGGTGGAT

TTGACTCTGTCTCCTGGTACCAACAATCCCCAGGGAAAGCCCCCAAAGTCAT

GGTTTTTGATGTCAGTCATCGGCCCTCAGGTATCTCTAATCGCTTCTCTGGCTC

CAAGTCCGGCAACACGGCCTCCCTGACCATCTCTGGGCTCCACATTGAGGAC

GAGGGCGATTATTTCTGCTCTTCACTGACAGACAGAAGCCATCGCATATTCGG

CGGCGGGACCAAGGTGACCGTTCTAGAGCGCAAATGTTGTGTCGAGTGCCCA

CCGTGCCCAGCACCACCTGTGGCAGGACCGTCAGTCTTCCTCTTCCCCCCAAA

ACCCAAGGACACCCTCATGATCTCCCGGACCCCTGAGGTCACGTGCGTGGTG

GTGGACGTGAGCCACGAAGACCCCGAGGTCCAGTTCAACTGGTACGTGGACG

GCGTGGAGGTGCATAATGCCAAGACAAAGCCACGGGAGGAGCAGTTCAACA

GCACGTTCCGTGTGGTCAGCGTCCTCACCGTTGTGCACCAGGACTGGCTGAA

CGGCAAGGAGTACAAGTGCAAGGTCTCCAACAAAGGCCTCCCAGCCCCCATC

GAGAAAACCATCTCCAAAACCAAAGGGCAGCCCCGAGAACCACAGGTGTAC

ACCCTGCCCCCATCCCGGGAGGAGATGACCAAGAACCAGGTCAGCCTGACCT

GCCTGGTCAAAGGCTTCTACCCCAGCGACATCGCCGTGGAGTGGGAGAGCAA

TGGGCAGCCGGAGAACAACTACAAGACCACACCTCCCATGCTGGACTCCGAC

GGCTCCTTCTTCCTCTACAGCAAGCTCACCGTGGACAAGAGCAGGTGGCAGC

AGGGGAACGTCTTCTCATGCTCCGTGATGCATGAGGCTCTGCACAACCACTA

CACGCAGAAGAGCCTCTCCCTGTCTCCGGGTAAATGA*GCGGCCGC*

Protein:

MEFGLSWVFLVAFLRGVQCQEQLVESGGGVVQPGGSLRLSCLASGFTFHKYGM

HWVRQAPGKGLEWVALISDDGMRKYHSDSMWGRVTISRDNSKNTLYLQFSSLK

VEDTAMFFCAREAGGPIWHDDVKYYDFNDGYYNYHYMDVWGKGTTVTVSSA

SGGGGSGGGGSGGGGSQSALTQPASVSGSPGQTITISCNGTSSDVGGFDSVSWYQ

QSPGKAPKVMVFDVSHRPSGISNRFSGSKSGNTASLTISGLHIEDEGDYFCSSLTD

RSHRIFGGGTKVTVLERKCCVECPPCPAPPVAGPSVFLFPPKPKDTLMISRTPEVT

CVVVDVSHEDPEVQFNWYVDGVEVHNAKTKPREEQFNSTFRVVSVLTVVHQD

WLNGKEYKCKVSNKGLPAPIEKTISKTKGQPREPQVYTLPPSREEMTKNQVSLTC

LVKGFYPSDIAVEWESNGQPENNYKTTPPMLDSDGSFFLYSKLTVDKSRWQQGN

VFSCSVMHEALHNHYTQKSLSLSPGK

5) VRC01-HC-2A-LC plasmid (hIgG1) (Plasmid VRC9715)

DNA:

*TCTAGACCACC*ATGGGATGGTCATGTATCATCCTTTTTCTAGTAGCAACTGCAA

CCGGTGTACATTCCCAGGTGCAGCTGGTGCAGTCTGGAGGTCAGATGAAGAA

GCCTGGCGAGTCGATGAGAATTTCTTGTCGGGCTTCTGGATATGAATTTATTG

ATTGTACGCTAAATTGGATTCGTCTGGCCCCCGGAAAAAGGCCTGAGTGGAT

GGGATGGCTGAAGCCTCGGGGGGGGGCCGTCAACTACGCACGTCCACTTCAG

GGCAGAGTGACCATGACTCGAGACGTTTATTCCGACACAGCCTTTTTGGAGCT

GCGCTCGTTGACAGTAGACGACACGGCCGTCTACTTTTGTACTAGGGGAAAA

AACTGTGATTACAATTGGGACTTCGAACACTGGGGCCGGGGCACCCCGGTCA

TCGTCTCATCACCGTCGACCAAGGGCCCATCGGTCTTCCCCCTGGCACCCTCC

TCCAAGAGCACCTCTGGGGGCACAGCGGCCCTGGGCTGCCTGGTCAAGGACT

ACTTCCCCGAACCGGTGACGGTGTCGTGGAACTCAGGCGCCCTGACCAGCGG

CGTGCACACCTTCCCGGCTGTCCTACAGTCCTCAGGACTCTACTCCCTCAGCA

GCGTGGTGACCGTGCCCTCCAGCAGCTTGGGCACCCAGACCTACATCTGCAA

CGTGAATCACAAGCCCAGCAACACCAAGGTGGACAAGAAAGTTGAGCCCAA

ATCTTGTGACAAAACTCACACATGCCCACCGTGCCCAGCACCTGAACTCCTG

GGGGGACCGTCAGTCTTCCTCTTCCCCCCAAAACCCAAGGACACCCTCATGA

TCTCCCGGACCCCTGAGGTCACATGCGTGGTGGTGGACGTGAGCCACGAAGA

CCCTGAGGTCAAGTTCAACTGGTACGTGGACGGCGTGGAGGTGCATAATGCC

AAGACAAAGCCGCGGGAGGAGCAGTACAACAGCACGTACCGTGTGGTCAGC

GTCCTCACCGTCCTGCACCAGGACTGGCTGAATGGCAAGGAGTACAAGTGCA

AGGTCTCCAACAAAGCCCTCCCAGCCCCCATCGAGAAAACCATCTCCAAAGC

CAAAGGGCAGCCCCGAGAACCACAGGTGTACACCCTGCCCCCATCCCGGGAT

GAGCTGACCAAGAACCAGGTCAGCCTGACCTGCCTGGTCAAAGGCTTCTATC

CCAGCGACATCGCCGTGGAGTGGGAGAGCAATGGGCAGCCGGAGAACAACT

ACAAGACCACGCCTCCCGTGCTGGACTCCGACGGCTCCTTCTTCCTCTACAGC

AAGCTCACCGTGGACAAGAGCAGGTGGCAGCAGGGGAACGTCTTCTCATGCT

CCGTGATGCATGAGGCTCTGCACAACCACTACACGCAGAAGAGCCTCTCCCT

GTCTCCGGGTAAACGGCGGCGGCGGGCCCCCGTGAAGCAGACCCTGAACTTC

GACCTGCTGAAGCTGGCCGGCGACGTGGAGAGCAACCCCGGCCCCATGGGAT

GGTCATGTATCATCCTTTTTCTAGTAGCAACTGCAACCGGTGTACATTCAGAA

ATTGTGTTGACACAGTCTCCAGGCACCCTGTCTTTGTCTCCAGGGGAAACAGC

CATCATCTCTTGTCGGACCAGTCAGTATGGTTCCTTAGCCTGGTATCAACAGA

GGCCCGGCCAGGCCCCCAGGCTCGTCATCTATTCGGGCTCTACTCGGGCCGCT

GGCATCCCAGACAGGTTCAGCGGCAGTCGGTGGGGGCCAGACTACAATCTCA

CCATCAGCAACCTGGAGTCGGGAGATTTTGGTGTTTATTATTGCCAGCAGTAT

GAATTTTTTGGCCAGGGGACCAAGGTCCAGGTCGACATTAAACGTACGGTGG

CTGCACCATCTGTCTTCATCTTCCCGCCATCTGATGAGCAGTTGAAATCTGGA

ACTGCCTCTGTTGTGTGCCTGCTGAATAACTTCTACCCCAGAGAAGCCAAAGT

GCAGTGGAAGGTGGACAACGCCCTGCAGAGCGGAAACAGCCAGGAAAGCGT

GACAGAGCAGGATTCCAAGGATTCCACATACAGCCTGAGCAGCACACTGACA

CTGTCCAAGGCCGACTACGAGAAGCACAAGGTGTACGCCTGCGAAGTGACAC

ACCAGGGACTGTCCTCCCCTGTGACAAAGAGCTTCAACAGAGGAGAATGCTG

ATAG*GATCC*

Protein:

MGWSCIILFLVATATGVHSQVQLVQSGGQMKKPGESMRISCRASGYEFIDCTLN

WIRLAPGKRPEWMGWLKPRGGAVNYARPLQGRVTMTRDVYSDTAFLELRSLT

VDDTAVYFCTRGKNCDYNWDFEHWGRGTPVIVSSPSTKGPSVFPLAPSSKSTSG

GTAALGCLVKDYFPEPVTVSWNSGALTSGVHTFPAVLQSSGLYSLSSVVTVPSSS

LGTQTYICNVNHKPSNTKVDKKVEPKSCDKTHTCPPCPAPELLGGPSVFLFPPKP

KDTLMISRTPEVTCVVVDVSHEDPEVKFNWYVDGVEVHNAKTKPREEQYNSTY

RVVSVLTVLHQDWLNGKEYKCKVSNKALPAPIEKTISKAKGQPREPQVYTLPPS

RDELTKNQVSLTCLVKGFYPSDIAVEWESNGQPENNYKTTPPVLDSDGSFFLYSK

LTVDKSRWQQGNVFSCSVMHEALHNHYTQKSLSLSPGKRRRRAPVKQTLNFDL

LKLAGDVESNPGPMGWSCIILFLVATATGVHSEIVLTQSPGTLSLSPGETAIISCRT

SQYGSLAWYQQRPGQAPRLVIYSGSTRAAGIPDRFSGSRWGPDYNLTISNLESGD

FGVYYCQQYEFFGQGTKVQVDIKRTVAAPSVFIFPPSDEQLKSGTASVVCLLNNF

YPREAKVQWKVDNALQSGNSQESVTEQDSKDSTYSLSSTLTLSKADYEKHKVY

ACEVTHQGLSSPVTKSFNRGEC

6) PG9 scFv-His$_6$ tagged:

DNA:

*GAATTCGCCGCCACC*ATGGAGTTTGGGCTGAGCTGGGTTTTCCTCGTTGCTTTC

TTAAGAGGTGTCCAGTGTCAGCGATTAGTGGAGTCTGGGGGAGGCGTGGTCC

AGCCTGGGTCGTCCCTGAGACTCTCCTGTGCAGCGTCCGGATTCGACTTCAGT

AGACAAGGCATGCACTGGGTCCGCCAGGCTCCAGGCCAGGGGCTGGAGTGG

GTGGCATTTATTAAATATGATGGAAGTGAGAAATATCATGCTGACTCCGTAT

GGGGCCGACTCAGCATCTCCAGAGACAATTCCAAGGATACGCTTTATCTCCA

AATGAATAGCCTGAGAGTCGAGGACACGGCTACATATTTTTGTGTGAGAGAG

GCTGGTGGGCCCGACTACCGTAATGGGTACAACTATTACGATTTCTATGATGG

TTATTATAACTACCACTATATGGACGTCTGGGGCAAAGGGACCACcGTgACaG

TCTCGAGCGGTGGCGGTGGCTCCGGAGGTGGTGGGAGCGGTGGCGGCGGATC

TCAGTCTGCCCTGACTCAGCCTGCCTCCGTGTCTGGGTCTCCTGGACAGTCGA

TCACCATCTCCTGCAATGGAACCAGCAATGATGTTGGTGGCTATGAATCTGTC

TCCTGGTACCAACAACATCCCGGCAAAGCCCCCAAAGTCGTGATTTATGATG

TCAGTAAACGGCCCTCAGGGGTTTCTAATCGCTTCTCTGGCTCCAAGTCCGGC

AACACGGCCTCCCTGACCATCTCTGGGCTCCAGGCTGAGGACGAGGGTGACT

ATTACTGCAAGTCTCTGACAAGCACGAGACGTCGGGTTTTCGGCACTGGGAC

CAAGCTGACCGTTCTACATCATCACCATCACCACTGA*GCGGCCGC*

Protein:

MEFGLSWVFLVAFLRGVQCQRLVESGGGVVQPGSSLRLSCAASGFDFSRQGMH

WVRQAPGQGLEWVAFIKYDGSEKYHADSVWGRLSISRDNSKDTLYLQMNSLRV

EDTATYFCVREAGGPDYRNGYNYYDFYDGYYNYHYMDVWGKGTTVTVSSGG

GGSGGGGSGGGGSQSALTQPASVSGSPGQSITISCNGTSNDVGGYESVSWYQQH

PGKAPKVVIYDVSKRPSGVSNRFSGSKSGNTASLTISGLQAEDEGDYYCKSLTST

RRRVFGTGTKLTVLHHHHHH

7) VRC01$_{scFv}$-E51 HC:

DNA:

*AATTCGCCGCCACC*ATGGGATGGTCATGTATCATCCTTTTTCTAGTAGCAACTG

CAACCGGTGTACATTCCCAGGTGCAGCTGGTGCAGTCTGGAGGTCAGATGAA

GAAGCCTGGCGAGTCGATGAGAATTTCTTGTCGGGCTTCTGGATATGAATTTA

TTGATTGTACGCTAAATTGGATTCGTCTGGCCCCCGGAAAAAGGCCTGAGTG

GATGGGATGGCTGAAGCCTCGGGGGGGGGCCGTCAACTACGCACGTCCACTT

CAGGGCAGAGTGACCATGACTCGAGACGTTTATTCCGACACAGCCTTTTTGG

AGCTGCGCTCGTTGACAGTAGACGACACGGCCGTCTACTTTTGTACTAGGGG

AAAAAACTGTGATTACAATTGGGACTTCGAACACTGGGGCCGGGGCACCCCG

GTCATCGTCTCATCAGGAGGGGGAAGCGGAGGGGGAAGCGGAGGGGGAAGC

GGAGGGGGATCCGAAATTGTGTTGACACAGTCTCCAGGCACCCTGTCTTTGTC

TCCAGGGGAAACAGCCATCATCTCTTGTCGGACCAGTCAGTATGGTTCCTTAG

CCTGGTATCAACAGAGGCCCGGCCAGGCCCCCAGGCTCGTCATCTATTCGGG

CTCTACTCGGGCCGCTGGCATCCCAGACAGGTTCAGCGGCAGTCGGTGGGGG

CCAGACTACAATCTCACCATCAGCAACCTGGAGTCGGGAGATTTTGGTGTTTA

TTATTGCCAGCAGTATGAATTTTTTGGCCAGGGGACCAAGGTCCAGGTCGAC

ATTAAAGCCGGCGGCAGCGGAGGAGGATCTGGGGGAGGGTCCGGAGGCGGA

TCCGGGGGCGGTTCAGGTGGGGGTAGCGGAGGGGGCTCAGGCGGAGCTAGC

GAGGTGCAGCTGGTGCAGTCTGGGGCTGAGGTGAACAAGCCTGGGTCCTCGG

TGAAGGTCTCCTGTCAGGCTTCTGGAGCCACCTTAAACAGTCATGCTTTCAGC

TGGGTGCGACAGGCCCCTGGACAAGGGCTTGAGTGGATGGCAGGGATCATCC

CTATATTTGGTTCATCACACTACGCACAAAAGTTCCAGGGCAGAGTCACGATT

ACCGCGGACGAGTCCACGCGCACAGTGTATTTGCATCTGAGAGGCCTGAGAT

CTGATGACACGGCCGTTTATTACTGTGCGAGTAATTCTATTGCCGGAGTAGCA

GCTGCCGGAGACTACGCTGACTACGATGGGGGCTACTACTACGATATGGATG

TCTGGGGCCAAGGGACCACGGTCACCGTCTCCTCAGCCTCCACCAAGGGCCC

ATCGGTCTTCCCCCTGGCACCCTCCTCCAAGAGCACCTCTGGGGGCACAGCG

GCCCTGGGCTGCCTGGTCAAGGACTACTTCCCCGAACCGGTGACGGTGTCGT

GGAACTCAGGCGCCCTGACCAGCGGCGTGCACACCTTCCCGGCTGTCCTACA

GTCCTCAGGACTCTACTCCCTCAGCAGCGTGGTGACCGTGCCCTCCAGCAGCT

TGGGCACCCAGACCTACATCTGCAACGTGAATCACAAGCCCAGCAACACCAA

GGTGGACAAGAAAGTTGAGCCCAAATCTTGTGACAAAACTCACACGTGCCCA

CCGTGCCCAGCACCTGAACTCCTGGGGGGACCGTCAGTCTTCCTCTTCCCCCC

AAAACCCAAGGACACCCTCATGATCTCCCGGACCCCTGAGGTCACATGCGTG

GTGGTGGACGTGAGCCACGAAGACCCTGAGGTCAAGTTCAACTGGTACGTGG

ACGGCGTGGAGGTGCATAATGCCAAGACAAAGCCGCGGGAGGAGCAGTACA

ACAGCACGTACCGGGTGGTCAGCGTCCTCACCGTCCTGCACCAGGACTGGCT

GAATGGCAAGGAGTACAAGTGCAAGGTCTCCAACAAAGCCCTCCCAGCCCCC

ATCGAGAAAACCATCTCCAAAGCCAAAGGTCAGCCCCGAGAACCACAGGTG

TACACCCTGCCCCCATCCCGGGATGAGCTGACCAAGAACCAGGTCAGCCTGA

CCTGCCTGGTCAAAGGCTTCTATCCCAGCGACATCGCCGTGGAGTGGGAGAG

CAATGGGCAGCCGGAGAACAACTACAAGACCACGCCTCCCGTGCTGGACTCC

GACGGCTCCTTCTTCCTCTACAGCAAGCTCACCGTGGACAAGAGCAGGTGGC

AGCAGGGGAACGTCTTCTCATGCTCCGTGATGCATGAGGCTCTGCACAACCA

CTACACGCAGAAGAGCCTCTCCCTGTCTCCGGGTAAATGA

Protein:

MGWSCIILFLVATATGVHSQVQLVQSGGQMKKPGESMRISCRASGYEFIDCTLN

WIRLAPGKRPEWMGWLKPRGGAVNYARPLQGRVTMTRDVYSDTAFLELRSLT

VDDTAVYFCTRGKNCDYNWDFEHWGRGTPVIVSSGGGSGGGSGGGSGGGSEIV

LTQSPGTLSLSPGETAIISCRTSQYGSLAWYQQRPGQAPRLVIYSGSTRAAGIPDRF

SGSRWGPDYNLTISNLESGDFGVYYCQQYEFFGQGTKVQVDIKAGGSGGGSGG

GSGGGSGGGSGGGSGGGSGGASEVQLVQSGAEVNKPGSSVKVSCQASGATLNS

HAFSWVRQAPGQGLEWMAGIIPIFGSSHYAQKFQGRVTITADESTRTVYLHLRGL

RSDDTAVYYCASNSIAGVAAAGDYADYDGGYYYDMDVWGQGTTVTVSSASTK

GPSVFPLAPSSKSTSGGTAALGCLVKDYFPEPVTVSWNSGALTSGVHTFPAVLQS

SGLYSLSSVVTVPSSSLGTQTYICNVNHKPSNTKVDKKVEPKSCDKTHTCPPCPA

PELLGGPSVFLFPPKPKDTLMISRTPEVTCVVVDVSHEDPEVKFNWYVDGVEVH

NAKTKPREEQYNSTYRVVSVLTVLHQDWLNGKEYKCKVSNKALPAPIEKTISKA

KGQPREPQVYTLPPSRDELTKNQVSLTCLVKGFYPSDIAVEWESNGQPENNYKT

TPPVLDSDGSFFLYSKLTVDKSRWQQGNVFSCSVMHEALHNHYTQKSLSLSPGK

8) VRC01$_{scFv}$–PG16 LC:

DNA:

*AATTCGCCGCCACC*ATGGGATGGTCATGTATCATCCTTTTTCTAGTAGCAACTG

CAACCGGTGTACATTCCCAGGTGCAGCTGGTGCAGTCTGGAGGTCAGATGAA

GAAGCCTGGCGAGTCGATGAGAATTTCTTGTCGGGCTTCTGGATATGAATTTA

TTGATTGTACGCTAAATTGGATTCGTCTGGCCCCCGGAAAAAGGCCTGAGTG

GATGGGATGGCTGAAGCCTCGGGGGGGGGCCGTCAACTACGCACGTCCACTT

CAGGGCAGAGTGACCATGACTCGAGACGTTTATTCCGACACAGCCTTTTTGG

AGCTGCGCTCGTTGACAGTAGACGACACGGCCGTCTACTTTTGTACTAGGGG

AAAAAACTGTGATTACAATTGGGACTTCGAACACTGGGGCCGGGGCACCCCG

GTCATCGTCTCATCAGGAGGGGGAAGCGGAGGGGGAAGCGGAGGGGGAAGC

GGAGGGGGATCCGAAATTGTGTTGACACAGTCTCCAGGCACCCTGTCTTTGTC

TCCAGGGGAAACAGCCATCATCTCTTGTCGGACCAGTCAGTATGGTTCCTTAG

CCTGGTATCAACAGAGGCCCGGCCAGGCCCCCAGGCTCGTCATCTATTCGGG

CTCTACTCGGGCCGCTGGCATCCCAGACAGGTTCAGCGGCAGTCGGTGGGGG

CCAGACTACAATCTCACCATCAGCAACCTGGAGTCGGGAGATTTTGGTGTTTA

TTATTGCCAGCAGTATGAATTTTTTGGCCAGGGGACCAAGGTCCAGGTCGAC

ATTAAAGCCGGCGGCAGCGGAGGAGGATCTGGGGGAGGGTCCGGAGGCGGA

TCCGGGGGCGGTTCAGGTGGGGGTAGCGGAGGGGGCTCAGGCGGAGCTAGC

CAGTCTGCCCTGACTCAGCCTGCCTCCGTGTCTGGGTCTCCTGGACAGACGAT

CACCATCTCCTGCAATGGAACCAGCAGTGACGTTGGTGGATTTGACTCTGTCT

CCTGGTACCAACAATCCCCAGGGAAAGCCCCCAAAGTCATGGTTTTTGATGT

CAGTCATCGGCCCTCAGGTATCTCTAATCGCTTCTCTGGCTCCAAGTCCGGCA

ACACGGCCTCCCTGACCATCTCTGGGCTCCACATTGAGGACGAGGGCGATTA

TTTCTGCTCTTCACTGACAGACAGAAGCCATCGCATATTCGGCGGCGGGACC

AAGGTGACCGTTCTAGGTCAGCCCAAGGCTGCCCCCTCGGTCACTCTGTTCCC

GCCCTCCTCTGAGGAGCTTCAAGCCAACAAGGCCACACTGGTGTGTCTCATA

AGTGACTTCTACCCGGGAGCCGTGACAGTGGCCTGGAAGGCAGATAGCAGCC

CCGTCAAGGCGGGAGTGGAGACCACCACACCCTCCAAACAAAGCAACAACA

AGTACGCGGCCAGCAGCTACCTGAGCCTGACGCCTGAGCAGTGGAAGTCCCA

CAAAAGCTACAGCTGCCAGGTCACGCATGAAGGGAGCACCGTGGAGAAGAC

AGTGGCCCCTACAGAATGTTCATAG

Protein:

MGWSCIILFLVATATGVHSQVQLVQSGGQMKKPGESMRISCRASGYEFIDCTLN

WIRLAPGKRPEWMGWLKPRGGAVNYARPLQGRVTMTRDVYSDTAFLELRSLT

VDDTAVYFCTRGKNCDYNWDFEHWGRGTPVIVSSGGGSGGGSGGGSGGGSEIV

LTQSPGTLSLSPGETAIISCRTSQYGSLAWYQQRPGQAPRLVIYSGSTRAAGIPDRF

SGSRWGPDYNLTISNLESGDFGVYYCQQYEFFGQGTKVQVDIKAGGSGGGSGG

GSGGGSGGGSGGGSGGGSGGASQSALTQPASVSGSPGQTITISCNGTSSDVGGFD

SVSWYQQSPGKAPKVMVFDVSHRPSGISNRFSGSKSGNTASLTISGLHIEDEGDY

FCSSLTDRSHRIFGGGTKVTVLGQPKAAPSVTLFPPSSEELQANKATLVCLISDFY

PGAVTVAWKADSSPVKAGVETTTPSKQSNNKYAASSYLSLTPEQWKSHKSYSC

QVTHEGSTVEKTVAPTECS

9) VRC01$_{scFv}$–ZAG 3–E51 HC:
DNA:

*GAATTCCCTCTAGACCACC*ATGGGATGGTCATGTATCATCCTTTTTCTAGTAGC

AACTGCAACCGGTGTACATTCCCAGGTGCAGCTGGTGCAGTCTGGAGGTCAG

ATGAAGAAGCCTGGCGAGTCGATGAGAATTTCTTGTCGGGCTTCTGGATATG

AATTTATTGATTGTACGCTAAATTGGATTCGTCTGGCCCCCGGAAAAAGGCCT

GAGTGGATGGGATGGCTGAAGCCTCGGGGGGGGGCCGTCAACTACGCACGTC

CACTTCAGGGCAGAGTGACCATGACTCGAGACGTTTATTCCGACACAGCCTTT

TTGGAGCTGCGCTCGTTGACAGTAGACGACACGGCCGTCTACTTTTGTACTAG

GGGAAAAAACTGTGATTACAATTGGGACTTCGAACACTGGGGCCGGGGCACC

CCGGTCATCGTCTCATCAGGAGGGGGAAGCGGAGGGGGAAGCGGAGGGGGA

AGCGGAGGGGGATCCGAAATTGTGTTGACACAGTCTCCAGGCACCCTGTCTT

TGTCTCCAGGGGAAACAGCCATCATCTCTTGTCGGACCAGTCAGTATGGTTCC

TTAGCCTGGTATCAACAGAGGCCCGGCCAGGCCCCCAGGCTCGTCATCTATT

CGGGCTCTACTCGGGCCGCTGGCATCCCAGACAGGTTCAGCGGCAGTCGGTG

GGGGCCAGACTACAATCTCACCATCAGCAACCTGGAGTCGGGAGATTTTGGT

GTTTATTATTGCCAGCAGTATGAATTTTTTGGCCAGGGGACCAAGGTCCAGGT

CGACATTAAATCCGGAGGTGGCGGTAGTGGGGGAGGCGACCCGCCAAGCGT

GGTGGTCACATCCCATCAAGCCCCTGGTGAAAAGAAGAAGCTCAAATGTTTG

GCCTACGATTTCTATCCAGGGAAGATCGACGTGCACTGGACTAGAGCCGGAG

AAGTCCAGGAGCCGGAACTCAGGGGTGATGTCCTGCACAACGGCAACGGCA

CTTACCAGTCTTGGGTCGTCGTAGCCGTGCCACCTCAGGACACGGCGCCATA

CTCCTGCCATGTGCAACATTCTTCCCTCGCACAGCCCCTGGTCGTGCCTTGGG

AGGCCTCCGGTGAGCCCAAATCTTGTGACAAAACTCACACATGCCCACCGTG

CCCAGCACCTGAACTCCTGGGGGGACCGTCAGTCTTCCTCTTCCCCCCAAAAC

CCAAGGACACCCTCATGATCTCCCGGACCCCTGAGGTCACATGCGTGGTGGT

GGACGTGAGCCACGAAGACCCTGAGGTCAAGTTCAACTGGTACGTGGACGGC

GTGGAGGTGCATAATGCCAAGACAAAGCCGCGGGAGGAGCAGTACAACAGC

ACGTACCGTGTGGTCAGCGTCCTCACCGTCCTGCACCAGGACTGGCTGAATG

GCAAGGAGTACAAGTGCAAGGTCTCCAACAAAGCCCTCCCAGCCCCCATCGA

GAAAACCATCTCCAAAGCCAAAGGGCAGCCCCGAGAACCACAGGTGTACAC

CCTGCCCCCATCCCGGGATGAGCTGACCAAGAACCAGGTCAGCCTGACCTGC

CTGGTCAAAGGCTTCTATCCCAGCGACATCGCCGTGGAGTGGGAGAGCAATG

GGCAGCCGGAGAACAACTACAAGACCACGCCTCCCGTGCTGGACTCCGACGG

CTCCTTCTTCCTCTACAGCAAGCTCACCGTGGACAAGAGCAGGTGGCAGCAG

GGGAACGTCTTCTCATGCTCCGTGATGCATGAGGCTCTGCACAACCACTACA

CGCAGAAGAGCCTCTCCCTGTCTCCGGGTAAATGA*TGAGGATCC*

Protein:

MGWSCIILFLVATATGVHS

QVQLVQSGGQMKKPGESMRISCRASGYEFIDCTLNWIRLAPGKRPEWMGWLKP

RGGAVNYARPLQGRVTMTRDVYSDTAFLELRSLTVDDTAVYFCTRGKNCDYN

WDFEHWGRGTPVIVSSGGGSGGGSGGGSGGGSEIVLTQSPGTLSLSPGETAIISCR

TSQYGSLAWYQQRPGQAPRLVIYSGSTRAAGIPDRFSGSRWGPDYNLTISNLESG

DFGVYYCQQYEFFGQGTKVQVDIKSGGGGSGGGDPPSVVVTSHQAPGEKKKLK

CLAYDFYPGKIDVHWTRAGEVQEPELRGDVLHNGNGTYQSWVVVAVPPQDTAP

YSCHVQHSSLAQPLVVPWEASGEPKSCDKTHTCPPCPAPELLGGPSVFLFPPKPK

DTLMISRTPEVTCVVVDVSHEDPEVKFNWYVDGVEVHNAKTKPREEQYNSTYR

VVSVLTVLHQDWLNGKEYKCKVSNKALPAPIEKTISKAKGQPREPQVYTLPPSR

DELTKNQVSLTCLVKGFYPSDIAVEWESNGQPENNYKTTPPVLDSDGSFFLYSKL

TVDKSRWQQGNVFSCSVMHEALHNHYTQKSLSLSPGK

10) VRC01 Fab HC (Fd)- His_7 tagged
DNA:

ATGGGATGGTCATGTATCATCCTTTTTCTAGTAGCAACTGCAACCGGTGTACA

TTCCCAGGTGCAGCTGGTGCAGTCTGGAGGTCAGATGAAGAAGCCTGGCGAG

TCGATGAGAATTTCTTGTCGGGCTTCTGGATATGAATTTATTGATTGTACGCT

AAATTGGATTCGTCTGGCCCCCGGAAAAAGGCCTGAGTGGATGGGATGGCTG

AAGCCTCGGGGGGGGGCCGTCAACTACGCACGTCCACTTCAGGGCAGAGTGA

CCATGACTCGAGACGTTTATTCCGACACAGCCTTTTTGGAGCTGCGCTCGTTG

ACAGTAGACGACACGGCCGTCTACTTTTGTACTAGGGGAAAAAACTGTGATT

ACAATTGGGACTTCGAACACTGGGGCCGGGGCACCCCGGTCATCGTCTCATC

ACCGTCGACCAAGGGCCCATCGGTCTTCCCCCTGGCACCCTCCTCCAAGAGC

ACCTCTGGGGGCACAGCGGCCCTGGGCTGCCTGGTCAAGGACTACTTCCCCG

AACCGGTGACGGTGTCGTGGAACTCAGGCGCCCTGACCAGCGGCGTGCACAC

CTTCCCGGCTGTCCTACAGTCCTCAGGACTCTACTCCCTCAGCAGCGTGGTGA

CCGTGCCCTCCAGCAGCTTGGGCACCCAGACCTACATCTGCAACGTGAATCA

CAAGCCCAGCAACACCAAGGTGGACAAGAAAGTTGAGCCCAAATCTTGTGA

CAAACATCATCACCATCACCACCAT

Protein:

MGWSCIILFLVATATGVHSQVQLVQSGGQMKKPGESMRISCRASGYEFIDCTLN

WIRLAPGKRPEWMGWLKPRGGAVNYARPLQGRVTMTRDVYSDTAFLELRSLT

VDDTAVYFCTRGKNCDYNWDFEHWGRGTPVIVSSPSTKGPSVFPLAPSSKSTSG

GTAALGCLVKDYFPEPVTVSWNSGALTSGVHTFPAVLQSSGLYSLSSVVTVPSSS

LGTQTYICNVNHKPSNTKVDKKVEPKSCDKHHHHHHH

11) PG9 Fab HC (Fd)- His_7 tagged

DNA:

ATGGAGTTTGGGCTGAGCTGGGTTTTCCTCGTTGCTTTCTTAAGAGGTGTCCA

GTGTCAGCGATTAGTGGAGTCTGGGGGAGGCGTGGTCCAGCCTGGGTCGTCC

CTGAGACTCTCCTGTGCAGCGTCCGGATTCGACTTCAGTAGACAAGGCATGC

ACTGGGTCCGCCAGGCTCCAGGCCAGGGGCTGGAGTGGGTGGCATTTATTAA

ATATGATGGAAGTGAGAAATATCATGCTGACTCCGTATGGGGCCGACTCAGC

ATCTCCAGAGACAATTCCAAGGATACGCTTTATCTCCAAATGAATAGCCTGA

GAGTCGAGGACACGGCTACATATTTTTGTGTGAGAGAGGCTGGTGGGCCCGA

CTACCGTAATGGGTACAACTATTACGATTTCTATGATGGTTATTATAACTACC

ACTATATGGACGTCTGGGGCAAAGGGACCACCGTGACAGTCTCGAGCGCCTC

CACCAAGGGCCCATCGGTCTTCCCCCTGGCACCCTCCTCCAAGAGCACCTCTG

GGGGCACAGCGGCCCTGGGCTGCCTGGTCAAGGACTACTTCCCCGAACCGGT

GACGGTGTCGTGGAACTCAGGCGCCCTGACCAGCGGCGTGCACACCTTCCCG

GCTGTCCTACAGTCCTCAGGACTCTACTCCCTCAGCAGCGTGGTGACCGTGCC

CTCCAGCAGCTTGGGCACCCAGACCTACATCTGCAACGTGAATCACAAGCCC

AGCAACACCAAGGTGGACAAGAGAGTTGAGCCCAAATCTTGTGACAAACATC

ATCACCATCACCACCAT

Protein:

MEFGLSWVFLVAFLRGVQCQRLVESGGGVVQPGSSLRLSCAASGFDFSRQGMH

WVRQAPGQGLEWVAFIKYDGSEKYHADSVWGRLSISRDNSKDTLYLQMNSLRV

EDTATYFCVREAGGPDYRNGYNYYDFYDGYYNYHYMDVWGKGTTVTVSSAS

KGPSVFPLAPSSKSTSGGTAALGCLVKDYFPEPVTVSWNSGALTSGVHTFPAVLQ

SSGLYSLSSVVTVPSSSLGTQTYICNVNHKPSNTKVDKRVEPKSCDKHHHHHHH

12) PG16 Fab HC (Fd)- His_7 tagged

DNA:

ATGGAGTTTGGGCTGAGCTGGGTTTTCCTCGCAACTCTGTTAAGAGTTGTGAA
GTGTCAGGAACAACTGGTGGAGTCTGGGGGAGGCGTGGTCCAGCCGGGGGG
GTCCCTGAGACTCTCCTGTTTAGCGTCTGGATTCACGTTTCACAAATATGGCA
TGCACTGGGTCCGCCAGGCTCCAGGCAAGGGCCTGGAGTGGGTGGCACTCAT
CTCAGATGACGGAATGAGGAAATATCATTCAGACTCCATGTGGGGCCGAGTC
ACCATCTCCAGAGACAATTCCAAGAACACTCTTTATCTGCAATTCAGCAGCCT
GAAAGTCGAAGACACGGCTATGTTCTTCTGTGCGAGAGAGGCTGGTGGGCCA
ATCTGGCATGACGACGTCAAATATTACGATTTTAATGACGGCTACTACAACTA
CCACTACATGGACGTCTGGGGCAAGGGGACCACGGTCACCGTCTCGAGCGCC
TCCACCAAGGGCCCATCGGTCTTCCCCCTGGCACCCTCCTCCAAGAGCACCTC
TGGGGGCACAGCGGCCCTGGGCTGCCTGGTCAAGGACTACTTCCCCGAACCG
GTGACGGTGTCGTGGAACTCAGGCGCCCTGACCAGCGGCGTGCACACCTTCC
CGGCTGTCCTACAGTCCTCAGGACTCTACTCCCTCAGCAGCGTGGTGACCGTG
CCCTCCAGCAGCTTGGGCACCCAGACCTACATCTGCAACGTGAATCACAAGC
CCAGCAACACCAAGGTGGACAAGAGAGTTGAGCCCAAATCTTGTGACAAAC
ATCATCACCATCACCACCAT

Protein:

MEFGLSWVFLATLLRVVKCQEQLVESGGGVVQPGGSLRLSCLASGFTFHKYGM
HWVRQAPGKGLEWVALISDDGMRKYHSDSMWGRVTISRDNSKNTLYLQFSSLK
VEDTAMFFCAREAGGPIWHDDVKYYDFNDGYYNYHYMDVWGKGTTVTVSSA

STKGPSVFPLAPSSKSTSGGTAALGCLVKDYFPEPVTVSWNSGALTSGVHTFPAV

LQSSGLYSLSSVVTVPSSSLGTQTYICNVNHKPSNTKVDKRVEPKSCDKHHHHH

HH

13) VRC01$_{scFv}$–PG16 HC:

DNA:

*GAATTCGCCGCCACC*ATGGGATGGTCATGTATCATCCTTTTTCTAGTAGCAACT

GCAACCGGTGTACATTCCCAGGTGCAGCTGGTGCAGTCTGGAGGTCAGATGA

AGAAGCCTGGCGAGTCGATGAGAATTTCTTGTCGGGCTTCTGGATATGAATTT

ATTGATTGTACGCTAAATTGGATTCGTCTGGCCCCCGGAAAAAGGCCTGAGT

GGATGGGATGGCTGAAGCCTCGGGGGGGGGCCGTCAACTACGCACGTCCACT

TCAGGGCAGAGTGACCATGACTCGAGACGTTTATTCCGACACAGCCTTTTTGG

AGCTGCGCTCGTTGACAGTAGACGACACGGCCGTCTACTTTTGTACTAGGGG

AAAAAACTGTGATTACAATTGGGACTTCGAACACTGGGGCCGGGGCACCCCG

GTCATCGTCTCATCAGGAGGGGGAAGCGGAGGGGGAAGCGGAGGGGGAAGC

GGAGGGGGATCCGAAATTGTGTTGACACAGTCTCCAGGCACCCTGTCTTTGTC

TCCAGGGGAAACAGCCATCATCTCTTGTCGGACCAGTCAGTATGGTTCCTTAG

CCTGGTATCAACAGAGGCCCGGCCAGGCCCCCAGGCTCGTCATCTATTCGGG

CTCTACTCGGGCCGCTGGCATCCCAGACAGGTTCAGCGGCAGTCGGTGGGGG

CCAGACTACAATCTCACCATCAGCAACCTGGAGTCGGGAGATTTTGGTGTTTA

TTATTGCCAGCAGTATGAATTTTTTGGCCAGGGGACCAAGGTCCAGGTCGAC

ATTAAAGCCGGCGGCAGCGGAGGAGGATCTGGGGGAGGGTCCGGAGGCGGA

TCCGGGGGCGGTTCAGGTGGGGGTAGCGGAGGGGGCTCAGGCGGAGCTAGC

CAGGAACAACTGGTGGAGTCTGGGGGAGGCGTGGTCCAGCCGGGGGGGTCC

CTGAGACTCTCCTGTTTAGCGTCTGGATTCACGTTTCACAAATATGGCATGCA

CTGGGTCCGCCAGGCTCCAGGCAAGGGCCTGGAGTGGGTGGCACTCATCTCA

GATGACGGAATGAGGAAATATCATTCAGACTCCATGTGGGGCCGAGTCACCA

TCTCCAGAGACAATTCCAAGAACACTCTTTATCTGCAATTCAGCAGCCTGAAA

GTCGAAGACACGGCTATGTTCTTCTGTGCGAGAGAGGCTGGTGGGCCAATCT

GGCATGACGACGTCAAATATTACGATTTTAATGACGGCTACTACAACTACCA

CTACATGGACGTCTGGGGCAAGGGGACCACGGTCACCGTCTCGAGCGCCTCC

ACCAAGGGCCCATCGGTCTTCCCCCTGGCACCCTCCTCCAAGAGCACCTCTGG

GGGCACAGCGGCCCTGGGCTGCCTGGTCAAGGACTACTTCCCCGAACCGGTG

ACGGTGTCGTGGAACTCAGGCGCCCTGACCAGCGGCGTGCACACCTTCCCGG

CTGTCCTACAGTCCTCAGGACTCTACTCCCTCAGCAGCGTGGTGACCGTGCCC

TCCAGCAGCTTGGGCACCCAGACCTACATCTGCAACGTGAATCACAAGCCCA

GCAACACCAAGGTGGACAAGAGAGTTGAGCCCAAATCTTGTGACAAAACTCA

CACATGCCCACCGTGCCCAGCACCTGAACTCCTGGGGGGACCGTCAGTCTTC

CTCTTCCCCCCAAAACCCAAGGACACCCTCATGATCTCCCGGACCCCTGAGGT

CACATGCGTGGTGGTGGACGTGAGCCACGAAGACCCTGAGGTCAAGTTCAAC

TGGTACGTGGACGGCGTGGAGGTGCATAATGCCAAGACAAAGCCGCGGGAG

GAGCAGTACAACAGCACGTACCGTGTGGTCAGCGTCCTCACCGTCCTGCACC

AGGACTGGCTGAATGGCAAGGAGTACAAGTGCAAGGTCTCCAACAAAGCCCT

CCCAGCCCCCATCGAGAAAACCATCTCCAAAGCCAAAGGGCAGCCCCGAGA

ACCACAGGTGTACACCCTGCCCCCATCCCGGGAGGAGATGACCAAGAACCAG

GTCAGCCTGACCTGCCTGGTCAAAGGCTTCTATCCCAGCGACATCGCCGTGG

AGTGGGAGAGCAATGGGCAGCCGGAGAACAACTACAAGACCACGCCTCCCG

TGCTGGACTCCGACGGCTCCTTCTTCCTCTATAGCAAGCTCACCGTGGACAAG

AGCAGGTGGCAGCAGGGGAACGTCTTCTCATGCTCCGTGATGCATGAGGCTC

TGCACAACCACTACACGCAGAAGAGCCTCTCCCTGTCTCCGGGTAAATGA*GC*

GGCCGC

Protein:

MGWSCIILFLVATATGVHSQVQLVQSGGQMKKPGESMRISCRASGYEFIDCTLN

WIRLAPGKRPEWMGWLKPRGGAVNYARPLQGRVTMTRDVYSDTAFLELRSLT

VDDTAVYFCTRGKNCDYNWDFEHWGRGTPVIVSSGGGSGGGSGGGSGGGSEIV

LTQSPGTLSLSPGETAIISCRTSQYGSLAWYQQRPGQAPRLVIYSGSTRAAGIPDRF

SGSRWGPDYNLTISNLESGDFGVYYCQQYEFFGQGTKVQVDIKAGGSGGGSGG

GSGGGSGGGSGGGSGGGSGGASQEQLVESGGGVVQPGGSLRLSCLASGFTFHKY

GMHWVRQAPGKGLEWVALISDDGMRKYHSDSMWGRVTISRDNSKNTLYLQFS

SLKVEDTAMFFCAREAGGPIWHDDVKYYDFNDGYYNYHYMDVWGKGTTVTV

SSASTKGPSVFPLAPSSKSTSGGTAALGCLVKDYFPEPVTVSWNSGALTSGVHTF

PAVLQSSGLYSLSSVVTVPSSSLGTQTYICNVNHKPSNTKVDKRVEPKSCDKTHT

CPPCPAPELLGGPSVFLFPPKPKDTLMISRTPEVTCVVVDVSHEDPEVKFNWYVD

GVEVHNAKTKPREEQYNSTYRVVSVLTVLHQDWLNGKEYKCKVSNKALPAPIE

KTISKAKGQPREPQVYTLPPSREEMTKNQVSLTCLVKGFYPSDIAVEWESNGQPE

NNYKTTPPVLDSDGSFFLYSKLTVDKSRWQQGNVFSCSVMHEALHNHYTQKSL

SLSPGK

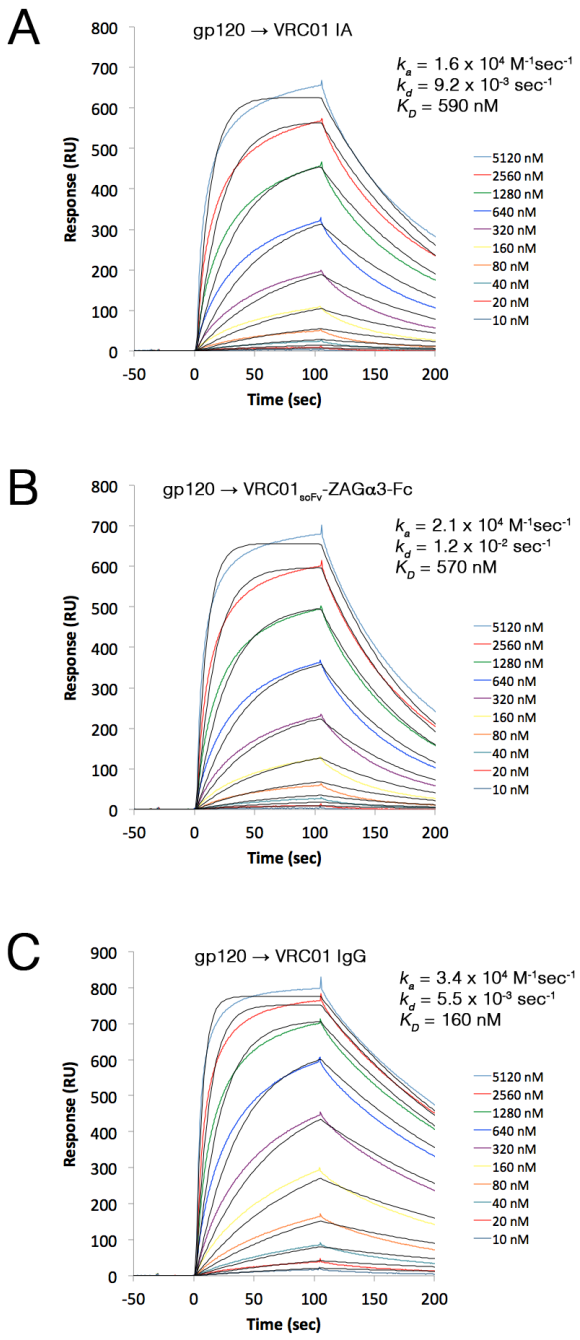

Supplemental Figure S2. Biosensor analyses of gp120 binding to immobilized VRC01 reagents. Sensorgrams (colored curves) of injected gp120 binding to VRC01 IA (**A**), VRC01$_{scFv}$-ZAG 3-Fc (**B**), and VRC01 IgG (**C**) immobilized using covalently attached protein A. Best fit binding curves (assuming a 1:1 binding model) are shown as thin black lines.

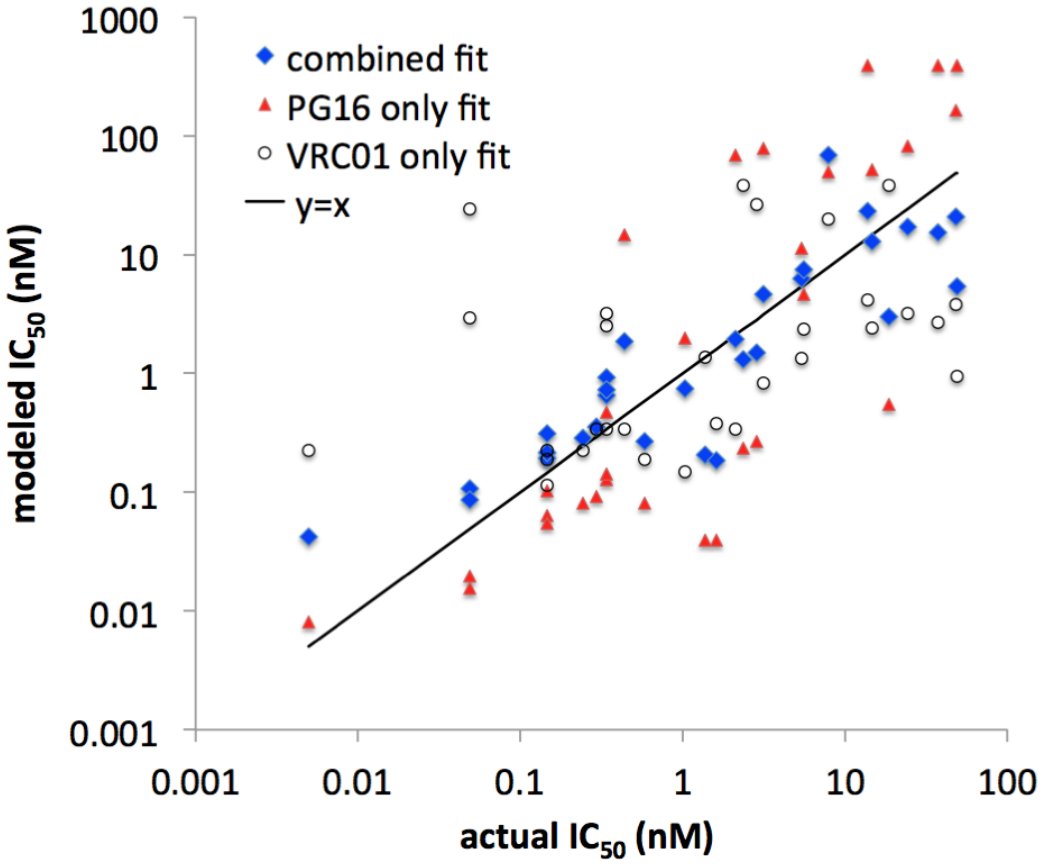

Supplemental Figure S3. Measured versus modeled IC_{50} values of $VRC01_{scFv}$–PG16. One parameter (PG16 or VRC01) or two parameter (combined fit; PG16 and VRC01) best fits based on IC_{50}s for PG16 IgG and VRC01 IgG. A 1:1 correlation between the modeled IC_{50} and the actual IC_{50} data is indicated by the y = x line. The parameters derived from the combined fit indicate that $VRC01_{scFv}$–PG16 has ~1/3 of the activity of PG16 IgG plus ~1/3 the activity of VRC01 IgG. The values of the correlation coefficient *R* for the combined, PG16 only, and VRC01 only fits are 0.877, 0.825, and 0.414, respectively. A reduced vs. full model *F*-test comparing the PG16 only fit with the 2-parameter fit demonstrates that the 2-parameter model is superior (*F*-test analysis significance $P<0.01$).

References:

1. Arndt KM, Muller KM, Pluckthun A. 1998. Factors influencing the dimer to monomer transition of an antibody single-chain Fv fragment. Biochemistry 37:12918–12926

2. Baba TW, et al. 2000. Human neutralizing monoclonal antibodies of the IgG1 subtype protect against mucosal simian-human immunodeficiency virus infection. Nat. Med. 6:200–206

3. Bennett MJ, Eisenberg D. 2004. The evolving role of 3D domain swapping in proteins. Structure12:1339–1341

4. Bird RE, Walker BW. 1991. Single chain antibody variable regions. Trends Biotechnol. 9:132–137

5. Corti D, et al. 2010. Analysis of memory B cell responses and isolation of novel monoclonal antibodies with neutralizing breadth from HIV-1-infected individuals. PLoS One 5:e8805.

6. Diskin R, Marcovecchio PM, Bjorkman PJ. 2010. Structure of a clade C HIV plus CD4 and CD4-induced antibody reveals anti-CD4 polyreactivity. Nat. Struct. Mol. Biol. 17:608–613

7. Dong JY, Fan PD, Frizzell RA. 1996. Quantitative analysis of the packaging capacity of recombinant adeno-associated virus. Hum. Gene Ther. 7:2101–2112

8. Durocher Y, Perret S, Kamen A. 2002. High-level and high-throughput recombinant protein production by transient transfection of suspension-growing human 293-EBNA1 cells. Nucleic Acids Res. 30:E9.

9. Fang J, et al. 2005. Stable antibody expression at therapeutic levels using the 2A peptide. Nat. Biotechnol. 23:584–590

10. Grimm D, Kay MA. 2003. From virus evolution to vector revolution: use of naturally occurring serotypes of adeno-associated virus (AAV) as novel vectors for human gene therapy. Curr. Gene Ther.3:281–304

11. Hessell AJ, et al. 2007. Fc receptor but not complement binding is important in antibody protection against HIV. Nature 449:101–104

12. Hessell AJ, et al. 2009. Effective, low-titer antibody protection against low-dose repeated mucosal SHIV challenge in macaques. Nat. Med. 15:951–954

13. Hessell AJ, et al. 2009. Broadly neutralizing human anti-HIV antibody 2G12 is effective in protection against mucosal SHIV challenge even at low serum neutralizing titers. PLoS Pathog.5:e1000433.

14. Huang C. 2009. Receptor-Fc fusion therapeutics, traps, and MIMETIBODY technology. Curr. Opin. Biotechnol. 20:692–699

15. Johnson PR, et al. 2009. Vector-mediated gene transfer engenders long-lived neutralizing activity and protection against SIV infection in monkeys. Nat. Med. 15:901–906

16. Johnson WE, et al. 2003. Assorted mutations in the envelope gene of simian immunodeficiency virus lead to loss of neutralization resistance against antibodies representing a broad spectrum of specificities. J. Virol. 77:9993–10003

17. Keele BF, et al. 2008. Identification and characterization of transmitted and early founder virus envelopes in primary HIV-1 infection. Proc. Natl. Acad. Sci. U. S. A. 105:7552–7557

18. Klein JS, Bjorkman PJ. 2010. Few and far between: how HIV may be evading antibody avidity.PLoS Pathog. 6:e1000908.

19. Labrijn AF, et al. 2003. Access of antibody molecules to the conserved coreceptor binding site on glycoprotein gp120 is sterically restricted on primary human immunodeficiency virus type 1. J. Virol.77:10557–10565

20. Lewis AD, Chen R, Montefiori DC, Johnson PR, Clark KR. 2002. Generation of neutralizing activity against human immunodeficiency virus type 1 in serum by antibody gene transfer. J. Virol.76:8769–8775

21. Li M, et al. 2005. Human immunodeficiency virus type 1 env clones from acute and early subtype B infections for standardized assessments of vaccine-elicited neutralizing antibodies. J. Virol.79:10108–10125

22. Li M, et al. 2006. Genetic and neutralization properties of subtype C human immunodeficiency virus type 1 molecular env clones from acute and early heterosexually acquired infections in Southern Africa. J. Virol. 80:11776–11790

23. Mascola JR, et al. 1999. Protection of macaques against pathogenic simian/human immunodeficiency virus 89.6PD by passive transfer of neutralizing antibodies. J. Virol. 73:4009–4018

24. Mascola JR, et al. 2000. Protection of macaques against vaginal transmission of a pathogenic HIV-1/SIV chimeric virus by passive infusion of neutralizing antibodies. Nat. Med. 6:207–210

25. McCarty DM, et al. 2003. Adeno-associated virus terminal repeat (TR) mutant generates self-complementary vectors to overcome the rate-limiting step to transduction in vivo. Gene Ther.10:2112–2118

26. Mehandru S, et al. 2007. Adjunctive passive immunotherapy in human immunodeficiency virus type 1-infected individuals treated with antiviral therapy during acute and early infection. J. Virol.81:11016–11031

27. Montefiori DC. 2005. Evaluating neutralizing antibodies against HIV, SIV, and SHIV in luciferase reporter gene assays. Curr. Protoc. Immunol. 2005:12.11 doi:10.1002/0471142735.im1211s64

28. Nelson AL. 2010. Antibody fragments: hope and hype. MAbs 2:77–83

29. Nishimura Y, et al. 2003. Transfer of neutralizing IgG to macaques 6 h but not 24 h after SHIV infection confers sterilizing protection: implications for HIV-1 vaccine development. Proc. Natl. Acad. Sci. U. S. A. 100:15131–15136

30. Parren PW, et al. 2001. Antibody protects macaques against vaginal challenge with a pathogenic R5 simian/human immunodeficiency virus at serum levels giving complete neutralization in vitro. J. Virol. 75:8340–8347

31. Poignard P, et al. 1999. Neutralizing antibodies have limited effects on the control of established HIV-1 infection in vivo. Immunity 10:431–438

32. Rerks-Ngarm S, et al. 2009. Vaccination with ALVAC and AIDSVAX to prevent HIV-1 infection in Thailand. N. Engl. J. Med. 361:2209–2220

33. Ritola K, et al. 2004. Multiple V1/V2 env variants are frequently present during primary infection with human immunodeficiency virus type 1. J. Virol. 78:11208–11218

34. Salazar-Gonzalez JF, et al. 2008. Deciphering human immunodeficiency virus type 1 transmission and early envelope diversification by single-genome amplification and sequencing. J. Virol. 82:3952–3970

35. Scheid JF, et al. 2011. Sequence and structural convergence of broad and potent HIV antibodies that mimic CD4 binding. Science 333:1633–1637

36. Shibata R, et al. 1999. Neutralizing antibody directed against the HIV-1 envelope glycoprotein can completely block HIV-1/SIV chimeric virus infections of macaque monkeys. Nat. Med. 5:204–210

37. Szymczak AL, et al. 2004. Correction of multi-gene deficiency in vivo using a single 'self-cleaving' 2A peptide-based retroviral vector. Nat. Biotechnol. 22:589–594

38. Trkola A, et al. 2005. Delay of HIV-1 rebound after cessation of antiretroviral therapy through passive transfer of human neutralizing antibodies. Nat. Med. 11:615–622

39. Virgin HW, Walker BD. 2010. Immunology and the elusive AIDS vaccine. Nature 464:224–231

40. Walker LM, Burton DR. 2010. Rational antibody-based HIV-1 vaccine design: current approaches and future directions. Curr. Opin. Immunol. 22:358–366

41. Walker LM, et al. 2011. Broad neutralization coverage of HIV by multiple highly potent antibodies. Nature 477:466–470

42. Walker LM, et al. 2009. Broad and potent neutralizing antibodies from an African donor reveal a new HIV-1 vaccine target. Science 326:285–289

43. Wei X, et al. 2003. Antibody neutralization and escape by HIV-1. Nature 422:307–312

44. Wu X, et al. 2010. Rational design of envelope identifies broadly neutralizing human monoclonal antibodies to HIV-1. Science 329:856–861

45. Zhou T, et al. 2010. Structural basis for broad and potent neutralization of HIV-1 by antibody VRC01. Science 329:811–817

Bibliography

Alkhatib, G.B., Edward A. (2007). HIV coreceptors: from discovery and designation to new paradigms and promise. European Journal of Medicine *12*, 375-384.

Altfeld, M., and Gale, M., Jr. (2015). Innate immunity against HIV-1 infection. Nat Immunol *16*, 554-562.

Altman, L. (1981). Rare Cancer Seen In 41 Homosexuals. In The New York Times (New York: The New York Times).

Arai, R., Ueda, H., Kitayama, A., Kamiya, N., and Nagamune, T. (2001). Design of the linkers which effectively separate domains of a bifunctional fusion protein. Protein Eng *14*, 529-532.

Argos, P. (1990). An investigation of oligopeptides linking domains in protein tertiary structures and possible candidates for general gene fusion. Journal of molecular biology *211*, 943-958.

ARTCC (2008). Life expectancy of individuals on combination antiretroviral therapy in high-income countries: a collaborative analysis of 14 cohort studies. The Lancet *372*, 293-299.

Atwell, S., Ridgway, J.B., Wells, J.A., and Carter, P. (1997). Stable heterodimers from remodeling the domain interface of a homodimer using a phage display library. J Mol Biol *270*, 26-35.

Baeuerle, P.A., and Reinhardt, C. (2009). Bispecific T-cell engaging antibodies for cancer therapy. Cancer Res *69*, 4941-4944.

Bai, Y., Ann, D.K., and Shen, W.-C. (2005). Recombinant granulocyte colony-stimulating factor-transferrin fusion protein as an oral myelopoietic agent.

Proceedings of the National Academy of Sciences of the United States of America *102*, 7292-7296.

Balazs, A.B., Bloom, J.D., Hong, C.M., Rao, D.S., and Baltimore, D. (2013). Broad protection against influenza infection by vectored immunoprophylaxis in mice. Nat Biotechnol *31*, 647-652.

Balazs, A.B., Chen, J., Hong, C.M., Rao, D.S., Yang, L., and Baltimore, D. (2012). Antibody-based protection against HIV infection by vectored immunoprophylaxis. Nature *481*, 81-84.

Balazs, A.B., Ouyang, Y., Hong, C.M., Chen, J., Nguyen, S.M., Rao, D.S., An, D.S., and Baltimore, D. (2014). Vectored immunoprophylaxis protects humanized mice from mucosal HIV transmission. Nat Med *20*, 296-300.

Balazs, A.B., and West, A.P., Jr. (2013). Antibody gene transfer for HIV immunoprophylaxis. Nat Immunol *14*, 1-5.

Baltimore, D. (1970). RNA-dependent DNA polymerase in virions of RNA tumour viruses. Nature *226*, 1209-1211.

Barbian, H.J., Decker, J.M., Bibollet-Ruche, F., Galimidi, R.P., West, A.P., Jr., Learn, G.H., Parrish, N.F., Iyer, S.S., Li, Y., Pace, C.S.*, et al.* (2015). Neutralization properties of simian immunodeficiency viruses infecting chimpanzees and gorillas. MBio *6*.

Barouch, D.H., Whitney, J.B., Moldt, B., Klein, F., Oliveira, T.Y., Liu, J., Stephenson, K.E., Chang, H.-W., Shekhar, K., Gupta, S.*, et al.* (2013). Therapeutic Efficacy of Potent Neutralizing HIV-1-Specific Monoclonal Antibodies in SHIV-Infected Rhesus Monkeys. Nature *503*, 224-228.

Barrett, D.M., Singh, N., Porter, D.L., Grupp, S.A., and June, C.H. (2014). Chimeric Antigen Receptor Therapy for Cancer. Annual Review of Medicine *65*, 333-347.

Bartesaghi, A., Merk, A., Borgnia, M.J., Milne, J.L., and Subramaniam, S. (2013). Prefusion structure of trimeric HIV-1 envelope glycoprotein determined by cryo-electron microscopy. Nat Struct Mol Biol *20*, 1352-1357.

Bednar, J., Furrer, P., Katritch, V., Stasiak, A.Z., Dubochet, J., and Stasiak, A. (1995). Determination of DNA persistence length by cryo-electron microscopy. Separation of the static and dynamic contributions to the apparent persistence length of DNA. J Mol Biol *254*, 579-594.

Berahovich, R.D., Lai, N.L., Wei, Z., Lanier, L.L., and Schall, T.J. (2006). Evidence for NK Cell Subsets Based on Chemokine Receptor Expression. The Journal of Immunology *177*, 7833-7840.

Bhatia, A.K., Kaushik, R., Campbell, N.A., Pontow, S.E., and Ratner, L. (2009). Mutation of critical serine residues in HIV-1 matrix result in an envelope incorporation defect which can be rescued by truncation of the gp41 cytoplasmic tail. Virology *384*, 233-241.

Blattner, C., Lee, J.H., Sliepen, K., Derking, R., Falkowska, E., de la Pena, A.T., Cupo, A., Julien, J.P., van Gils, M., Lee, P.S.*, et al.* (2014). Structural delineation of a quaternary, cleavage-dependent epitope at the gp41-gp120 interface on intact HIV-1 Env trimers. Immunity *40*, 669-680.

Boffey, P.M. (1986). AIDS IN THE FUTURE: EXPERTS SAY DEATHS WILL CLIMB SHARPLY. In The New York Times (New York: New York Times).

Boggiano, C., and Littman, D.R. (2007). HIV's vagina travelogue. Immunity *26*, 145-147.

Bonner, A., Furtado, P.B., Almogren, A., Kerr, M.A., and Perkins, S.J. (2008). Implications of the near-planar solution structure of human myeloma dimeric IgA1 for mucosal immunity and IgA nephropathy. Journal of immunology *180*, 1008-1018.

Bournazos, S., Klein, F., Pietzsch, J., Seaman, M.S., Nussenzweig, M.C., and Ravetch, J.V. (2014). Broadly neutralizing anti-HIV-1 antibodies require Fc effector functions for in vivo activity. Cell *158*, 1243-1253.

Briggs, J.A., and Krausslich, H.G. (2011). The molecular architecture of HIV. J Mol Biol *410*, 491-500.

Bruno, C.J., and Jacobson, J.M. (2010). Ibalizumab: an anti-CD4 monoclonal antibody for the treatment of HIV-1 infection. The Journal of antimicrobial chemotherapy *65*, 1839-1841.

Buchacher, A., Predl, R., Strutzenberger, K., Steinfellner, W., Trkola, A., Purtscher, M., Gruber, G., Tauer, C., Steindl, F., Jungbauer, A*., et al.* (1994). Generation of human monoclonal antibodies against HIV-1 proteins; electrofusion and Epstein-Barr virus transformation for peripheral blood lymphocyte immortalization. AIDS Res Hum Retroviruses *10*, 359-369.

Büning, H., Uckert, W., Cichutek, K., Hawkins, R.E., and Abken, H. (2010). Do CARs Need a Driver's License? Adoptive Cell Therapy with Chimeric Antigen Receptor-Redirected T Cells Has Caused Serious Adverse Events. Human Gene Therapy *21*, 1039-1042.

Buonaguro, L., Tornesello, M.L., and Buonaguro, F.M. (2007). Human immunodeficiency virus type 1 subtype distribution in the worldwide epidemic: pathogenetic and therapeutic implications. J Virol *81*, 10209-10219.

Burton, D.R., Pyati, J., Koduri, R., Sharp, S.J., Thornton, G.B., Paul, W.H.I.P., Lynette, S.W.S., Hendry, R.M., Dunlop, N., Nara, P.L.*, et al.* (1994). Efficient Neutralization of Primary Isolates of HIV-1 by a Recombinant Human Monoclonal Antibody. Science *266*, 1024-1027.

Burton, D.R., Williamson, R.A., and Parren, P.W. (2000). Antibody and virus: binding and neutralization. Virology *270*, 1-3.

Capon, D.J., and Ward, R.H.R. (1991). The CD4-gpl20 Interaction and Aids Pathogenesis. Annual Review of Immunology *9*, 649-678.

Caskey, M., Klein, F., Lorenzi, J.C.C., Seaman, M.S., West Jr, A.P., Buckley, N., Kremer, G., Nogueira, L., Braunschweig, M., Scheid, J.F.*, et al.* (2015). Viraemia suppressed in HIV-1-infected humans by broadly neutralizing antibody 3BNC117. Nature *522*, 487-491.

CDC, C.f.D.C.a.P. (2012). Estimated HIV incidence among adults and adolescents in the United States, 2007-2010. In HIV Surveillance Supplemental Report (Atlanta, GA: Centers for Disease Control).

Chan, D.C., Fass, D., Berger, J.M., and Kim, P.S. (1997). Core structure of gp41 from the HIV envelope glycoprotein. Cell *89*, 263-273.

Chan, D.C., and Kim, P.S. (1998). HIV entry and its inhibition. Cell *93*, 681-684.

Chang, C.H., Short, M.T., Westholm, F.A., Stevens, F.J., Wang, B.C., Furey, W., Jr., Solomon, A., and Schiffer, M. (1985). Novel arrangement of immunoglobulin

variable domains: X-ray crystallographic analysis of the lambda-chain dimer Bence-Jones protein Loc. Biochemistry *24*, 4890-4897.

Chen, X., Zaro, J.L., and Shen, W.C. (2013). Fusion protein linkers: property, design and functionality. Advanced drug delivery reviews *65*, 1357-1369.

Chertova, E., Bess Jr, J.W., Jr., Crise, B.J., Sowder, I.R., Schaden, T.M., Hilburn, J.M., Hoxie, J.A., Benveniste, R.E., Lifson, J.D., Henderson, L.E*., et al.* (2002a). Envelope glycoprotein incorporation, not shedding of surface envelope glycoprotein (gp120/SU), Is the primary determinant of SU content of purified human immunodeficiency virus type 1 and simian immunodeficiency virus. J Virol *76*, 5315-5325.

Chertova, E., Bess, J.W., Jr., Crise, B.J., Sowder, I.R., Schaden, T.M., Hilburn, J.M., Hoxie, J.A., Benveniste, R.E., Lifson, J.D., Henderson, L.E*., et al.* (2002b). Envelope glycoprotein incorporation, not shedding of surface envelope glycoprotein (gp120/SU), Is the primary determinant of SU content of purified human immunodeficiency virus type 1 and simian immunodeficiency virus. J Virol *76*, 5315-5325.

Chi, Q., Wang, G., and Jiang, J. (2013). The persistence length and length per base of single-stranded DNA obtained from fluorescence correlation spectroscopy measurements using mean field theory. Physica A: Statistical Mechanics and its Applications *392*, 1072-1079.

Chiang, J.J., Gardner, M.R., Quinlan, B.D., Dorfman, T., Choe, H., and Farzan, M. (2012). Enhanced Recognition and Neutralization of HIV-1 by Antibody-Derived CCR5-Mimetic Peptide Variants. Journal of Virology *86*, 12417-12421.

Chojnacki, J., Staudt, T., Glass, B., Bingen, P., Engelhardt, J., Anders, M., Schneider, J., Muller, B., Hell, S.W., and Krausslich, H.G. (2012). Maturation-dependent HIV-1 surface protein redistribution revealed by fluorescence nanoscopy. Science *338*, 524-528.

Churchill, M.J., Deeks, S.G., Margolis, D.M., Siliciano, R.F., and Swanstrom, R. (2016). HIV reservoirs: what, where and how to target them. Nat Rev Microbiol *14*, 55-60.

Coffin, J., and Swanstrom, R. (2013). HIV pathogenesis: dynamics and genetics of viral populations and infected cells. Cold Spring Harb Perspect Med *3*, a012526.

Colman, P.M., Epp, O., Fehlhammer, H., Bode, W., Schiffer, M., Lattman, E.E., Jones, T.A., and Palm, W. (1974). X-ray studies on antibody fragments. FEBS Lett *44*, 194-199.

Cook, L.B., Melamed, A., Niederer, H., Valganon, M., Laydon, D., Foroni, L., Taylor, G.P., Matsuoka, M., and Bangham, C.R. (2014). The role of HTLV-1 clonality, proviral structure, and genomic integration site in adult T-cell leukemia/lymphoma. Blood *123*, 3925-3931.

Corti, D., and Lanzavecchia, A. (2013). Broadly neutralizing antiviral antibodies. Annu Rev Immunol *31*, 705-742.

Crooks, E.T., Jiang, P., Franti, M., Wong, S., Zwick, M.B., Hoxie, J.A., Robinson, J.E., Moore, P.L., and Binley, J.M. (2008). Relationship of HIV-1 and SIV envelope glycoprotein trimer occupation and neutralization. Virology *377*, 364-378.

Crotty, S. (2011). Follicular helper CD4 T cells (TFH). Annu Rev Immunol *29*, 621-663.

D'Andrea, L.D., and Regan, L. (2003). TPR proteins: the versatile helix. Trends in biochemical sciences *28*, 655-662.

Dahabieh, M.S., Battivelli, E., and Verdin, E. (2015). Understanding HIV latency: the road to an HIV cure. Annu Rev Med *66*, 407-421.

Deeks, S.G., Wagner, B., Anton, P.A., Mitsuyasu, R.T., Scadden, D.T., Huang, C., Macken, C., Richman, D.D., Christopherson, C., June, C.H.*, et al.* (2002). A phase II randomized study of HIV-specific T-cell gene therapy in subjects with undetectable plasma viremia on combination antiretroviral therapy. Mol Ther *5*, 788-797.

Dev, S., and Surolia, A. (2006). Dynamic light scattering study of peanut agglutinin: size, shape and urea denaturation. Journal of biosciences *31*, 551-556.

Diskin, R., Klein, F., Horwitz, J.A., Halper-Stromberg, A., Sather, D.N., Marcovecchio, P.M., Lee, T., West, A.P., Gao, H., Seaman, M.S.*, et al.* (2013a). Restricting HIV-1 pathways for escape using rationally designed anti–HIV-1 antibodies. The Journal of Experimental Medicine *210*, 1235-1249.

Diskin, R., Klein, F., Horwitz, J.A., Halper-Stromberg, A., Sather, D.N., Marcovecchio, P.M., Lee, T., West, A.P., Jr., Gao, H., Seaman, M.S.*, et al.* (2013b). Restricting HIV-1 pathways for escape using rationally designed anti-HIV-1 antibodies. J Exp Med *210*, 1235-1249.

Diskin, R., Marcovecchio, P.M., and Bjorkman, P.J. (2010). Structure of a clade C HIV-1 gp120 bound to CD4 and CD4-induced antibody reveals anti-CD4 polyreactivity. Nat Struct Mol Biol *17*, 608-613.

Diskin, R., Scheid, J.F., Marcovecchio, P.M., West, A.P., Jr., Klein, F., Gao, H., Gnanapragasam, P.N., Abadir, A., Seaman, M.S., Nussenzweig, M.C.*, et al.* (2011a). Increasing the potency and breadth of an HIV antibody by using structure-based rational design. Science *334*, 1289-1293.

Diskin, R., Scheid, J.F., Marcovecchio, P.M., West, A.P., Klein, F., Gao, H., Gnanapragasam, P.N.P., Abadir, A., Seaman, M.S., Nussenzweig, M.C.*, et al.* (2011b). Increasing the Potency and Breadth of an HIV Antibody by using Structure-Based Rational Design. Science (New York, NY) *334*, 1289-1293.

Do Kwon, Y., Pancera, M., Acharya, P., Georgiev, I.S., Crooks, E.T., Gorman, J., Joyce, M.G., Guttman, M., Ma, X., Narpala, S.*, et al.* (2015). Crystal structure, conformational fixation and entry-related interactions of mature ligand-free HIV-1 Env. Nat Struct Mol Biol *22*, 522-531.

Doria-Rose, N.A., Klein, R.M., Manion, M.M., O'Dell, S., Phogat, A., Chakrabarti, B., Hallahan, C.W., Migueles, S.A., Wrammert, J., Ahmed, R.*, et al.* (2009). Frequency and Phenotype of Human Immunodeficiency Virus Envelope-Specific B Cells from Patients with Broadly Cross-Neutralizing Antibodies. Journal of Virology *83*, 188-199.

Dörner, T., and Radbruch, A. (2007). Antibodies and B Cell Memory in Viral Immunity. Immunity *27*, 384-392.

Dybul, M., Fauci, A.S., Bartlett, J.G., Kaplan, J.E., and Pau, A.K. (2002). Guidelines for Using Antiretroviral Agents among HIV-Infected Adults and Adolescents: The Panel on Clinical Practices for Treatment of HIV*. Annals of Internal Medicine *137*, 381-433.

Edelman, G.M. (1973). Antibody structure and molecular immunology. Science *180*, 830-840.

Eisen, H.N., and Siskind, G.W. (1964). Variations in Affinities of Antibodies during the Immune Response*. Biochemistry *3*, 996-1008.

Euler, Z., van Gils, M.J., Bunnik, E.M., Phung, P., Schweighardt, B., Wrin, T., and Schuitemaker, H. (2010). Cross-Reactive Neutralizing Humoral Immunity Does Not Protect from HIV Type 1 Disease Progression. Journal of Infectious Diseases *201*, 1045-1053.

Evers, T.H., van Dongen, E.M., Faesen, A.C., Meijer, E.W., and Merkx, M. (2006). Quantitative understanding of the energy transfer between fluorescent proteins connected via flexible peptide linkers. Biochemistry *45*, 13183-13192.

Feinberg, M.B., Baltimore, D., and Frankel, A.D. (1991). The role of Tat in the human immunodeficiency virus life cycle indicates a primary effect on transcriptional elongation. Proc Natl Acad Sci U S A *88*, 4045-4049.

Felber, B.K., Drysdale, C.M., and Pavlakis, G.N. (1990). Feedback regulation of human immunodeficiency virus type 1 expression by the Rev protein. J Virol *64*, 3734-3741.

Ferrantelli, F., Rasmussen, R.A., Buckley, K.A., Li, P.L., Wang, T., Montefiori, D.C., Katinger, H., Stiegler, G., Anderson, D.C., McClure, H.M.*, et al.* (2004). Complete protection of neonatal rhesus macaques against oral exposure to pathogenic simian-human immunodeficiency virus by human anti-HIV monoclonal antibodies. J Infect Dis *189*, 2167-2173.

Fischl, M.A., Richman, D.D., Grieco, M.H., Gottlieb, M.S., Volberding, P.A., Laskin, O.L., Leedom, J.M., Groopman, J.E., Mildvan, D., Schooley, R.T.*, et al.* (1987). The efficacy of azidothymidine (AZT) in the treatment of patients with AIDS and AIDS-related complex. A double-blind, placebo-controlled trial. N Engl J Med *317*, 185-191.

Flint, S.J., Enquist, L.W., Racaniello, V.R., and Skalka, A.M. (2008). Principles of Virology (ASM Press).

Freed, E.O., and Mouland, A.J. (2006). The cell biology of HIV-1 and other retroviruses. Retrovirology *3*, 77.

Gallo, R., and Montagnier, L. (2003). PERSPECTIVE: The Discovery of HIV as the Cause of AIDS. The New England Journal of Medicine *349*, 2283-2285.

Gallo, R.C. (2005). The discovery of the first human retrovirus: HTLV-1 and HTLV-2. Retrovirology *2*, 17.

Ganser-Pornillos, B., Yeager, M., and Sundquist, W.I. (2008). The Structural Biology of HIV Assembly. Current opinion in structural biology *18*, 203.

Garces, F., Lee, Jeong H., de Val, N., Torrents de la Pena, A., Kong, L., Puchades, C., Hua, Y., Stanfield, Robyn L., Burton, Dennis R., Moore, John P.*, et al.* (2015). Affinity Maturation of a Potent Family of HIV Antibodies Is Primarily Focused on Accommodating or Avoiding Glycans. Immunity *43*, 1053-1063.

Garces, F., Sok, D., Kong, L., McBride, R., Kim, Helen J., Saye-Francisco, Karen F., Julien, J.-P., Hua, Y., Cupo, A., Moore, John P.*, et al.* (2014). Structural Evolution of Glycan Recognition by a Family of Potent HIV Antibodies. Cell *159*, 69-79.

Gardner, M.R., Kattenhorn, L.M., Kondur, H.R., von Schaewen, M., Dorfman, T., Chiang, J.J., Haworth, K.G., Decker, J.M., Alpert, M.D., Bailey, C.C*., et al.* (2015). AAV-expressed eCD4-Ig provides durable protection from multiple SHIV challenges. Nature *519*, 87-91.

Geijtenbeek, T.B., Kwon, D.S., Torensma, R., van Vliet, S.J., van Duijnhoven, G.C., Middel, J., Cornelissen, I.L., Nottet, H.S., KewalRamani, V.N., Littman, D.R*., et al.* (2000). DC-SIGN, a dendritic cell-specific HIV-1-binding protein that enhances trans-infection of T cells. Cell *100*, 587-597.

George, R.A., and Heringa, J. (2002). An analysis of protein domain linkers: their classification and role in protein folding. Protein Eng *15*, 871-879.

Go, E.P., Liao, H.X., Alam, S.M., Hua, D., Haynes, B.F., and Desaire, H. (2013). Characterization of host-cell line specific glycosylation profiles of early transmitted/founder HIV-1 gp120 envelope proteins. J Proteome Res *12*, 1223-1234.

Goodall, J. (1983). Population Dynamics during a 15 Year Period in one Community of Free-living Chimpanzees in the Gombe National Park, Tanzania. Zeitschrift für Tierpsychologie *61*, 1-60.

Gottlieb, M.S., Schroff, R., Schanker, H.M., Weisman, J.D., Fan, P.T., Wolf, R.A., and Saxon, A. (1981). Pneumocystis carinii pneumonia and mucosal candidiasis in previously healthy homosexual men: evidence of a new acquired cellular immunodeficiency. The New England Journal of Medicine *305*, 1425-1431.

Graham, B.S. (2002). Clinical Trials of HIV Vaccines. Annual Review of Medicine *53*, 207-221.

Grimm, D., and Kay, M.A. (2003). From Virus Evolution to Vector Revolution: Use of Naturally Occurring Serotypes of Adeno-associated Virus (AAV) as Novel Vectors for Human Gene Therapy. Current Gene Therapy *3*, 281-304.

Guimaraes, C.P., Witte, M.D., Theile, C.S., Bozkurt, G., Kundrat, L., Blom, A.E., and Ploegh, H.L. (2013). Site-specific C-terminal and internal loop labeling of proteins using sortase-mediated reactions. Nat Protoc *8*, 1787-1799.

Haase, A.T. (1999). Population Biology of HIV-1 Infection: Viral and CD4+ T Cell Demographics and Dynamics

in Lymphatic Tissues. Annual Review of Immunology *17*, 625-656.

Halper-Stromberg, A., Lu, C.L., Klein, F., Horwitz, J.A., Bournazos, S., Nogueira, L., Eisenreich, T.R., Liu, C., Gazumyan, A., Schaefer, U*., et al.* (2014). Broadly neutralizing antibodies and viral inducers decrease rebound from HIV-1 latent reservoirs in humanized mice. Cell *158*, 989-999.

Hao, S., and Baltimore, D. (2009). The stability of mRNA influences the temporal order of the induction of genes encoding inflammatory molecules. Nature immunology *10*, 281-288.

Harris, A., Borgnia, M.J., Shi, D., Bartesaghi, A., He, H., Pejchal, R., Kang, Y.K., Depetris, R., Marozsan, A.J., Sanders, R.W*., et al.* (2011). Trimeric HIV-1 glycoprotein gp140 immunogens and native HIV-1 envelope glycoproteins display the same closed and open quaternary molecular architectures. Proc Natl Acad Sci U S A *108*, 11440-11445.

Harris, M., Nosyk, B., Harrigan, R., Lima, V.D., Cohen, C., and Montaner, J. (2012). Cost-Effectiveness of Antiretroviral Therapy for Multidrug-Resistant HIV: Past, Present, and Future. AIDS Research and Treatment *2012*, 595762.

Harrison, S.C. (2015). Viral membrane fusion. Virology *479-480*, 498-507.

Hendrickson, E.R., Truby, T.M., Joerger, R.D., Majarian, W.R., and Ebersole, R.C. (1995). High sensitivity multianalyte immunoassay using covalent DNA-labeled antibodies and polymerase chain reaction. Nucleic Acids Res *23*, 522-529.

Hermonat, P.L., Quirk, J.G., Bishop, B.M., and Han, L. (1997). The packaging capacity of adeno-associated virus (AAV) and the potential for wild-type-plus AAV gene therapy vectors. FEBS Lett *407*, 78-84.

Hessell, A.J. (2007). Fc receptor but not complement binding is important in antibody protection against HIV. Nature *449*, 101-104.

Hessell, A.J., Poignard, P., Hunter, M., Hangartner, L., Tehrani, D.M., Bleeker, W.K., Parren, P.W.H.I., Marx, P.A., and Burton, D.R. (2009). Effective, low-titer antibody protection against low-dose repeated mucosal SHIV challenge in macaques. Nat Med *15*, 951-954.

Hofmann-Lehmann, R., Vlasak, J., Rasmussen, R.A., Smith, B.A., Baba, T.W., Liska, V., Ferrantelli, F., Montefiori, D.C., McClure, H.M., Anderson, D.C.*, et al.* (2001). Postnatal passive immunization of neonatal macaques with a triple combination of human monoclonal antibodies against oral simian-human immunodeficiency virus challenge. J Virol *75*, 7470-7480.

Horton, H.M., Bernett, M.J., Pong, E., Peipp, M., Karki, S., Chu, S.Y., Richards, J.O., Vostiar, I., Joyce, P.F., Repp, R.*, et al.* (2008). Potent In vitro and In vivo Activity

of an Fc-Engineered Anti-CD19 Monoclonal Antibody against Lymphoma and Leukemia. Cancer Research *68*, 8049-8057.

Horwitz, J.A., Halper-Stromberg, A., Mouquet, H., Gitlin, A.D., Tretiakova, A., Eisenreich, T.R., Malbec, M., Gravemann, S., Billerbeck, E., Dorner, M.*, et al.* (2013). HIV-1 suppression and durable control by combining single broadly neutralizing antibodies and antiretroviral drugs in humanized mice. Proceedings of the National Academy of Sciences *110*, 16538-16543.

Houghton, A.N., and Guevara-Patino, J.A. (2004). Immune recognition of self in immunity against cancer. J Clin Invest *114*, 468-471.

Huang, J., Kang, B.H., Pancera, M., Lee, J.H., Tong, T., Feng, Y., Imamichi, H., Georgiev, I.S., Chuang, G.-Y., Druz, A.*, et al.* (2014). Broad and potent HIV-1 neutralization by a human antibody that binds the gp41-gp120 interface. Nature *515*, 138-142.

Huang, J., Ofek, G., Laub, L., Louder, M.K., Doria-Rose, N.A., Longo, N.S., Imamichi, H., Bailer, R.T., Chakrabarti, B., Sharma, S.K.*, et al.* (2012a). Broad and potent neutralization of HIV-1 by a gp41-specific human antibody. Nature *491*, 406-412.

Huang, J., Ofek, G., Laub, L., Louder, M.K., Doria-Rose, N.A., Longo, N.S., Imamichi, H., Bailer, R.T., Chakrabarti, B., Sharma, S.K.*, et al.* (2012b). Broad and potent neutralization of HIV-1 by a gp41-specific human antibody. Nature *491*, 406-412.

Hutchinson, J.F. (2001). The Biology and Evolution of HIV. Annual Review of Anthropology *30*, 85-108.

Icenogle, J., Shiwen, H., Duke, G., Gilbert, S., Rueckert, R., and Anderegg, J. (1983). Neutralization of poliovirus by a monoclonal antibody: kinetics and stoichiometry. Virology *127*, 412-425.

Jowett, J.B., Planelles, V., Poon, B., Shah, N.P., Chen, M.L., and Chen, I.S. (1995). The human immunodeficiency virus type 1 vpr gene arrests infected T cells in the G2 + M phase of the cell cycle. J Virol *69*, 6304-6313.

Julien, J.-P., Sok, D., Khayat, R., Lee, J.H., Doores, K.J., Walker, L.M., Ramos, A., Diwanji, D.C., Pejchal, R., Cupo, A.*, et al.* (2013a). Broadly Neutralizing Antibody PGT121 Allosterically Modulates CD4 Binding via Recognition of the HIV-1 gp120 V3 Base and Multiple Surrounding Glycans. PLoS Pathog *9*, e1003342.

Julien, J.P., Cupo, A., Sok, D., Stanfield, R.L., Lyumkis, D., Deller, M.C., Klasse, P.J., Burton, D.R., Sanders, R.W., Moore, J.P.*, et al.* (2013b). Crystal structure of a soluble cleaved HIV-1 envelope trimer. Science *342*, 1477-1483.

Julien, J.P., Lee, J.H., Cupo, A., Murin, C.D., Derking, R., Hoffenberg, S., Caulfield, M.J., King, C.R., Marozsan, A.J., Klasse, P.J.*, et al.* (2013c). Asymmetric recognition of the HIV-1 trimer by broadly neutralizing antibody PG9. Proc Natl Acad Sci U S A *110*, 4351-4356.

Kajander, T., Cortajarena, A.L., Mochrie, S., and Regan, L. (2007a). Structure and stability of designed TPR protein superhelices: unusual crystal packing and implications for natural TPR proteins. Acta Crystallographica Section D-Biological Crystallography *63*, 800-811.

Kajander, T., Cortajarena, A.L., Mochrie, S., and Regan, L. (2007b). Structure and stability of designed TPR protein superhelices: unusual crystal packing and implications for natural TPR proteins. Acta crystallographica Section D, Biological crystallography *63*, 800-811.

Kalos, M., Levine, B.L., Porter, D.L., Katz, S., Grupp, S.A., Bagg, A., and June, C.H. (2011). T Cells with Chimeric Antigen Receptors Have Potent Antitumor Effects and Can Establish Memory in Patients with Advanced Leukemia. Science Translational Medicine *3*, 95ra73-95ra73.

Karush, F. (1976). Multivalent binding and functional affinity. Contemp Top Mol Immunol *5*, 217-228.

Keele, B.F., Jones, J.H., Terio, K.A., Estes, J.D., Rudicell, R.S., Wilson, M.L., Li, Y., Learn, G.H., Beasley, T.M., Schumacher-Stankey, J.*, et al.* (2009). Increased mortality and AIDS-like immunopathology in wild chimpanzees infected with SIVcpz. Nature *460*, 515-519.

Kilby, J.M., Hopkins, S., Venetta, T.M., DiMassimo, B., Cloud, G.A., Lee, J.Y., Alldredge, L., Hunter, E., Lambert, D., Bolognesi, D.*, et al.* (1998). Potent suppression of HIV-1 replication in humans by T-20, a peptide inhibitor of gp41-mediated virus entry. Nat Med *4*, 1302-1307.

Klasse, P.J., Depetris, R.S., Pejchal, R., Julien, J.P., Khayat, R., Lee, J.H., Marozsan, A.J., Cupo, A., Cocco, N., Korzun, J.*, et al.* (2013). Influences on trimerization and aggregation of soluble, cleaved HIV-1 SOSIP envelope glycoprotein. J Virol *87*, 9873-9885.

Klasse, P.J., and Sattentau, Q.J. (2002). Occupancy and mechanism in antibody-mediated neutralization of animal viruses. J Gen Virol *83*, 2091-2108.

Klein, F., Gaebler, C., Mouquet, H., Sather, D.N., Lehmann, C., Scheid, J.F., Kraft, Z., Liu, Y., Pietzsch, J., Hurley, A.*, et al.* (2012a). Broad neutralization by a combination of antibodies recognizing the CD4 binding site and a new conformational epitope on the HIV-1 envelope protein. The Journal of Experimental Medicine *209*, 1469-1479.

Klein, F., Halper-Stromberg, A., Horwitz, J.A., Gruell, H., Scheid, J.F., Bournazos, S., Mouquet, H., Spatz, L.A., Diskin, R., Abadir, A.*, et al.* (2012b). HIV therapy by a combination of broadly neutralizing antibodies in humanized mice. Nature *492*, 118-122.

Klein, F., Mouquet, H., Dosenovic, P., Scheid, J.F., Scharf, L., and Nussenzweig, M.C. (2013). Antibodies in HIV-1 vaccine development and therapy. Science *341*, 1199-1204.

Klein, F., Nogueira, L., Nishimura, Y., Phad, G., West, A.P., Halper-Stromberg, A., Horwitz, J.A., Gazumyan, A., Liu, C., Eisenreich, T.R.*, et al.* (2014a). Enhanced HIV-1 immunotherapy by commonly arising antibodies that target virus escape variants. The Journal of Experimental Medicine *211*, 2361-2372.

Klein, J.S., and Bjorkman, P.J. (2010). Few and far between: how HIV may be evading antibody avidity. PLoS Pathog *6*, e1000908.

Klein, J.S., Gnanapragasam, P.N., Galimidi, R.P., Foglesong, C.P., West, A.P., Jr., and Bjorkman, P.J. (2009a). Examination of the contributions of size and avidity to

the neutralization mechanisms of the anti-HIV antibodies b12 and 4E10. Proc Natl Acad Sci USA *106*, 7385-7390.

Klein, J.S., Gnanapragasam, P.N., Galimidi, R.P., Foglesong, C.P., West, A.P., Jr., and Bjorkman, P.J. (2009b). Examination of the contributions of size and avidity to the neutralization mechanisms of the anti-HIV antibodies b12 and 4E10. Proc Natl Acad Sci U S A *106*, 7385-7390.

Klein, J.S., Jiang, S., Galimidi, R.P., Keeffe, J.R., and Bjorkman, P.J. (2014b). Design and characterization of structured protein linkers with differing flexibilities. Protein Engineering, Design, and Selection *27*, 325-330.

Kong, L., Lee, J.H., Doores, K.J., Murin, C.D., Julien, J.-P., McBride, R., Liu, Y., Marozsan, A., Cupo, A., Klasse, P.-J.*, et al.* (2013). Supersite of immune vulnerability on the glycosylated face of HIV-1 envelope glycoprotein gp120. Nat Struct Mol Biol *20*, 796-803.

Kunert, R., Wolbank, S., Stiegler, G., Weik, R., and Katinger, H. (2004). Characterization of molecular features, antigen-binding, and in vitro properties of IgG and IgM variants of 4E10, an anti-HIV type 1 neutralizing monoclonal antibody. AIDS Res Hum Retroviruses *20*, 755-762.

Kurosaki, T., Kometani, K., and Ise, W. (2015). Memory B cells. Nat Rev Immunol *15*, 149-159.

Kwong, J.A., Dorfman, T., Quinlan, B.D., Chiang, J.J., Ahmed, A.A., Choe, H., and Farzan, M. (2011). A Tyrosine-Sulfated CCR5-Mimetic Peptide Promotes Conformational Transitions in the HIV-1 Envelope Glycoprotein. Journal of Virology *85*, 7563-7571.

Kwong, P.D., Doyle, M.L., Casper, D.J., Cicala, C., Leavitt, S.A., Majeed, S., Steenbeke, T.D., Venturi, M., Chaiken, I., Fung, M.*, et al.* (2002). HIV-1 evades antibody-mediated neutralization through conformational masking of receptor-binding sites. Nature *420*, 678-682.

Kwong, P.D., Wyatt, R., Robinson, J., Sweet, R.W., Sodroski, J., and Hendrickson, W.A. (1998). Structure of an HIV gp120 envelope glycoprotein in complex with the CD4 receptor and a neutralizing human antibody. Nature *393*, 648-659.

Labrijn, A.F., Meesters, J.I., de Goeij, B.E., van den Bremer, E.T., Neijssen, J., van Kampen, M.D., Strumane, K., Verploegen, S., Kundu, A., Gramer, M.J.*, et al.* (2013). Efficient generation of stable bispecific IgG1 by controlled Fab-arm exchange. Proc Natl Acad Sci U S A *110*, 5145-5150.

Labrijn, A.F., Meesters, J.I., Priem, P., de Jong, R.N., van den Bremer, E.T., van Kampen, M.D., Gerritsen, A.F., Schuurman, J., and Parren, P.W. (2014). Controlled Fab-arm exchange for the generation of stable bispecific IgG1. Nat Protoc *9*, 2450-2463.

Labrijn, A.F., Poignard, P., Raja, A., Zwick, M.B., Delgado, K., Franti, M., Binley, J., Vivona, V., Grundner, C., Huang, C.C.*, et al.* (2003). Access of antibody molecules to the conserved coreceptor binding site on glycoprotein gp120 is sterically restricted on primary human immunodeficiency virus type 1. J Virol *77*, 10557-10565.

Lake, J.-a., Carr, J., Feng, F., Mundy, L., Burrell, C., and Li, P. (2003). The role of Vif during HIV-1 infection: interaction with novel host cellular factors. Journal of Clinical Virology *26*, 143-152.

Lama, J., Mangasarian, A., and Trono, D. (2001). Cell-surface expression of CD4 reduces HIV-1 infectivity by blocking Env incorporation in a Nef- and Vpu-inhibitable manner. Current Biology *9*, 622-631.

Lazar-Molnar, E., Almo, S.C., and Nathenson, S.G. (2006). The interchain disulfide linkage is not a prerequisite but enhances CD28 costimulatory function. Cellular immunology *244*, 125-129.

Leen, A.M., Myers, G.D., Sili, U., Huls, M.H., Weiss, H., Leung, K.S., Carrum, G., Krance, R.A., Chang, C.C., Molldrem, J.J.*, et al.* (2006). Monoculture-derived T lymphocytes specific for multiple viruses expand and produce clinically relevant effects in immunocompromised individuals. Nat Med *12*, 1160-1166.

Levitt, N., Briggs, D., Gil, A., and Proudfoot, N.J. (1989). Definition of an efficient synthetic poly(A) site. Genes Dev *3*, 1019-1025.

Levy, J.A. (1993). Pathogenesis of human immunodeficiency virus infection. Microbiol Rev *57*, 183-289.

Lichty, J.J., Malecki, J.L., Agnew, H.D., Michelson-Horowitz, D.J., and Tan, S. (2005). Comparison of affinity tags for protein purification. Protein expression and purification *41*, 98-105.

Liljeroos, L., Krzyzaniak, M.A., Helenius, A., and Butcher, S.J. (2013). Architecture of respiratory syncytial virus revealed by electron cryotomography. Proc Natl Acad Sci U S A *110*, 11133-11138.

Liu, H.L., Doleyres, Y., Coutinho, P.M., Ford, C., and Reilly, P.J. (2000). Replacement and deletion mutations in the catalytic domain and belt region of Aspergillus awamori glucoamylase to enhance thermostability. Protein Eng *13*, 655-659.

Liu, J., Bartesaghi, A., Borgnia, M.J., Sapiro, G., and Subramaniam, S. (2008). Molecular architecture of native HIV-1 gp120 trimers. Nature *455*, 109-113.

Liu, L., Patel, B., Ghanem, M.H., Bundoc, V., Zheng, Z., Morgan, R.A., Rosenberg, S.A., Dey, B., and Berger, E.A. (2015). Novel CD4-Based Bispecific Chimeric Antigen Receptor Designed for Enhanced Anti-HIV Potency and Absence of HIV Entry Receptor Activity. J Virol *89*, 6685-6694.

Loeb, J.E., Cordier, W.S., Harris, M.E., Weitzman, M.D., and Hope, T.J. (1999). Enhanced expression of transgenes from adeno-associated virus vectors with the woodchuck hepatitis virus posttranscriptional regulatory element: implications for gene therapy. Hum Gene Ther *10*, 2295-2305.

Luftig, M.A., Mattu, M., Di Giovine, P., Geleziunas, R., Hrin, R., Barbato, G., Bianchi, E., Miller, M.D., Pessi, A., and Carfi, A. (2006). Structural basis for HIV-1 neutralization by a gp41 fusion intermediate-directed antibody. Nat Struct Mol Biol *13*, 740-747.

Lyumkis, D., Julien, J.P., de Val, N., Cupo, A., Potter, C.S., Klasse, P.J., Burton, D.R., Sanders, R.W., Moore, J.P., Carragher, B.*, et al.* (2013). Cryo-EM structure of a fully glycosylated soluble cleaved HIV-1 envelope trimer. Science *342*, 1484-1490.

Maes, R., Sedwick, W., and Vaheri, A. (1967). Interaction between DEAE-dextran and nucleic acids. Biochemica et Biophysica ACTA (BBA) - Nucleic Acids and Protein Synthesis *134*, 269-276.

Magadán, J.G., Pérez-Victoria, F.J., Sougrat, R., Ye, Y., Strebel, K., and Bonifacino, J.S. (2010). Multilayered Mechanism of CD4 Downregulation by HIV-1 Vpu

Involving Distinct ER Retention and ERAD Targeting Steps. PLoS Pathog *6*, e1000869.

Main, E.R., Jackson, S.E., and Regan, L. (2003). The folding and design of repeat proteins: reaching a consensus. Current opinion in structural biology *13*, 482-489.

Marsden, M.D., and Zack, J.A. (2015). Double trouble: HIV latency and CTL escape. Cell Host Microbe *17*, 141-142.

Marx, J.L. (1975). Antibody structure: now in three dimensions. Science *189*, 1075-1114.

Mascola, J.R. (1997). Potent and synergistic neutralization of human immunodeficiency virus (HIV) type 1 primary isolates by hyperimmune anti-HIV immunoglobulin combined with monoclonal antibodies 2F5 and 2G12. J Virol *71*, 7198-7206.

Mascola, J.R. (1999). Protection of macaques against pathogenic simian/human immunodeficiency virus 89.6PD by passive transfer of neutralizing antibodies. J Virol *73*, 4009-4018.

Mascola, J.R. (2000). Protection of macaques against vaginal transmission of a pathogenic HIV-1/SIV chimeric virus by passive infusion of neutralizing antibodies. Nat Med *6*, 207-210.

Mascola, J.R., and Montefiori, D.C. (2010). The role of antibodies in HIV vaccines. Annu Rev Immunol *28*, 413-444.

Mattes, M.J. (2004). Binding parameters of antibodies: pseudo-affinity and other misconceptions. Cancer Immunology, Immunotherapy *54*, 513-516.

Mattes, M.J. (2005). Binding parameters of antibodies: pseudo-affinity and other misconceptions. Cancer Immunol Immunother *54*, 513-516.

Maude, S.L., Frey, N., Shaw, P.A., Aplenc, R., Barrett, D.M., Bunin, N.J., Chew, A., Gonzalez, V.E., Zheng, Z., Lacey, S.F., *et al.* (2014). Chimeric Antigen Receptor T Cells for Sustained Remissions in Leukemia. New England Journal of Medicine *371*, 1507-1517.

Maul, R.W., and Gearhart, P.J. (2010). AID and somatic hypermutation. Adv Immunol *105*, 159-191.

McCoy, L.E., Quigley, A.F., Strokappe, N.M., Bulmer-Thomas, B., Seaman, M.S., Mortier, D., Rutten, L., Chander, N., Edwards, C.J., Ketteler, R., *et al.* (2012). Potent and broad neutralization of HIV-1 by a llama antibody elicited by immunization. The Journal of Experimental Medicine *209*, 1091-1103.

McLaughlin, S.K., Collis, P., Hermonat, P.L., and Muzyczka, N. (1988). Adeno-associated virus general transduction vectors: analysis of proviral structures. J Virol *62*, 1963-1973.

McLellan, J.S., Pancera, M., Carrico, C., Gorman, J., Julien, J.-P., Khayat, R., Louder, R., Pejchal, R., Sastry, M., Dai, K., *et al.* (2011). Structure of HIV-1 gp120 V1/V2 domain with broadly neutralizing antibody PG9. Nature *480*, 336-343.

McMichael, A.J. (2006). HIV vaccines. Annu Rev Immunol *24*, 227-255.

McNatt, M.W., Zang, T., and Bieniasz, P.D. (2013). Vpu Binds Directly to Tetherin and Displaces It from Nascent Virions. PLoS Pathog *9*, e1003299.

Medzhitov, R. (2007). Recognition of microorganisms and activation of the immune response. Nature *449*, 819-826.

Medzhitov, R., and Janeway, C., Jr. (2000). Innate immunity. N Engl J Med *343*, 338-344.

Mehellou, Y., and De Clercq, E. (2010). Twenty-six years of anti-HIV drug discovery: where do we stand and where do we go? J Med Chem *53*, 521-538.

Merk, A., and Subramaniam, S. (2013). HIV-1 envelope glycoprotein structure. Curr Opin Struct Biol *23*, 268-276.

Mitsuyasu, R.T., Anton, P.A., Deeks, S.G., Scadden, D.T., Connick, E., Downs, M.T., Bakker, A., Roberts, M.R., June, C.H., Jalali, S.*, et al.* (2000). Prolonged survival and tissue trafficking following adoptive transfer of CD4zeta gene-modified autologous CD4(+) and CD8(+) T cells in human immunodeficiency virus-infected subjects. Blood *96*, 785-793.

Moir, S., Chun, T.W., and Fauci, A.S. (2011). Pathogenic mechanisms of HIV disease. Annu Rev Pathol *6*, 223-248.

Monahan, P.E., and Samulski, R.J. (2000). AAV vectors: is clinical success on the horizon? Gene Ther *7*, 24-30.

Montefiori, D.C. (1996). Neutralizing and infection-enhancing antibody responses to human immunodeficiency virus type 1 in long-term nonprogressors. J Infect Dis *173*, 60-67.

Montefiori, D.C. (2005). Evaluating neutralizing antibodies against HIV, SIV, and SHIV in luciferase reporter gene assays. Current protocols in immunology / edited by John E Coligan [et al *Chapter 12*, Unit 12 11.

Montefiori, D.C., Hill, T.S., Vo, H.T., Walker, B.D., and Rosenberg, E.S. (2001). Neutralizing antibodies associated with viremia control in a subset of individuals after treatment of acute human immunodeficiency virus type 1 infection. J Virol *75*, 10200-10207.

Moody, M.A., Santra, S., Vandergrift, N.A., Sutherland, L.L., Gurley, T.C., Drinker, M.S., Allen, A.A., Xia, S.M., Meyerhoff, R.R., Parks, R.*, et al.* (2014). Toll-like receptor 7/8 (TLR7/8) and TLR9 agonists cooperate to enhance HIV-1 envelope antibody responses in rhesus macaques. J Virol *88*, 3329-3339.

Moore, J.P., and Sodroski, J. (1996). Antibody cross-competition analysis of the human immunodeficiency virus type 1 gp120 exterior envelope glycoprotein. J Virol *70*, 1863-1872.

Mouquet, H., Scharf, L., Euler, Z., Liu, Y., Eden, C., Scheid, J.F., Halper-Stromberg, A., Gnanapragasam, P.N., Spencer, D.I., Seaman, M.S.*, et al.* (2012a). Complex-type N-glycan recognition by potent broadly neutralizing HIV antibodies. Proc Natl Acad Sci U S A *109*, E3268-3277.

Mouquet, H., Scharf, L., Euler, Z., Liu, Y., Eden, C., Scheid, J.F., Halper-Stromberg, A., Gnanapragasam, P.N.P., Spencer, D.I.R., Seaman, M.S.*, et al.* (2012b). Complex-type N-glycan recognition by potent broadly neutralizing HIV antibodies. Proceedings of the National Academy of Sciences *109*, E3268-E3277.

Mouquet, H., Scheid, J.F., Zoller, M.J., Krogsgaard, M., Ott, R.G., Shukair, S., Artyomov, M.N., Pietzsch, J., Connors, M., Pereyra, F.*, et al.* (2010). Polyreactivity increases the apparent affinity of anti-HIV antibodies by heteroligation. Nature *467*, 591-595.

Munro, J.B., Gormann, J., Ma, X., Zhou, Z., Arthos, J., Burton, D.R., Koff, W.C., Courtner, J.R., Smith, A.B., 3rd, Kwong, P.D.*, et al.* (2014). Conformational dynamics of single HIV-1 envelope trimers on the surface of native virions.

Science Xpress *published online 8 October 2014 [DOI:10.1126/science.1254426]*.

Murphy, K., Travers, P., Walport, M., and Janeway, C. (2012). Janeway's immunobiology (New York: Garland Science).

Neefjes, J., Jongsma, M.L., Paul, P., and Bakke, O. (2011). Towards a systems understanding of MHC class I and MHC class II antigen presentation. Nat Rev Immunol *11*, 823-836.

Nobbmann, U., Connah, M., Fish, B., Varley, P., Gee, C., Mulot, S., Chen, J., Zhou, L., Lu, Y., Shen, F.*, et al.* (2007). Dynamic light scattering as a relative tool for assessing the molecular integrity and stability of monoclonal antibodies. Biotechnology & genetic engineering reviews *24*, 117-128.

O'Shea, E.K., Lumb, K.J., and Kim, P.S. (1993). Peptide 'Velcro': design of a heterodimeric coiled coil. Curr Biol *3*, 658-667.

Ostertag, W., Roesler, G., Krieg, C.J., Kind, J., Cole, T., Crozier, T., Gaedicke, G., Steinheider, G., Kluge, N., and Dube, S. (1974). Induction of endogenous virus and of thymidine kinase by bromodeoxyuridine in cell cultures transformed by Friend virus. Proc Natl Acad Sci U S A *71*, 4980-4985.

Pace, C.S., Song, R., Ochsenbauer, C., Andrews, C.D., Franco, D., Yu, J., Oren, D.A., Seaman, M.S., and Ho, D.D. (2013). Bispecific antibodies directed to CD4 domain 2 and HIV envelope exhibit exceptional breadth and picomolar potency against HIV-1. Proc Natl Acad Sci U S A *110*, 13540-13545.

Palella, F.J., Jr., Delaney, K.M., Moorman, A.C., Loveless, M.O., Fuhrer, J., Satten, G.A., Aschman, D.J., and Holmberg, S.D. (1998). Declining morbidity and

mortality among patients with advanced human immunodeficiency virus infection. HIV Outpatient Study Investigators. N Engl J Med *338*, 853-860.

Pancera, M., Zhou, T., Druz, A., Georgiev, I.S., Soto, C., Gorman, J., Huang, J., Acharya, P., Chuang, G.Y., Ofek, G.*, et al.* (2014a). Structure and immune recognition of trimeric pre-fusion HIV-1 Env. Nature *514*, 455-461.

Pancera, M., Zhou, T., Druz, A., Georgiev, I.S., Soto, C., Gorman, J., Huang, J., Acharya, P., Chuang, G.Y., Ofek, G.*, et al.* (2014b). Structure and immune recognition of trimeric pre-fusion HIV-1 Env. Nature.

Pantophlet, R., and Burton, D.R. (2006). GP120: target for neutralizing HIV-1 antibodies. Annu Rev Immunol *24*, 739-769.

Pardridge, W.M. (2010). Biopharmaceutical drug targeting to the brain. Journal of drug targeting *18*, 157-167.

Parkin, N.T., Chamorro, M., and Varmus, H.E. (1992). Human immunodeficiency virus type 1 gag-pol frameshifting is dependent on downstream mRNA secondary structure: demonstration by expression in vivo. J Virol *66*, 5147-5151.

Parren, P.W., Poignard, P., Ditzel, H.J., Williamson, R.A., and Burton, D.R. (2000). Antibodies in human infectious disease. Immunol Res *21*, 265-278.

Pauling, L., Pressman, D., and Grossberg, A.L. (1944). The Serological Properties of Simple Substances. VII. A Quantitative Theory of the Inhibition by Haptens of the Precipitation of Heterogeneous Antisera with Antigens, and Comparison with Experimental Results for Polyhaptenic Simple Substances and for Azoproteins. Journal of the American Chemical Society *66*, 784-792.

Paxton, W., Connor, R.I., and Landau, N.R. (1993). Incorporation of Vpr into human immunodeficiency virus type 1 virions: requirement for the p6 region of gag and mutational analysis. J Virol *67*, 7229-7237.

Pegu, A., Asokan, M., Wu, L., Wang, K., Hataye, J., Casazza, J.P., Guo, X., Shi, W., Georgiev, I., Zhou, T.*, et al.* (2015). Activation and lysis of human CD4 cells latently infected with HIV-1. Nat Commun *6*, 8447.

Pegu, A., Yang, Z.Y., Boyington, J.C., Wu, L., Ko, S.Y., Schmidt, S.D., McKee, K., Kong, W.P., Shi, W., Chen, X.*, et al.* (2014). Neutralizing antibodies to HIV-1 envelope protect more effectively in vivo than those to the CD4 receptor. Science translational medicine *6*, 243ra288.

Pejchal, R., Doores, K.J., Walker, L.M., Khayat, R., Huang, P.-S., Wang, S.-K., Stanfield, R.L., Julien, J.-P., Ramos, A., Crispin, M.*, et al.* (2011). A potent and broad neutralizing antibody recognizes and penetrates the HIV glycan shield. Science (New York, Ny) *334*, 1097-1103.

Peled, J.U., Kuang, F.L., Iglesias-Ussel, M.D., Roa, S., Kalis, S.L., Goodman, M.F., and Scharff, M.D. (2008). The Biochemistry of Somatic Hypermutation. Annual Review of Immunology *26*, 481-511.

Perelson, A.S., Neumann, A.U., Markowitz, M., Leonard, J.M., and Ho, D.D. (1996). HIV-1 dynamics in vivo: virion clearance rate, infected cell life-span, and viral generation time. Science *271*, 1582-1586.

Pettit, S.C., Everitt, L.E., Choudhury, S., Dunn, B.M., and Kaplan, A.H. (2004). Initial cleavage of the human immunodeficiency virus type 1 GagPol precursor by its activated protease occurs by an intramolecular mechanism. J Virol *78*, 8477-8485.

Picker, L.J., Hansen, S.G., and Lifson, J.D. (2012). New paradigms for HIV/AIDS vaccine development. Annu Rev Med *63*, 95-111.

Pieper, K., Grimbacher, B., and Eibel, H. (2013). B-cell biology and development. Journal of Allergy and Clinical Immunology *131*, 959-971.

Porter, D.L., Levine, B.L., Kalos, M., Bagg, A., and June, C.H. (2011). Chimeric Antigen Receptor–Modified T Cells in Chronic Lymphoid Leukemia. New England Journal of Medicine *365*, 725-733.

Pritchard, L.K., Harvey, D.J., Bonomelli, C., Crispin, M., and Doores, K.J. (2015a). Cell- and Protein-Directed Glycosylation of Native Cleaved HIV-1 Envelope. J Virol *89*, 8932-8944.

Pritchard, L.K., Vasiljevic, S., Ozorowski, G., Seabright, G.E., Cupo, A., Ringe, R., Kim, H.J., Sanders, R.W., Doores, K.J., Burton, D.R.*, et al.* (2015b). Structural Constraints Determine the Glycosylation of HIV-1 Envelope Trimers. Cell Rep *11*, 1604-1613.

Purtscher, M., Trkola, A., Gruber, G., Buchacher, A., Predl, R., Steindl, F., Tauer, C., Berger, R., Barrett, N., Jungbauer, A.*, et al.* (1994). A broadly neutralizing human monoclonal antibody against gp41 of human immunodeficiency virus type 1. AIDS Res Hum Retroviruses *10*, 1651-1658.

Rispens, T., Meesters, J., den Bleker, T.H., Ooijevaar-De Heer, P., Schuurman, J., Parren, P.W., Labrijn, A., and Aalberse, R.C. (2013). Fc-Fc interactions of human IgG4 require dissociation of heavy chains and are formed predominantly by the intra-chain hinge isomer. Mol Immunol *53*, 35-42.

Rizzuto, C.D., Wyatt, R., Hernandez-Ramos, N., Sun, Y., Kwong, P.D., Hendrickson, W.A., and Sodroski, J. (1998). A conserved HIV gp120 glycoprotein structure involved in chemokine receptor binding. Science *280*, 1949-1953.

Roben, P., Moore, J.P., Thali, M., Sodroski, J., Barbas, C.F., 3rd, and Burton, D.R. (1994). Recognition properties of a panel of human recombinant Fab fragments to the CD4 binding site of gp120 that show differing abilities to neutralize human immunodeficiency virus type 1. Journal of virology *68*, 4821-4828.

Roberts, M.R., Qin, L., Zhang, D., Smith, D.H., Tran, A.C., Dull, T.J., Groopman, J.E., Capon, D.J., Byrn, R.A., and Finer, M.H. (1994). Targeting of human immunodeficiency virus-infected cells by CD8+ T lymphocytes armed with universal T-cell receptors. Blood *84*, 2878-2889.

Ross, T.M., Oran, A.E., and Cullen, B.R. (1999). Inhibition of HIV-1 progeny virion release by cell-surface CD4 is relieved by expression of the viral Nef protein. Current Biology *9*, 613-621.

Rossi, D.L., Rossi, E.A., Cardillo, T.M., Goldenberg, D.M., and Chang, C.H. (2014). A new class of bispecific antibodies to redirect T cells for cancer immunotherapy. MAbs *6*, 381-391.

Rudicell, R.S., Holland Jones, J., Wroblewski, E.E., Learn, G.H., Li, Y., Robertson, J.D., Greengrass, E., Grossmann, F., Kamenya, S., Pintea, L.*, et al.* (2010). Impact of Simian Immunodeficiency Virus Infection on Chimpanzee Population Dynamics. PLoS Pathog *6*, e1001116.

Rutledge, T., Cosson, P., Manolios, N., Bonifacino, J.S., and Klausner, R.D. (1992). Transmembrane helical interactions: zeta chain dimerization and functional association with the T cell antigen receptor. The EMBO Journal *11*, 3245-3254.

Sanchez, L.M., Chirino, A.J., and Bjorkman, P. (1999). Crystal structure of human ZAG, a fat-depleting factor related to MHC molecules. Science *283*, 1914-1919.

Sanders, R.W., Derking, R., Cupo, A., Julien, J.P., Yasmeen, A., de Val, N., Kim, H.J., Blattner, C., de la Pena, A.T., Korzun, J.*, et al.* (2013). A next-generation cleaved, soluble HIV-1 Env trimer, BG505 SOSIP.664 gp140, expresses multiple epitopes for broadly neutralizing but not non-neutralizing antibodies. PLoS Pathog *9*, e1003618.

Sanders, R.W., Vesanen, M., Schuelke, N., Master, A., Schiffner, L., Kalyanaraman, R., Paluch, M., Berkhout, B., Maddon, P.J., Olson, W.C.*, et al.* (2002). Stabilization of the soluble, cleaved, trimeric form of the envelope glycoprotein complex of human immunodeficiency virus type 1. J Virol *76*, 8875-8889.

Sather, D.N., Carbonetti, S., Kehayia, J., Kraft, Z., Mikell, I., Scheid, J.F., Klein, F., and Stamatatos, L. (2012). Broadly Neutralizing Antibodies Developed by an HIV-Positive Elite Neutralizer Exact a Replication Fitness Cost on the Contemporaneous Virus. Journal of Virology *86*, 12676-12685.

Sattentau, Q.J., and Moore, J.P. (1991). Conformational changes induced in the human immunodeficiency virus envelope glycoprotein by soluble CD4 binding. J Exp Med *174*, 407-415.

Schaefer, W., Regula, J.T., Bahner, M., Schanzer, J., Croasdale, R., Durr, H., Gassner, C., Georges, G., Kettenberger, H., Imhof-Jung, S.*, et al.* (2011). Immunoglobulin

domain crossover as a generic approach for the production of bispecific IgG antibodies. Proc Natl Acad Sci U S A *108*, 11187-11192.

Scharf, L., Scheid, Johannes F., Lee, Jeong H., West, Anthony P., Jr., Chen, C., Gao, H., Gnanapragasam, Priyanthi N.P., Mares, R., Seaman, Michael S., Ward, Andrew B.*, et al.* (2014). Antibody 8ANC195 Reveals a Site of Broad Vulnerability on the HIV-1 Envelope Spike. Cell Reports *7*, 785-795.

Scharf, L., Wang, H., Gao, H., Chen, S., McDowall, A.W., and Bjorkman, P.J. (2015). Broadly Neutralizing Antibody 8ANC195 Recognizes Closed and Open States of HIV-1 Env. Cell *162*, 1379-1390.

Scheid, J., Mouquet, H., Feldhahn, N., Walker, B., Pereyra, F., Cutrell, E., Seaman, M., Mascola, J., Wyatt, R., Wardemann, H.*, et al.* (2009a). A method for identification of HIV gp140 binding memory B cells in human blood. Journal of immunological methods *343*, 65-67.

Scheid, J.F., Mouquet, H., Feldhahn, N., Seaman, M.S., Velinzon, K., Pietzsch, J., Ott, R.G., Anthony, R.M., Zebroski, H., Hurley, A.*, et al.* (2009b). Broad diversity of neutralizing antibodies isolated from memory B cells in HIV-infected individuals. Nature *458*, 636-640.

Scheid, J.F., Mouquet, H., Ueberheide, B., Diskin, R., Klein, F., Oliveira, T.Y.K., Pietzsch, J., Fenyo, D., Abadir, A., Velinzon, K.*, et al.* (2011a). Sequence and Structural Convergence of Broad and Potent HIV Antibodies That Mimic CD4 Binding. Science (New York, Ny) *333*, 1633-1637.

Scheid, J.F., Mouquet, H., Ueberheide, B., Diskin, R., Klein, F., Olivera, T.Y., Pietzsch, J., Fenyo, D., Abadir, A., Velinzon, K.*, et al.* (2011b). Sequence and Structural

Convergence of Broad and Potent HIV Antibodies That Mimic CD4 Binding. Science *333*, 1633-1637.

Scheufler, C., Brinker, A., Bourenkov, G., Pegoraro, S., Moroder, L., Bartunik, H., Hartl, F.U., and Moarefi, I. (2000). Structure of TPR domain-peptide complexes: critical elements in the assembly of the Hsp70-Hsp90 multichaperone machine. Cell *101*, 199-210.

Schmidt, T.G., and Skerra, A. (2007). The Strep-tag system for one-step purification and high-affinity detection or capturing of proteins. Nat Protoc *2*, 1528-1535.

Schnepp, B.C., Jensen, R.L., Clark, K.R., and Johnson, P.R. (2009). Infectious molecular clones of adeno-associated virus isolated directly from human tissues. J Virol *83*, 1456-1464.

Schofield, D.J., Stephenson, J.R., and Dimmock, N.J. (1997). Variations in the neutralizing and haemagglutination-inhibiting activities of five influenza A virus-specific IgGs and their antibody fragments. J Gen Virol *78 (Pt 10)*, 2431-2439.

Scholler, J., Brady, T.L., Binder-Scholl, G., Hwang, W.T., Plesa, G., Hege, K.M., Vogel, A.N., Kalos, M., Riley, J.L., Deeks, S.G.*, et al.* (2012). Decade-long safety and function of retroviral-modified chimeric antigen receptor T cells. Sci Transl Med *4*, 132ra153.

Schrödinger, L. (2011). The PyMOL Molecular Graphics System (The PyMOL Molecular Graphics System).

Schuler, B., Lipman, E.A., Steinbach, P.J., Kumke, M., and Eaton, W.A. (2005). Polyproline and the "spectroscopic ruler" revisited with single-molecule

fluorescence. Proceedings of the National Academy of Sciences of the United States of America *102*, 2754-2759.

Schulke, N., Vesanen, M.S., Sanders, R.W., Zhu, P., Lu, M., Anselma, D.J., Villa, A.R., Parren, P.W., Binley, J.M., Roux, K.H.*, et al.* (2002). Oligomeric and conformational properties of a proteolytically mature, disulfide-stabilized human immunodeficiency virus type 1 gp140 envelope glycoprotein. J Virol *76*, 7760-7776.

Schultz, B.R., and Chamberlain, J.S. (2008). Recombinant adeno-associated virus transduction and integration. Mol Ther *16*, 1189-1199.

Schuurman, J., Labrijn, A.F., and Parren, P.W. (2012). Fab-arm exchange: what's in a name? MAbs *4*, 636.

Seaman, M.S., Janes, H., Hawkins, N., Grandpre, L.E., Devoy, C., Giri, A., Coffey, R.T., Harris, L., Wood, B., Daniels, M.G.*, et al.* (2010). Tiered categorization of a diverse panel of HIV-1 Env pseudoviruses for assessment of neutralizing antibodies. J Virol *84*, 1439-1452.

Sharp, P.M., and Hahn, B.H. (2011). Origins of HIV and the AIDS pandemic. Cold Spring Harb Perspect Med *1*, a006841.

Shental-Bechor, D., and Levy, Y. (2008). Effect of glycosylation on protein folding: a close look at thermodynamic stabilization. Proceedings of the National Academy of Sciences of the United States of America *105*, 8256-8261.

Sheskin, D. (2004). Handbook of Parametric and Nonparametric Statistical Procedures, 3rd edn (Boca Raton: Chapman & Hall/CRC).

Shingai, M., Nishimura, Y., Klein, F., Mouquet, H., Donau, O.K., Plishka, R., Buckler-White, A., Seaman, M., Piatak, M., Lifson, J.D.*, et al.* (2013). Antibody-mediated immunotherapy of macaques chronically infected with SHIV suppresses viraemia. Nature *advance online publication*.

Sievers, S.A., Scharf, L., West, A.P., Jr., and Bjorkman, P.J. (2015). Antibody engineering for increased potency, breadth and half-life. Current Opinion in HIV and AIDS *10*.

Simon, V., Ho, D.D., and Abdool Karim, Q. (2006). HIV/AIDS epidemiology, pathogenesis, prevention, and treatment. The Lancet *368*, 489-504.

Sok, D., van Gils, M.J., Pauthner, M., Julien, J.-P., Saye-Francisco, K.L., Hsueh, J., Briney, B., Lee, J.H., Le, K.M., Lee, P.S.*, et al.* (2014). Recombinant HIV envelope trimer selects for quaternary-dependent antibodies targeting the trimer apex. Proceedings of the National Academy of Sciences *111*, 17624-17629.

Solis, M., Nakhaei, P., Jalalirad, M., Lacoste, J., Douville, R., Arguello, M., Zhao, T., Laughrea, M., Wainberg, M.A., and Hiscott, J. (2011). RIG-I-mediated antiviral signaling is inhibited in HIV-1 infection by a protease-mediated sequestration of RIG-I. J Virol *85*, 1224-1236.

Sougrat, R., Bartesaghi, A., Lifson, J.D., Bennett, A.E., Bess, J.W., Zabransky, D.J., and Subramaniam, S. (2007). Electron tomography of the contact between T cells and SIV/HIV-1: implications for viral entry. PLoS Pathog *3*, e63.

Staerz, U.D., Kanagawa, O., and Bevan, M.J. (1985). Hybrid antibodies can target sites for attack by T cells. Nature *314*, 628-631.

Stanfield, R.L., Zemla, A., Wilson, I.A., and Rupp, B. (2006). Antibody elbow angles are influenced by their light chain class. J Mol Biol *357*, 1566-1574.

Starcich, B.R., Hahn, B.H., Shaw, G.M., McNeely, P.D., Modrow, S., Wolf, H., Parks, E.S., Parks, W.P., Josephs, S.F., Gallo, R.C.*, et al.* (1986). Identification and characterization of conserved and variable regions in the envelope gene of HTLV-III/LAV, the retrovirus of AIDS. Cell *45*, 637-648.

Stiegler, G., Kunert, R., Purtscher, M., Wolbank, S., Voglauer, R., Steindl, F., and Katinger, H. (2001). A potent cross-clade neutralizing human monoclonal antibody against a novel epitope on gp41 of human immunodeficiency virus type 1. AIDS Res Hum Retroviruses *17*, 1757-1765.

Stieh, D.J., King, D.F., Klein, K., Liu, P., Shen, X., Hwang, K., Ferrari, G., Montefiori, D.C., Haynes, B., Pitisuttithum, P.*, et al.* (2014). Aggregate complexes of HIV-1 induced by multimeric antibodies. Retrovirology *11*, 78.

Stopak, K., de Noronha, C., Yonemoto, W., and Greene, W.C. (2003). HIV-1 Vif Blocks the Antiviral Activity of APOBEC3G by Impairing Both Its Translation and Intracellular Stability. Molecular Cell *12*, 591-601.

Tamamis, P., and Floudas, C.A. (2014). Molecular recognition of CCR5 by an HIV-1 gp120 V3 loop. PLoS One *9*, e95767.

Thaxton, M. (2006). Why the Chimpanzees of Gombe National Park are in Jeopardy (Population Reference Bureau).

Tiselius, A., and Kabat, E.A. (1938). ELECTROPHORESIS OF IMMUNE SERUM. Science *87*, 416-417.

Tiselius, A., and Kabat, E.A. (1939). An Electrophoretic Study of Immune Sera and Purified Antibody Preparations. J Exp Med *69*, 119-131.

Tonegawa, S. (1983). Somatic generation of antibody diversity. Nature *302*, 575-581.

Topalian, S.L., Weiner, G.J., and Pardoll, D.M. (2011). Cancer immunotherapy comes of age. J Clin Oncol *29*, 4828-4836.

Tran, E.E., Borgnia, M.J., Kuybeda, O., Schauder, D.M., Bartesaghi, A., Frank, G.A., Sapiro, G., Milne, J.L., and Subramaniam, S. (2012). Structural mechanism of trimeric HIV-1 envelope glycoprotein activation. PLoS Pathog *8*, e1002797.

Trinh, C.H., Smith, D.P., Kalverda, A.P., Phillips, S.E., and Radford, S.E. (2002). Crystal structure of monomeric human beta-2-microglobulin reveals clues to its amyloidogenic properties. Proceedings of the National Academy of Sciences of the United States of America *99*, 9771-9776.

Trkola, A., Kuster, H., Rusert, P., Joos, B., Fischer, M., Leemann, C., Manrique, A., Huber, M., Rehr, M., Oxenius, A.*, et al.* (2005). Delay of HIV-1 rebound after cessation of antiretroviral therapy through passive transfer of human neutralizing antibodies. Nat Med *11*, 615-622.

Trkola, A., Purtscher, M., Muster, T., Ballaun, C., Buchacher, A., Sullivan, N., Srinivasan, K., Sodroski, J., Moore, J.P., and Katinger, H. (1996). Human monoclonal antibody 2G12 defines a distinctive neutralization epitope on the gp120 glycoprotein of human immunodeficiency virus type 1. Journal of Virology *70*, 1100-1108.

Tu, H., Bonura, C., Giannini, C., Mouly, H., Soussan, P., Kew, M., Paterlini-Brechot, P., Brechot, C., and Kremsdorf, D. (2001). Biological impact of natural COOH-

terminal deletions of hepatitis B virus X protein in hepatocellular carcinoma tissues. Cancer Res *61*, 7803-7810.

UNAIDS (2015). UNAIDS Facts Sheet 2015, UNAIDS, ed. (UNAIDS.org: UNAIDS).

UNAIDS, and Sabin, K., eds. (2015). UNAIDS Report: How AIDS changed everything (Switzerland: UNAIDS).

van Gils, M.J., Euler, Z., Schweighardt, B., Wrin, T., and Schuitemaker, H. (2009). Prevalence of cross-reactive HIV-1-neutralizing activity in HIV-1-infected patients with rapid or slow disease progression. AIDS *23*.

van Gils, M.J., and Sanders, R.W. (2013). Broadly neutralizing antibodies against HIV-1: Templates for a vaccine. Virology *435*, 46-56.

Victora, G.D., and Mesin, L. (2014). Clonal and cellular dynamics in germinal centers. Curr Opin Immunol *28*, 90-96.

Victora, G.D., and Nussenzweig, M.C. (2012). Germinal Centers. Annual Review of Immunology *30*, 429-457.

Vijay-Kumar, S., Bugg, C.E., and Cook, W.J. (1987). Structure of ubiquitin refined at 1.8 A resolution. Journal of molecular biology *194*, 531-544.

Walker, L.M., Huber, M., Doores, K.J., Falkowska, E., Pejchal, R., Julien, J.-P., Wang, S.-K., Ramos, A., Chan-Hui, P.-Y., Moyle, M.*, et al.* (2011). Broad neutralization coverage of HIV by multiple highly potent antibodies. Nature *477*, 466-470.

Walker, L.M., Phogat, S.K., Chan-Hui, P.-Y., Wagner, D., Phung, P., Goss, J.L., Wrin, T., Simek, M.D., Fling, S., Mitcham, J.L.*, et al.* (2009a). Broad and Potent Neutralizing Antibodies from an African Donor Reveal a New HIV-1 Vaccine Target. Science (New York, Ny) *326*, 285-289.

Walker, L.M., Phogat, S.K., Chan-Hui, P.Y., Wagner, D., Phung, P., Goss, J.L., Wrin, T., Simek, M.D., Fling, S., Mitcham, J.L*., et al.* (2009b). Broad and Potent Neutralizing Antibodies from an African Donor Reveal a New HIV-1 Vaccine Target. Science *326*, 285-289.

Waters, L., Mandalia, S., Randell, P., Wildfire, A., Gazzard, B., and Moyle, G. (2008). The Impact of HIV Tropism on Decreases in CD4 Cell Count, Clinical Progression, and Subsequent Response to a First Antiretroviral Therapy Regimen. Clinical Infectious Diseases *46*, 1617-1623.

Watkins, D.I. (2008). The Vaccine Search Goes On. In Scientific American (SCIENTIFIC AMERICAN, INC.), pp. 69-77.

Weissenhorn, W., Dessen, A., Harrison, S.C., Skehel, J.J., and Wiley, D.C. (1997). Atomic structure of the ectodomain from HIV-1 gp41. Nature *387*, 426-430.

West, A.P., Jr., Galimidi, R.P., Foglesong, C.P., Gnanapragasam, P.N., Klein, J.S., and Bjorkman, P.J. (2010). Evaluation of CD4-CD4i antibody architectures yields potent, broadly cross-reactive anti-human immunodeficiency virus reagents. J Virol *84*, 261-269.

West, A.P., Jr., Galimidi, R.P., Gnanapragasam, P.N., and Bjorkman, P.J. (2012). Single-chain Fv-based anti-HIV proteins: potential and limitations. J Virol *86*, 195-202.

West, A.P., Jr., Scharf, L., Scheid, J.F., Klein, F., Bjorkman, P.J., and Nussenzweig, M.C. (2014). Structural insights on the role of antibodies in HIV-1 vaccine and therapy. Cell *156*, 633-648.

Witte, M.D., Theile, C.S., Wu, T., Guimaraes, C.P., Blom, A.E., and Ploegh, H.L. (2013). Production of unnaturally linked chimeric proteins using a combination of sortase-catalyzed transpeptidation and click chemistry. Nat Protoc *8*, 1808-1819.

Wolbank, S., Kunert, R., Stiegler, G., and Katinger, H. (2003). Characterization of human class-switched polymeric (immunoglobulin M [IgM] and IgA) anti-human immunodeficiency virus type 1 antibodies 2F5 and 2G12. J Virol *77*, 4095-4103.

Wu, H., Pfarr, D.S., Tang, Y., An, L.L., Patel, N.K., Watkins, J.D., Huse, W.D., Kiener, P.A., and Young, J.F. (2005). Ultra-potent antibodies against respiratory syncytial virus: effects of binding kinetics and binding valence on viral neutralization. J Mol Biol *350*, 126-144.

Wu, J., Fu, J., Zhang, M., and Liu, D. (2015). Blinatumomab: a bispecific T cell engager (BiTE) antibody against CD19/CD3 for refractory acute lymphoid leukemia. J Hematol Oncol *8*, 104.

Wu, X., Yang, Z.-Y., Li, Y., Hogerkorp, C.-M., Schief, W.R., Seaman, M.S., Zhou, T., Schmidt, S.D., Wu, L., Xu, L.*, et al.* (2010a). Rational Design of Envelope Identifies Broadly Neutralizing Human Monoclonal Antibodies to HIV-1. Science (New York, NY) *329*, 856-861.

Wu, X., Yang, Z.Y., Li, Y., Hogerkorp, C.M., Schief, W.R., Seaman, M.S., Zhou, T., Schmidt, S.D., Wu, L., Xu, L.*, et al.* (2010b). Rational design of envelope identifies broadly neutralizing human monoclonal antibodies to HIV-1. Science *329*, 856-861.

Wu, Y. (2015). STRUCTURAL CHARACTERIZATIONS OF THE DIMERIC ANTI-HIV ANTIBODY 2G12 AND THE HIV-2 ENVELOPE GLYCOPROTEIN. In

Biology and Biological Engineering (Pasadena, CA: California Institute of Technology), pp. 155.

Wyatt, R., Kwong, P.D., Desjardins, E., Sweet, R.W., Robinson, J., Hendrickson, W.A., and Sodroski, J.G. (1998). The antigenic structure of the HIV gp120 envelope glycoprotein. Nature *393*, 705-711.

Xu, L., Daly, T., Gao, C., Flotte, T.R., Song, S., Byrne, B.J., Sands, M.S., and Parker Ponder, K. (2001). CMV-beta-actin promoter directs higher expression from an adeno-associated viral vector in the liver than the cytomegalovirus or elongation factor 1 alpha promoter and results in therapeutic levels of human factor X in mice. Hum Gene Ther *12*, 563-573.

Yu, X., Yuan, X., Matsuda, Z., Lee, T.H., and Essex, M. (1992). The matrix protein of human immunodeficiency virus type 1 is required for incorporation of viral envelope protein into mature virions. J Virol *66*, 4966-4971.

Zadeh, J.N., Steenberg, C.D., Bois, J.S., Wolfe, B.R., Pierce, M.B., Khan, A.R., Dirks, R.M., and Pierce, N.A. (2011). NUPACK: Analysis and design of nucleic acid systems. J Comput Chem *32*, 170-173.

Zhang, J., Yun, J., Shang, Z., Zhang, X., and Pan, B. (2009). Design and optimization of a linker for fusion protein construction. Progress in Natural Science *19*, 1197-1200.

Zhen, A., Kamata, M., Rezek, V., Rick, J., Levin, B., Kasparian, S., Chen, I.S., Yang, O.O., Zack, J.A., and Kitchen, S.G. (2015). HIV-specific Immunity Derived From Chimeric Antigen Receptor-engineered Stem Cells. Mol Ther *23*, 1358-1367.

Zhong, X.S., Matsushita, M., Plotkin, J., Riviere, I., and Sadelain, M. (2010). Chimeric antigen receptors combining 4-1BB and CD28 signaling domains augment PI3kinase/AKT/Bcl-XL activation and CD8+ T cell-mediated tumor eradication. Mol Ther *18*, 413-420.

Zhou, H.X. (2004). Polymer models of protein stability, folding, and interactions. Biochemistry *43*, 2141-2154.

Zhu, P., Chertova, E., Bess, J., Lifson, J.D., Arthur, L.O., Liu, J., Taylor, K.A., and Roux, K.H. (2003). Electron tomography analysis of envelope glycoprotein trimers on HIV and simian immunodeficiency virus virions. Proceedings of the National Academy of Sciences *100*, 15812-15817.

Zhu, P., Liu, J., Bess, J., Jr., Chertova, E., Lifson, J.D., Grise, H., Ofek, G.A., Taylor, K.A., and Roux, K.H. (2006). Distribution and three-dimensional structure of AIDS virus envelope spikes. Nature *441*, 847-852.

Zhu, T., Korber, B.T., Nahmias, A.J., Hooper, E., Sharp, P.M., and Ho, D.D. (1998). An African HIV-1 sequence from 1959 and implications for the origin of the epidemic. Nature *391*, 594-597.

Zingler, K., and Littman, D.R. (1993). Truncation of the cytoplasmic domain of the simian immunodeficiency virus envelope glycoprotein increases env incorporation into particles and fusogenicity and infectivity. J Virol *67*, 2824-2831.

Zou, Y., Weis, W.I., and Kobilka, B.K. (2012). N-terminal T4 lysozyme fusion facilitates crystallization of a G protein coupled receptor. PloS one *7*, e46039.